A ROLE FOR THE PHOSPHOINOSITIDE LIPID KINASE PI4KIIIB IN BREAST ONCOGENSIS AND AKT ACTIVATION

Anne Morrow, B.Sc.

Thesis submitted to the Faculty of Graduate and Postdoctoral Studies in partial fulfillment of the requirements for the degree of

Doctor of Philosophy
In
Biochemistry

Department of Biochemistry, Microbiology and Immunology
Faculty of Medicine
University of Ottawa
Ottawa, Ontario, Canada

ABSTRACT

The lipid kinase phosphatidylinositol 4-kinase III β (PI4KIIIβ) phosphorylates phosphatidylinositol (PtdIns) to generate PI(4)P in the Golgi. PI4KIIIβ is likely involved in the development of breast cancer as it has been reported genetically amplified in a subset of human breast tumours and is a downstream effector of the eukaryotic elongation factor 1 alpha 2 (eEF1A2), a transforming gene that is amplified and highly expressed in approximately 60% of human breast tumours. The goal of my thesis is to investigate a role for PI4KIIIβ in breast oncogenesis.

We show that PI4KIIIβ is highly expressed in approximately 20% of primary human breast tumours. Overexpression of PI4KIIIβ in an invasive breast ductal carcinomas cell line, BT549, increased the production of filopodial actin filament protrusions and enhanced *in vitro* proliferative capacity. Enhanced PI4KIIIβ expression did not impact the migratory rate of these breast cancer cells.

We found that PI4KIIIβ expression activates Akt kinase in the BT549 breast cancer cell line. PI4KIIIβ overexpression led to an increase in the plasma membrane abundance of the PI3K derived $PI(3,4,5)P_3$/$PI(3,4)P_2$ lipids, upstream activators of Akt signalling. PI(4)P and $PI(4,5)P_2$ are precursors to $PI(3,4,5)P_3$ and $PI(3,4)P_2$ generation, however, no changes in the overall cellular abundance or localization of PI(4)P or $PI(4,5)P_2$ were detected in PI4KIIIβ-overexpressing cells. Inhibition of PI4KIIIβ kinase activity, using the drug Pik93, had no effect on PI4KIIIβ-mediated Akt activation. Additionally, ectopic expression of a catalytically inactive PI4KIIIβ also led to increased Akt activity and $PI(3,4,5)P_3$/$PI(3,4)P_2$

plasma membrane abundance. Together, this implies that PI4KIIIβ regulates Akt independently of PI(4)P generation. The PI4KIIIβ interacting protein, Rab11, is likely involved in PI4KIIIβ mediated Akt activation, as RNAi-mediated depletion of Rab11 suppressed the effect of PI4KIIIβ overexpression on Akt activation. Furthermore, PI4KIIIβ overexpression altered cellular Rab11 distribution and led to enhanced recruitment of PI4KIIIβ and Rab11 to recycling endosomes.

Therefore, PI4KIIIβ is highly expressed in a subset of breast tumours and upregulated PI4KIIIβ expression enhances filopodia production and cell growth *in vitro*. Enhanced PI4KIIIβ expression increases $PI(3,4,5)P_3$/$PI(3,4)P_2$ plasma membrane abundance and Akt activation independently of its kinase function, through a mechanism that likely involves Rab11. This work suggests that PI4KIIIβ impacts breast oncogenesis by regulating PI3K/Akt signalling through Rab11 and endosomal trafficking.

Keywords: Breast cancer; phosphoinositides; phosphatidylinositol 4-kinase III β; filopodia, Akt; Rab11

DEDICATION

This work is in honour of my mother, Suzanne L. Blais and my grandfather, Harry M. Morrow.

ACKNOWLEDGEMENTS

I would like to begin by thanking my supervisor, Dr. Jonathan Lee, for taking me on as an honours student and offering me the opportunity to continue on to do my Ph.D. I am grateful for all I have learned from you and for the encouragement you gave me throughout the course of my studies. I would also like to thank all of the members of Dr. Lee's lab, past and present, who have contributed to my training and who offered their support over the years. I would like to particularly thank Dixie Pinke and Sandy Szeto. Dixie, I am grateful that you were there with me from start and am thankful for the great friendship that we built out of this shared experience. Sandy, thank you for your continued support throughout our time together in the lab.

I would like to take this opportunity to thank my thesis advisory committee members, Dr. Ilona Skerjanc and Dr. Zemin Yao. They consistently pushed my work further and offered great insight into my research and invaluable guidance on my academic journey. I would also like to thank the many professors, technicians and support staff at the University of Ottawa, and especially within the departments of Biochemistry, Microbiology and Immunology as well as Cellular and Molecular Medicine, who offered technical assistance and research support. In addition, I would like to thank the graduate students at the University of Ottawa who shared in my journey, offering both their scientific knowledge and their camaraderie.

Finally, I would like to thank my friends and family for their unfailing support throughout my graduate studies. Thank you for your encouragement through the struggles and for sharing in the joy of the successes.

TABLE OF CONTENTS

LIST OF ABBREVIATIONS

ADP	Adenosine diphosphate
AP	Adaptor protein
APPL1	Adaptor protein, phosphotyrosine interaction, PH domain and leucine zipper containing 1
ARF	ADP ribosylation factor
Arp2/3	Actin-related protein-2/3
ATCC	American Type Culture Collection
ATP	Adenosine triphosphate
BSA	Bovine serum albumin
cAMP	Cyclic adenosine monophosphate
CERT	Ceramide transfer
CFP	Cyan fluorescent protein
CHO	Chinese hamster ovary
DAG	Diacylglycerol
DMSO	Dimethyl sulfoxide
DN	Dominant negative
ECM	Extracellular matrix
EDTA	Ethylenediaminetetraacetic acid
EEA1	Early endosome antigen 1
eEF	Eukaryotic elongation factor
EGFR	Epidermal growth factor receptor
ENTH	Epsin N-terminal homology
ER	Endoplasmic reticulum
F-actin	Filamentous actin
FAPP	Four-phosphate-adaptor protein
FBS	Fetal bovine serum
Fwd	Four wheel drive
FYVE	Fab1, YotB, Vac1 and EEA1 binding
G-actin	Globular actin
GalT	Galactosyltransferase
GAP	GTPase-activating protein
GDP	Guanosine diphosphate

GEF	Guanine nucleotide exchange factor
GF	Growth factor
GFP	Green fluorescent protein
GGA	Golgi-localised, γ adaptin ear-containing, Arf-binding
GPCR	G protein-coupled receptor
GTP	Guanosine triphosphate
HCl	Hydrochloric acid
HEPES	Hydroxyethyl piperazineethanesulfonic acid
HER2	Human epidermal growth factor 2
HPLC	High-performance liquid chromatography
HRP	Horseradish peroxidase
Hrs	Hepatocyte growth factor–regulated tyrosine kinase substrate
INPP4	Inositol polyphosphate 4-phosphatase
IP_3	Inositol trisphosphate
IRS-1	Insulin receptor substrate-1
LOH	Loss of heterozygosity
LPA	Lysophosphatic acid
KD	Kinase-dead
MAPK	Mitogen-activated protein kinase
MDCK	Madin-Darby Canine Kidney
MOI	Multiplicity of infection
mRNA	Messenger RNA
mTOR	Mammalian target of rapamycin
N-WASP	Neural WASP
N-terminal	Amino-terminal
NCS-1	Neuronal calcium sensor-1
OSBP	Oxysterol-binding protein
PAGE	Polyacrylamide gel electrophoresis
PBS	Phosphate buffered saline
PDGF	Platelet-derived growth factor
PDK1	Phosphoinositide-dependent kinase-1
PH	Pleckstrin homology
PI	Phosphoinositide
PI3K	Phosphatidylinositol 3-kinase
PI(3)P	Phosphatidylinositol 3-phosphate
$PI(3,4)P_2$	Phosphatidylinositol 3,4-bisphosphate
$PI(3,5)P_2$	Phosphatidylinositol 3,5-bisphosphate
$PI(3,4,5)P_3$	Phosphatidylinositol 3,4,5-trisphosphate

PI4K	Phosphatidylinositol 4-kinase
PI(4)P	Phosphatidylinositol 4-phosphate
PI(4,5)P_2	Phosphatidylinositol 4,5-bisphosphate
PI(5)P	Phosphatidylinositol 5-phosphate
PIKfyve	Phosphatidylinositol 3-phosphate 5-kinase
PKC	Protein kinase C
PKD	Protein kinase K
PLC	Phospholipase C
PTEN	Phosphatase and tensin homolog deleted on chromosome ten
PtdIns	Phosphatidylinositol
PVDF	Polyvinylidene fluoride
PX	Phox homology
RIPA	Radioimmunoprecipitation assay
RNA	Ribonucleic acid
RTK	Receptor tyrosine kinase
S.D.	Standard deviation
SDS	Sodium dodecyl sulphate
S.E.M.	Standard error of the mean
SHIP	SH2 domain-containing 5'-inositol phosphate
SNARE	Soluble N-ethylamide-sensitive factor activating protein receptor
siRNA	Small interfering RNA
TCA	Trichloroactic acid
TGN	Trans-Golgi network
TMA	Tissue microarray
tRNA	Transfer RNA
V_{max}	Maximum velocity
WASP	Wiskott Alderich syndrome protein
WAVE	WASP-family verprolin-homologous protein
WT	Wild type

LIST OF FIGURES

LIST OF TABLES

CHAPTER 1: GENERAL INTRODUCTION

1.1 Phosphoinositides

Phosphoinositides (PI) are negatively charged membrane-bound phospholipids that play important and diverse roles in regulating cell signalling and transport (1-3). Phosphoinositides are phosphorylated derivations of phosphatidylinositol (PtdIns), which is comprised of a glycerol backbone esterified to two fatty acid chains and a phosphate group and attached to a polar D-*myo*-inositol head group that extends into the cytoplasm (Fig. 1.1). The diacylglycerol (DAG) component of PtdIns is predominantly 1-stearoyl-2-arachanonyl-3-phosphoglycerol (4). Reversible phosphorylation of three of the free hydroxyl groups (D3, D4 and D5) in the inositol ring give rise to seven distinct phosphoinositide species: PI(3)P, PI(4)P, PI(5)P, PI(3,4)P_2, PI(3,5)P_2, PI(4,5)P_2 and PI(3,4,5)P_3 (Fig. 1.1). PtdIns is synthesized in the endoplasmic reticulum (ER) through the addition of a myo-inositol head group to activated cytidine diphosphate-diacylglecerol (CDP-DAG) by PtdIns synthase (PIS) (5). PtdIns is then delivered to other cellular membranes by vesicular transport or cytosolic PtdIns transfer proteins. There the combined action of lipid kinases and phosphatases regulate the production of phosphoinositide species (2, 6).

PtdIns and phosphoinositide lipids are found in relatively low abundance within eukaryotic cells, with PtdIns representing less than 15% of total phospholipids and phosphoinositides being present at levels of between 0.01-5% of that observed for PtdIns (1, 2, 7). However, phosphoinositides are able to regulate a great diversity of signalling events due to the structural variances of the phosphorylated species and the different interactions that each mediate through the binding of their head group to cytosolic proteins or cytosolic domains of membrane proteins. The polyanionic nature of phosphoinositides allows them to interact with proteins containing clusters of basic residues through non-specific electrostatic

Figure 1.1: Phosphoinositide species.

Phosphatidylinositol (PtdIns) consists of a D-myo-inositol 1-phosphate headgroup attached, almost exclusively, to 1-stearoyl, 2-arachanonyl, 3-phosphoglycerol as depicted. Seven distinct phosphoinositide species can be derived from the reversible phosphorylation of PtdIns at the 3-, 4- and 5- position of the inositol ring. Adapted from (1).

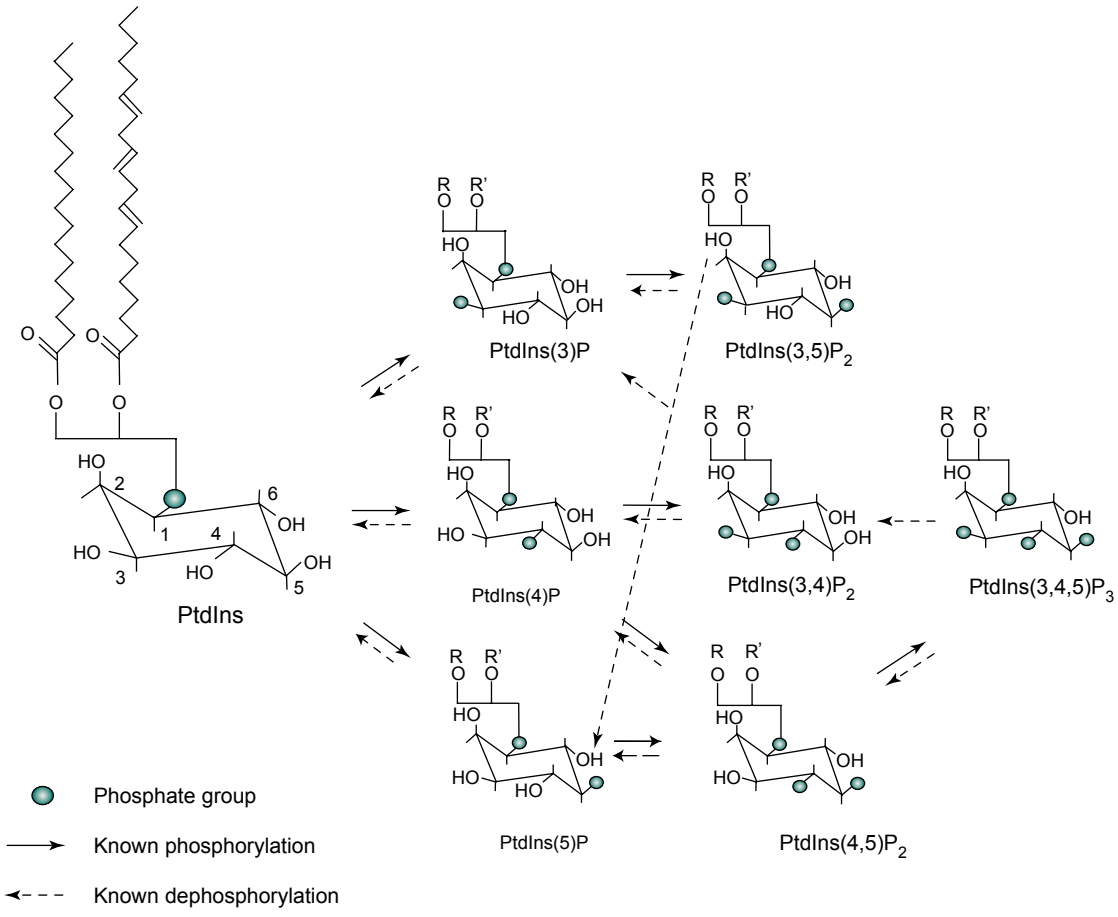
PtdIns
PtdIns(3)P
PtdIns(5)P
PtdIns(4)P
PtdIns(3,5)P2
PtdIns(3,4)P2
PtdIns(4,5)P2
PtdIns(3,4,5)P3
Phosphate group
Known phosphorylation
Known dephosphorylation

interactions. Basic/aromatic amino acid motifs have been shown to be the primary binding site for a number of phosphoinositide interacting proteins such as KRAS and Rab35, as well a number of actin-binding proteins, such as profilin, cofilin and gelsolin (8-10). Phosphoinositides can also bind proteins with more specificity through folded modules termed phosphoinositide recognition or binding domains (11, 12). These phosphoinositide binding domains include the plexstrin homology (PH) domain, the phox-homology (PX) domain, the FYVE (for Fab1, YotB, Vac1 and early antigen endosome 1 (EEA1) binding) domain and the epsin amino-terminal (ENTH) domain (Fig. 1.2). Some recognition domains have a high affinity for only one phosphoinositide, such as the unique recognition of PI(3)P by FYVE domains (K_d = 50 nM), while other domains, such as PH domains, bind several different phosphoinositides (12). Though PH domains interact with phosphoinositides with a broad range of specificity and affinity, a subset of PH domains bind specific phosphoinositide species with high affinity (13). For example, the PH domain of phospholipase C δ 1 (PLC-δ1) has a specific and high affinity for the phosphoinositide lipid $PI(4,5)P_2$ (K_d = 1.7 μM), whereas the PH domain of Akt binds $PI(3,4,5)P_3$ and $PI(3,4)P_2$ with similar affinity (K_d = 0.4 and 0.57 μM respectively) (14, 15). In comparison, the N-terminal PH domain of pleckstrin-1 binds to $PI(4,5)P_2$ and phosphatidylserine with similar affinity, signalling that the PH domain of pleckstrin binds non-specifically to membranes via electrostatic interactions (13, 16). Furthermore, higher affinity binding can be achieved through coincidence detection, when multiple signals act in concert to direct protein effector membrane binding, such as dual binding of proteins to phosphoinositides and membrane co-receptors, cargo proteins or small GTPases (1, 2). These interactions together serve to target proteins to specific locations within the cell.

Figure 1.2: Phosphoinositide recognition domains.

Phosphoinositide protein binding domains have been identified that bind phosphoinositide species with varying specificity and affinity. Phosphoinositide binding modules are presented schematically, along with their target phosphoinositides. Abbreviations: ANTH, AP180 N-terminal homology; ENTH, Epsin N-terminal homology; FERM, 4.1 protein, ezrin, radixin and moesin binding; Fyve, Fab1, YotB, Vac1 and EEA1 binding; GOLPH3, Golgi phosphoprotein 3; PH, pleckstrin homology; PROPPIN, β-propellers that bind polyphosphoinositides; PX, phox homology; PTB, phosphotyrosine-binding. Adapted from (17).

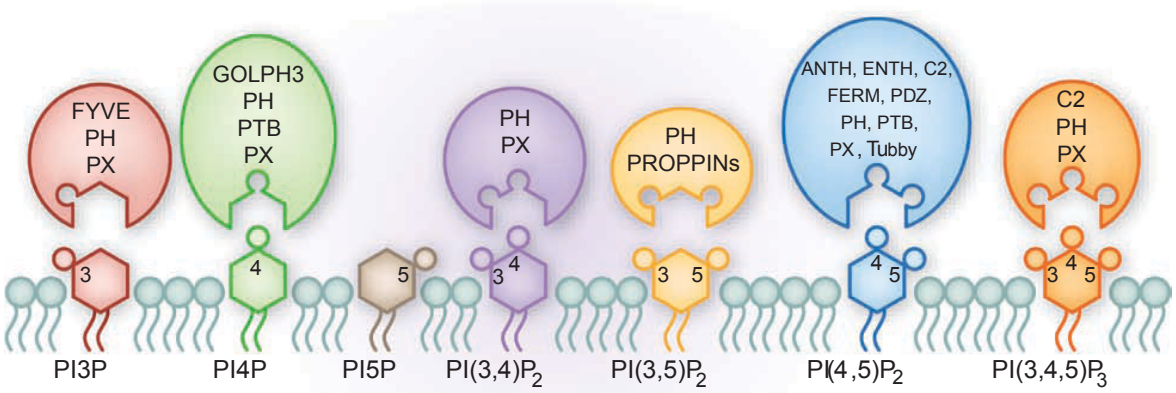
FYVE
PH
PX
GOLPH3
PH
PTB
PX
PH
PX
PH
PROPPINs
ANTH, ENTH, C2,
FERM, PDZ,
PH, PTB,
PX, Tubby
C2
PH
PX
3
4
5
3 4
3 5
4 5
3 4 5
PI3P
PI4P
PI5P
PI(3,4)P2
PI(3,5)P2
PI(4,5)P2
PI(3,4,5)P3

Phosphoinositides are differentially distributed on cellular membranes (Fig. 1.3). This segregation of phosphoinositide species on distinct subcellular membranes is critical in the control of directional membrane traffic, with phosphoinositide identity directing the transport of cargo from one membrane compartment to another (18, 19). For example, budding vesicles must contain lipids that will recruit the surface factors needed for fusion with a given acceptor membrane and these factors must be shed after fusion. The rapid conversion of phosphoinositide lipids from one species to another by kinases and phosphatases whose activity is spatially regulated makes this possible. A phosphoinositide-based code is thought to define organelle identity (20). As such, PI(4)P is enriched at the Golgi, PI(3)P and PI(3,5)P_2 are concentrated in early and late endosomes respectively and PI(4,5)P_2, PI(3,4,5)P_3 are predominantly found at the plasma membrane (2).

An imaging tool that takes advantage of protein phosphoinositide recognition domains was devised in order to study the spatial distribution of the various phosphoinositides and better understand the localized regulatory functions these lipids exert. Fluorescent probes were generated, fusing high affinity and specificity inositide lipid protein binding modules, such as the subset of high affinity binding PH domains described above, to green fluorescent protein (GFP) (21). These probes allow visualization of specific pools of phosphoinositide lipids in live cells and offer the advantage of resolving issues of fixation and sensitivity initially encountered in work done with anti-phosphoinositide antibodies (22, 23). However, imaging PIs using fluorescent probes has certain limitations. It is important to consider that PH domains are recruited by multiple membrane interactions and that a specific reporter will detect a given phosphoinositide only in the molecular context of the probe being used (22). For example the FAPP1 PH domain will only bind to PI(4)P associated with Arf1

Figure 1.3: Subcellular localization of phosphoinositides.

The predominant subcellular localization of phosphoinositide species is shown schematically. Phosphoinositides are concentrated in distinct pools of cytosolic membranes and serve as markers of various cell compartments. A heterogeneous distribution of phosphoinositides within a given membrane has also been observed. Abbreviations: EE, early endosomes; MVB, multi-vesicular bodies; PI(3)P, phosphatidylinositol 3-phosphate; PI(3,4)P_2, phosphatidylinositol 3,4-bisphosphate; PI(3,5)P_2, phosphatidylinositol 3,5-bisphosphate; PI(3,4,5)P_3, phosphatidylinositol 3,4,5-trisphosphate; PI(4)P, phosphatidylinositol 4-phosphate; PI(4,5)P_2, phosphatidylinositol 4,5-bisphosphate. Adapted from (17).

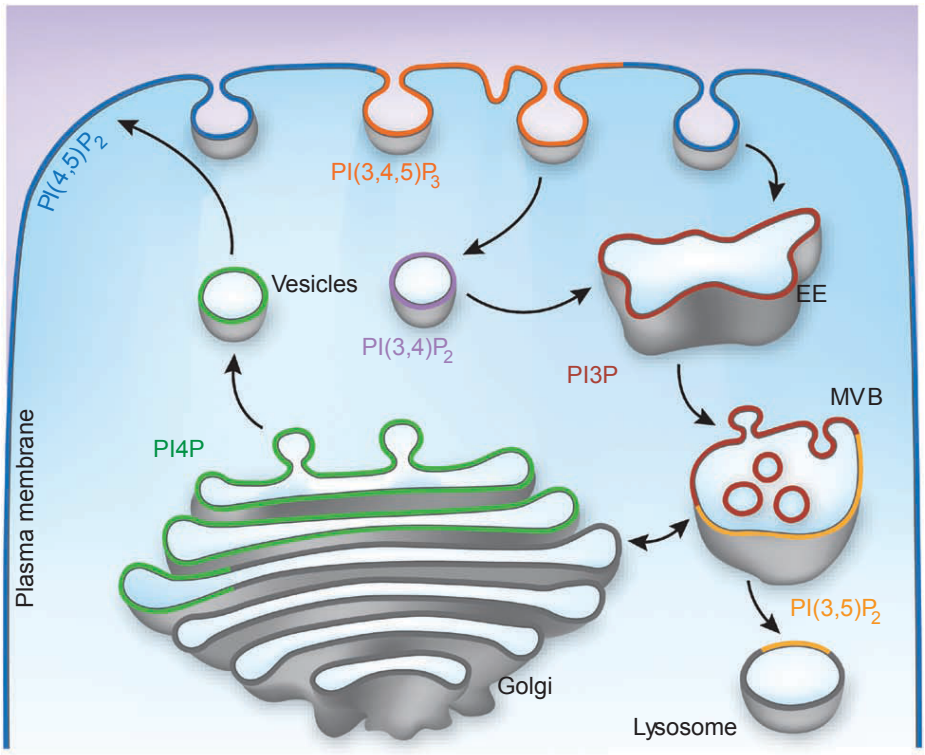
PI(4,5)P2
PI(3,4,5)P3
Vesicles
PI(3,4)P2
EE
PI3P
MVB
PI4P
Plasma membrane
PI(3,5)P2
Golgi
Lysosome

(24). Moreover, the probe can only bind to free lipids that are not in complex and will therefore have restricted access to certain lipid pools (22). Finally, binding of the PH domain-GFP reporters to phosphoinositides also inhibits the signalling processes regulated by the targeted phosphoinositide(s) (22). As a consequence, long term expression of the reporter constructs can be cytotoxic. To circumvent these limitations, recent work by Hammond et al. demonstrated that anti-phosphoinositide antibodies give more reliable results when used with specific fixation techniques (25). It is likely that a combination of visualization techniques will allow a full picture to emerge of the cellular dynamics of phosphoinositide generation.

1.2 PI(4)P

PI(4)P is produced by phosphorylation at the D4 position of the inositol ring of PtdIns by phosphatidylinositol 4-kinases (PI4K) (26). PI(4)P is the second most abundant phosphoinositide species, accounting for 30% of phosphoinositides in mammalian cells (7). PI(4)P is also the most abundant monophosphorylated phosphoinositide derivative, accounting for 95% of the PIP in the cell (11, 27). It is also the predominant phosphoinositide of the Golgi complex, where it has essential roles in Golgi function (2). PI(4)P regulates Golgi morphology, vesicle-mediated export from the trans-Golgi network (TGN) and lipid biogenesis. PI(4)P regulates Golgi morphology through the recruitment of GOLPH3, which interacts with the unconventional myosin motor protein MYO18A (28). Together GOLPH3 and MYO18A provide a tensile force that maintains the shape of the Golgi (28). PI(4)P also directs clathrin coated vesicle adaptor recruitment, which promotes sorting of cargo at the TGN into vesicles destined for the endolysosomal system (29). The clathrin adaptor proteins, adaptor protein 1 (AP-1) and the Golgi-localised, γ adaptin ear-

containing, ADP-ribosylation factor 1 (Arf)-binding proteins (GGAs) all bind to PI(4)P (19, 30-32). In addition, PI(4)P also recruits lipid transfer proteins to the Golgi through conserved N-terminal PH domains (33). PI(4)P binds to ceramide-transfer protein (CERT), oxysterol-binding protein 1 (OSPB1) and four-phosphate-adaptor protein (FAPP) 1 and 2 (33-35). These lipid transfer proteins mediate non-vesicular lipid transport between membranes and regulate sphingolipid and sterol metabolism, as well as vesicular trafficking from the TGN to the plasma membrane (34, 36, 37). AP-1, GGAs, FAPP1 and OSBP also bind the small GTPase Arf1, allowing for dual recognition and more specific membrane targeting (31, 33, 34, 38).

The phosphatase responsible for dephosphorylating PI(4)P, Sac1, is localized in the ER and early Golgi compartments (39, 40). This localization of Sac1 is believed to prevent retrograde trafficking of PI(4)P from the Golgi to the ER and creates a gradient in which PI(4)P, and its effectors, are enriched in late Golgi compartments (29, 39, 41). Within these late Golgi compartments, PI(4)P is a central regulator of protein and lipid transport to the cell surface. Depletion of PI(4)P at the Golgi impairs the exit of cargo from the Golgi to both the plasma membrane and late endosomes (42). Furthermore, depletion of PI(4)P impairs the replenishment of plasma membrane $PI(4,5)P_2$ (42). This suggests that Golgi derived PI(4)P has a role in regulating plasma membrane $PI(4,5)P_2$ production.

1.3 $PI(4,5)P_2$

$PI(4,5)P_2$, along with PI(4)P, form the bulk of phosphoinositide lipids in mammalian cells; $PI(4,5)P_2$ accounts for 60% of phosphoinositide species (2, 7). In addition, $PI(4,5)P_2$ is the most abundant form of PIP_2 in mammalian cells, accounting for an estimated 99% of the

total PIP_2 (11). $PI(4,5)P_2$ is primarily synthesized from PI(4)P by PI(4)P 5-kinases (PIPKIs) and may also be formed, in a more minor pathway, by PI(5)P 4-kinase (PIPKII) directed phosphorylation of PI(5)P (43). $PI(4,5)P_2$ is concentrated in the plasma membrane, where it plays critical roles in signal transduction, actin polymerization and anchoring, exocytosis and endocytosis, as well as in the regulation of integral plasma membrane proteins (2). $PI(4,5)P_2$ functions as a classic signal transduction molecule as it can be hydrolysed by phospholipase C (PLC), leading to the generation of the second messengers DAG and inositol 1,4,5-trisphosphate, which activate protein kinase C (PKC) and release intracellular stores of Ca^{2+} respectively (44). $PI(4,5)P_2$ can also be hydrolysed by inositol polyphosphate phosphatases (INPP5s), regenerating PI(4)P (26).

$PI(4,5)P_2$ itself is a regulator of various cellular processes. Firstly, $PI(4,5)P_2$ impacts the organization of the actin cytoskeleton. $PI(4,5)P_2$ directly induces actin filament polymerization by binding to Wiskott–Aldrich syndrome protein (WASP), along with the small GTPase Cdc42, leading to activation of the actin-related protein complex 2/3 (Arp2/3) (45). $PI(4,5)P_2$ also binds to and regulates the function of actin binding proteins found at cell adhesion sites (46-49). For example, talin, when bound to $PI(4,5)P_2$ has enhanced affinity for integrins, which are cell-surface-adhesion receptors that mediate the attachment between a cell and the extracellular matrix (ECM) (46). Secondly, $PI(4,5)P_2$ is involved in regulating exocytic and endocytic trafficking. $PI(4,5)P_2$ has a specific role in vesicle priming (*i.e.,* pre-fusion stage) (50, 51). $PI(4,5)P_2$ has been shown to be required for Ca^{2+}-triggered exocytosis in PC12 and chromaffin cells, likely via interaction with synaptotagmin-1, the calcium sensor for exocytosis (52-54). Plasma membrane $PI(4,5)P_2$ binds to synaptotagmin-1, which is anchored to the membrane of secretory granules, facilitating the juxtaposition of the

vesicle and the plasma membrane (55). $PI(4,5)P_2$ also regulates endocytosis as a co-receptor for the recruitment and regulation of endocytic clathrin adaptors such AP-2 and epsin, as well as dynamin, which controls vesicular fission (18, 56, 57). Finally, $PI(4,5)P_2$ can also regulate the function of integral membrane proteins, such as ion exchangers and transporters (58, 59). $PI(4,5)P_2$ positively regulates the activity of sodium-calcium exchangers (NCX-1), sodium-proton exchangers (NHE1-4), epithelial sodium channels (ENaC) and voltage gated sodium channels (KCNQ) (58, 59). In addition, $PI(4,5)P_2$ has also been shown to inhibit the capsaicin receptor (TRPV1), a heat activated ion channel of the pain pathway, allowing $PI(4,5)P_2$ hydrolysis to direct TRPV1 activation or potentiation (60).

1.4 $PI(3,4,5)P_3$/$PI(3,4)P_2$

$PI(4,5)P_2$ can also be further phosphorylated by type I PI3Ks to produce $PI(3,4,5)P_3$ (26). In quiescent cells, $PI(3,4,5)P_3$ is a rare lipid species, comprising 0.1% of its precursor, $PI(4,5)P_2$, though upon tyrosine kinase stimulation, $PI(3,4,5)P_3$ levels can increase from 2- to 100-fold (3). $PI(3,4)P_2$, in turn, is generated by dephosphorylation of $PI(3,4,5)P_3$ at the D5 position by the SH2 domain containing inositol phosphatases (SHIP) 1 and 2 (26). $PI(3,4,5)P_3$ and $PI(3,4)P_2$ are grouped together as they both have the capacity to activate Akt, a central signalling molecule (61, 62). Akt is a serine/threonine kinase that regulates anti-apoptotic, proliferative and protein synthesis pathways, as well as regulating cell migration and invasion (62, 63). As will be discussed later, $PI(3,4,5)P_3$ and $PI(3,4)P_2$ are responsible for recruiting Akt to the plasma membrane via its PH domain, where it can be activated by protein-dependent kinase-1 (PDK1) and mammalian target of rapamycin complex 2 (mTORC2)-dependent phosphorylation (61, 62). Evidence suggests that $PI(3,4,5)P_3$ and

$PI(3,4)P_2$ also direct PDK1 recruitment to the plasma membrane through its PH binding domain (64).

Furthermore, $PI(3,4,5)P_3$ is involved in the regulation of actin cytoskeleton dynamics. $PI(3,4,5)P_3$ interacts with and activates the WASP-family verprolin-homologous protein (WAVE), mediating the formation of lamellipodia, a peripheral actin meshwork found at the leading edge of motile cells (65). $PI(3,4,5)P_3$ also interacts with a number of guanine nucleotide exchange factors (GEFs) and GTPases activating proteins (GAPs) that regulate the activity of the Rho family of small GTPases, which in turn regulate actin cytoskeleton remodeling (66, 67). In contrast, to date only one $PI(3,4)P_2$ specific interaction has been characterized, with an adaptor protein, the tandem PH (pleckstrin homology)-domain-containing protein (TAPP) 1 and 2, which appears to function as part of a feedback loop that downregulates tyrosine kinase signalling (68, 69). The fact that these lipid species regulate both common and independent signalling pathways illustrates the complex and fine-tuned nature of phosphoinositide regulated cellular processes within the cell.

1.5 PI(3)P/PI(3,5)P_2/PI(5)P

PI(3)P and $PI(3,5)P_2$ are relatively minor phosphoinositide species; however, they play crucial roles in the biology of endosomes, a heterogeneous system of membranes responsible for the sorting and delivery of proteins and lipids to and from the plasma membrane, Golgi and lysosomes . PI(3)P is generated from PI by type III PI3Ks (43). PI(3)P is a major determinant of early endosome identity and binds a variety of endosomal proteins, such as EEA1, hepatocyte growth factor–regulated tyrosine kinase substrate (Hrs) and the microtubule-dependent motor protein KIF16B, regulating vesicle tethering and fusion, receptor sorting, and endosomal interactions with the cytoskeleton (70-72). $PI(3,5)P_2$ is

generated by PIKfyve (PIPKIII) phosphorylation of PI(3)P, with PIKfyve localizing to early and late endosomes as well as lysosomes in mammalian cells (43, 73-75). $PI(3,5)P_2$ plays an important role in endosomal trafficking and vesicle budding (74, 76, 77). $PI(3,5)P_2$ is also believed to be the major precursor for most of the cellular pools of PI(5)P, through dephosphorylation by the myotubularin phosphatases (78).

PI(5)P has also been reported to be generated by PIKfyve phosphorylaton of PI and in addition by $PI(4,5)P_2$ 4 -phosphatases (type I and type II) dephosphorylation of $PI(4,5)P_2$ *in vitro* (79, 80). The novel PTEN-like phosphatase (PLIP) has been shown to dephosphorylate PI(5)P, regenerating PI, *in vitro (81)*. The role of PI(5)P is the least well defined of the phosphoinositide species. It has been reported localized to the nucleus, plasma membrane, Golgi and sarco/endoplasmic reticulum (82-84). Within the nucleus, PI(5)P has been found to regulate nuclear protein function, activating the ubiquitin-ligase Cu13-SPOP (85). Outside of the nucleus, the function of PI(5)P is less clear. This phosphoinositide is reported to prolong or enhance PI3K/Akt signalling and possibly play a role in late endosome to plasma membrane trafficking (86-89).

1.6 Phosphatidylinositol 4-Kinases

PI4Ks are responsible for phosphorylating PtdIns at the D4 position of the inositol ring, generating PI(4)P, the precursor to $PI(4,5)P_2$, $PI(3,4)P_2$ and $PI(3,4,5)P_3$ generation (Fig 1.4). There are four mammalian PI4Ks: PI4KIIα, PI4KIIβ, PI4KIIIα and PI4KIIIβ. PI4Ks are classified as either type II or type III based on biochemical properties: type II PI4Ks (α and β) have a high affinity for ATP, are sensitive to inhibition by low concentrations of adenosine and are wortmannin insensitive; type III PI4Ks (α and β) have lower affinity for ATP, have low sensitivity to adenosine inhibition and are wortmannin-sensitive (90). All

Figure 1.4: The phosphoinositide signalling pathway catalyzed by PI4K.

PI4K catalyzes the phosphorylation of PtdIns at the D4 position of the inositol ring to PI(4)P. The Sac1 phosphatase converts PI(4)P back into PtdIns. PI(4)P is a precursor for $PI(3,4)P_2$, $PI(4,5)P_2$ and $PI(3,4,5)P_3$ generation by PI3K (type II), PI(4)P 5-kinase and PI3K (type I) phosphorylation respectively. $PI(3,4)P_2$ generation via desphorylation of $PI(3,4,5)P_3$ by SHIP1/2 and PI(3)P generation via INPP4 dephosphorylation of $PI(3,4)P_2$ are also possible. In addition the $PI(4,5)P_2$ and $PI(3,4,5)P_3$ phosphatases INPP5 and PTEN are presented.

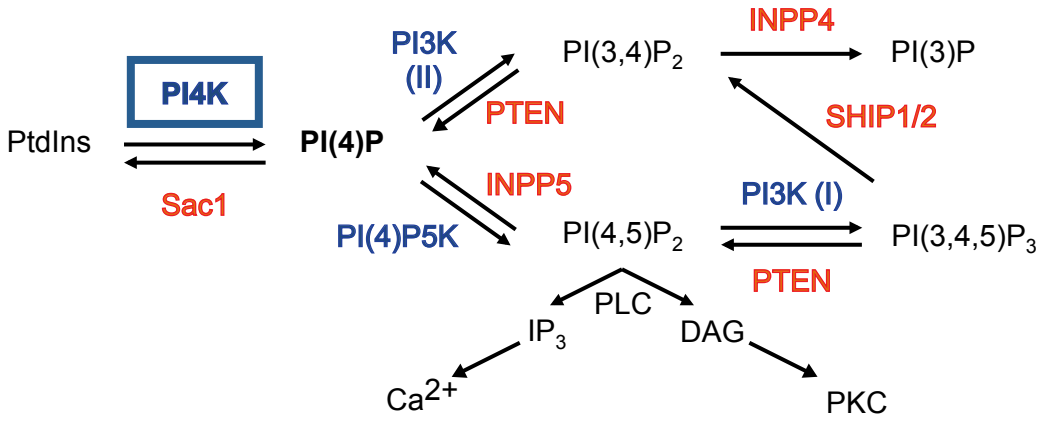
PI4K
PtdIns
PI(4)P
Sac1
PI3K
(II)
PTEN
PI(3,4)P2
INPP4
PI(3)P
SHIP1/2
INPP5
PI(4)P5K
PI(4,5)P2
PI3K (I)
PI(3,4,5)P3
PTEN
PLC
IP3
DAG
Ca2+
PKC

four PI4K enzymes show a wide tissue distribution, indicating that these enzymes play essential roles throughout the body (91, 92). While all performing the same catalytic function, each PI4K has unique structural features (Fig. 1.5). The type II and type III PI4Ks do not share sequence homology and all four isoforms differ in their N-terminal regulatory domains (90). As a consequence, the four different isoforms localize to discrete subcellular membrane compartments (Fig. 1.6).

Type II PI4K enzymes undergo palmitoylation on a conserved stretch of cysteine residues (93). PI4KIIα is tightly membrane-bound and localizes primarily to the TGN and to endosomes (19, 91). Consistent with its localization, PI4KIIα is involved in regulating intracellular trafficking. Knockdown of PI4KIIα abolishes AP-1 adaptor recruitment to the Golgi and impairs AP-3 adaptor recruitment to endosomes (19, 94). PI4KIIα also mediates the endosomal trafficking and lysosomal degradation of the epidermal growth factor receptor (EGFR) (95). Mice lacking PI4KIIα kinase activity develop late onset degeneration of spinal cord axons, likely as a result of a neuronal trafficking defects (96). PI4KIIβ in contrast, is primarily cytosolic, reflecting a difference in steady state palmitoylation (97). PI4IIβ can be recruited to the plasma membrane after platelet-derived growth factor stimulation, in a mechanism mediated by Rac1-GTP (98). PI4KIIβ has also been reported localized to endosomes when overexpressed in COS-7 monkey kidney fibroblast cells (91). Currently, however, a distinct function for PI4KIIβ has not been ascribed to this enzyme. Relatively recent work has been done using fluorescence correlation spectroscopy to study the localization of green fluorescent protein (GFP)-tagged PI4KII*β* in the cytoplasm (99). PI4KII*β* was found highly enriched in small molecular complexes, and using a palmitoylation-defective mutant, PI4KII*β*-FFPFF, it was shown that this clustering is

Figure 1.5: Structural features of PI4K isoforms.

The structural features of the mammalian isoforms of PI4K (PI4KIIIβ, PI4KIIα and PI4KIIIα) are illustrated. The yeast ortholog for each PI4K (Pik1p, Lsbp and Stt4p) is placed underneath the corresponding enzyme. PI4KIIβ is not shown as, structurally, the type II PI4Ks are very similar, with the only notable difference being that in lieu of the proline-rich sequence at its N-terminus, the β enzyme contains a highly acidic region. The PI4K type II and type III kinase domains differ in sequence homology. It is however, the N-terminus of all three PI4Ks that differ the most between isoforms. The scale indicates length of proteins in amino acids. Abbreviations: Pro-rich, proline-rich; Ser-rich, serine-rich; cys-rich, cysteine-rich; LKU, lipid kinase unique domain; Fq, frequenin-binding site; Hom2, PI4KIIIβ and Pik1p homology domain; NLS, purported nuclear localization signal. Adapted from (90).

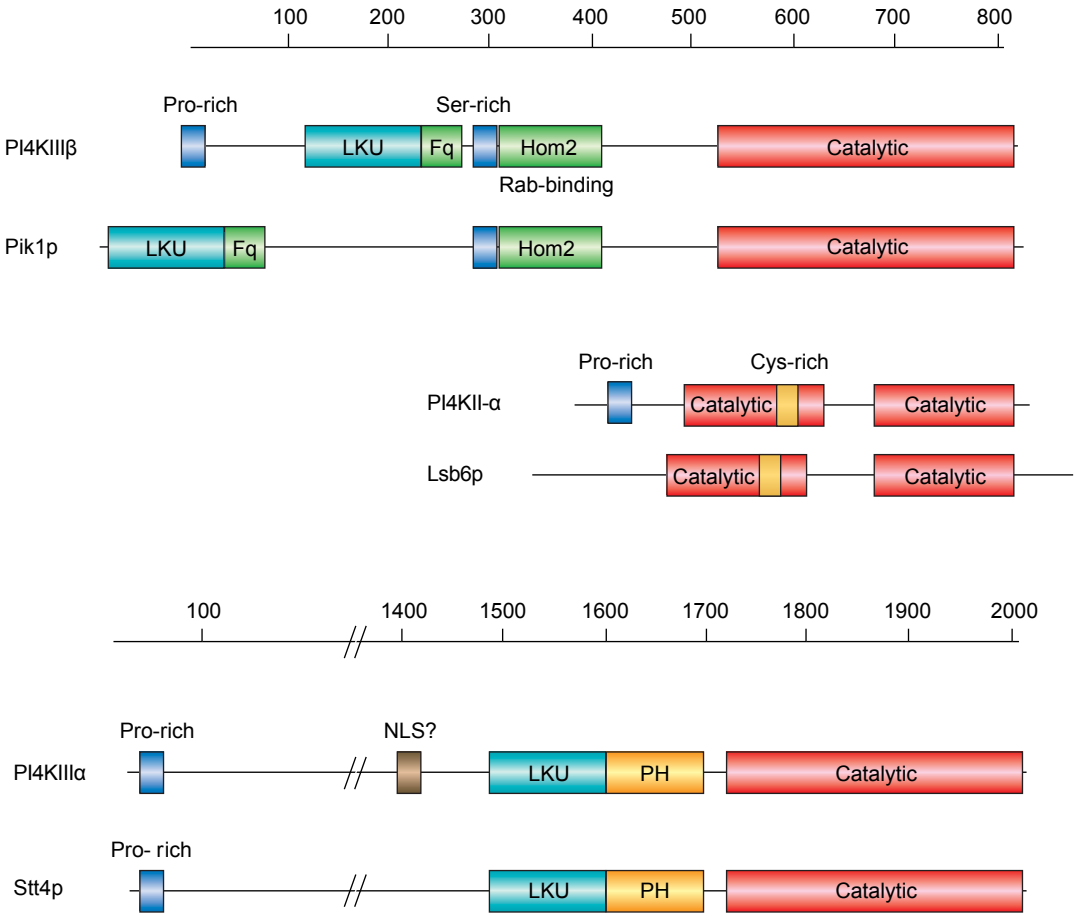
100
200
300
400
500
600
700
800
Pro-rich
Ser-rich
PI4KIIIβ
LKU
Fq
Hom2
Catalytic
Rab-binding
Pik1p
LKU
Fq
Hom2
Catalytic
Pro-rich
Cys-rich
PI4KII-α
Catalytic
Catalytic
Lsb6p
Catalytic
Catalytic
100
1400
1500
1600
1700
1800
1900
2000
Pro-rich
NLS?
PI4KIIIα
LKU
PH
Catalytic
Pro- rich
Stt4p
LKU
PH
Catalytic

Figure 1.6: Cellular localization of PI4K enzymes.

The localization of the four different mammalian isoforms of PI4K in the cell and the major routes of vesicular transport are shown. Abbreviations: EE, early endosomes; ER, endoplasmic reticulum; Lys, lysosomes; MVB, multivesicular body; PI4K, phosphatidylinositol 4-kinase; PM, plasma membrane; TGN, trans-Golgi network. Adapted from (90).

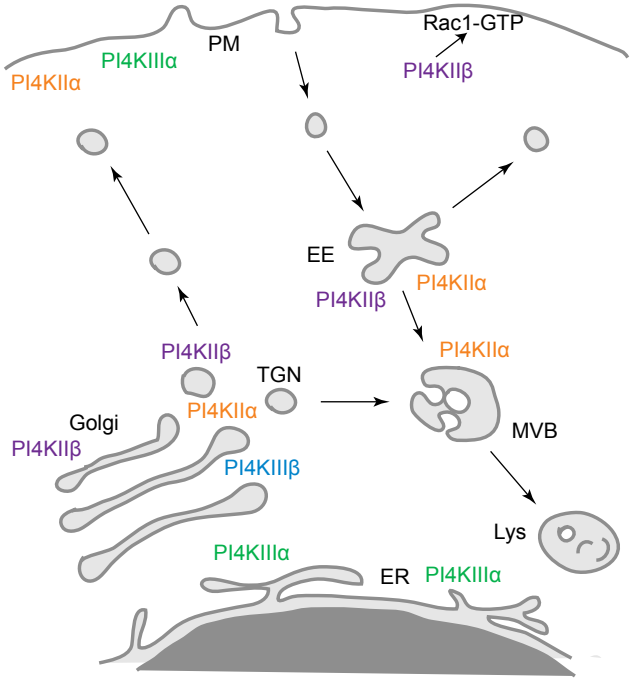
PM
Rac1-GTP
PI4KIIIα
PI4KIIα
PI4KIIβ
EE
PI4KIIα
PI4KIIβ
PI4KIIβ
PI4KIIα
TGN
PI4KIIα
Golgi
PI4KIIβ
MVB
PI4KIIIβ
Lys
PI4KIIIα
ER
PI4KIIIα

dependent on PI4KIIβ's membrane association (99). A dual-colour brightness analysis technique allows the authors to determine that PI4KII*β* codistributes with clathrin light chain and the clathrin adaptor protein, AP-2 (99). These results suggest that PI4KIIβ localizes to clathrin-coated vesicles and is involved in an early endocytic pathway. Together, type II PI4Ks are responsible for synthesizing ~ 50% of the total cellular PI(4,5)P_2 pool (100). There is one yeast ortholog for the type II PI4K enzymes, Lsb6p (also termed Pik2p), which contributes minimally to PI(4)P generation (101, 102). Inactivation of the protein causes only a mild defect in endocytic trafficking (103). This defect can be rescued by expressing a construct that does not contain the catalytic domain, but requires a region that interacts with the yeast ortholog of WASP protein, which is involved in regulating actin polymerization (103). This suggests that the catalytic function of Lsb6p may not be essential and that the protein likely functions as a scaffold regulating the movement of vesicles. The type II PI4K ortholog found in *Drosophila* is involved in regulating the trafficking of secretory granule proteins (104). Through the study of PI4KII null mutant flies, PI4KII was shown to be required during development for the formation of secretory glue granules of normal size in *Drosophila* salivary glands (104). Loss of PI4KII led to the production of smaller granules, the formation of enlarged late endosomes and the accumulation of the granule SNARE Snap24 and glue marker Sg3 in these enlarged endosomes (104). Re-introduction of wild-type PI4KII restored glue granule size and normal late endosome morphology, whereas expression of a catalytically inactive PI4KII failed to do so (104), illustrating the importance of the catalytic function of PI4KII in the trafficking of secretory granules in *Drosophila* (104).

PI4KIIIα was initially reported at the ER in mammalian cells, however a role at the ER for PI4KIIIα has not been determined (105). Instead, PI4KIIIα has been attributed a role in the maintenance of phosphoinositide pools at the plasma membrane. In particular, PI4KIIIα was shown to be responsible for the production of PI(4)P and PI(4,5)P_2 at the plasma membrane during agonist-induced Ca^{2+} signalling (106). Recent work by De Camilli's lab showed that PI4KIIIα, a primarily cytoplasmic protein, transiently interacts with the plasma membrane, through binding to two interactor proteins (EFR3B and TTC7B) (107). The authors used a conditional gene knockout approach to study the effect of loss of PI4KIIIα on cellular functions, as conventional PI4KIIIα mouse knockouts were embryonic lethal . In MEF cells with a complete loff of PI4KIIIα a selective loss of plasma membrane PI(4)P and PI(4,5)P2 were observed. This work highlights the importance of PI4KIIIα in plasma membrane phosphoinositide production. It has also been proposed that PI4KIIIα is involved in generating membrane alterations necessary for hepatitis C virus replication (108). In addition, PI4KIIIα has been identified as a principal component of the PI3K branch of FGF signalling in zebrafish, playing a crucial role in pectoral fin development (109). The yeast ortholog of PI4KIIIα, Stt4p, is an essential gene and is localized to the plasma membrane (110). It is necessary for the maintenance of cell wall integrity, vacuole morphology and actin cytoskeleton organization (111).

1.7 PI4KIIIβ

The focus of my project is on PI4KIIIβ. PI4KIIIβ is primarily Golgi localized and is also found in the cytosol and in the nucleus (105, 112). The small GTPase Arf1, in its active GTP-bound state, is responsible for recruiting soluble PI4KIIIβ to the Golgi and activating PI4KIIIβ (105, 113). When monkey kidney fibroblast-like cells (Cos7) were transfected with

a catalytically inactive PI4KIIIβ and treated with Brefeldin A (BFA), a fungal toxin that prevents the activation of Arf and induces the disassembly of the Golgi, Golgi retubulation was impaired following removal of the drug, suggesting that Arf-regulated PI4KIIIβ kinase activity may be required to maintain the structural integrity of the Golgi (113). PI4KIIIβ physically interacts with another Golgi localized protein, neuronal calcium sensor-1 (NCS-1), which enhances the kinase activity of PI4KIIIβ in a Ca^{2+} dependent manner (114-117). Myristoylation of NCS-1 is required for its interaction with PI4KIIIβ (117). NCS-1 regulates exocytosis in neuroendocrine cells and siRNA depletion of PI4KIIIβ has been shown to prevent the stimulatory effect of NCS-1 expression on regulated exocytosis in PC12 cells (117). NCS-1 can also bind Arf1 (115). Haynes et al. found that the binding of PI4KIIIβ to Arf1 and NCS-1 is mutually exclusive in direct binding assays, as PI4KIIIβ was not found to bind Arf1 and NCS-1 simultaneously under conditions where the Arf1-NCS-1 interaction was detected (115). Furthermore, inclusion of NCS-1 in *in vitro* kinase assays led to a loss of Arf1 mediated PI4KIIIβ activation (115). Additionally, Arf1 co-expression with NCS-1 in PC12 cells abolished the stimulatory effect of NCS-1 expression on regulated secretion (115). The authors posit that the direct interaction between Arf1 and NCS-1 allows for bidirectional control of PI4KIIIβ; Arf1 and NCS-1 can activate PI4KIIIβ independently, but their interaction prevents the dual or combined activation of PI4KIIIβ by both effectors, should they overlap in the cell (115). This is likely due to the fact that Arf1 and NCS-1 regulate independent trafficking pathways and this would allow for these pathways to remain spatially and temporally distinct within the cell.

In addition to its role in regulated secretion in neuroendocrine cells, PI4KIIIβ has been shown to regulate TGN to plasma membrane protein delivery in polarized Madin-

Darby canine kidney (MDCK) cells (118). Furthermore, PI4KIIIβ, in concert with NCS-1, regulates extracellular signal-regulated kinase (ERK) 1/2 signalling via endocytic trafficking (119). Previous studies have established that the mitogen-activated protein kinase (MAPK) cascade, in which ERK propagates mitogenic signals from receptors at the plasma membrane to targets in the nucleus, requires endosomal trafficking (120-122). Trafficking of signalling intermediates within endocytic vesicles has been hypothesized to be an efficient way of propagating signals from the plasma membrane to the nucleus by temporally and spatially regulating components of the signalling cascade (120, 121). Kapp-Barnea et al. found that the endocytic recycling compartment (ERC), a perinuclear compartment from which recycling endosomes emerge, is an intermediate step in ERK1/2 trafficking and that overexpression of NCS-1 increases the rate of endocytic trafficking, the amount of ERC localized ERK1/2 and nuclear pERK1/2 levels; inversely expression of a catalytically inactive PI4KIIIβ decreased these events (119, 123). This work demonstrates a role for PI4KIIIβ and NCS-1 in endosomal recycling and signal transduction.

Recently, a role for PI4KIIIβ in lysosomal sorting has also been revealed (124). Sridhar et al. found that a fraction of PI4KIIIβ is stably associated with lysosomes and that PI4KIIIβ depletion resulted in loss of lysosomal contents through the uncontrolled tubulation of lysosomal compartments (124). shRNA knockdown of PI4KIIIβ in NIH3T3 mouse fibroblast cells led to a decrease in protein secretion, as well as reduced levels of lysosomal membrane proteins and the formation of abnormally long tubules from lysosome-associated membrane protein-1 (LAMP-1) positive compartments (124). In fractionated control cells, PI4KIIIβ was detected in the small vesicular fraction enriched for clathrin and adaptor proteins, proteins involved in vesicular fission/fusion and motor proteins (124). Together,

these results suggest that PI4KIIIβ has a role in both vesicle formation and lysosomal cargo sorting (124). Expression of a catalytically inactive PI4KIIIβ cannot rescue the hypertubulation lysosomal phenotype, suggesting that the role of PI4KIIIβ in lysosomal structure and function is contingent on PI(4)P generation (124).

PI4KIIIβ is also responsible for regulating CERT-mediated transport of ceramide between the ER and the Golgi (125). Treatment of COS7 cells with Pik93, a PI4KIIIβ specific inhibitor, inhibits the transport of fluorescent ceramide analogues from the ER to the Golgi, which in turn inhibits sphingomyelin synthesis in the Golgi (125).

There are no mouse knockout models for PI4KIIIβ, however male flies null for the *Drosophila* PI4KIIIβ, *fwd*, are sterile, with defects in spermatocyte cytokinesis linked to secretory trafficking (126, 127). Fwd was shown to be required for tyrosine phosphorylation in the cleavage furrow and for normal organization of actin filaments in the constricting contractile ring in dividing spermatocytes (127). Polevoy et al. showed that Fwd is required for PI(4)P synthesis at the Golgi and for the formation of PI(4)P-containing secretory vesicles, which localize to the midzone of late-stage dividing *Drosophila* spermatocytes (126). Expression of a catalytically inactive Fwd was able to partially restore fertility to *fwd* mutant flies, suggesting that Fwd regulates cytokinesis, in part, independently of its kinase activity (126). Rab11, a small GTPase, was shown to interact with Fwd, at the Golgi and at the midzone of dividing cells, independently of its kinase function, and was found to act downstream of Fwd in regulating cytokinesis (126). This work demonstrates that PI4KIIIβ has a conserved role in the regulation of cellular trafficking events.

The yeast ortholog of PI4KIIIβ, Pik1, is an essential gene (128). Temperature sensitive Pik1 strains display defects in Golgi morphology and secretion, as well as a defect

in the polarization of the actin cytoskeleton and are often multinucleated suggesting a defect in cytokinesis (111, 129). Pik1 localizes to the Golgi and the nucleus, and has essential roles in both (130). Using Pik1 mutants that exclusively localize to either the cytoplasm or the nucleus, Strahl et al. showed that neither mutant can rescue Pik1Δ spore viability on their own, suggesting that discrete pools of PI(4)P are required for nuclear function and Golgi secretion (130). Pik1 localization at the Golgi is mediated by its interaction with the yeast ortholog of NCS-1, Frq1 (131). Pik1 and Arf1 do not physically interact in yeast cells, however Pik1 has a genetic interaction with Arf1 and binds Sec7, the GEF that activates Arf1, suggesting that they localize to common areas and function in a similar pathway in yeast cells (129, 132). Though both Pik1 and PI4KIIIβ have been reported localized to the nucleus, the role of nuclear PI4KIIIβ remains unknown (112, 130).

A number of phosphorylation sites have been mapped to PI4KIIIβ (133). Hausser et al. demonstrated that, at the Golgi, protein kinase D (PKD) phosphorylates PI4KIIIβ at Ser294, increasing the lipid kinase activity of the enzyme and enhancing protein transport from the TGN to the plasma membrane (134). 14-3-3 proteins bind PI4KIIIβ when phosphorylated at Ser294, protecting it from dephosphorylation at this residue and therefore maintaining activation of the lipid kinase via phosphorylation at Ser294 (135). PI4KIIIβ has also been shown to localize to nuclear speckles when phosphorylated at Ser496 and Thr504 (136). Therefore both activation and localization of PI4KIIIβ can be regulated by phosphorylation states.

1.8 Rab11

PI4KIIIβ is itself required for recruitment of the small GTPase Rab11 to the TGN (137). Rab11 is a member of the Ras superfamily of GTPases (138). All GTPases are

molecular switches, cycling between active GTP and inactive GDP states and serve as scaffolds, integrating membrane trafficking and signalling, both temporally and spatially (139). Among the over 60 human Rab and Rab-like proteins identified, 36 have been attributed defined cellular functions (140). Rab11 localizes to the TGN, early endosomes and recycling endosomes and plays a key role in slow endosomal recycling and post-Golgi trafficking (141-143). Rab11 has also been shown to regulate exocytosis of recycling vesicles at the plasma membrane (144).

The interaction between PI4KIIIβ and Rab11 regulates transport from the Golgi to the plasma membrane (137). PI4KIIIβ specifically interacts with the active GTP-bound form of Rab11 but this interaction is not dependent on the kinase activity of PI4KIIIβ, as a kinase-dead PI4KIIIβ mutant and the wild type protein bind Rab11 with the same affinity (137). Likewise, in *Drosophila*, Fwd interacts with Rab11, independently of its kinase activity and regulates Rab11 localization during cytokinesis (126). Rab11 was shown to function downstream of Fwd, as overexpression of Rab11 can partially suppress the cytokinesis defect in in *fwd* mutant male fly spermatocytes (126). Therefore, there is a conserved role for Rab11 as a downstream effector of PI4KIIIβ in the regulation of cell trafficking.

Of interest to my work, Rab11 has also been shown to mediate G-protein-coupled receptor (GPCR) signalling dependent PI3K/Akt activation on recycling endosomes (Fig. 1.7) (145). More specifically, in HEK-293T, human embryonic kidney cells, lysophosphatic acid (LPA) stimulates GPCR activation, leading to the dissociation of Gβγ, which then interacts with Rab11 on early and recycling endosomes, leading to the recruitment of PI3Kγ and the activation of Akt at these endosomal compartments (145).

Figure 1.7: Model depicting the role of Rab11 in Akt activation.

GPCR activation induces the dissociation of heterotrimeric G proteins into Gα and Gβγ subunits. The liberated Gβγ heterodimer activates its effectors such as PI3Kγ at the plasma membrane, leading to the activation of Akt (1). Gβγ also interacts with Rab11a, promoting Gβγ trafficking to early and slowly recycling endosomes (as defined by presence of Rab11a) (2). The assembly of a signalling complex occurs at endosomes after recruitment of PI3Kγ followed by activation of Akt (steps 3 and 4). A fraction of Akt is associated with this endosomal fraction even in nonstimulated cells, but the association of this protein is further increased in response to receptor stimulation leading to the phosphorylation of endosomal Akt (5). To complete the cycle Gβγ is recycled to the plasma membrane to start a new cycle of signalling. Adapted from (145).

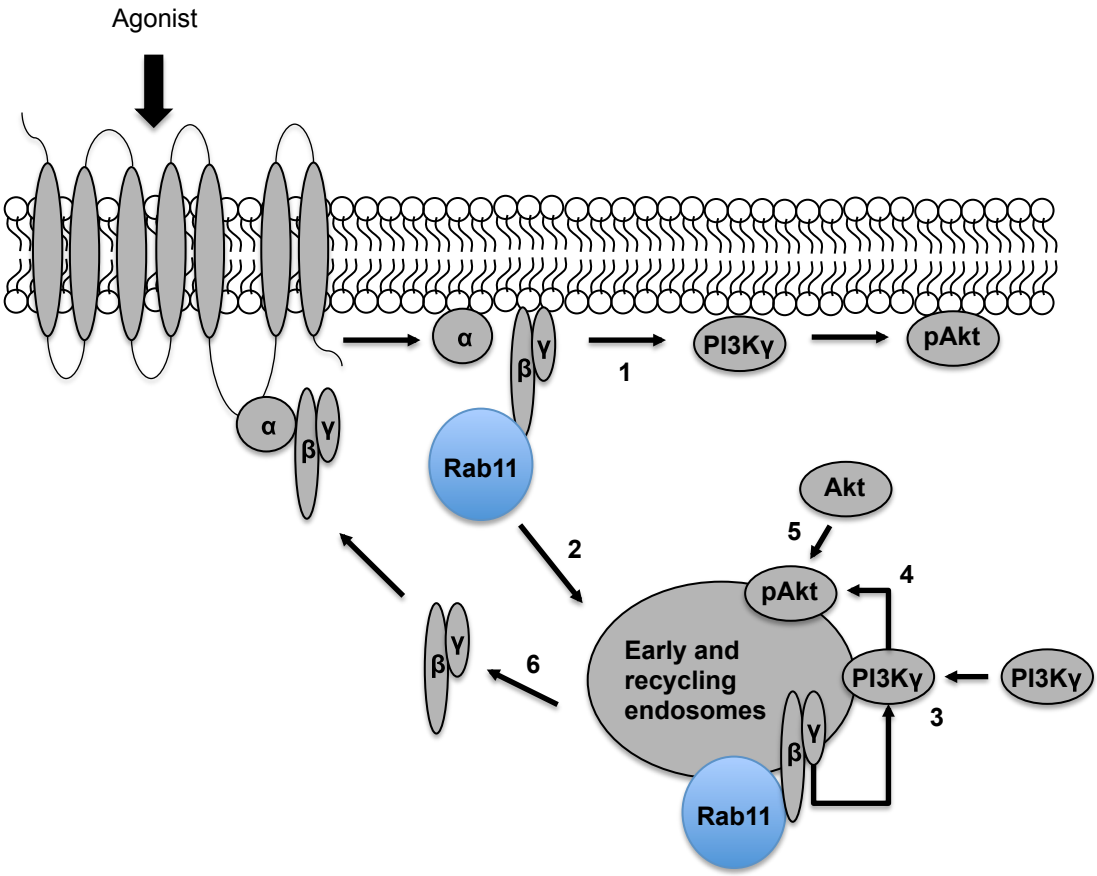
Agonist
α
β
γ
1
PI3Kγ
pAkt
Rab11
2
Akt
5
pAkt
4
Early and
recycling
endosomes
PI3Kγ
PI3Kγ
3
6
β
γ
Rab11

1.9 eEF1A2: An Oncogenic PI4KIIIβ Interacting Protein

PI4KIIIβ has also been identified as a binding partner of the eukaryotic elongation factor 1 alpha 2 (eEF1A2). eEF1A2 directly binds to and activates PI4KIIIβ. The two proteins interact with a 1:1 stoichiometry and this interaction doubles the enzyme's maximum velocity *in vitro* (146). Ectopic expressing of eEF1A2 leads to an increase in overall cellular PI(4)P and PI(4,5)P_2 lipid abundance, with PI4KIIIβ required for eEF1A2-mediated PI(4,5)P_2 accumulation at the plasma membrane (146, 147).

eEF1A2 is one of two isoforms of eEF1A, GTP hydrolysing enzymes that bind amino-acylated tRNA and recruit it to the ribosome during the elongation phase of protein synthesis in eukaryotic cells (148). In its GTP-bound form, eEF1A2 brings amino-acylated tRNA to the A-site of the ribosome, where it is then hydrolysed and eEF1A-GDP is released (149). The two eEF1A isoforms share > 90% sequence homology and perform the same function during protein translation (150). However, the two proteins differ in their tissue-specific expression patterns: eEF1A1 is expressed ubiquitously, whereas eEF1A2 is normally only expressed in the heart, brain and skeletal muscle (150).

The best characterized function of eEF1A is in protein translation, however a number of non-canonical roles have been attributed to the protein. First, eEF1A interacts with the cytoskeleton. eEF1A has been shown to bind microtubules in a calcium/calmodulin dependent manner (151, 152). In a co-precipitation assay in whole cell extracts, eEF1A and actin were also shown to interact in a 1:2 molar ratio, with the binding of actin and amino-acylated tRNA being mutually exclusive (153, 154). It has been shown that eEF1A regulates

the cytoskeleton by stabilizing microtubules and binding and bundling actin (152, 154). In addition, eEF1A is a cytoplasmic mediator of nuclear protein export (155). Finally, eEF1A2 has a particular anti-apoptotic role: eEF1A2 protects cells against programmed cell death during oxidative stress-induced, growth factor withdrawal-induced and ER stress induced apoptosis (156, 157).

1.10 eEF1A2 and Cancer

Outside of its role in protein translation, eEF1A2 has also been identified as a breast, ovarian and lung cancer oncogene. The human eEF1A2 gene, *EEF1A2*, maps to 20q13.3, which is genetically amplified in breast, ovarian and lung cancers (158-160). In addition, eEF1A2 is overexpressed in ~ 60% of breast tumours, ~ 30% of ovarian tumours and 28% of lung tumours (161-164). eEF1A2 expression was found to be independent of HER-2 and estrogen receptor expression in a study of 345 breast tumour samples (163). Interestingly, eEF1A2 expression predicts increased survival probability in breast and ovarian cancer patients (161, 163). Though the study of eEF1A2 as an oncogene has been most extensively done in the context of breast, ovarian and lung cancer, aberrant eEF1A2 expression has also been reported for a number of other cancers, including pancreatic, hepatocellular, colon and kidney carcinomas, as well as multiple myelomas (157, 165-167).

eEF1A2 displays transforming properties associated with oncogenes. Rodent fibroblast cells expressing eEF1A2 are able to form foci, grow as colonies in soft agar and proliferate at an increased rate (162). In addition, eEF1A2 expression is sufficient to induce *in vivo* tumorigenicity, as eEF1A2-expressing NIH 3T3 cells grow as tumours in nude mice (162). Ectopic expression of eEF1A2 in human ovarian adenocarcinoma cells enhances their *in vitro* proliferative capacity and ability to form tumour-like spheroids in hanging drop

culture (161). eEF1A2 expression also stimulates actin remodelling, leading to increased filopodia formation in rodent fibroblast and breast cancer cells and enhancing breast cancer cell migration and invasion (168). Previous work has shown that PI4KIIIβ is required for eEF1A2-induced filopodia formation (147). Finally, eEF1A2 expression leads to the activation of the PI3K/Akt signalling pathway (157, 168).

1.11 PI4K and Cancer

Recently a role for PI4Ks has been emerging in cancer. PI4KIIα expression is upregulated in a number of cancers, with particularly high expression reported in breast, and thyroid cancers, as well as in fibrosarcomas, malignant melanomoas and bladder transitional cell carcinomas (169). PI4KIIα was found to regulate tumour growth by promoting tumour angiogenesis through increased accumulation of hypoxia-induced factor-1 α (HIF-1α) and as a result leading to increased production of vascular endothelial growth factor (VEGF) (169). This increase in PI4KIIα mediated HIF-1α accumulation is dependent on human epidermal growth factor receptor 2 (HER2), PI3K and extracellular signal-regulated protein kinase (ERK) signalling cascades (169).

PI4KIIβ has been shown to have an anti-metastatic role in hepatocellelular carcinoma (170). PI4KIIα interacts with the transmembrane protein tetraspanin CD81, which leads to the formation of CD81 enriched vesicles (170). These vesicles sequester α-actinin-4, an actin binding and bundling protein, from the plasma membrane, leading to remodelling of the actin cytoskeleton and ultimately inhibiting cell migration (170, 171). PI4KIIIα has been found highly expressed in a highly invasive and metastatic pancreatic ductal carcinoma cell line as compared to a weakly invasive and metastatic one (172). PI4KIIIα was also identified as being important for resistance to the chemotherapeutic agent gemcitabine in a pancreatic

adenocarcinoma cell line (173). In addition, PI4KIIIα was identified as a mediator of cisplatin chemoresistance in medulloblastoma cell lines (174). The research to date suggests that PI4KIIIα likely has a role in pancreatic cancer and more widely in chemoresistance.

1.12 PI4KIIIβ and Breast Cancer

PI4KIIIβ appears to have a particularly important role in breast cancer. The 1q21 chromosomal locus encoding PI4KIIIβ has been reported highly amplified in subset of breast tumours (175-177). A recent study found that PI4KIIIβ was genetically amplified in a large-scale transcriptional analysis of 2000 breast tumours, positing PI4KIIIβ as a putative breast cancer driver (178). At a functional level, PI4KIIIβ ectopic expression disrupts the three dimensional *in vitro* acinar morphogenesis of breast epithelial cells, leading to the formation of a multi-acinar structure, a morphological phenotype of oncogene expression (179). In addition, PI4KIIIβ expression appears to have an anti-apoptotic role in MDA-MB-231 breast cancer cells (180). Together with the observation that PI4KIIIβ is downstream of the eEF1A2 oncoprotein (146), which is upregulated in breast cancer (163), it is likely that PI4KIIIβ is mechanistically involved in breast cancer oncogenesis.

1.13 Breast Cancer

According to the Canadian Cancer Society, breast cancer is the most commonly diagnosed cancer and the second leading cause of cancer death in Canadian women (181). The organization estimates that 23 400 Canadian women were diagnosed with breast cancer in 2011 (181). Though advancements in early detection and improved treatment options have led to steadily decreasing mortality rates associated with breast cancer, an estimated 5 100 deaths of Canadian women were attributed to breast cancer in 2011 (181).

Breast cancer is a heterogeneous disease. It encompasses neoplasms that originate from breast tissue, either from epithelial cells from the inner lining of milk ducts or the lobules that supply the ducts with milk (182). Breast tumours can be confined to a primary site, spread to regional lymph nodes or metastasize, invading distant sites from the breast (183). Invasive ductal and lobular carcinomas account for 90% of all breast tumours (184), with metastasis being the primary cause of death for breast cancer patients (185). Breast tumours can be broadly classified into three major subtypes with distinct morphological features and clinical behaviours: luminal, HER2 positive ($HER2^+$) and basal-like. Luminal tumours, which form the major breast tumour subtype, tend to be positive for the estrogen and/or progesterone hormone receptors and for the most part respond well to hormonal interventions (186, 187). $HER2^+$ tumours have amplification and overexpression of the ERBB2/HER2 oncogene and can be effectively treated with anti-HER2 therapies (186, 187). Finally, basal-like tumours in general lack hormone receptors and HER2 expression and are therefore also often classified as triple-negative breast cancers (186). There is currently no single molecular based therapy that is effective for the treatment of triple-negative breast cancer and only 20% of this breast tumour subtype respond well to conventional chemotherapeutic treatment (186). There is a high degree of diversity within each tumour subtype and in addition, there are frequently differences in tumorigenic traits, such as angiogenic, invasive and metastatic potential, between cells within a given tumour (186). This coupled to the fact that the particular microenvironment surrounding a tumour has an impact on its development (188), demonstrates how varied breast tumour progression and therapeutic responses can be. Understanding the multiple molecular mechanisms of breast cancer development is key for the advancement of personalized medicine (189). Coupled with the advances in high-throughput genomic, transcriptomic and proteomic technologies,

this would ideally allow for the development of individualized treatment plans for breast cancer patients.

1.14 Regulation of the Actin Cytoskeleton in Cancer Cell Migration

My project focuses, in part, on the role of PI4KIIIβ in the process of actin remodelling and cell migration. Cancer cell migration and invasion allow neoplastic cells to invade tissue barriers, disseminate into circulation and metastasize to distant organs (190). Cell migration involves multiple steps and the formation of different actin filament structures that contribute to altering the cell's shape (Fig. 1.8). Firstly, a moving cell becomes polarized and actin protrusions are extended in the desired direction of movement; secondly, the cell anchors itself to the ECM through focal adhesions; finally contraction of actin stress fibres, followed by disassembly of focal adhesions at the rear, allow the cell to move forward (191). Cell migration is initiated by the formation of protrusive actin structures, which include: lamellipodia, filopodia and invadopodia (190). Filopodia and lamellipodia are both found at the leading edge of a migrating cell and together promote directed cell migration (192). Lamellipodia are broad, sheet-like membrane protrusions formed by branched actin filaments (193, 194). Filopodia are thin, finger-like membrane protrusions comprised of tight parallel bundles of filamentous actin (192, 195). Invadopodia are ventral membrane projections that perform proteolytic ECM degradation and have a filopodia-like morphology (193, 196). My work will look specifically at filopodia formation as an important component of cell migration.

1.14.1 Mechanism of Filopodia Formation

There are two forms of actin in the cell: globular actin (G-actin) and filamentous actin (F-

Figure 1.8: Cell migration is dependent on different actin filament structures.

Directed cell migration involves a multi-step process. **(i)** Motility is initiated by an actin-dependent protrusion of the leading edge, which is composed of lamellipodia and filopodia. These protrusive structures contain actin filaments, with barbed ends oriented towards the plasma membrane. **(ii)** During cellular extension, new adhesions with the substratum are formed under the leading edge. **(iii)** Next, the nucleus and the cell body are translocated forward through actomysin-based contraction forces that might be mediated by focal adhesion-linked stress fibres, which also mediate the attachment to the substratum**. (iv)** Then, retraction fibres pull the rear of the cell forward, adhesions at the rear of the cell dissassemble and the trailing edge retracts. Adapted from (192).

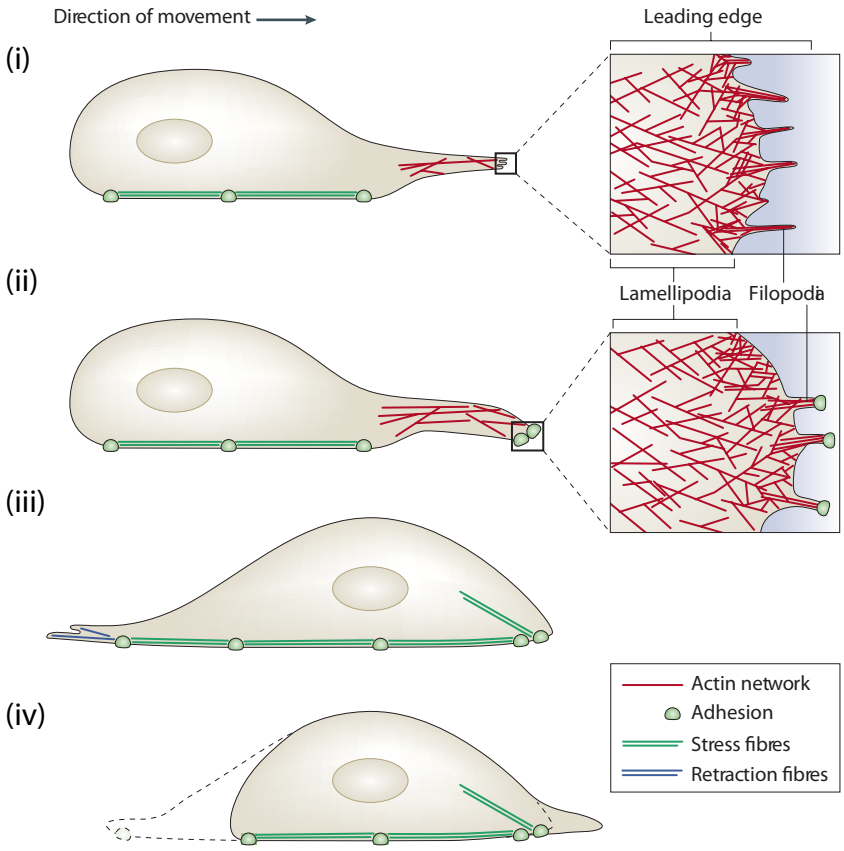
Direction of movement
Leading edge
(i)
(ii)
Lamellipodia
Filopodia
(iii)
(iv)
Actin network
Adhesion
Stress fibres
Retraction fibres

actin). G-actin are monomeric actin units, whereas F-actin is composed of actin monomers assembled into polar helical filaments (197). Parallel bundled F-actin filaments are the primary constituents of filopodia (192). Filopodial actin filaments are polar structures with a rapidly growing filament end, called the barbed end, which is pointed towards the membrane, and a slow growing end, called the pointed end (192). During actin filament polymerization, actin monomers bind to the barbed end at 10 times the rate of addition to the pointed end (198). Actin monomers bind to adenosine triphosphate/adenosine diphosphate (ATP/ADP) as well as divalent cations, such as calcium (Ca^{2+}) and magnesium (Mg^{2+}). These interactions stabilize the nucleotide-actin bound complex (199). Hydrolysis of the actin-bound ATP subsequently destabilizes the filament, resulting in dissociation of the actin subunits at the pointed end (200). This ATP-dependent polymerization at barbed ends and depolymerization at pointed ends leads to filament treadmilling (or turnover), which drives motility processes (200, 201).

Actin-binding proteins within the cell regulate the structure and dynamics of actin filaments. Actin sequestering, capping and severing (or depolymerizing) proteins all contribute to actin filament formation. Profilin is a small globular protein that acts as an ATP-actin sequestering protein in the absence of free filament ends, while promoting actin polymerization in the presence of free barbed ends (202-204). Capping proteins block the elongation of actin filament barbed ends (200). Gelsolin is both an actin filament capping and severing protein (205, 206). Cofilin promotes rapid actin filament disassembly by depolymerizing and severing actin filaments (207, 208).

The polymerization of new actin filaments requires actin nucleation, followed by barbed-end filament elongation (209). There are two major filopodial actin-nucleating

machineries. The first actin-nucleating process is directed by the Arp2/3 complex. Arp2/3 is a stable complex of seven subunits, which binds to the side of pre-existing filaments, where it nucleates new actin filament polymerization (192). Activation of the Arp2/3 complex is induced by WASP proteins (WASP and N-WASP), which are activated by the small Rho GTPase, Cdc42 (210). The second actin-nucleating process is directed by formins, large multidomain proteins that nucleate polymerization of unbranched actin filaments (192). The formin Dia2 has been shown to have an essential role in filopodia formation through knockout studies done in *Dictyostelium discoideum* (211). The formin homology-2 (FH2) domain initiates filament assembly and remains associated with the barbed end, protecting it from capping proteins, whereas the formin homology-1 (FH1) domain recruits profilin-G-actin complexes to the barbed end, allowing filament elongation (192). It is important to note that there is a third alternative mechanism that can stimulate filopodia formation, directed by Cdc42 independently of the WASP/Arp2/3 pathway (192). Cdc42 can bind to the insulin-receptor substrate p53 (IRSp53), which is an I-BAR domain-containing protein that allows it to bind to and deform lipid membranes (192). IRSp53 also binds to the WAVE2 protein complex and the EVA/VASP family protein MENA (212). WAVE2 is essential for lamellipodium formation and may also contribute to the generation of filopodia protrusions in concert with IRSp53 (213-215). ENA/VASP proteins localize to filopodia tips and protect them from capping (216, 217).

A current working model for filopodia formation describes the convergence of nucleated and elongating actin filaments within the lamellipodial network, and subsequent parallel bundling of these actin filaments, which lead to the formation of filopodia at the leading edge of a motile cell (Figure 1.9) (192). The known mechanisms of filopodia

Figure 1.9: A working model for filopodia formation.

A subset of uncapped actin filaments of the Arp2/3-nucleated dendritic network are targeted for continued elongation by the formin Dia2 and/or by ENA/VASP proteins. The barbed ends of these elongating actin filaments are brought together through the motor activity of Myosin-X, leading to the formation of a fillipodium. IRSp53 may further facilitate plasma membrane protrusions by directly deforming the membrane. The incorporation of the actin crosslinking protein fascin in the shaft of the fillopodium bundles the actin filaments. Adapted from (192).

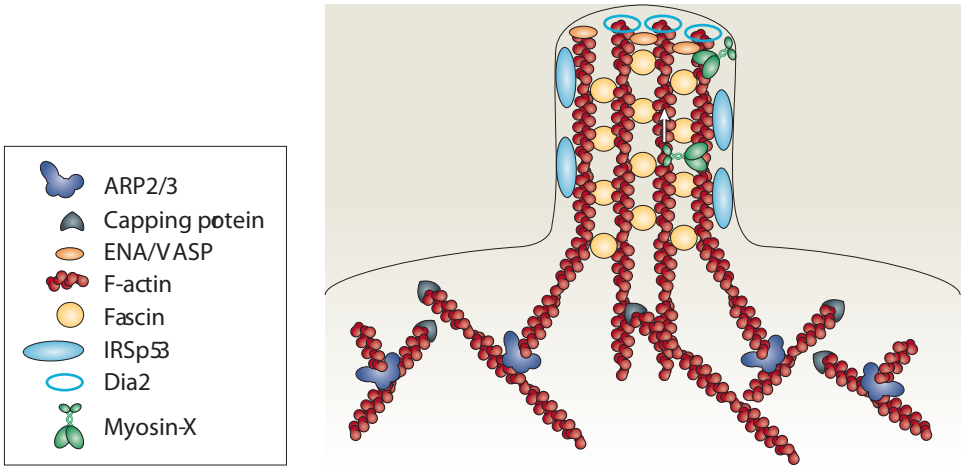
ARP2/3
Capping protein
ENA/VASP
F-actin
Fascin
IRSp53
Dia2
Myosin-X

nucleation and elongation have been covered above. Myosin-X, an actin-based motor protein is believed to play a role in the convergence of actin filaments, while also transporting filopodial components to the tips of growing filopodia (218, 219). Finally, fascin, an actin bundling protein, is responsible for crosslinking actin filaments as they polymerize, creating stiff and parallel actin bundles (220, 221).

1.14.2 The Role of Phosphoinositides in Actin Dynamics and Cell Migration

Phosphoinositides play an important role in regulating actin cytoskeleton dynamics. $PI(4,5)P_2$ interacts with and regulates the function of several actin-binding proteins that control actin filament polymerization (Fig. 1.10). $PI(4,5)P_2$, in concert with Cdc42, activates WASP and N-WASP proteins, relieving them from an auto-inhibitory state, which induces Arp2/3 complex-dependent actin filament nucleation (222). In addition, $PI(4,5)P_2$ binds to gelsolin and cofilin inhibiting their ability to cap and sever actin filaments, respectively (200). Moreover, $PI(4,5)P_2$ can interact with profilin, disrupting the protein's ability to sequester actin monomers within the cell, further facilitating actin filament assembly (200). Finally, the presence of negatively charged $PI(4,5)P_2$ lipids may itself contribute to promoting membrane curvature, by recruiting I-BAR domain containing proteins which deform $PI(4,5)P_2$-riche membranes into tubular structures, facilitating the formation of filopodial membrane protrusions (223, 224). $PI(3,4,5)P_3$ also regulates actin polymerization. Along with prenylated Rac-GTP, $PI(3,4,5)P_3$ binds to the WAVE2 protein complex, which activates actin nucleation (225-228). In addition, $PI(3,4,5)P_3$ binds and activates Rac GEFs, allowing exchange of Rac from a GDP- to a GTP-bound state, which has been shown to induce actin filament assembly (214, 229). Moreover, $PI(3,4,5)P_3$ has been found to bind to myosin-X and is required for myosin-X localization to filopodia tips (230). Using mutant

Figure 1.10: Regulation of actin filament assembly by PI(4,5)P_2.

PI(4,5)P_2 interacts with and regulates the function of a number of actin-binding proteins that impact actin filament assembly. **A.** The activity of WASP family proteins is enhanced by PI(4,5)P2, promoting Arp2/3-mediated actin filament assembly. **B.** Filament barbed end capping proteins, such as gelsolin are inhibited by PI(4,5)P_2. **C.** Actin filament disassembly is diminished through inhibition of ADF/cofilin by PI(4,5)P_2. **D.** Actin monomer sequestering is diminished through inhibition of profilin by PI(4,5)P_2. Adapted from (200).

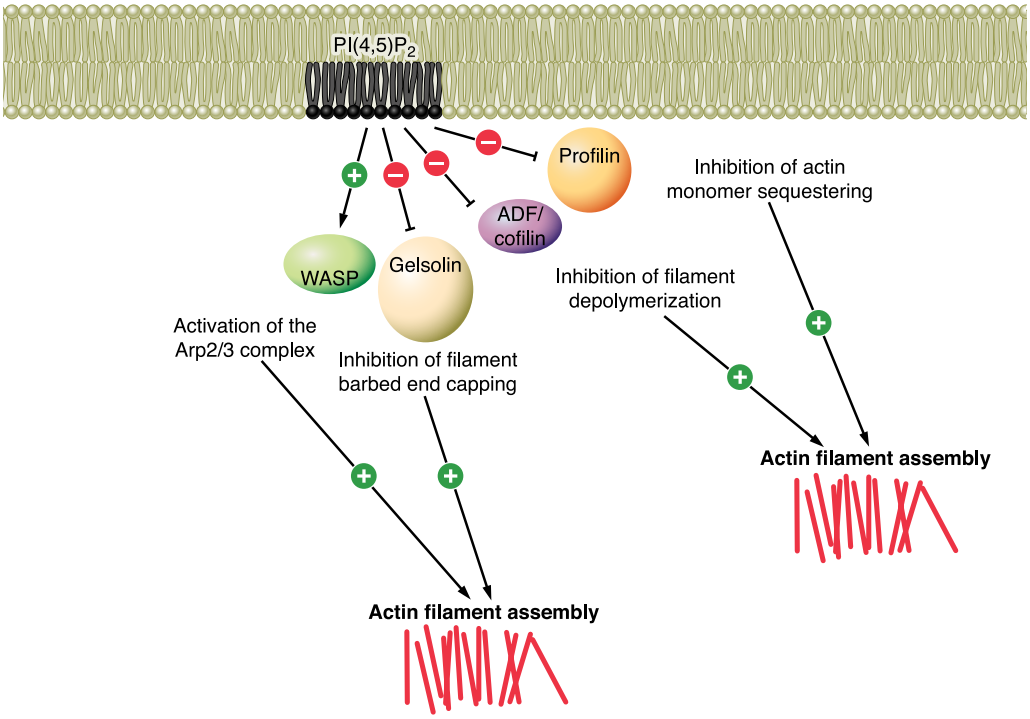
PI(4,5)P2
Profilin
ADF/
cofilin
WASP
Gelsolin
Activation of the
Arp2/3 complex
Inhibition of filament
barbed end capping
Inhibition of actin
monomer sequestering
Inhibition of filament
depolymerization
Actin filament assembly
Actin filament assembly

constructs, Plantard et al. were also able to show that expression of myosin-X induces filopodia formation only when able to bind $PI(3,4,5)P_3$ (230). Recent work has also revealed that $PI(3,4)P_2$ has a role in the regulation of invadopodia assembly (231). Lastly, $PI(4,5)P_2$ and $PI(3,4,5)P_3$ are crucial determinants of cell polarity during cell migration (232-234). Though phosphoinositide lipids are involved in the regulation of filopodial dynamics and cell migration through multiple mechanisms, a role for PI4Ks in filopodia formation and cell migration remains largely unknown.

1.14.3 The Role of Filopodia in Cancer

Abundant filopodia are a characteristic of invasive cancer cells (235). Moreover, several proteins implicated in filopodia formation have been linked to cancer progression and invasion. Firstly, expression of Arp2/3, WASP and WAVE actin-nucleating complex proteins has been reported upregulated in a number of cancers, including breast, lung and colorectal (236-241). Notably, co-expression of Arp2 and WAVE2 predicts poor outcome in invasive breast carcinoma (241). Secondly, expression of the actin-bundling protein fascin has been found upregulated in a number of carcinomas (242). High expression of fascin is linked to an increased risk of invasion and appears to contribute to a more aggressive clinical course of cancer (243-247). Fascin expression has also been shown to stimulate cell migration *in vitro* (248). Finally, formins, activators of actin filament assembly, are also overexpressed in a number of cancers including T-cell lymphomas and colorectal cancer (242). The human diaphanous homologue 1 (DIAPH1) formin, in particular, was shown to be required for invadopodia formation in motile breast tumour cells (249). Understanding the multiple mechanisms of filopodia formation is therefore critical to understanding the

metastatic progression of cancer. In addition, uncovering the molecular determinants of filopodia formation offers potential therapeutic targets for invasive cancer treatment.

1.15 PI3K/Akt Signalling in Cancer

My project will also focus on the role of PI4KIIIβ in the activation of Akt signalling. Akt, a serine/threonine kinase, is a central regulator of multiple biological processes, including cell survival, proliferation, growth and migration, which when deregulated promote neoplastic transformation (250, 251). Akt recognizes and phosphorylates the consensus sequence RXRXX(S/T) when surrounded by hydrophobic residues (252). Numerous Akt targets have been identified within the cell. Akt target effectors include BAD, a pro-apoptotic member of the BCL2 family of cell death inducing proteins, whose ability to form a non-functional hetero-dimer with the survival factor BCL-XL is inhibited when phosphorylated by Akt (253). Akt also directly phosphorylates glycogen synthase kinase-3β (GSK3β), blocking its kinase activity and impeding its ability to phosphorylate Cyclin D1, for proteosomal degradation, thereby allowing Cyclin D1 to accumulate and promoting cell proliferation (254). Another target of Akt phosphorylation is the tumour sclerosis protein 2 (TSC2), which regulates cell growth via the mTORC1 signalling pathway (255). Akt phosphorylation of TSC2 inactivates the inhibitory TSC1/2 complex, allowing activation of the raptor protein containing mTORC1 (256). mTORC1 positively regulates protein synthesis by phosphorylating the eukaryotic initiation factor 4E (eIF4E)-binding protein 1 (4E-BP1) and the p70 ribosomal S6 kinase 1 (S6K1) (255). 4E-BP1 phosphorylation prevents its binding to eIF4E, allowing it to promote cap-dependent translation (257). Phosphorylation of S6K1 increases mRNA biogenesis, cap-dependent translation and elongation and translation of ribosomal proteins (258). Finally, Akt signalling can impact the

migratory and invasive properties of a cell. Akt regulates the conversion of epithelial cells into mesenchymal cells through the epithelial to mesenchymal transition (EMT), a process required for embryogenesis, tissue repair and carcinoma progression (259). Akt induces EMT through induction of Snail expression via Akt-mediated nuclear factor-kappaB (NF-kB) activation (260).

1.15.1 Akt Activation is Regulated by PI(3,4,5)P_3/ PI(3,4)P_2

Akt activity is itself regulated by PI(3,4,5)P_3/ PI(3,4)P_2 abundance at the plasma membrane (Fig. 1.11). PI(3,4,5)P_3/ PI(3,4)P_2 lipids are able to direct the recruitment of Akt to the plasma membrane through interaction with the kinase's PH domain; it is at the plasma membrane that Akt activation via phosphorylation is initiated (62). PI(3,4,5)P_3 phospholipids are generated at the plasma membrane by class I PI3K-mediated phosphorylation of PI(4,5)P_2 (26). PI(3,4)P_2 is then produced by SHIP1/2 dephosphorylation of PI(3,4,5)P_3 (26). Class I PI3Ks are comprised of a catalytic and a regulatory subunit. The regulatory subunit is activated by interaction with membrane receptors, which relieve its inhibition of the catalytic subunit, allowing active PI3K to be recruited to the plasma membrane. Class IA catalytic subunits (p110α/β/δ), paired with one of five regulatory subunits (p85α/β, p55α/γ, p50α), are activated by receptor tyrosine kinases, whereas the class IB p110γ catalytic subunit, which binds either a p101, p87 or p84 catalytic subunit, is activated by GPCRs (26, 261). The production of PI(3,4,5)P_3/PI(3,4)P_2 lipids then leads to the translocation of Akt to the plasma membrane via the protein's PH domain (61, 62). Akt is then activated by PDK1 phosphorylation at Thr308, within the catalytic domain's activation loop, and Ser473 phosphorylation by the rapamycin-insensitive mTORC2 complex, within the C-terminal hydrophobic domain (262-264). Phosphorylation at these two sites restructures the enzyme

Figure 1.11: Akt activation is regulated by $PI(3,4,5)P_3$/$PI(3,4)P_2$.

Akt signalling is initiated by receptor tyrosine kinase (RTK) activation by growth factors. (GF). This leads to the activation of PI3K, which converts $PI(4,5)P_2$ into $PI(3,4,5)P_3$. $PI(3,4,5)P_3$ can subsequently be dephosphorylated, at the D5 position, by SHIP1/2 to generate $PI(3,4)P_2$. $PI(3,4,5)P_3$ and $PI(3,4)P_2$ are responsible for the recruitment of Akt to the plasma membrane where it is activated by phosphorylation at Thr308 by PDK1 and at Ser473 by mTORC2. PDK1 recruitment to the plasma membrane is also directed by $PI(3,4,5)P_3$ and $PI(3,4)P_2$. Once active, Akt can phosphorylate a multitude of downstream targets, which together promote cell growth, proliferation, survival and invasion. Akt signalling can be shut off through $PI(3,4,5)P_3$ and $PI(3,4)P_2$ hydrolysis by PTEN and INPP4B, respectively.

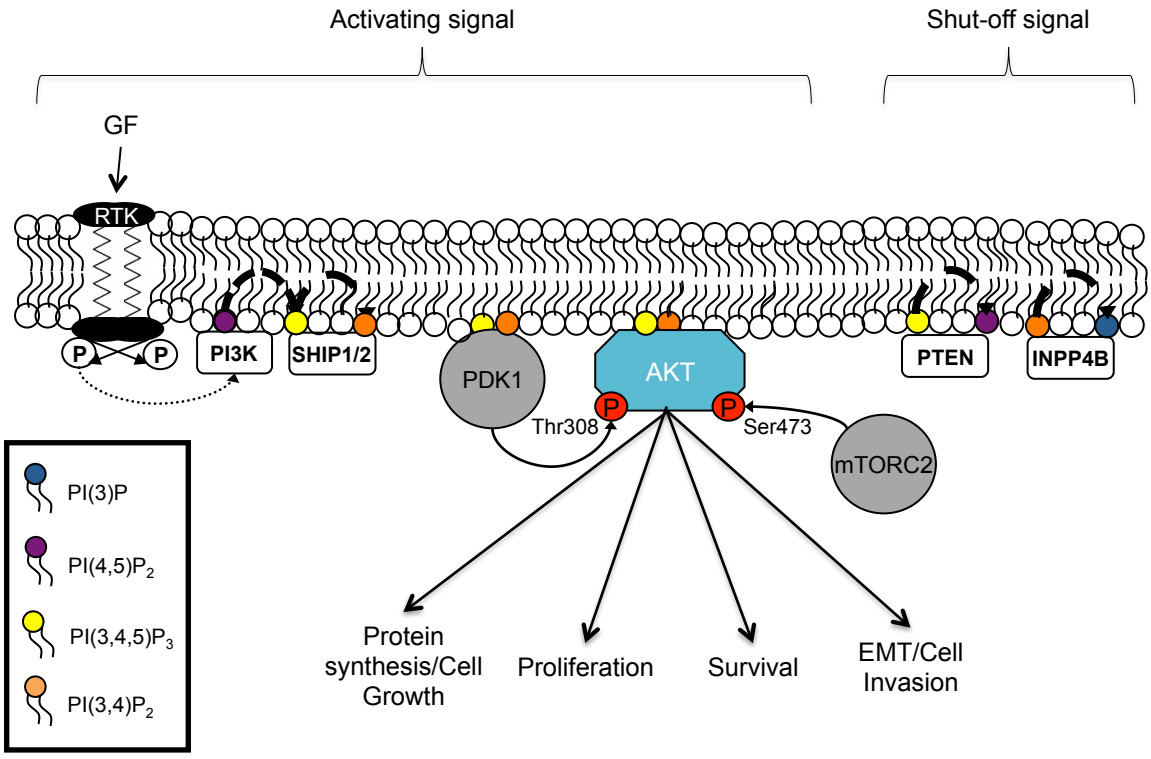
Activating signal
Shut-off signal
GF
RTK
P
P
PI3K
SHIP1/2
PDK1
AKT
P
P
Thr308
Ser473
mTORC2
PTEN
INPP4B
PI(3)P
PI(4,5)P2
PI(3,4,5)P3
PI(3,4)P2
Protein synthesis/Cell Growth
Proliferation
Survival
EMT/Cell Invasion

into its fully active conformation (265). It has been proposed that the Akt PH domain covers Thr308 and Ser473 and interaction of the PH domain with $PI(3,4,5)P_3$ (and presumably $PI(3,4)P_2$) exposes these sites to phosphorylation (266). Once fully active, Akt can phosphorylate its numerous downstream targets.

1.15.2 Akt Isoforms

There are three highly homologous Akt isoforms: Akt1, Akt2 and Akt3. The Thr308 and Ser473 activating phosphorylation sites are conserved across all three isoforms (267, 268). The study of isoform-specific knockout mice suggests that the three Akt isoforms regulate distinct cellular functions. Akt1-null cells display higher rates of apoptosis, indicating a critical role for Akt1 in cell survival (269). Akt2-null mice develop a type 2 diabetes-like phenotype, suggesting a specific role for Akt2 in glucose homeostasis (270). Akt3 knockout mice display a reduction in brain mass, pointing to a specific role for Akt3 in brain development (271). However, there is likely overlap of Akt isoform function as well, as Akt isoform double knockouts cause lethality in mouse models, whereas the single knockouts are viable (194, 272). It has been hypothesized that Akt isoforms regulate distinct cellular processes through: (1) distinct tissue distribution; (2) differential activation by extracellular stimuli; (3) distinct intrinsic catalytic activity; and (4) cell context specific subcellular factors that confer substrate specificity (273). All three Akt isoforms are expressed in normal breast tissue (274). However, differential Akt isoform genetic amplification, expression and kinase activity have been detected in breast tumours: Akt2 has been detected genetically amplified; and both Akt1 and Akt2 expression levels and activity have been reported elevated (275-278).

1.15.3 Akt Signalling in Cancer

Akt is an important regulator of oncogenesis. Expression of constitutively activated Akt1 (myristolated so as to be constitutively bound to the membrane) transforms rodent fibroblast cells, allowing them to grow on soft agar and form tumours in nude mice (278). PI3K also has a central role in cancer, as an upstream regulator of Akt activity, via $PI(3,4,5)P_3$ production. A study of five different transgenic mouse models of malignant transformation found PI3K activity contributed to all the transformed phenotypes, and particularly to anchorage independent growth (279). The p110 catalytic subunit of PI3K has been reported genetically amplified in ovarian cancer (280). Furthermore, the gene encoding the p85 regulatory subunit of PI3K contains somatic mutations, which render PI3K constitutively active, in ovarian and colon tumours (281). PI3K expression (p85 regulatory subunit) and activity has also been specifically found increased in breast tumours (282, 283). The importance of PI3K-Akt signalling in cancer is also evidenced by studies done on PTEN, the phosphatase responsible for converting $PI(3,4,5)P_3$ back into $PI(4,5)P_2$ (284). Loss of PTEN expression or function is frequent in human cancers, due to gene deletion, inactivating or protein destabilizing mutations and protein transcriptional silencing (285-288). Enforced PTEN expression, in PTEN-null breast cancer cell lines, leads to a decrease in cell growth and induces apoptosis (289). The inositol polyphosphate 4-phosphatase type II (INPP4B), which hydrolyses $PI(3,4)P_2$, has also been identified as a tumour suppressor, illustrating the importance of $PI(3,4)P_2$, along with $PI(3,4,5)P_3$, in Akt activation (290). Loss of heterozygosity (LOH) at the INPP4B locus has been detected in a large proportion of basal-like breast cancers (290).

1.16 Research Hypothesis and Objectives

There are two parts to my thesis. In the first part, my aim is to assess the impact of enhanced PI4KIIIβ expression on the oncogenic processes of filopodia driven cell migration and cell proliferation in breast cancer cells. The second aim of my project is to investigate how PI4KIIIβ expression impacts Akt activation in breast cancer cells.

1.16.1 Aim 1: Assessing a role for PI4KIIIβ in breast oncogenesis

As the chromosomal locus encoding PI4KIIIβ has been reported highly amplified in breast cancers (175-177) and PI4KIIIβ was found genetically amplified in a large-scale transcriptional analysis of breast tumours (178), we wanted to assess whether PI4KIIIβ protein levels were increased in breast tumours. To this end, immunohistochemical staining of 169 commercially available breast tumour samples, composed of 160 invasive ductal carcinomas and 9 medullary carcinomas, was performed. The PI4KIIIβ expression levels in these were compared to 34 normal breast tissue samples immunostained in parallel. We found that PI4KIIIβ expression was increased in a subset of breast tumours. I then wanted to assess the impact of increased PI4KIIIβ expression in breast cancer, by studying its overexpression in the BT549 breast cancer cell line. The primary objective of this aim was to study the effect of increased PI4KIIIβ expression in BT549 breast cancer cells on filopodia production and cell migration, as well as on rates of cell proliferation.

Objective 1: As PI4KIIIβ expression is increased in a subset of primary human breast tumours, determine the impact of enhanced PI4KIIIβ expression on filopodia formation, cell migration and proliferation in the BT549 breast cancer cell line

In order to determine what role increased PI4KIIIβ may have in breast oncogenesis, several different parameters that are associated with malignancy were examined. Ectopic expression of the breast cancer oncogene eEF1A2 has been shown to induce filopodia formation and cell migration/invasion in breast cancer cells (146, 163, 164, 168). eEF1A2 expression also increases ovarian cancer cell proliferation (161). Work in our lab has identified that PI4KIIIβ physically interacts with eEF1A2, leading to direct activation of the enzyme's lipid kinase activity (146). *We therefore hypothesized that enhanced PI4KIIIβ expression would phenocopy the effects observed in cells aberrantly expressing eEF1A2.* To test this hypothesis, BT549 breast cancer cells, initially derived from an invasive ductal carcinoma, were engineered to stably ectopically express PI4KIIIβ. These BT549 cells overexpressing PI4KIIIβ were then studied for filopodia production, cell migration rates and proliferative capacity.

1.16.2 Aim 2: The role of PI4KIIIβ in Akt activation

Expression of the PI4KIIIβ-activator, eEF1A2, had also previously been shown to increase Akt activation (157, 168), leading me to investigate the role of PI4KIIIβ in Akt activation in a breast cancer cell model. This second aim had two main objectives: the first objective was to determine the impact of PI4KIIIβ expression on Akt activation; the second objective was to investigate the mechanism through which PI4KIIIβ was mediating activation of this oncogenic signalling pathway.

Objective 1: Determine the impact of PI4KIIIβ expression on Akt activation

BT549 cells overexpressing PI4KIIIβ were studied to determine if enhanced PI4KIIIβ expression led to increased Akt activation. In addition, BT549 parental cells were treated

with siRNA targeted to PI4KIIIβ, to determine a role for endogenous PI4KIIIβ in Akt activation.

Objective 2: Investigate the mechanism through which PI4KIIIβ activates Akt

PI4KIIIβ expression was found to regulate Akt activation, which led to the investigation of the mechanism through which this lipid kinase was contributing to Akt activation. *We hypothesized that PI4KIIIβ was regulating Akt activation either through increased PI(4)P production, generating more PI(3,4,5)P_3/PI(3,4)P_3 lipids downstream, or via a protein interaction*. Rab11 was a likely candidate interacting protein through which PI4KIIIβ could be impacting Akt signalling, as Rab11 had previously been shown to mediate Akt activation on endosomal membranes (145). Based on this hypothesis, the following three experimental goals were put forth to investigate how PI4KIIIβ expression was mediating Akt activation:

i. Examine the phosphoinositide signalling pathway potentially implicated in PI4KIIIβ-mediated Akt activation.

ii. Determine if PI4KIIIβ-mediated Akt activation is dependent on the enzyme's catalytic function.

iii. Determine the role of the PI4KIIIβ binding partner, Rab11, in PI4KIIIβ-mediated Akt activation.

1.17 Thesis Summary

In the second chapter of my thesis PI4KIIIβ is shown to be highly expressed in 18% of human primary breast tumours assayed. I find that elevated expression of PI4KIIIβ increases filopodia formation in BT549 breast cancer cells and in Rat2 rodent fibroblast

cells. This increase in filopodia production is not sufficient, however, to increase the migratory rate of breast cancer cells. Elevated expression of PI4KIIIβ does lead to an increase in the *in vitro* proliferative capacity of breast cancer cells. These results suggest that PI4KIIIβ is involved in breast oncogenesis, with a specific role in the process of cell proliferation.

In the third chapter of my thesis, I show that in the BT549 breast cancer cell line PI4KIIIβ expression regulates the activation of the pro-survival, growth and proliferation signalling protein, Akt. PI4KIIIβ activates Akt via PI3K, as elevated expression of PI4KIIIβ leads to an increase in PI(3,4,5)P_3/PI(3,4)P_2 lipids at the plasma membrane. However, no increases in PI(4)P or PI(4,5)P_2 lipids were detected. Furthermore, inhibition of PI4KIIIβ by the inhibitor Pik93 does not impede PI4KIIIβ-mediated Akt activation. In addition, ectopic expression of a catalytically inactive PI4KIIIβ also leads to an increase in Akt activation and plasma membrane levels of PI(3,4,5)P_3/PI(3,4)P_2. Together, this suggests that PI4KIIIβ expression activates Akt in a manner that is not dependent on its catalytic activity. I then verified, through immunoprecipitation and immunofluorescence that PI4KIIIβ and Rab11 were interacting in our cell system and found an enhanced interaction between the two proteins in the PI4KIIIβ-overexpressing BT549 cells. Furthermore, PI4KIIIβ and the recycling endosome marker, transferrin receptor, were found to co-localize to a greater extent in the PI4KIIIβ-overexpressing cells. This suggested that PI4KIIIβ and Rab11 are recruited to recycling endosomes in cells with increased PI4KIIIβ expression. Elevated PI4KIIIβ expression also led to a redistribution of Rab11 within the cell, shifting it from a primarily Golgi localization to a broader more punctate distribution within the cytoplasm. To investigate if the Rab11/PI4KIIIβ interaction was mediating Akt activation, I treated the

PI4KIIIβ-overexpressing cells with siRNA targeted to Rab11 and found that this led to a decrease in Akt activation. This suggests that PI4KIIIβ is working in concert with Rab11 to activate Akt, likely by altering intracellular trafficking.

CHAPTER 2: ENHANCED PI4KIIIB EXPRESSION IMPACTS THE ORGANIZATION OF THE ACTIN CYTOSKELETON AND THE PROLIFERATION OF BREAST CANCER CELLS*

* Modified versions of elements in this chapter have been published:

Nilufar, S., **Morrow, A.A.,** Jonathan, J.M. and Perkins, T.J. 2013. FiloDetect: Automatic detection of filopodia from fluorescence microscopy images. *BMC Syst Biol*. 7:66

Jeganathan, S., **Morrow, A.A.,** Amiri, A. and Lee, J.M. 2008. Elongation factor eEF1A2 cooperates with phosphatidylinositol-4 kinase IIIβ to stimulate PI(4,5)P_2 generation and filopodia production. *Mol. Cell. Biol.* 28:4549-61

2.1 Introduction

Membrane phosphoinositide lipids, the phosphorylated derivatives of phosphatidylinositol (PtdIns), and the kinases/phosphatases that regulate their generation play critical roles in cancer. They do so by controlling apoptotic and proliferative pathways and stimulating cell migration and cytoskeletal remodelling (232, 291-294). There has been an emerging role for PI 4-kinases (PI4K), that generate phosphatidylinositol 4-phosphate (PI(4)P) from PtdIns, in cancer (295). In particular, recent work points to a role for PI4KIIIβ, one of four mammalian PI4Ks, in breast cancer. Firstly, Curtis *et al* showed that *PI4KB*, the 1q21 gene encoding PI4KIIIβ, was frequently amplified in breast tumours (178). Based on a large-scale transcriptional analysis of 2000 tumours, the authors concluded that *PIK4B* is a novel breast cancer driver (178). Additionally, 1q21 has previously been reported highly amplified in breast cancers (175-177). At a functional level, we have shown that ectopic PI4KIIIβ expression disrupts *in vitro* three-dimensional acinar development of MCF10A breast epithelial cells (179). We have also identified PI4KIIIβ as a downstream effector of the eukaryotic elongation factor 1 alpha 2 (eEF1A2), a transforming gene that is amplified and highly expressed in 30-50% of breast, ovarian and lung tumours (146, 158, 162-164). Finally, PI4KIIIβ expression has also been shown to inhibit apoptosis in MDA-MB 231 cells (180). Taken together, these observations suggest a likely role for PI4KIIIβ in breast tumorigenesis.

Tumorigenesis is a multistep process reflecting the various genetic alterations that drive the progressive transformation of normal human cells into cancerous cells. Hanahan and Weinberg have classified six essential changes in cell physiology that collectively lead to malignant transformation: self-sufficiency in growth signals, insensitivity to growth

inhibitory signals, evasion of programmed cell death, limitless replicative potential, sustained angiogenesis and tissue invasion and metastasis (296). In short, cells acquire genetic alterations in proto-oncogenes and tumour suppressors that lead to enhanced cell proliferation and survival and ultimately tumour invasion and metastasis (297). Metastasis, the dissemination of cancer cells from the primary tumour to distant organs, is the major cause of cancer-related deaths (298).

We have previously identified PI4KIIIβ as a direct target of the breast, ovarian and lung cancer oncogene, eEF1A2 (146, 158, 162-164). The two proteins interact with 1:1 stoichiometry and eEF1A2 doubles the PI4KIIIβ V_{max} (146). Aberrant expression of the PI4KIIIβ activator, eEF1A2, has been linked to two hallmarks of malignant transformation: increased cell proliferation and enhanced migration. We have reported that eEF1A2 expression increases the proliferative capacity of ovarian cancer cells (161). We have also reported that eEF1A2 expression induces actin remodelling, increasing filopodia formation and stimulating breast cancer cell migration and invasion. (168). Furthermore, eEF1A2 has been reported to be overexpressed in metastatic rat mammary adenocarcinoma cell lines when compared to non-metastatic controls (299). We found that eEF1A2 expression stimulates the formation of filopodia in both transformed, BT549 breast cancer cells, as well in non-transformed, Rat2 rodent fibroblast cells (168). Filopodia are thin, finger-like cellular protrusions, comprised of tight parallel bundles of filamentous actin (192). These protrusions are found at the leading edge of motile cells and are used to sense the cell's microenvironment (192, 195). Filopodia have been shown to regulate cancer cell motility *in vitro*, and metastasis in *in vivo* mouse experiments (222, 300).

In this chapter, I seek to determine what impact enhanced expression of PI4KIIIβ has on breast cancer cells. More specifically I will determine if elevated expression of PI4KIIIβ is sufficient to impact breast cancer cell actin remodelling and migration, as well as proliferation.

We find that approximately 20% of primary human breast tumours show increased PI4KIIIβ protein expression relative to normal breast tissue. In addition, I show that elevated expression of PI4KIIIβ leads to actin cytoskeleton remodelling, specifically an increase in the production of filopodia in both breast cancer cells and non-transformed cells. This increase in filopodia is not, however, sufficient to impact breast cancer cell migration, suggesting that eEF1A2 expression likely impacts cell migration through additional mechanisms outside of its interaction with PI4KIIIβ. Increased expression of PI4KIIIβ does lead to increased breast cancer cell proliferation. Therefore, elevated PI4KIIIβ expression in breast cancer may play a more specific role in regulating cell replication and tumour growth.

2.2 Materials and Methods

Cell culture. The BT549 cell line was purchased from the American Tissue Culture Collection (ATCC, Manassas, VA, USA) and grown in RPMI medium 1640 (Life Technologies, Carlsbad, CA, USA) supplemented with 10% FBS (Life Technologies), 1 mM sodium pyruvate (Life Technologies), 10 nM HEPES buffer and 0.023 IU/ml insulin (from bovine pancreas, # I-5500; Sigma, Oakville, ON, Canada). The Rat2 cell line was obtained from the American Tissue Culture Collection (ATCC) and grown in DMEM supplemented with 10% FBS. BT549 and Rat2 cell lines stably expressing ectopic PI4KIIIβ were generated using a pLXSN retroviral system as previously described (301). Infected cells were selected in 0.4 mg/ml G418 (BioShop, Burlington, ON, Canada). All cell lines were cultured at 37°C in a humidified atmosphere with 5% CO_2.

Plasmids. Full-length human PI4KIIIβ (MGC-1921, Mammalian Genome Collection, ATCC) was cloned into the pLXSN retroviral vector in the EcoRI and XhoI sites. Nucleotides 1-3303 (RefSeq: NM_001198774.1) were included in pLXSN.

Immunohistochemistry. Tumour tissue microarrays (TMAs) were obtained from US Biomax (BC08013a, BC08023 and BC08032; Rockville, MD, USA) and staining was performed by Dr. Jonathan Lee. For TMA staining, the slide was sequentially deparaffinized (2x xylenes, 2x 100% ethanol, 1x 95% ethanol, 1x 70% ethanol, 1x water), boiled in 0.1 M sodium citrate (pH 6.0) for 10 min and then allowed to cool in the citrate buffer for 10 min. Slides were then rinsed twice in PBS/0.2 % Tween 20 and blocked in 10% FCS/1% BSA/PBS/0.2% Tween for 1 hr at room temperature in a humidified chamber. Slides were

then incubated overnight at 4°C with PI4KIIIβ antibody (BD Biosciences, Mississauga, ON, CA) diluted 1:150 in 1% BSA/PBS/0.2% Tween 20. The primary antibody was then removed by three rinses of 5 min each in PBS/0.2% Tween 20. Antibody staining was detected using biotinylated VECTASTAIN anti-mouse IgG antibody and alkaline phosphatase according to the manufacturer's instructions (Vector Laboratories, Burlington, ON, CA). Slides were counterstained using hematoxylin. Staining was visualized using a Zeiss Axio Imager.A1 microscope with images acquired using a Zeiss AxioCam MrRc5 camera and AxioVision 4.6 software (Zeiss, Toronto, ON, CA). Images were scored qualitatively as low, moderate or high depending on the intensity of the staining in the cytoplasm. Counting was performed in triplicate with discrepancies resolved by a fourth count. Statistical analysis was performed using GraphPad Prism 6.0 software.

Western blotting. Cells were lysed using radioimmunoprecipitation assay (RIPA) buffer (50 nM Tris-Cl; pH 7.4, 1% Triton X-100, 1% sodium dodecyl sulfate (SDS), 1 mM ethylenediaminetetraacetic acid (EDTA); pH 7.0, 150 mM NaCl) supplemented with protease and phosphatase inhibitor cocktail tablets (Roche Diagnostics, Mississauga, ON, CA). Protein concentrations were determined by Bradford protein assay (Bio-Rad, Hercules, CA, USA). SDS sample buffer was added to 10 μg of protein lysate, resolved by SDS-PAGE and transferred onto PVDF membrane (Millipore, Bellerica, MA, USA). PI4KIIIβ (1:10 000; BD Biosciences) and β-actin (1:20 000; Sigma, Oakville, ON, CA) antibodies were used according to the manufacturer's instructions.

Immunofluorescence. Immunostaining was performed on 1 x 10^5 cells plated in 6-well plates (Corning, Tewksbury, MA, USA) containing coverslips. 24 hr after plating, cells were fixed with 3.7%/PBS formaldehyde for 15 min, permeabilized with 0.1% Triton X-100/PBS for 10 min and blocked with 5% FBS/PBS for 1 hr. Cells were then incubated with Phalloidin 546 or 594 (1:200/PBS; Molecular Probes, Life Technologies, Carlsbad, CA, USA) for 1 hr. Slides were mounted using fluorescent mounting media (Dako, Burlington, ON, CA). Fixed cell images were acquired using an Olympus FluoView FV1000 laser scanning confocal microscope with an Olympus UPLSAPO 100X/1.40 oil objective (Richmond Hill, ON, Canada). Images were collected using Olympus software (FV100, version 01.04a). Filopodia were quantified in the Rat2 cell lines using the Olympus software. Filopodia were quantified in the BT549 cells using FiloDetect, an automated computational tool designed to detect, count and measure the length of filopodia in fluorescence microscopy images (302).

Scratch wound assay. Cells were suspended by trypsinization and diluted to 5 x 10^5 cells/ml. Silicone culture inserts (Ibidi, Minitube Canada, Ingersoll, ON, CA) were placed on 35 mm dishes (Ibidi). 80 µl of the cell suspension was seeded into each well and the outer area filled with complete growth media. Cells were allowed to adhere for 16-24 hr to reach confluence. Media around the inserts and culture-inserts were then gently removed and the plate replenished with growth media. The wound was then imaged using a Leica DM IRE phase contrast microscope using a HC PL APO CS 10X/0.40 objective hourly until wound closure (Leica Microsystems, Concord, ON, CA). Images were analyzed by calculating wound area over time normalized to initial wound area using the manual area calculation function on ImageJ (NIH).

Cell proliferation assay. Cell proliferation was measured using the CyQUANT cell proliferation assay as per the manufacturer's instructions (Molecular Probes, Life Technologies). Briefly, 2000 cells were initially plated per well in 96 well plates, approximately 15 hr prior to taking the zero time point. Plates were frozen at -80°C at given time points and were subsequently quantified along with standards at the end point of the experiment. Cell count was measured using a green fluorescent dye (CyQUANT GR), which produces a strong fluorescent emission when bound to nucleic acids (303). The fluorometric signal was measured at 485 nm using a Tecan Spectra plate reader.

2.3 Results

2.3.1 PI4KIIIβ expression is enhanced in a subset of breast tumours

To determine whether PI4KIIIβ expression might be altered in breast cancer, PI4KIIIβ protein expression was analyzed in 169 primary human breast tumours (160 invasive ductal carcinomas and 9 medullary carcinomas). For this purpose, a commercially available PI4KIIIβ antibody and two commercially available human breast tumour TMAs were used. PI4KIIIβ staining in each section was categorized as low, moderate or high. Representative images of the three categories are shown in Fig. 2.1. PI4KIIIβ protein expression was detected at a low level in all normal breast tissue samples (34/34) (Table 2.1). The majority of primary human breast tumours assayed also express PI4KIIIβ protein at this low, but detectable level (138/169). However, 18% of primary tumours assayed (26/160 invasive ductal carcinomas and 5/9 medullary carcinomas) expressed higher than normal levels of the protein, i.e. either moderate or high. These results are statistically significant, yielding a p-value of 0.0032 (Fisher's exact test). There were no significant differences in tumour grade or age of patients at diagnosis between the groups with normal or higher PI4KIIIβ expression. These results show that PI4KIIIβ expression is enhanced in a subset of primary human breast tumours.

2.3.2 Elevated expression of PI4KIIIβ increases filopodia production *in vitro*

To investigate the impact of elevated PI4KIIIβ on cytoskeletal rearrangement in breast cancer cells, BT549 breast ductal carcinoma cells were engineered to ectopically and stably express PI4KIIIβ (Fig. 2.2A). Cells overexpressing PI4KIIIβ show increased filopodia production as compared to vector control cells (Fig. 2.2B). A significant increase in both the total number and average length of filopodia per cell were detected in cells ectopically

Figure 2.1: PI4KIIIβ expression in primary breast tumours in a tissue microarray.

Representative images of PI4KIIIβ immunostaining in normal breast tissue and breast tumours classified as showing low, moderate or high expression of PI4KIIIβ. Scale bars represent 100 μm.

PI4KIIIβ

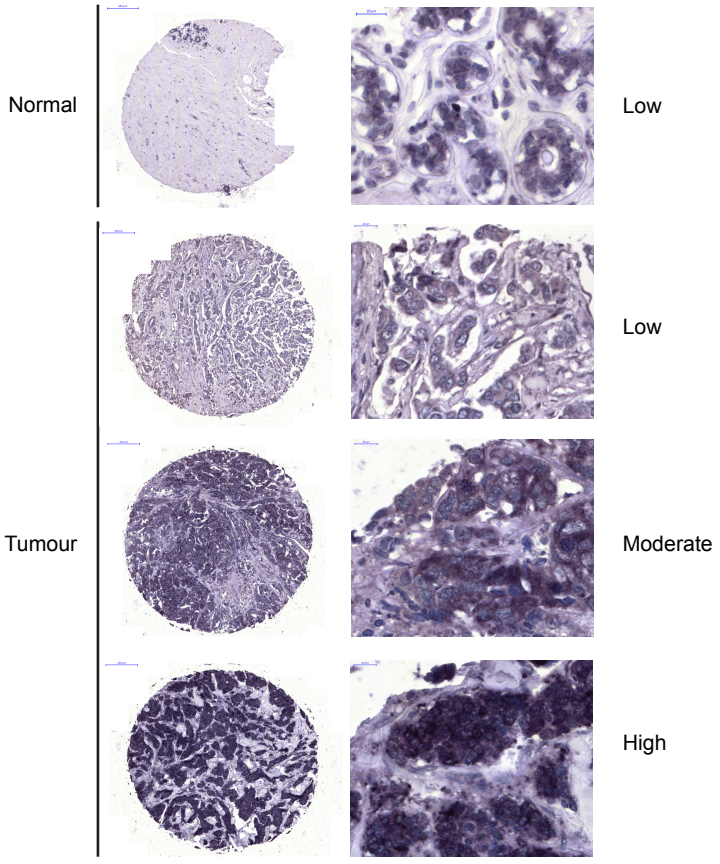

Table 2.1: Evaluation of PI4KIIIβ expression in breast cancer.

PI4KIIIβ protein expression was categorized as, either low, moderate or high for the microarray tissue samples stained. The *n* value indicates the number of each tissue type assayed.

Breast tissue	PI4KIIIβ expression	Number of samples	Percentage of samples (%)
Normal (*n*=34)	Low	34	100
	Moderate, high	0	0
All Tumours (*n*=169)	Low	138	82
	Moderate, high	31	18
Invasive ductal carcinoma (*n*=160)	Low	134	84
	Moderate	18	11
	High	8	5
Medullary carcinoma (*n*=9)	Low	4	44
	Moderate	5	56
	High	0	0

Figure 2.2: Elevated expression of PI4KIIIβ increases filopodia formation in breast cancer cells.

A. Western blot analysis showing PI4KIIIβ protein expression in parental, vector control and PI4KIIIβ-overexpressing BT549 cell lines. **B.** Confocal images showing the enhanced production of filopodia (indicated by arrows) in PI4KIIIβ expressing cells as compared to vector control cells. The actin cytoskeleton was visualized by Phalloidin staining. Scale bars represent 10 μm. **C.** Quantification of the total number of filopodia per cell for vector control and PI4KIIIβ expressing BT549 cells (n = 30 cells for each cell line). The points are laid over a 1.96 S.E.M. (95% confidence interval) in light grey and a 1 S.D. in dark grey. The difference in the total number of filopodia per cell in the vector control and PI4KIIIβ expressing cells is statistically significant ($p < 0.001$, Student's t-test). **D.** Quantification of the average length of filopodia in μm per cell for vector control and PI4KIIIβ expressing BT549 cells (n = 30 cells for each cell line). The points are laid over a 1.96 S.E.M. (95% confidence interval) in light grey and a 1 S.D. in dark grey. The difference in average filopodium length in the vector control and PI4KIIIβ expressing cells is statistically significant ($p < 0.001$, Student's t-test).

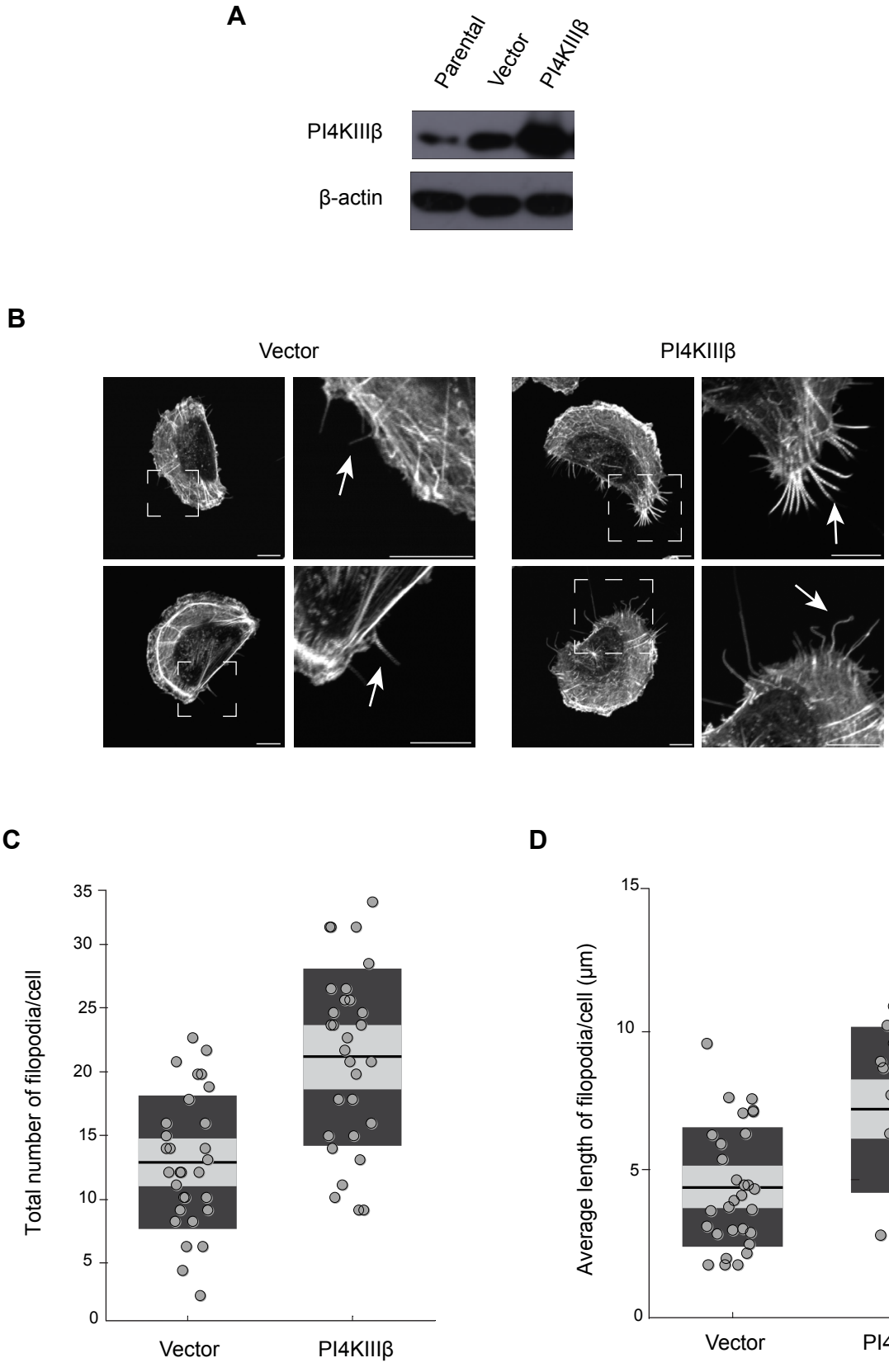
A
Parental
Vector
PI4KIIIβ
PI4KIIIβ
β-actin
B
Vector
PI4KIIIβ
C
Total number of filopodia/cell
35
30
25
20
15
10
5
0
Vector
PI4KIIIβ
D
Average length of filopodia/cell (μm)
15
10
5
0
Vector
PI4KIIIβ

expressing PI4KIIIβ as compared to vector controls ($p < 0.001$, Student's *t*-test) (Fig. 2.2C). PI4KIIIβ-overexpressing cells have an average of 21 filopodia per cell and an average length of 7.10 μm per filopodia as compared to vector control cells, which have an average of 13 filopodia per cell and an average length of 4.45 μm per filopodia. The quantification of BT549 filopodia length and number was done using FiloDetect, an automatic detection tool for filopodia in fluorescent microscopy images, developed collaboratively with Dr. Sharmin Nilufar and Dr. Ted Perkins.

To determine if elevated PI4KIIIβ expression can also impact filopodia production in non-transformed cells, I generated Rat2 rodent fibroblast cells that ectopically express PI4KIIIβ (Fig. 2.3A). The Rat2 cells overexpressing PI4KIIIβ also showed increased filopodia production as compared to vector control cells (Fig. 2.3B). I observed a significant approximately 4-fold increase in the number of cells with at least ten filopodia greater than 3 μm in length in the cell line stably overexpressing PI4KIIIβ as compared to the vector control ($p < 0.05$, Student's *t*-test) (Fig. 2.3C). The average filopodia length in the PI4KIIIβ overexpressing cell line was 5.13 μm, as compared to 2.03 μm in the vector control cell line (304). These results indicate that elevated PI4KIIIβ expression can increase filopodia formation in both transformed and non-transformed cells.

2.3.3 Elevated expression of PI4KIIIβ does not affect cell migration

As increased filopodia formation has been shown to promote cell migration (222), I next assessed whether the increase in filopodia detected in the BT549 PI4KIIIβ-overexpressing cells led to more migratory breast cancer cells. A scratch wound assay was used to study cell migration (Fig. 2.4A). No difference was found in the rate of wound closure between PI4KIIIβ-overexpressing cells and vector control cells (Fig. 2.4B). These

Figure 2.3: Elevated expression of PI4KIIIβ increases filopodia production in non-transformed cells.

A. Western blot analysis showing increased PI4KIIIβ protein expression over the vector control in Rat2 cells. **B.** Confocal images showing the enhanced production of filopodia (indicated with arrows) in PI4KIIIβ-expressing cells as compared to vector control cells. The actin cytoskeleton was visualized by Phalloidin staining. Scale bars represent 10 μm. **C.** Quantification of the increase in longer filopodia in Rat2 cells ± S.D. (n = 134 and 118 for vector control and PI4KIIIβ stable cells, respectively). Filled columns indicate cells with at least 10 filopodia greater than or equal to 3 μm in length. Open columns indicate cells with any number of filopodia less than 3 μm in length. Statistical significance ($p < 0.05$, Student's t-test) is indicated by (*).

A

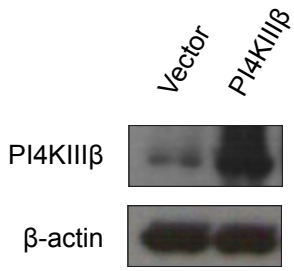
Vector
PI4KIIIβ
PI4KIIIβ
β-actin

B

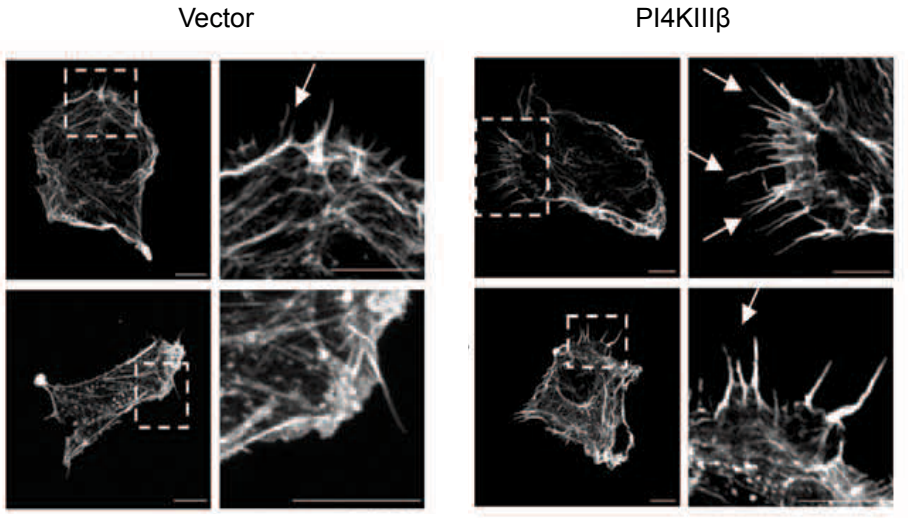
Vector
PI4KIIIβ

C

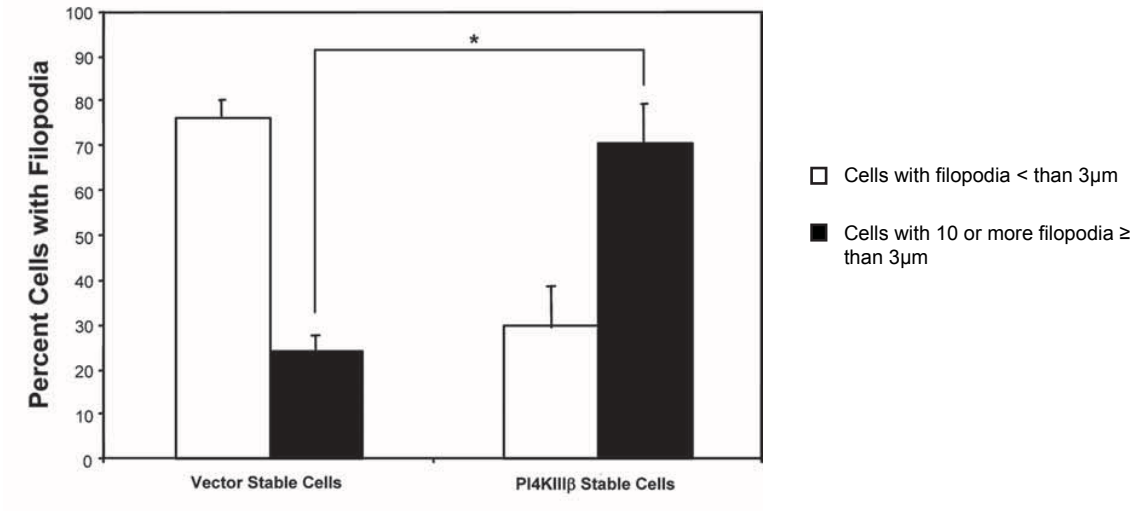
Percent Cells with Filopodia
100
90
80
70
60
50
40
30
20
10
0
*
Vector Stable Cells
PI4KIIIβ Stable Cells
Cells with filopodia < than 3μm
Cells with 10 or more filopodia ≥ than 3μm

Figure 2.4: Elevated PI4KIIIβ expression does not alter the migration of breast cancer cells.

A. Confocal images of a representative wound closure assay performed on the vector control and PI4KIIIβ-expressing BT549 cell lines. **B.** Quantification of three independent wound closure assays showing no change in the time course of wound area closure over 20 hr for PI4KIIIβ-expressing cell lines as compared to the vector control cell line. Data are presented as mean of wound area at given time point ± S.D.

A

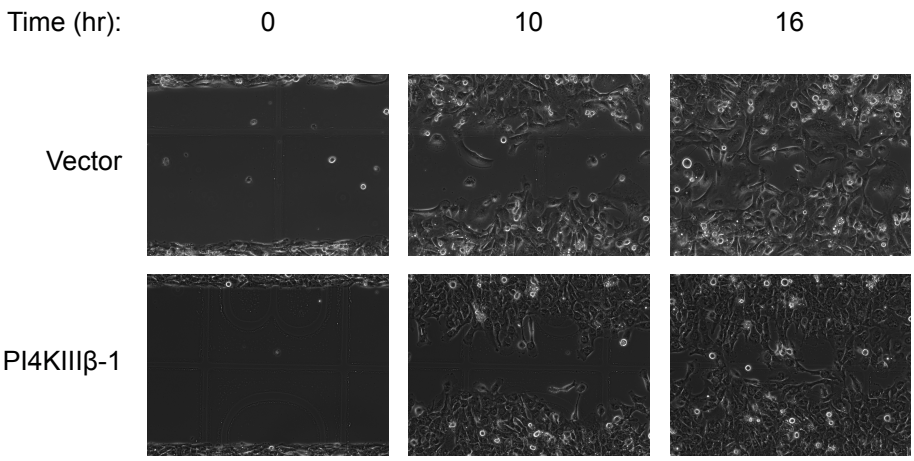
Time (hr):
0
10
16
Vector
PI4KIIIβ-1

B

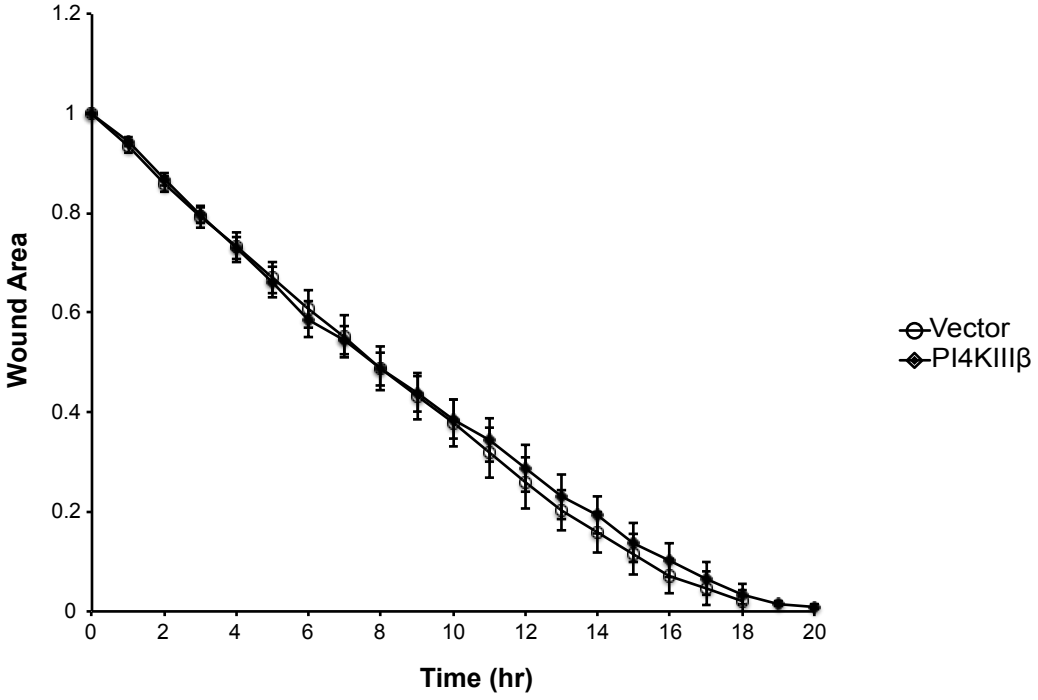
Wound Area
1.2
1
0.8
0.6
0.4
0.2
0
0
2
4
6
8
10
12
14
16
18
20
Time (hr)
Vector
PI4KIIIβ

results suggest that elevated PI4KIIIβ expression does not substantially increase the migration of BT549 breast cancer cells.

2.3.4 Elevated expression of PI4KIIIβ increases cell proliferation

We next determined whether ectopic PI4KIIIβ expression could impact breast cancer cell proliferation. As shown in Fig. 2.5, BT549 cells overexpressing PI4KIIIβ proliferate at a faster rate than their parental or vector control counterparts. Parental and empty vector control cells had doubling times of 38.8 hr and 37.3 hr respectively, whereas PI4KIIIβ-overexpressing cells had a doubling time of 17.2 hr. This indicates that elevated expression of PI4KIIIβ increases the *in vitro* proliferative capacity of breast cancer cells.

Figure 2.5: Elevated expression of PI4KIIIβ enhances cell proliferation.

PI4KIIIβ-overexpressing BT549 cells (closed symbols) proliferate at a faster rate than the parental and vector control cells (open symbols). Each point represents the average fold growth of cells at a given time point over the number of cells measured at the initial time point (0 hr) in triplicate experiments ± S.D.

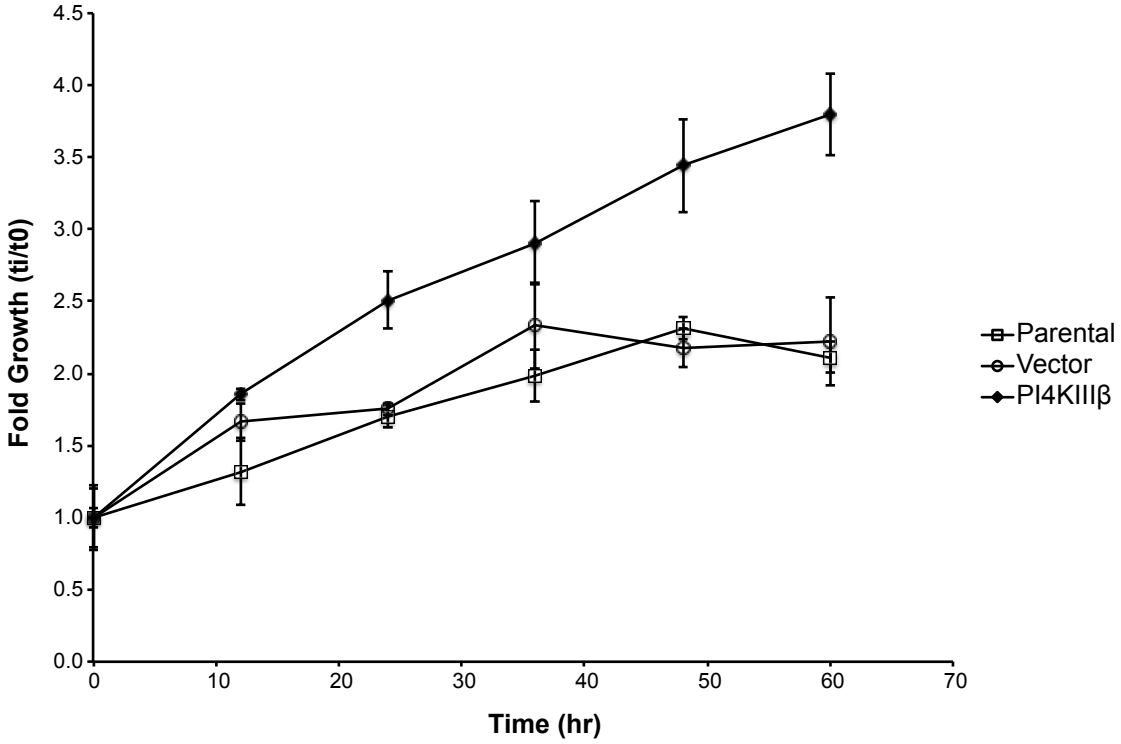
Fold Growth (ti/t0)
4.5
4.0
3.5
3.0
2.5
2.0
1.5
1.0
0.5
0.0
0
10
20
30
40
50
60
70
Time (hr)
Parental
Vector
PI4KIIIβ

2.4 Discussion

A number of PI4K enzymes have been linked to cancer development. For example, PI4KIIα has been reported highly expressed in malignant melanoma, fibrosarcoma, bladder, thyroid and breast cancer and its expression has been shown to promote tumor angiogenesis (169). High levels of PI4KIIIα expression are also associated with invasive and metastatic pancreatic cancer development (172). Furthermore, a large-scale genomic and transcriptome analysis identified *PI4KB*, the gene encoding PI4KIIIβ, as a breast cancer driver (178). Supporting a role for PI4KIIIβ in breast cancer development, we show here that PI4KIIIβ protein levels are increased in ~ 20% of primary human breast tumours assayed, implying that PI4KIIIβ upregulation plays a role in breast cancer neoplastic development. We also find that overexpression of PI4KIIIβ alters the actin cytoskeleton, specifically enhancing production of filopodial protrusions, and also increases the rate of cell proliferation.

We have previously reported that PI4KIIIβ directly interacts with and is activated by the oncogene, eEF1A2 (146, 158, 162-164). eEF1A2 is one of two isoforms of eEF1A, a GTP hydrolyzing enzyme that binds amino-acylated tRNAs and recruits them to the ribosome during the elongation phase of protein synthesis (148). eEF1A2 is genetically amplified and highly expressed in ~30-60% of breast, ovarian and lung tumours (158, 162, 163), but is normally only expressed in heart, brain and skeletal muscle tissue (150, 305, 306). Importantly, eEF1A2 is a transforming gene and its expression in rodent fibroblast cells increases proliferation, allows substrate-independent growth and enhances their tumorigenicity in mouse xenograft models (162). We have also shown that eEF1A2 expression increases filopodia formation and cell migration and invasion in breast cancer cells (168), and increases the proliferative rate of ovarian cancer cells (161). Because

eEF1A2 is a protein translation elongation factor, at first glance it seems likely that it might enhance tumorigenicity by activating protein translation (307). However, protein initiation is thought to be the limiting factor in protein translation rather than protein elongation (308). As such, we believe that eEF1A2 is regulating oncogenesis via a mechanism independent from its role in protein translation. For example, eEF1A2 expression leads to an increase in Akt activation without altering its protein abundance (146, 168). We therefore hypothesized that eEF1A2 was likely regulating oncogenesis via one or more effector proteins. This study demonstrates that one possible pathway through which eEF1A2 likely impacts filopodia production and cell proliferation is through its interaction with PI4KIIIβ, as ectopic PI4KIIIβ expression is sufficient to affect both processes.

Though PI4KIIIβ overexpression leads to greater filopodia production, it does not have the capacity to impact cell migration rates. This result was somewhat surprising, as enhanced filopodia is a hallmark of migratory cells and eEF1A2 expression leads to an increase in filopodia production in a PI4KIIIβ-dependent fashion and stimulates cell migration and invasion in breast cancer cells (222, 300). The BT549 breast cancer cell line is highly migratory and invasive (309, 310). It is possible that even though filopodia production is increased through ectopic expression of PI4KIIIβ in BT549 cells, that the number and length of filopodia are not increased to a level that would push the cell's migratory velocity rate any further. The impact of filopodia production on cell migration may follow a threshold effect in this cell system, in which signals that are below a given threshsold trigger little or no response but once they reach a certain level they trigger a response that increases sharply to reach a maximum (311). Goldbeter and Koshland first described this phenomenon in relation to biological systems in 1981 (312). Though this concept has primarily been used to describe enzymatic signalling systems such as the mitogen-activated protein kinase (MAPK)

cascade and the regulation of heterotrimeric G-protein signalling, it could be applied to more complex biological systems (311, 313). In this case, changes in filopodia production below a certain threshold may not have the capacity to further impact migration velocity rates in this transformed cell line and once a critical level is reached this would lead to a rapid change in the rate of migration.

Cell migration is a multistep process that drives cancer progression (314). It is also possible that eEF1A2 expression impacts more than one cellular process regulating cytoskeletal architecture, which in combination leads to an increase in cell migration and invasion. In a number of different organisms, EF1A proteins have been shown to have cellular functions outside of their canonical role in protein translation, with a particular role in actin cytoskeleton remodelling. *Dictostylium* EF1A directly binds F-actin, enhancing actin bundling (315). The capacity of EF1A to directly bind to actin has also been demonstrated in maize and carrots (316, 317). Interestingly, the carrot EF1A isoform was found to facilitate actin polymerization (317). In addition, ectopic expression of *Saccharomyces cereviseae* eEF1A2 genes (TEF1 and TEF2) leads to a general disorganization of the actin cytoskeleton (318). As eEF1A proteins appear to play a conserved role in actin binding and cytoskeleton remodelling, it is likely that eEF1A2 is involved in regulating actin cytoskeleton remodelling events in a number of ways, both directly though interaction with F-actin and indirectly though binding partners such as PI4KIIIβ, leading to the enhanced cell migration observed in breast cancer cells expressing eEF1A2. The work presented here suggests that PI4KIIIβ overexpression on its own is not sufficient to enhance cancer cell migration, however it does not rule out the possibility that the interaction between PI4KIIIβ and eEF1A2 may contribute to eEF1A2's capacity to enhance cell migration. Further work would be necessary to definitively answer that question, such as looking at the effect of expressing a mutant

eEF1A2, lacking the ability to bind PI4KIIIβ, on breast cancer cell migration, as well as studying the impact of PI4KIIIβ siRNA depletion on the migration rate of eEF1A2-expressing breast cancer cells.

Though enhanced PI4KIIIβ expression does not impact BT549 directional cell migration in two-dimension (2D), it does not exclude the possibilities that enhanced PI4KIIIβ could impact cell migration in three-dimensional (3D) matrices. It has been established that the 2D surface of *in vitro* cultured cells varies substantively from the 3D extracellular environment of cells in vivo (319). Previous work has revealed that 2D migration properties do not always correlate with the migratory behaviour of cells in 3D (320). Researchers found that growth factor stimulated breast cancer cell motility responses in 2D were not predictive of cell migration behaviour in 3D; however, increased membrane protrusions were tightly correlated to enhanced 3D migration (320). To test the impact of enhanced PI4KIIIβ expression on cell migration in 3D under a chemotactic signal, experiments should be performed in the future using a Boyden chamber-based cell invasion assay. In this assay cells are placed in an upper compartment and migrate across a collagen coated membrane into a lower compartment containing chemotactic agents (321).

In summary, we have identified that PI4KIIIβ expression levels are increased in a subset of human breast tumours and that ectopic expression of PI4KIIIβ enhances filopodia production and cell proliferation in breast cancer cells. This suggests that PI4KIIIβ may have a role in breast oncogenesis.

CHAPTER 3: ELEVATED EXPRESSION OF PI4KIIIB LEADS TO AKT ACTIVATION INDEPENDENTLY OF ITS KINASE FUNCTION IN BREAST CANCER CELLS*

* Modified versions of elements in this chapter are being prepared for manuscript submission:

Morrow, A.A., Alipour, M.A., Bridges, D., Yao, Z., Saltiel, A. and Lee, J.M. 2013. Elevated expression of PI4KIIIβ leads to Akt activation independently of its kinase function.

3.1 Introduction

PI4KIIIβ likely has a functional role in breast oncogenesis. As described in the previous chapter, large-scale genomic and transcriptome analysis identified *PI4KB*, the gene encoding PI4KIIIβ, as a breast cancer driver (178). We have also previously implicated PI4KIIIβ in oncogenesis as the protein is bound and activated by the breast and ovarian cancer oncogene eEF1A2 and its high expression disrupts *in vitro* three-dimensional mammary epithelial morphogenesis (146, 162-164, 179). We have also found that approximately 20% of human breast tumours have elevated levels of PI4KIIIβ protein expression, relative to normal breast tissue, and that ectopic expression of PI4KIIIβ leads to an increase in breast cancer cell proliferation (results presented in chapter 2). However, the mechanism by which PI4KIIIβ might promote neoplasia is still unclear.

Expression of the PI4KIIIβ activator eEF1A2 has been shown to increase Akt activation and impact PI3K-dependent cytoskeletal remodelling in breast cancer cells, in addition to its capacity to increase cancer cell migration and proliferation (161, 168). We therefore sought to determine whether elevated PI4KIIIβ expression can regulate the activation of Akt, a serine/threonine kinase and a central regulator of multiple biological processes, among them cell survival, proliferation, and growth (62, 322).

Akt activity is increased in multiple human malignancies, with aberrant activation reported in as many as 70% of breast cancers (323-327). Akt activity is regulated, in large part, by PI3K-generated $PI(3,4,5)P_3$ and $PI(3,4)P_2$ phosphoinositide lipids (61, 62). $PI(3,4,5)P_3$/$PI(3,4)P_2$ recruit Akt to the plasma membrane through its pleckstrin- PH domain, allowing phosphorylation at Thr308, within the activation loop of the protein, by PDK1. mTORC2 phosphorylates Akt at Ser473, within the carboxyl-terminal tail (262, 263, 328). The tumor suppressors, PTEN and INPP4 antagonise PI3K/Akt signalling by

dephosphorylating PI(3,4,5)P_3 at the D3 position, and PI(3,4)P_2 at the D4 position respectively (290, 329, 330).

We find that ectopic PI4KIIIβ expression leads to Akt activation in a PI(3,4,5)P_3-dependent manner. Surprisingly, PI4KIIIβ-mediated Akt activation is not dependent on PI4KIIIβ lipid kinase activity but likely involves its interaction with the small GTPase, Rab11. Rab11 regulates vesicular trafficking, playing a role in slow endosomal recycling and has previously been shown to interact with PI4KIIIβ (137, 142). Our work suggests that PI4KIIIβ has an important role in breast cancer and that cooperation between Rab11 and PI4KIIIβ represents a putative novel Akt activation pathway.

3.2 Materials and Methods

Cell culture. The BT549 cell line was purchased from the American Tissue Culture Collection (ATCC) and grown in RPMI medium 1640 (Life Technologies) supplemented with 10% FBS (Life Technologies), 1 mM sodium pyruvate (Life Technologies), 10 nM HEPES buffer and 0.023 IU/ml insulin (from bovine pancreas, I-5500; Sigma). BT549 cell lines stably expressing ectopic PI4KIIIβ were generated using a pLXSN retroviral system as previously described (301). Infected cells were selected in 0.4 mg/ml G418 (BioShop). All cell lines were cultured at 37°C in humidified atmosphere with 5% CO_2.

Plasmids. Full-length human PI4KIIIβ (MGC-1921, Mammalian Genome Collection, ATCC) was cloned into the pLXSN retroviral vector in the EcoRI and XhoI sites. Nucleotides 1-3303 (RefSeq: NM_001198774.1) were included in pLXSN. Kinase-dead (D656A) PI4KIIIβ (gift from A. Hausser, University of Stuttgart) was cloned into the pLXSN retroviral vector in the HpaI and XhoI sites. Nucleotides 474-2879 (CDS; RefSeq: NM_001198774.1) were included in pLXSN. Wild type and kinase-dead plasmids were sequenced prior to cloning, ensuring that the only sequence difference between the two constructs is the D656A mutation. The PI(3,4,5)P_3/ PI(3,4)P_2 reporter construct, Akt-PH-GFP, and PI(4)P reporter construct, FAPP1-PH-GFP, were gifts from T. Balla (National Institutes of Health). The GFP-PI4KIIIβ construct was a gift from A. Hausser (University of Stuttgart).

siRNA and transfections. PI4KIIIβ targeted siRNA sequence 1 is 5'-GGAGGUGUUGGAGAAAGUCtt-3' (catalog number AM51331, siRNA ID no. 283) and

siRNA sequence 2 is 5'-GCACUGUGCCCAACUAUGAtt -3' (catalog number AM51331; siRNA ID no.184). The Rab11 targeted siRNA sequence used was 5'-CAACAAUGUGGUUCCUAUUtt-3' (catalog number 442708, siRNA ID no. s16702). All siRNAs and the negative control siRNA (catalog number 4611) were purchased from Life Technologies. siRNA transfections were performed in 1% serum media with 10 nM siRNA using Lipofectamine RNAiMAX (Life Technologies) as per the manufacturer's instructions. Lysates were collected either 48 hr or 72 hr post transfection for PI4KIIIβ and Rab11 targeted siRNA transfections respectively. Cells were transfected using Lipofectamine LTX and Plus Reagents (Life Technologies) according to the manufacturer's instructions.

Adenoviral infection. Cells were plated (5×10^5 cells per 10 cm plate) 24 hr prior to infection. On the day of infection, cells were placed in 5 ml serum free growth media with adenoviral particles at an MOI of 200. Cells were collected for Western blotting 24 hr post infection. The adenovirus expressing wild type PTEN was kindly provided by M. J. Lee (Wayne State University).

Western blotting. Cells were plated (2×10^5 cells per 6 cm plate) 48 hr prior to lysate taking and serum depleted (placed in 1% serum containing growth media) 24 hr prior. Cells were lysed using radioimmunoprecipitation assay (RIPA) buffer (50 nM Tris-Cl; pH 7.4, 1% Triton X-100, 1% sodium dodecyl sulfate (SDS), 1 mM ethylenediaminetetraacetic acid (EDTA); pH 7.0, 150 mM NaCl) supplemented with protease and phosphatase inhibitor cocktail tablets (Roche Diagnostics). Protein concentrations were determined by Bradford protein assay (Bio-Rad). SDS sample buffer was added to 10 μg of protein lysate, resolved

by SDS-PAGE and transferred onto PVDF membrane (Millipore). PI4KIIIβ (1:10 000) (BD Biosciences), pAkt-S473 (1:2000), pAkt-T308 (1:1000), Akt (1:1000), p-cRaf (1:1000) and cRaf (1:1000) (all Cell Signaling Technology, Danvers, MA, USA), Rab11 (Millipore) and β-actin (1:20 000) (Sigma) antibodies were used according to the manufacturer's instructions at the indicated dilutions.

Immunoprecipitation. Cells were lysed in 50 mM Tris, pH 7.5, 0.15 mM NaCl, 0.5% Triton X-100 supplemented with protease and phosphatase inhibitor cocktail tablets (Roche Diagnostics). Immunoprecipitation with PI4KIIIβ (Millipore) was performed with 5 ug of antibody per 1 mg/ml of lysate using Protein A agarose beads (Millipore).

Immunofluorescence. Protein immunostaining was performed on cells plated in 6-well plates (Corning) containing glass coverslips. Cells were fixed with 3.7% formaldehyde for 15 min and either permeabilized with 0.1% Triton X-100 for 10 min and blocked with 3% FBS for 1 hr (PI4KIIIβ/Giantin, PI4KIIIβ) or permeabilized and blocked in 0.5% saponin (from Quillaja Bark; Sigma), 3% FBS for 1 hr (PI4KIIIβ/TfR). Cells were then incubated with primary antibodies overnight in 3% FBS. The following primary antibodies were used as per the manufacturer's instructions at the indicated dilutions: PI4KIIIβ (1:200) (BD Biosciences), Giantin (1:200) (Abcam, Toronto, ON, CA), Transferrin Receptor (1:200) (Abcam). This was followed by a 1 hr incubation with Alexa Fluor 488 and Alexa Fluor 647 conjugated secondary antibodies in 3% FBS (1:200, Molecular Probes, Life Technologies) and a 20 min incubation with Hoechst 33258 dye (Sigma) for DNA labeling (0.5 μg/ml). PI(4)P and PI(4,5)P_2 lipid antibody staining was performed on cells plated in 4-well plates

(BD Biosciences) according to the Golgi and plasma membrane specific immunostaining protocols as previously described (25). Briefly, for lipid staining at the Golgi, cells were fixed with 2% methanol-free formaldehyde/PBS (TAAB Laboratories, Aldermaston, Berkshire, UK) followed by permeabilization with 20 μM digitonin (Sigma) and blocking in 5% goat serum. Primary monoclonal anti-PI(4,5)P_2 mouse IgM antibody was used at 2.5 μg/ml and primary monoclonal anti-PI(4)P mouse IgM antibody was used at 8 μg/ml (both from Echelon Biosciences, Salt Lake City, UT, USA), followed by Alexa Fluor 647 secondary antibody incubation (1:200, Molecular Probes, Life Technologies). Permeabilization, blocking and antibody incubations were done in buffer A: 20 mM PIPES, pH6.8; 137 mM NaCl, 2.7 mM KCl. For lipid staining at the plasma membrane cells were first fixed in 4% methanol-free formaldehyde containing 0.2% gluteraldehyde (Sigma). Cells were then placed on ice and all subsequent steps were carried out at 4°C. Cells were blocked and permeabilized in Buffer A containing 5% goat serum, 50 mM NH_4Cl (used to quench aldehyde groups and reduce background staining) and 0.5% Saponin. Cells were then incubated with primary (anti-PI(4)P; 8 μg/ml, Echelon Biosciences) and secondary antibodies (Alexa Fluor 647; 1:200, Molecular Probes, Life Technologies) in Buffer A containing 5% goat serum and 0.1% saponin. All slides were mounted using fluorescent mounting media (Dako). Fixed cell images were all acquired by sequential excitation using an Olympus FluoView FV1000 laser scanning confocal microscope with an Olympus UPLSAPO 100X/1.40 oil objective. Images were collected using Olympus software (FV100, version 01.04a).

Quantification of immunofluorescent images. Akt-PH-GFP reporter construct membrane recruitment and Rab11-GFP distribution quantification were performed using ImageJ

software (NIH). For the Akt-PH-GFP reporter, the cell periphery was delineated as 20% of the total cell area at the outer edge of the cell. Quantification of reporter construct recruitment to the plasma membrane is presented as the GFP fluorescent intensity (total integrated density of pixels) detected at the periphery over the total cellular fluorescent intensity. Rab11-GFP fluorescent intensity was measured at the Golgi, as defined by the area marked by GALT-CFP fluorescence, and converted to a proportion of the total Rab11-GFP fluorescent intensity. The proportion of extra-Golgi Rab11-GFP was defined as the difference between whole cell and Golgi-area GFP fluorescence, divided by whole cell fluorescence. A total of 20 cells were quantified from 4 independent trials for each cell line in each experiment. Background was subtracted from all fluorescent (integrated density) measurements. Quantification of the Pearson's coefficient of correlation (*r*) was performed using Olympus software (FV100, version 01.04a).

Live cell imaging. FAPP1-PH-GFP imaging in Pik93 treated Bt549 cells was performed by Dr. Jonathan Lee. 1 x 10^5 BT549 cells were plated on uncoated 35mm glass bottom plates (MatTek P35G-0-20-C) 24 hr prior to transfection. Cells were then transfected with FAPP1-PH-GFP using Liopfectamine LTX as per the manufacturer's instructions (Life technologies). 24 hr after transfection, cells were treated with either DMSO or 250 nM PIK93 in DMSO. Cell images were acquired by an ORCA-R2 Hammamatsu CCD camera in an Olympus VivaView FL microscope using the 20X objective and an X-cite eXacte mercury arc illumination with a GFP filter cube. Images were processed in VivaView FL software.

Rab11/GALT imaging was performed by Dr. Amir Alipour. Vector control, WT- and KD-PI4KIIIβ-expressing BT549 cells were plated on MatTek coverslips (MatTek

Corporation, Ashland, MA, USA) 24 hr prior to transfection. Cells were co-transfected with GFP-Rab11 and CFP-Galt, using FuGENE HP extreme as per the manufacturer's instructions (Roche Diagnostics). Time lapse images were acquired 24 hr after transfection using an inverted confocal laser scanning microscope, LSM 510, (Zeiss) equipped with a stage heated to 37°C in a chamber containing 5 % CO_2 (v/v)/95 % (v/v) air. CFP and GFP were excited using 417–442 nm and 486–498 nm band-pass filters, respectively. Fluorescence emission spectra were collected using 455–475 nm (CFP) and 510–545 nm (GFP) band-pass filters. Images were acquired at a rate of 1/s. Captured images were converted to animation and exported to QuickTime movie using the Image J software (NIH software).

Competitive ELISA. We determined the relative amount of $PI(3,4,5)P_3$ present in the stable cell lines using a competitive PIP_3 Mass ELISA kit (Echelon Biosciences). Lipids were extracted and purified PIP_3-containing suspensions were treated according to the manufacturer's instructions. Briefly, $3x10^6$ cells per experimental point, plated 24 hr prior, were scraped and rinsed using cold 0.5 M trichloroacetic acid (TCA). Cells were then rinsed twice in 5% TCA/1 mM EDTA. Neutral lipids were then removed using MeOH : $CHCl_3$ (2:1). Following this, acidic lipids were extracted using MeOH : $CHCl_3$: 12 M HCl (80:40:1). The extracted supernatant was then phase split using 0.1 M HCl : $CHCl_3$ (1.8:1) and the organic phase was dried under a stream of gaseous nitrogen. The dried lipids were then resuspended in PIP_3 buffer (50 mM Hepes, 150 mM NaCl, 1.5% sodium cholate, pH7.4), sonicated in a water bath for 5 min and left overnight at 4°C. Lipid extracts were quantified alongside PIP_3 standards the following day. Briefly, samples and standards were first incubated with a PIP_3 detector protein and then subsequently added to a microplate pre-coated with PIP_3, which will serve to competitively bind the PIP_3 detector protein added to

samples. Unbound detector protein is then removed by washing the plates and a peroxidase-linked secondary antibody and colorimetric substrate is added to detect the PIP_3 detector protein bound to the plate. The colorimetric signal was measured at 450 nm using the Tecan Spectra plate reader. The colorimetric signal is inversely proportional to the amount of PIP_3 extracted from the cells.

HPLC analysis. Labelling, extraction, and quantification of phosphatidylinositol phosphates were performed as previously described by Dr. Dave Bridges (331). Briefly, cells were labelled in inositol-free media with [^{3}H]myo-inositol for 48 hr. Cells were then scraped into ice-cold 4.5% perchloric acid and lysed for 15 min at room temperature. Phospholipids were then extracted and deacylated with a solution of 26% methylamine, 45% MeOH, and 11% butanol. Inositol lipids were separated on a Partisphere 5-SAX column with a 0–0.8 M ammonium phosphate, pH 3.8 gradient. Lipid levels were normalized to total phosphatidylinositol levels. There were no differences in the total phosphatidylinositol between the groups (not shown).

3.3 Results

3.3.1 PI4KIIIβ expression regulates Akt activation

To investigate a potential role of PI4KIIIβ expression in the regulation of Akt signalling in breast cancer cells, BT549, human breast ductal carcinoma cell lines, were generated to ectopically express PI4KIIIβ (Fig. 3.1A). These same cell lines were used in the studies presented in Chapter 2, pertaining to BT549 cells stably ectopically expressing PI4KIIIβ. In two independent BT549 cell lines with enhanced PI4KIIIβ expression, a significant approximate 2-fold increase in Akt phosphorylation at Thr308 and at Ser473 was detected as compared to the vector control ($p < 0.05$, Student's *t*-test) (Fig. 3.1A-B). To determine whether this increase in Akt phosphorylation increases intracellular activity of the protein, we probed the cell lines for the level of phosphorylation of c-Raf (Ser259), a known Akt kinase target that has been shown to shift human breast cancer cells from cell cycle arrest to proliferation (332). A significant 1.8-fold increase in c-Raf phosphorylation was detected in the PI4KIIIβ-overexpressing cell lines relative to the vector control, indicating a higher level of Akt kinase activity following enhanced PI4KIIIβ expression ($p < 0.05$, Student's *t*-test) (Fig. 3.1C-D). Moreover, this increase in Akt phosphorylation was observed in BT549 cells overexpressing PI4KIIIβ in full serum, reduced serum and serum-free growth conditions (Fig. 3.1E). This shows that PI4KIIIβ activates Akt, in BT549 cells, in a manner that is independent of serum levels.

We next determined whether a loss of PI4KIIIβ protein expression might lead to a decrease in Akt activation. To this end, BT549 parental cells were treated with two distinct siRNA sequences targeted to PI4KIIIβ. Concomitant with a decrease in PI4KIIIβ protein levels, we observed a consistent and significant decrease (~ 40-50%) in Akt phosphorylation

Figure 3.1: Enhanced PI4KIIIβ expression increases Akt activity.

A. Western blot analysis showing levels of phosphorylation of Akt at Ser473 and at Thr308 in two independent BT549 cell lines with increased PI4KIIIβ protein expression as compared to parental and vector controls. **B.** Quantification of the relative increase in Akt phosphorylation over total Akt levels in the PI4KIIIβ-expressing cell lines as compared to the vector control. Data are presented as mean ± S.E.M. of three independent trials and (*) indicates statistical significance ($p < 0.05$, Student's *t*-test). **C.** Western blot analysis showing phosphorylation of c-Raf at Ser259 in two independent BT549 cell lines with increased PI4KIIIβ protein expression as compared to parental and vector controls. **D.** Quantification of the relative increase in c-Raf phosphorylation over total c-Raf levels in the PI4KIIIβ-expressing cell lines as compared to the vector control. Data are presented as mean ± S.E.M. of two independent trials for two independent cell lines ($n = 4$) and (*) indicates statistical significance ($p < 0.05$, Student's *t*-test). **E.** Western blot analysis showing increased Akt phosphorylation at Ser473 and Thr308 for PI4KIIIβ-overexpressing cells as compared to vector controls grown overnight in media containing no serum, 1% serum or full (10%) serum.

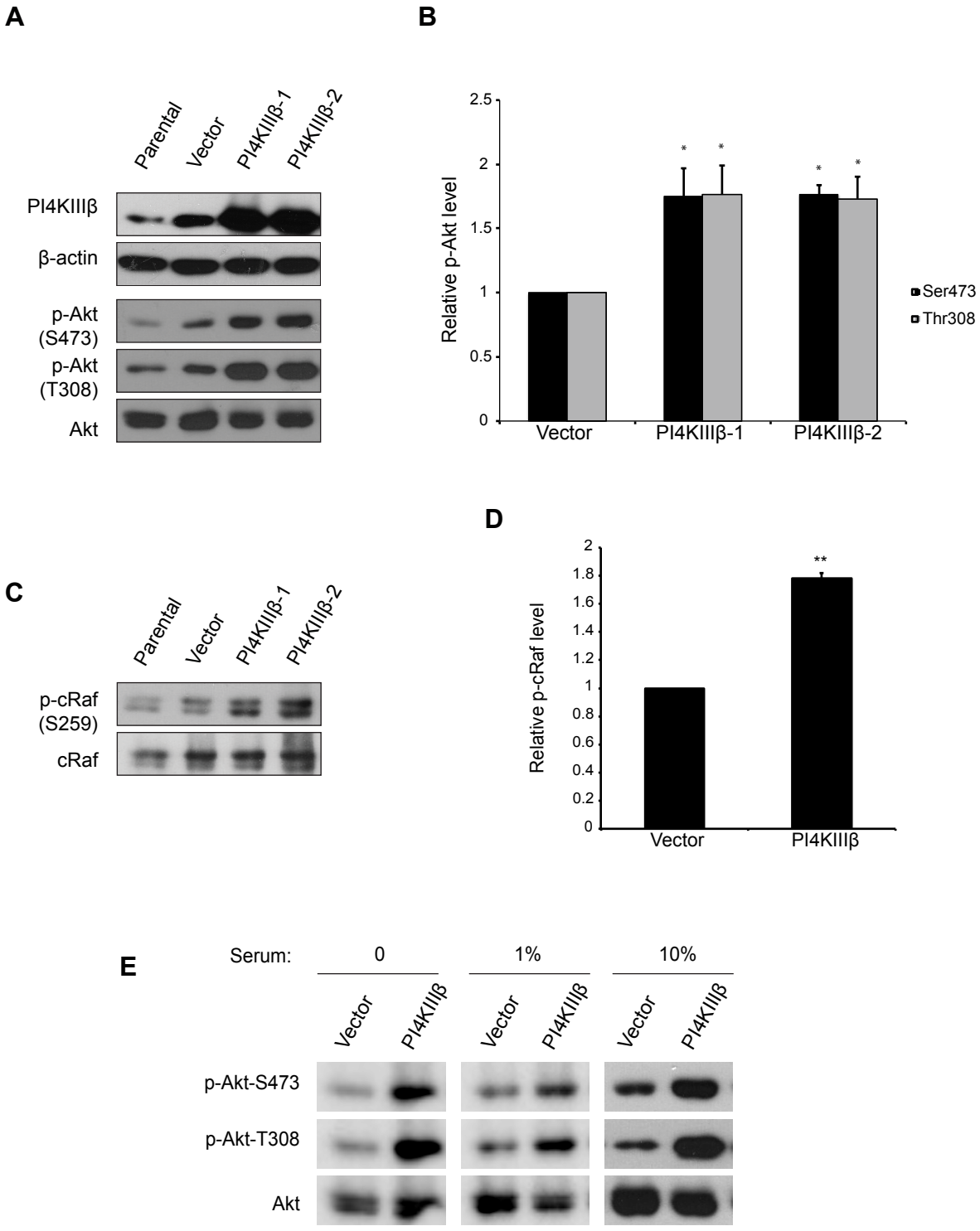
A
Parental
Vector
PI4KIIIβ-1
PI4KIIIβ-2
PI4KIIIβ
β-actin
p-Akt (S473)
p-Akt (T308)
Akt
B
Relative p-Akt level
2.5
2
1.5
1
0.5
0
Vector
PI4KIIIβ-1
PI4KIIIβ-2
Ser473
Thr308
C
Parental
Vector
PI4KIIIβ-1
PI4KIIIβ-2
p-cRaf (S259)
cRaf
D
Relative p-cRaf level
2
1.8
1.6
1.4
1.2
1
0.8
0.6
0.4
0.2
0
Vector
PI4KIIIβ
E
Serum:
0
1%
10%
Vector
PI4KIIIβ
p-Akt-S473
p-Akt-T308
Akt

at Ser473 and Thr308 ($p < 0.05$, Student's *t*-test) (Fig. 3.2A-B). PI4KIIIβ has been shown to be required for structural integrity of the Golgi complex (113). We therefore wanted to ensure that siRNA depletion of PI4KIIIβ was not leading to gross changes in Golgi morphology, which could impact cell trafficking and signalling as a whole. siRNA treated cells were therefore stained for the cis-medial Golgi marker, Giantin, as well as PI4KIIIβ protein. PI4KIIIβ protein expression was effectively decreased in the BT549 cells treated with each of the siRNA sequences against PI4KIIIβ, as compared to BT549 cells treated with the negative control siRNA (Fig. 3.2C). The Golgi morphology was then scored as intact, disrupted or partially disrupted in each of the cell treatments stained, depending on whether the Golgi was imaged as a punctate structure or as a more dispersed organelle at a 40X maginification. Representative images are shown in Fig. 3.2C. There were no significant changes in the proportion of cells scored for each Golgi state in the siRNA treated cells as compared to control treated cells and the vast majority of cells (≥ 90%), in siRNA treated cells, display an intact Golgi (Fig 3.2D). This suggests that siRNA knockdown of PI4KIIIβ does not have a detectable effect on Golgi morphology and depletion of PI4KIIIβ is not impacting Akt regulation by a gross deregulation of Golgi function. These results suggest that PI4KIIIβ is involved in regulating Akt activation in BT549 breast cancer cells and that overexpression of PI4KIIIβ leads to an increase in Akt activation.

3.3.2 PI4KIIIβ expression activates Akt via PI(3,4,5)P_3 signalling

Because Akt activation is dependent, in large measure, on PI(3,4,5)P_3 levels, we next determined the effect of PI4KIIIβ expression on the overall cellular abundance of PI(3,4,5)P_3 using a competitive ELISA. We observed a significant increase (~ 60%) in PI(3,4,5)P_3

Figure 3.2: PI4KIIIβ siRNA depletion leads to a decrease in Akt activation.

A. Western blot analysis showing Akt phosphorylation at Ser473 and Thr308 in BT549 parental cells treated with two distinct siRNA sequences targeted to PI4KIIIβ as compared to cells treated with the negative control siRNA. **B.** Quantification of relative decrease in Akt phosphorylation in cells treated with siRNA targeted to PI4KIIIβ as compared to cells treated with negative control siRNA. Data are presented as mean ± S.E.M. of three independent experiments and (*) indicates statistical significance ($p < 0.05$, Student's *t*-test). **C.** BT549 parental cells treated with two distinct siRNA sequences targeted to PI4KIIIβ , as well as negative control siRNA, immunostained for PI4KIII (green) and the cis-medial Golgi marker Giantin (red). Representative images for Golgi morphology scoring are shown and described as intact, disrupted or partially disrupted (partial). Scale bars represent 10 μm. **D.** Quantification of Golgi morphology scoring in siRNA treated cells. Quantification was done on three independent trials each containing 100 stained and scored cells. Results are presented as the average proportion of total Golgi scored per trial ± S.E.M.

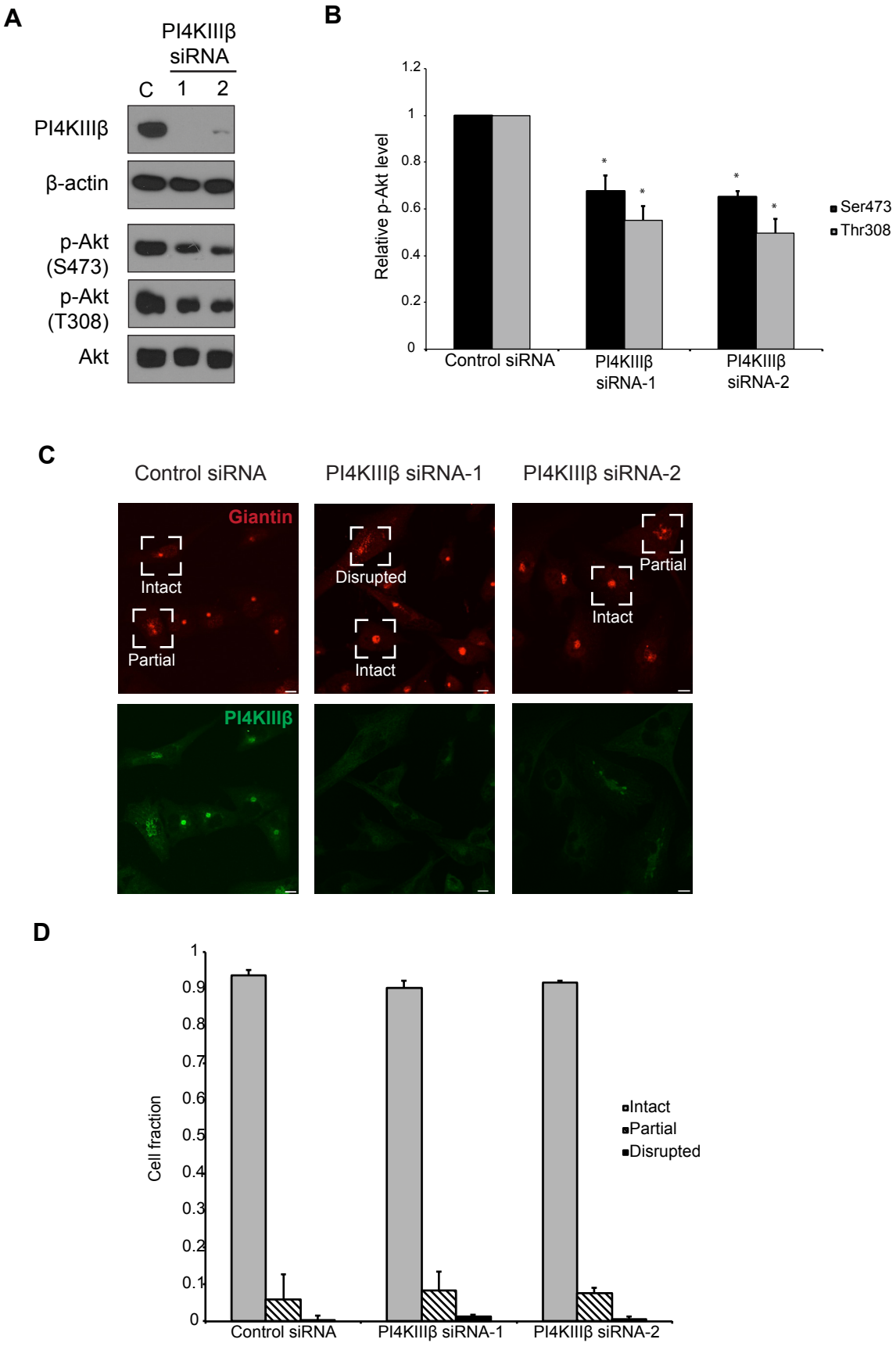
A
PI4KIIIβ siRNA
C 1 2
PI4KIIIβ
β-actin
p-Akt (S473)
p-Akt (T308)
Akt
B
Relative p-Akt level
1.2
1
0.8
0.6
0.4
0.2
0
Control siRNA
PI4KIIIβ siRNA-1
PI4KIIIβ siRNA-2
Ser473
Thr308
C
Control siRNA
PI4KIIIβ siRNA-1
PI4KIIIβ siRNA-2
Giantin
Intact
Partial
Disrupted
Intact
Partial
Intact
PI4KIIIβ
D
Cell fraction
1
0.9
0.8
0.7
0.6
0.5
0.4
0.3
0.2
0.1
0
Control siRNA
PI4KIIIβ siRNA-1
PI4KIIIβ siRNA-2
Intact
Partial
Disrupted

abundance in the PI4KIIIβ-overexpressing cell lines compared to the vector control ($p < 0.05$, Student's *t*-test) (Fig. 3.3A). We then visualized the intracellular localization of $PI(3,4,5)P_3$ using a fluorescent reporter composed of the PH domain of Akt fused to GFP (GFP-Akt PH), which binds to $PI(3,4,5)P_3$ and $PI(3,4)P_2$ lipids (22). Cell lines with increased PI4IIIβ expression showed increased plasma membrane recruitment of the reporter construct, indicating higher levels of $PI(3,4,5)P_3$ and/or $PI(3,4)P_2$ at the cell membrane, where Akt activation is directed by these lipid species (Fig. 3.3B, *Left*). When cells were transfected with GFP alone, no enhanced reporter recruitment could be observed at the cell membrane for the PI4KIIIβ-overexpressing cells as compared the vector control (Fig. 3.3B, *Right*). Quantification of reporter construct recruitment to the plasma membrane was measured as the percentage of total GFP fluorescent intensity detected at the cell periphery. A significant increase ($p < 0.01$, Student's *t*-test) in fluorescent intensity at the cell periphery was detected for the GFP-Akt-PH lipid reporter in both the vector control and PI4KIIIβ-overexpressing cells as compared to each cell line transfected with GFP alone (Fig. 3.3C). Approximately 14% of total GFP fluorescence was detected at the cell membrane in both cell lines. In comparison, 19% and 31% of total GFP-Akt-PH fluorescence, was detected at the cell membrane in the vector control and PI4KIIIβ-overexpressing cells, respectively. This illustrates the membrane binding specificity of the GFP-Akt-PH reporter. The further increase (~ 10%; $p < 0.01$, Student's *t*-test) in membrane association of the GFP-Akt-PH reporter detected in the PI4KIIIβ-overexpressing cells as compared to vector control cells, indicates increased abundance of $PI(3,4,5)P_3$/$PI(3,4)P_2$ lipids at the cell membrane in cells with elevated PI4KIIIβ expression (Fig. 3.3C).

Figure 3.3: Enhanced PI4KIIIβ expression increases total PI(3,4,5)P_3 cellular abundance and plasma membrane localization.

A. PI(3,4,5)P_3 abundance is shown as a concentration of pmol per 10^6 cells and is the mean ± S.E.M. of duplicate samples from three independent experiments in the case of the vector control and from two independent experiments for each of the BT549 PI4KIIIβ-expressing cell lines. Increased PI(3,4,5)P_3 production in PI4KIIIβ-expressing cell lines as compared to the empty vector control is statistically significant ($p < 0.05$, Student's *t*-test) and is indicated by (*). **B.** Confocal images of BT549 vector control and PI4KIIIβ overexpressing cell lines transfected with the PI(3,4,5)P_3/ PI(3,4)P_2 reporter Akt-PH-GFP or GFP alone. Scale bars represent 10 μm. **C.** Quantification of plasma membrane recruitment of the GFP-Akt-PH reporter or GFP alone in vector control or PI4KIIIβ overexpressing cells. Quantification is presented as the mean of GFP fluorescence intensity at the cell periphery over total cell fluorescence ± S.E.M. for 20 cells from four independent trials. (**) indicates statistical significance ($p < 0.01$, Student's *t*-test).

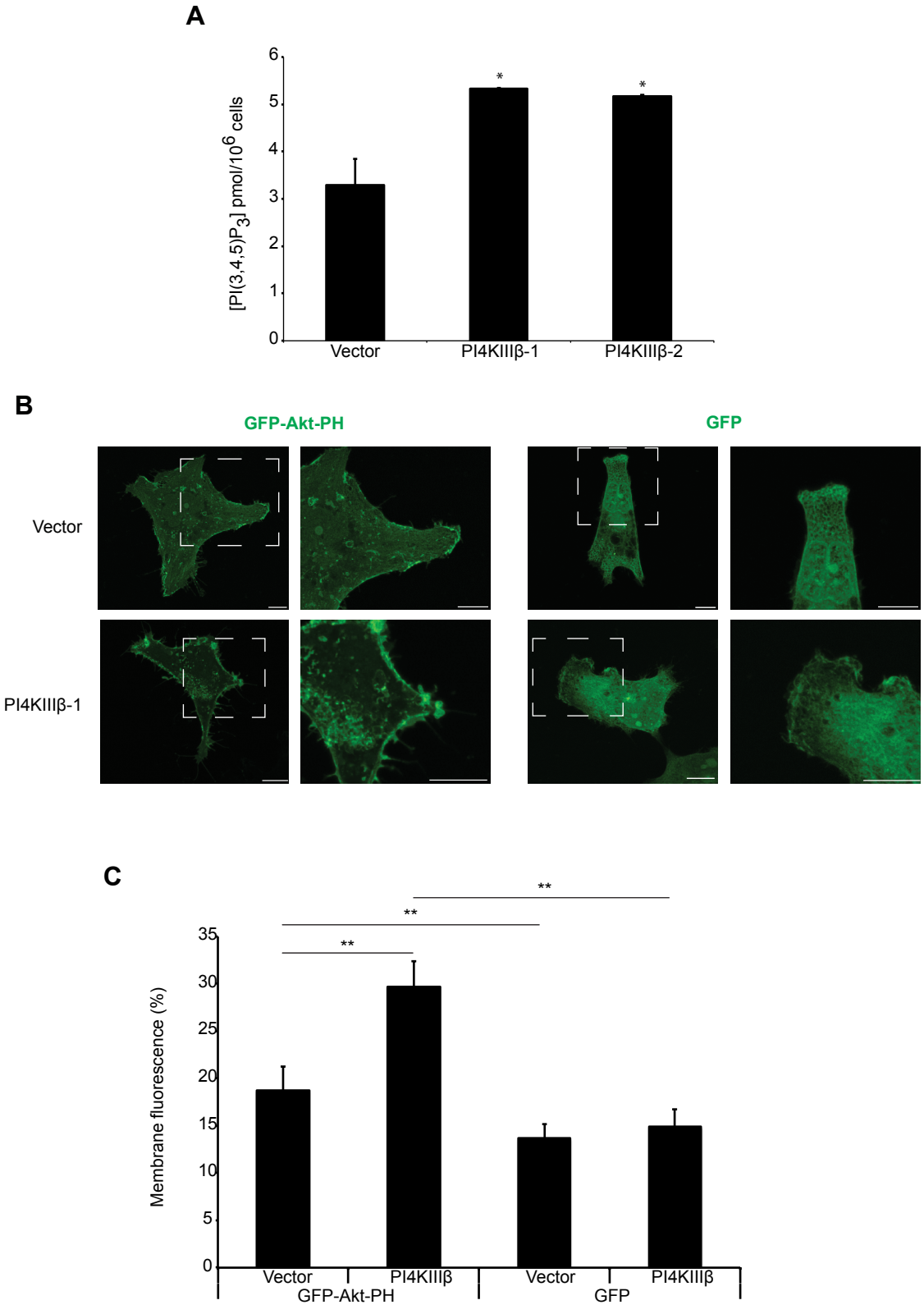
A
[PI(3,4,5)P3] pmol/10^6 cells
0
1
2
3
4
5
6
*
*
Vector
PI4KIIIβ-1
PI4KIIIβ-2
B
GFP-Akt-PH
GFP
Vector
PI4KIIIβ-1
C
Membrane fluorescence (%)
0
5
10
15
20
25
30
35
**
**
**
Vector
PI4KIIIβ
Vector
PI4KIIIβ
GFP-Akt-PH
GFP

BT549 cells are PTEN-null, as they contain a truncation mutation in *PTEN*, which leads to the rapid degradation of the truncated protein (333, 334). We therefore next determined the effect of re-introducing wild type PTEN on Akt activation, in the cell lines with enhanced PI4KIIIβ expression. Expression of wild-type PTEN by adenoviral infection led to a decrease in Akt phosphorylation in both the BT549 cells with enhanced PI4KIIIβ expression and the vector control cells (Fig. 3.4A). PTEN expression led to a significant decrease in Akt phosphorylation by approximately 50% in both the vector control and PI4KIIIβ-overexpressing cells ($p < 0.01$, Student's t-test)) (Fig. 3.4B). As PTEN is responsible for dephosphorylating $PI(3,4,5)P_3$ into $PI(4,5)P_2$, this result suggests that the increase in Akt activation in the PI4KIIIβ-expressing cells is dependent on cellular $PI(3,4,5)P_3$ lipid levels. Therefore PI4KIIIβ-mediated Akt activation likely occurs via the canonical PI3K signalling pathway.

3.3.3 PI4KIIIβ mediated Akt activation is independent of its kinase activity

$PI(3,4,5)P_3$ is principally generated by the sequential phosphorylation of PI, at positions D4, D5 and D3 respectively, by PI 4-kinases, PI4P 5-kinases and PI 3-kinases. We therefore hypothesized that enhanced PI4KIIIβ expression might increase the cellular abundance of $PI(3,4,5)P_3$ by increasing its precursors PI(4)P and $PI(4,5)P_2$. To test this idea, we measured the PI levels in the cell lines stably ectopically expressing PI4KIIIβ using HPLC separation of ^3H labelled inositol lipids. Surprisingly, there was no significant difference detected in the relative abundance of PI(4)P or $PI(4,5)P_2$ lipids in the PI4KIIIβ-overexpressing cell lines as compared to the vector or parental control cell lines (Fig. 3.5A). Thus, enhanced PI4IIIβ expression appears to increase $PI(3,4,5)P_3$ levels without having an impact on total cellular PI(4)P or $PI(4,5)P_2$ abundance. To determine if ectopic expression of

Figure 3.4: PI4KIIIβ-mediated Akt activation is lost in the BT549-PTEN null cell line upon expression of a functional PTEN.

A. Western blot analysis showing Akt phosphorylation at Ser473 and Thr308 in vector control and PI4KIIIβ-overexpressing cell lines infected with adenovirus expressing wild-type PTEN as compared to the untreated cell lines. **B.** Quantification of the relative decrease in Akt phosphorylation in cells treated with adenovirus expressing wild-type PTEN as compared to untreated controls. Data are presented as the mean ± S.E.M. of three independent experiments and (**) indicates statistical significance ($p < 0.01$, Student's *t*-test) for each PTEN expressing cell line compared to its untreated control.

A

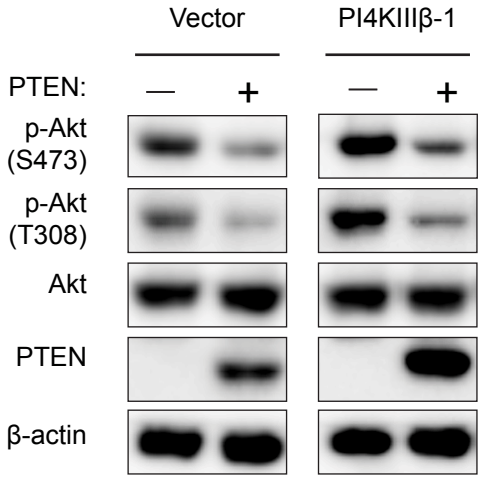
Vector
PI4KIIIβ-1
PTEN:
—
+
—
+
p-Akt (S473)
p-Akt (T308)
Akt
PTEN
β-actin

B

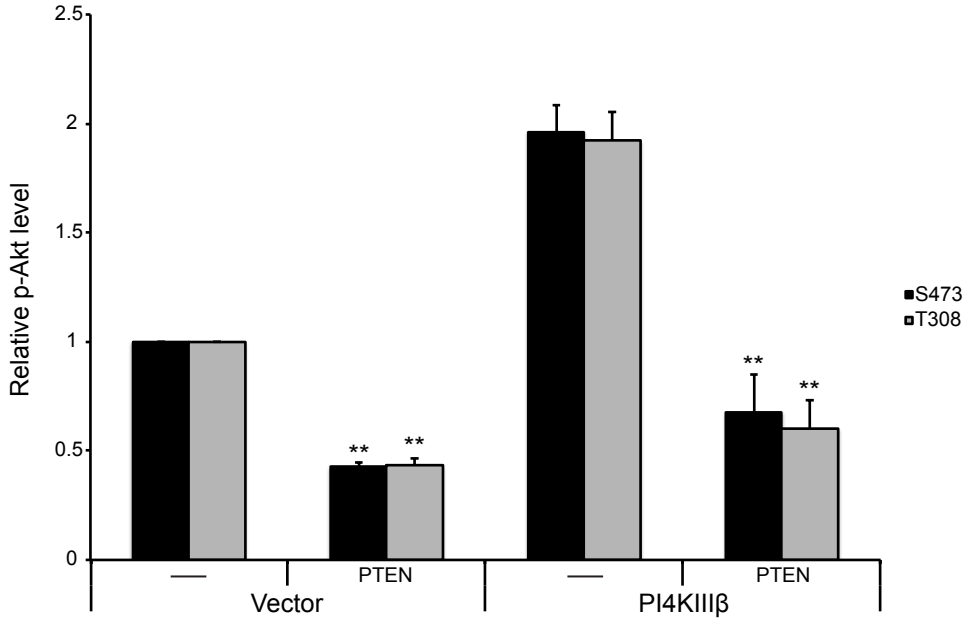
Relative p-Akt level
2.5
2
1.5
1
0.5
0
**
**
**
**
S473
T308
—
PTEN
—
PTEN
Vector
PI4KIIIβ

Figure 3.5: Increased PI4KIIIβ expression does not alter the cellular abundance of either PI(4)P or PI(4,5)P nor the localization of PI(4)P

A. HPLC analysis of PI(4)P and PI(4,5)P_2 phosphoinositide levels as a percent of total radiolabeled inositol in the parental, vector control and two independent PI4KIIIβ-expressing BT549 cell lines. Data are presented as mean ± S.E.M. of three independent experiments. **B.** Confocal images of BT549 vector control and PI4KIIIβ overexpressing cell lines transfected with the PI(4)P reporter FAPP1-PH-GFP. Scale bars represent 10 μm. **C.** Lipid antibody immunostaining (red) of PI(4)P at the Golgi and PI(4)P and PI(4,5)P_2 at the plasma membrane in BT549 cells transiently transfected with PI4KIIIβ-GFP. Transfected cells are designated by an arrow. All other cells in the field are untransfected (i.e. control cells). Scale bar indicates 10 μm.

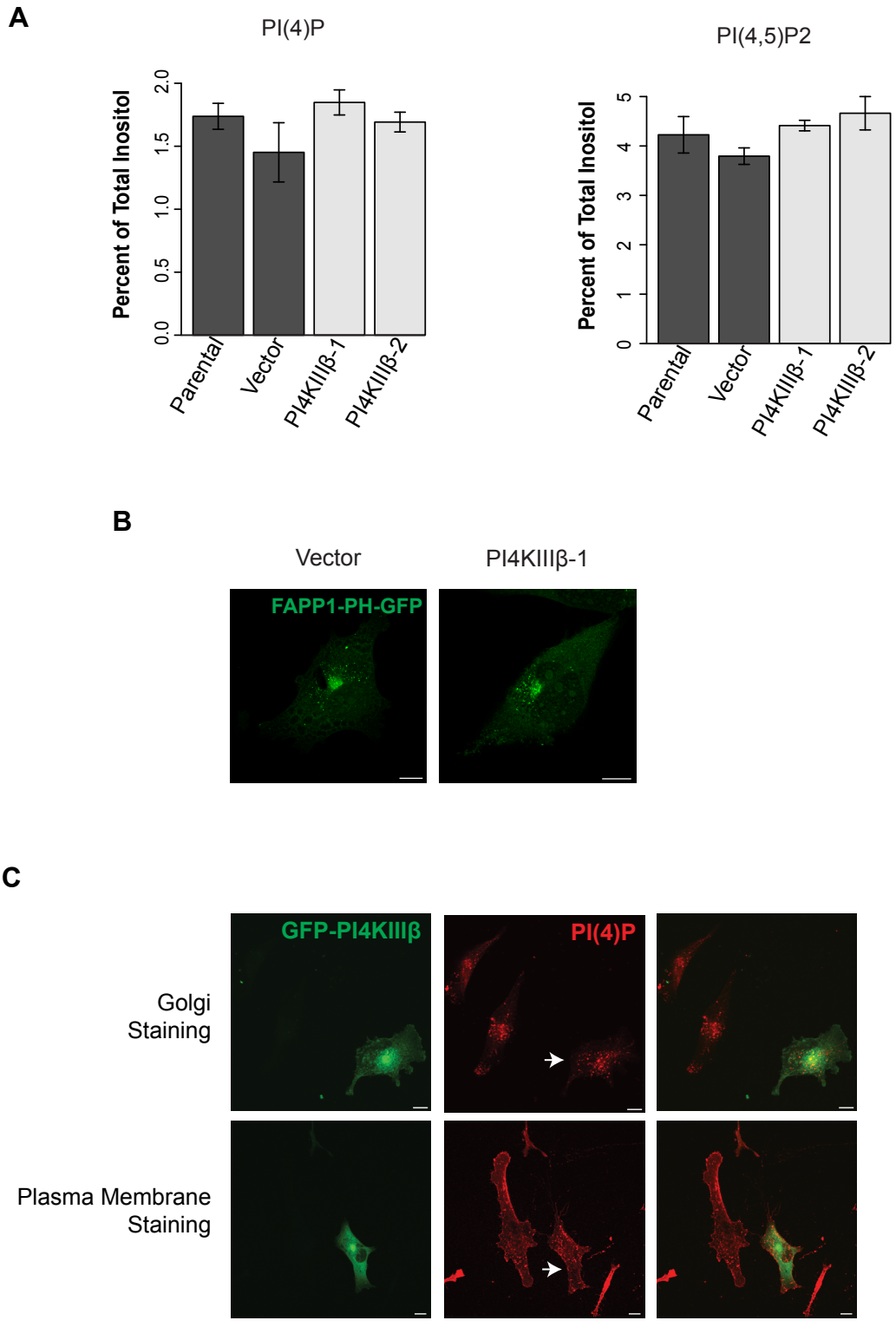
A
PI(4)P
Percent of Total Inositol
0.0
0.5
1.0
1.5
2.0
Parental
Vector
PI4KIIIβ-1
PI4KIIIβ-2
PI(4,5)P2
Percent of Total Inositol
0
1
2
3
4
5
Parental
Vector
PI4KIIIβ-1
PI4KIIIβ-2
B
Vector
PI4KIIIβ-1
FAPP1-PH-GFP
C
GFP-PI4KIIIβ
PI(4)P
Golgi Staining
Plasma Membrane Staining

PI4KIIIβ leads to an altered distribution of PI(4)P lipid, cells were transfected with the FAPP1-PH-GFP, a reporter construct which binds to PI(4)P in a Golgi specific context (33, 34). No evident changes in FAPP1-PH-GFP, and therefore PI(4)P lipid distribution, were observed between vector control and PI4KIIIβ-expressing BT549 cells (Fig. 3.5B). To further verify if ectopic expression of PI4KIIIβ alters the distribution of either PI(4)P or $PI(4,5)P_2$ lipid immunostaining was performed on BT549 cells transiently transfected with GFP-PI4KIIIβ, following specific protocols that enable the preservation of the Golgi and plasma membrane respectively (25). There did not appear to be any gross changes in intensity or distribution patterns of PI(4)P at the Golgi or of PI(4)P and $PI(4,5)P_2$ at the plasma membrane in cells transfected with GFP-PI4KIIIβ compared to untransfected cells in the same field (Fig. 3.5C). This suggests that enhanced PI4KIIIβ expression does not lead to a substantive change in PI(4)P or $PI(4,5)P_2$ lipid production or localization.

In light of these findings, we then asked whether or not the kinase activity of PI4KIIIβ was required for Akt activation. To this end, we treated the BT549 cells stably expressing ectopic PI4KIIIβ with a drug that inhibits PI4KIIIβ, Pik93. This drug inhibits only the PI4KIIIβ isoform (and not PI4KIIIα) at a molar concentration of 250 nM, though at this molar range Pik93 also inhibits PI3Kγ (106, 335, 336). In addition, Pik93 can inhibit PI3Kα, PI3Kβ and PI3Kδ but only at higher concentrations (336). Overnight treatment of cells with Pik93 had no effect on PI4KIIIβ-mediated Akt activation, as the same increase in Akt phosphorylation is observed in PI4KIIIβ-expressing cells as compared to vector control cells, when treated with DMSO (vehicle control) or Pik93 (Fig 3.6A). To ensure that Pik93 was in fact inhibiting PI4KIIIβ in our cell system, we followed the distribution of the PI(4)P lipid reporter, FAPP1-PH-GFP, in BT549 parental cells treated with either DMSO or Pik93.

Figure 3.6: Inhibition of PI4KIIIβ activity does not impede PI4KIIIβ-mediated Akt activation.

A. Western blot showing that PI4KIIIβ-overexpression leads to an increase in activating Akt phosphorylation in BT549 cells, when treated with either the PI4KIII inhibitor Pik93 (250 nM) or the vehicle control, DMSO. **B.** Confocal images taken during live cell imaging, following a given BT549 cell transiently transfected with FAPP1-PH-GFP and treated with either DMSO (vehicle control) or Pik93 (250 nM) over 60 min. The PI(4)P reporter construct can be seen redistributing to the cytoplasm in cells treated with Pik93 at the 30 min mark. This same effect is not observed in cells treated with DMSO. Scale bars represent 10 μm.

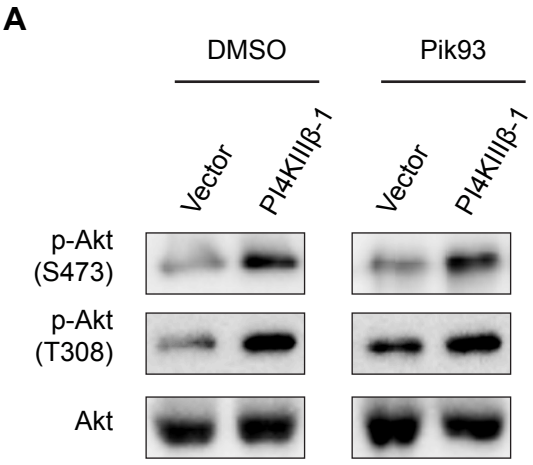
A
DMSO
Pik93
Vector
PI4KIIIβ-1
Vector
PI4KIIIβ-1
p-Akt (S473)
p-Akt (T308)
Akt

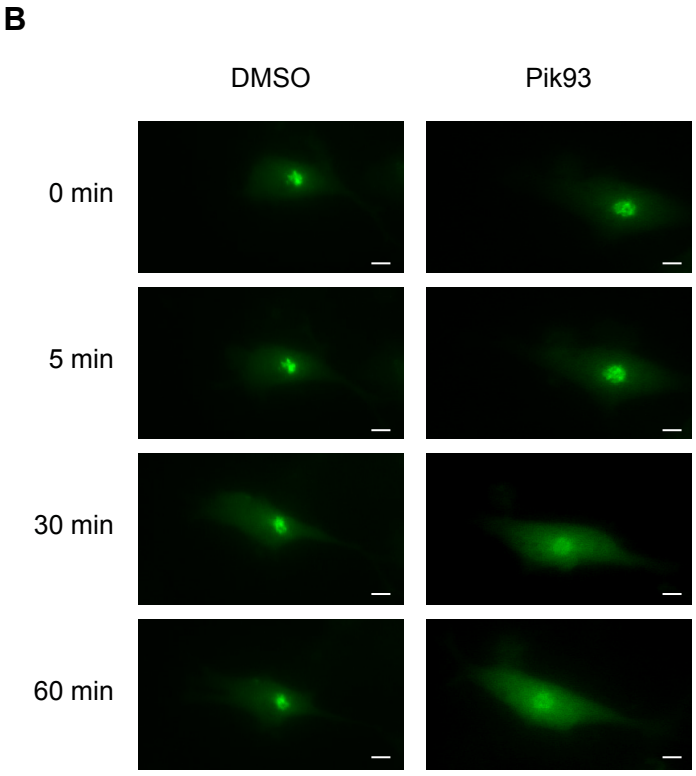
B
DMSO
Pik93
0 min
5 min
30 min
60 min

Pik93 inhibition of PI4KIIIβ has previously been shown to lead to a reduction of FAPP1-PH-GFP Golgi localization (337). We found that treatment of cells with 250 nM of Pik93 effectively led to loss of Golgi reporter fluorescence by 30 min time (Fig. 3.6B). In contrast, FAPP1-PH-GFP remained primarily Golgi localized in DMSO treated cells. This, presumably, reflects the loss of PI(4)P lipid at the Golgi due to Pik93 inhibition of PI4KIIIβ. As treatment with the PI4KIIIβ inhibitor Pik93 had no effect on PI4KIIIβ-mediated Akt activation, this indicates that PI4KIIIβ catalytic activity is not required for its role in Akt activation.

To further investigate the catalytic role of PI4KIIIβ in Akt activation, we next generated BT549 cells ectopically expressing a kinase-dead (KD) PI4KIIIβ. KD-PI4KIIIβ contains a substitution of an aspartic acid residue for alanine at position 656, rendering it catalytically inactive (113, 137). Previous work has demonstrated that the PI4K activity of KD-PI4KIIIβ is < 0.2% that of wild type (WT) PI4KIIIβ (113, 137). With respect to Akt activation, two independent cell lines expressing KD-PI4KIIIβ showed significant increases (~ 2-fold) in Akt phosphorylation at Thr308 and at Ser473 as compared to the vector control and at levels comparable to those observed in BT549 cells ectopically expressing WT-PI4KIIIβ ($p < 0.05$, Student's *t*-test) (Fig 3.7A-B). This indicates that PI4KIIIβ expression leads to Akt activation independently of its catalytic activity. We also found that BT549 cells expressing KD-PI4KIIIβ proliferate at a faster rate than vector control cells (Fig. 3.7C). Ectopic expression of both KD- and WT-PI4KIIIβ decreased the doubling time of BT549 cells to 27 hr, as compared to vector control cells, which had a doubling time of 47 hr. It has been previously reported that kinase activity is not required for the Golgi localization of the soluble PI4KIIIβ protein (137). Therefore, we next wanted to verify that ectopic expression

Figure 3.7: Ectopic expression of a catalytically inactive PI4KIIIβ (D656A) increases Akt activation.

A. Western blot analysis of Akt phosphorylation at Ser473 and at Thr308 in WT-and two independent KD-PI4KIIIβ-expressing BT549 cell lines as compared to the vector control. **B.** Quantification of the relative increase in Akt phosphorylation over total Akt levels is shown in the WT-PI4KIIIβ-overexpressing and KD-PI4KIIIβ-expressing cell lines as compared to the vector control. Data are presented as mean ± S.E.M. of three independent experiments and (*) indicates statistical significance ($p < 0.05$, Student's *t*-test). **C.** KD-PI4KIIIβ-expressing BT549 cells (closed triangle-purple line) proliferate at a faster rate than vector control cells (open symbol) and at a comparable rate as WT-PI4KIIIβ-overexpressing cells (closed diamond-blue line). Each point represents the average fold growth of cells at a given time point over the number of cells measured at the initial time point (0 hr) for three independent experiments for each cell line ± S.D. **D.** Confocal images of PI4KIIIβ localization (green) in vector control, WT- PI4KIIIβ-overexpressing and KD-PI4KIIIβ expressing cells. Golgi, as identified by the cis-medial Golgi marker Giantin, is seen in red and DNA is blue. Scale bar indicates 10 μm. **E.** Confocal images of BT549 vector control and KD-PI4KIIIβ-expressing cells transfected with the $PI(3,4,5)P_3$/ $PI(3,4)P_2$ reporter, Akt-PH-GFP. Scale bars indicate 10 μm. **F**. Quantification of the plasma membrane recruitment of the Akt-PH-GFP reporter in the vector control and KD-PI4KIIIβ-expressing cells presented as the mean ± S.E.M. for 20 cells from 4 independent experiments. Statistical significance ($p < 0.01$, Student's *t*-test) is indicated by (**).

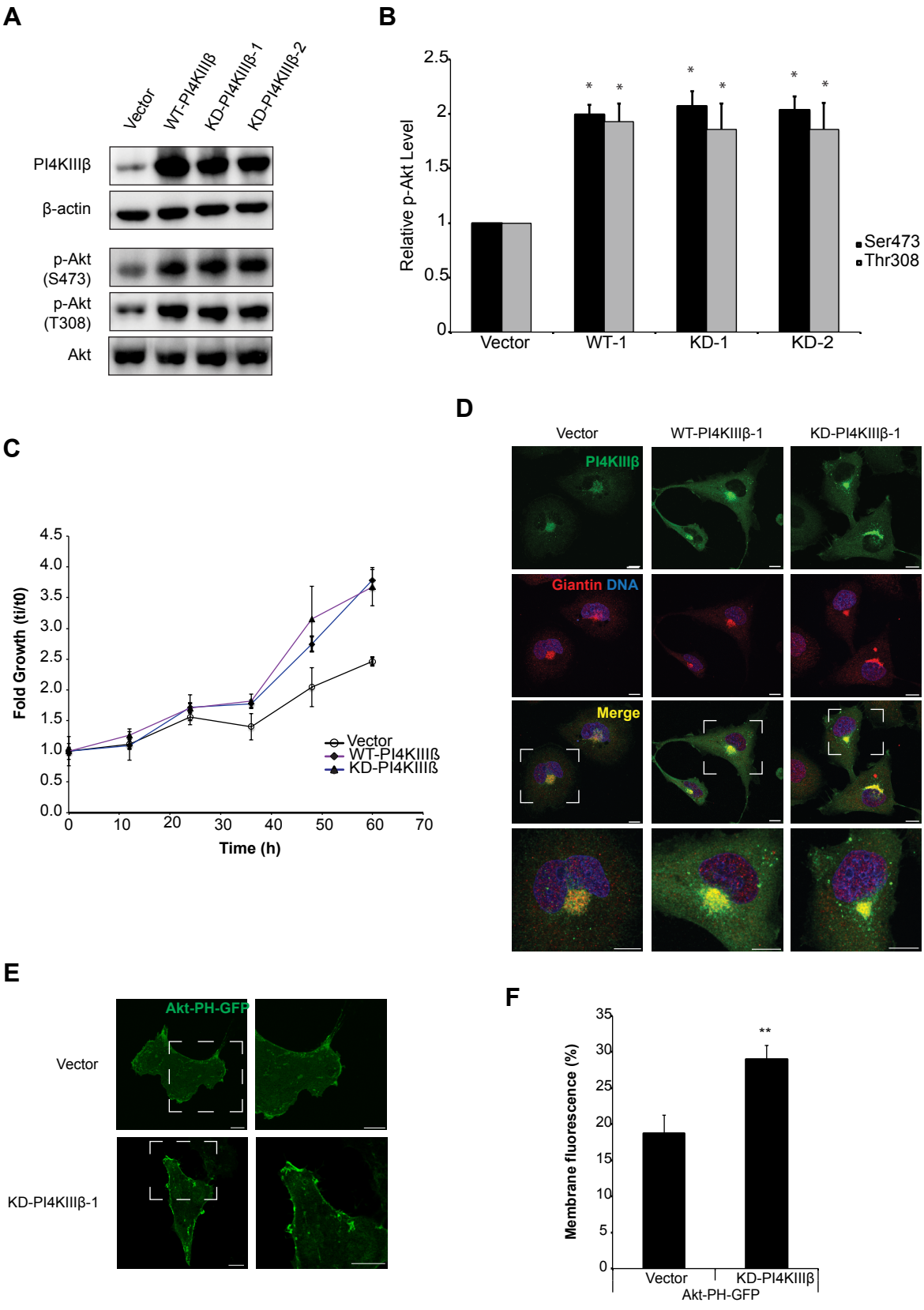
A
Vector
WT-PI4KIIIβ
KD-PI4KIIIβ-1
KD-PI4KIIIβ-2
PI4KIIIβ
β-actin
p-Akt (S473)
p-Akt (T308)
Akt
B
Relative p-Akt Level
2.5
2
1.5
1
0.5
0
Vector
WT-1
KD-1
KD-2
Ser473
Thr308
C
Fold Growth (ti/t0)
4.5
4.0
3.5
3.0
2.5
2.0
1.5
1.0
0.5
0.0
0
10
20
30
40
50
60
70
Time (h)
Vector
WT-PI4KIIIß
KD-PI4KIIIß
D
Vector
WT-PI4KIIIβ-1
KD-PI4KIIIβ-1
PI4KIIIβ
Giantin DNA
Merge
E
Akt-PH-GFP
Vector
KD-PI4KIIIβ-1
F
Membrane fluorescence (%)
35
30
25
20
15
10
5
0
**
Vector
KD-PI4KIIIβ
Akt-PH-GFP

of KD-PI4KIIIβ did not alter the subcellular localization of PI4KIIIβ protein in our cell system. We found that in all cell lines, the PI4KIIIβ protein co-localized with the cis-medial Golgi marker Giantin and could also be observed in the cytoplasm (Fig 3.7D). As expected, the Golgi and cytoplasmic pools of PI4KIIIβ appear more abundant in cells ectopically expressing either WT- or KD-PI4KIIIβ as compared to vector controls. Importantly, no dramatic differences in PI4KIIIβ cellular distribution were detected between the cells ectopically expressing either WT- or KD-PI4KIIIβ.

We next investigated whether KD-PI4KIIIβ-expressing cells showed increased $PI(3,4,5)P_3$ plasma membrane abundance, similarly to WT-PI4KIIIβ expressing cells. To this end, cells were transfected with the $PI(3,4,5)P_3/PI(3,4)P_2$ reporter construct, Akt-PH-GFP. A significant increase in cell membrane association of the GFP-Akt-PH reporter was detected in the KD-PI4KIIIβ-expressing cells, as compared to vector controls ($p < 0.01$, Student's *t*-test) (Fig. 3.7D-E). This increase in $PI(3,4,5)P_3$ reporter plasma membrane recruitment is similar in amplitude (~ 10%) to that observed in WT-PI4KIIIβ-overexpressing cells (Fig. 3.3C). Thus, ectopic expression of a kinase inactive PI4KIIIβ also has the capacity to increase the plasma membrane abundance of $PI(3,4,5)P_3$ and increase Akt activation in breast cancer cells, to similar levels observed in cells ectopically expressing the wild type PI4KIIIβ protein.

3.3.4 A role for Rab11 in PI4KIIIβ-mediated Akt activation

As we determined that the kinase function of PI4KIIIβ is not necessary for Akt activation it was likely that an accessory PI4KIIIβ binding protein was involved in this activation process. The endosomal trafficking protein, Rab11, was an attractive candidate as it had already been shown to bind PI4KIIIβ independently of kinase activity (126, 137). We

first verified that PI4KIIIβ and Rab11 interact in our cells lines by co- immunoprecipitation. Rab11 co-immunoprecipiated with PI4KIIIβ in the vector control, WT-PI4KIIIβ-overexpressing and KD-PI4KIIIβ-expressing cell lines, with a greater amount of Rab11 found with PI4KIIIβ in the cell lines ectopically expressing WT- or KD-PI4KIIIβ, suggesting that a proportion of exogenous PI4KIIIβ interacts with Rab11 in these cell lines (Fig 3.8A). This interaction between PI4KIIIβ and Rab11 was visualized by immunofluorescence in the vector control, WT-PI4KIIIβ-overexpressing and KD-PI4KIIIβ-expressing BT549 cells, which were transfected with Rab11-GFP (Fig. 3.8B). Quantification of the Pearson's correlation coefficient (*r*) for PI4KIIIβ and Rab11-GFP shows a significant increase in the colocalization of these two proteins in WT- PI4KIIIβ-overexpressing and KD-PI4KIIIβ-expressing cells, as compared to vector control cells ($p < 0.01$, Student's *t*-test) (Fig. 3.8C). Furthermore, in the WT-PI4KIIIβ-overexpressing and KD-PI4KIIIβ-expressing cells, PI4KIIIβ appears to co-localize with the recycling endosome marker, the transferrin receptor (TfR), to a greater degree than in vector control cells (Fig. 3.9A). A significant increase in the Pearson's correlation coefficient (*r*) for PI4KIIIβ and the transferrin receptor was also detected in the WT-PI4KIIIβ-overexpressing and KD-PI4KIIIβ-expressing cells, as compared to the vector control cells ($p < 0.01$, Student's *t*-test) (Fig. 3.9B). This suggests that PI4KIIIβ and Rab11 recruitment to recycling endosomes is enhanced in cells with increased PI4KIIIβ expression.

We then examined the localization of Rab11 in the expressing cell lines by live cell imaging. Cells were transfected with Rab11-GFP and GalT-CFP to mark the TGN. Rab11 localizes to the TGN, early and recycling endosomes (142). Still images taken during live cell imaging show that Rab11 distribution is altered in cells ectopically expressing either WT- or KD-PI4KIIIβ (Fig.3.10A). In vector control cells Rab11 is detected primarily in the

Figure 3.8: PI4KIIIβ interacts with Rab11 in vector control, WT-PI4KIIIβ-overexpressing and KD-PI4KIIIβ expressing cells.

A. Co-immunoprecipitation (Co-IP) was performed on whole cell lysates of vector control, WT- PI4KIIIβ-overexpressing and KD-PI4KIIIβ-expressing BT549 cells. Each lane contains 10 µg of total protein. Co-IP was performed using a PI4KIIIβ specific antibody. Agarose beads alone were used as a negative control. Interacting proteins were identified by Western blot using PI4KIIIβ and Rab11 antibodies. **B.** Confocal images of Rab11-GFP and PI4KIIIβ (red) in the vector control, WT- PI4KIIIβ-overexpressing and KD-PI4KIIIβ-expressing BT549 cells. Scale bars represent 10 µm. **C.** The Pearson's correlation coefficient (*r*) for PI4KIIIβ and Rab11-GFP in the vector control, WT-PI4KIIIβ-overexpressing and KD-PI4KIIIβ-expressing BT549 cells. Data is presented as the mean ± S.E.M. for 15 cells imaged from three independent experiments for each cell line. Statistical significance ($p < 0.01$, Student's *t*-test) is indicated by (**).

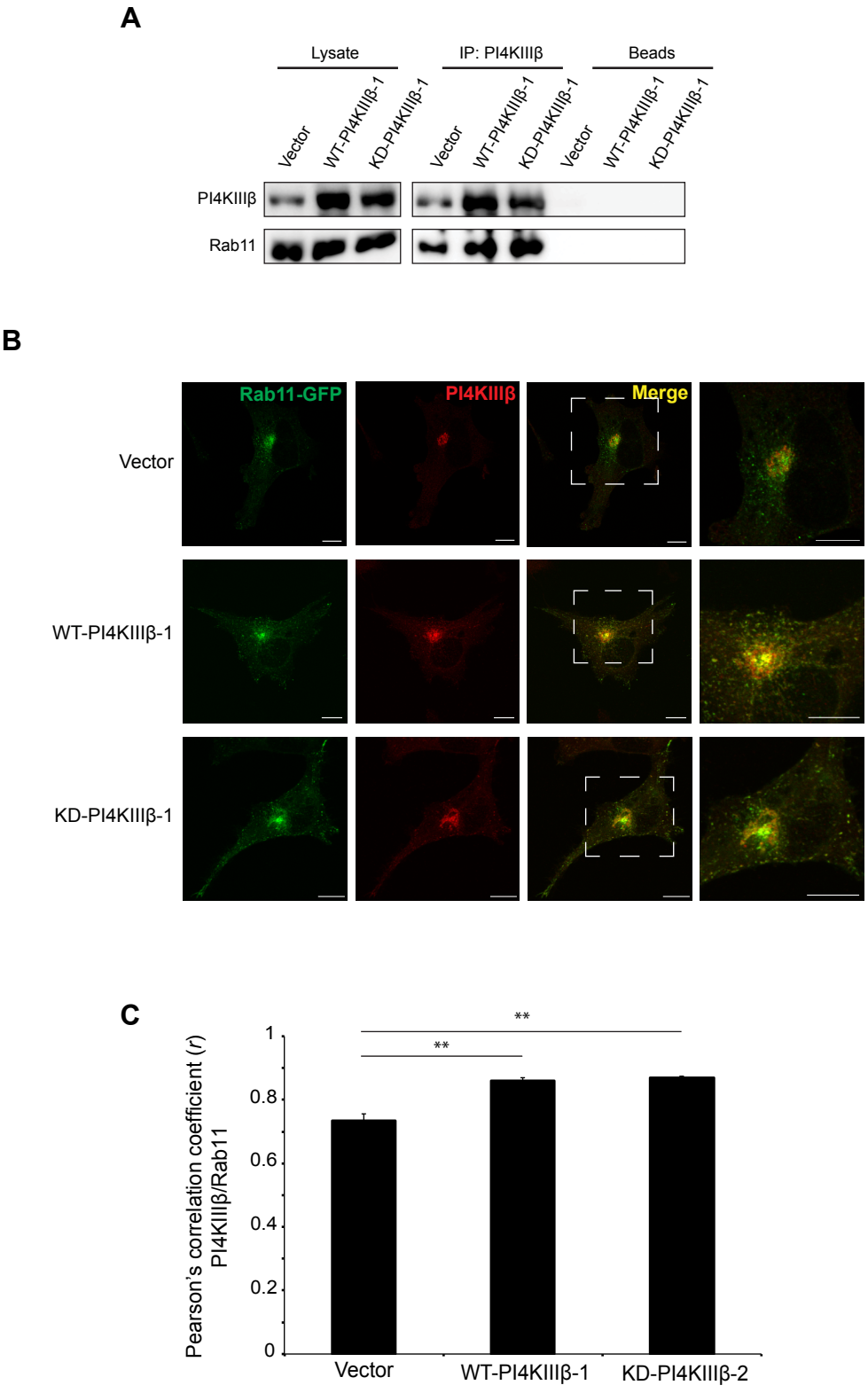
A
Lysate
IP: PI4KIIIβ
Beads
Vector
WT-PI4KIIIβ-1
KD-PI4KIIIβ-1
Vector
WT-PI4KIIIβ-1
KD-PI4KIIIβ-1
Vector
WT-PI4KIIIβ-1
KD-PI4KIIIβ-1
PI4KIIIβ
Rab11
B
Rab11-GFP
PI4KIIIβ
Merge
Vector
WT-PI4KIIIβ-1
KD-PI4KIIIβ-1
C
Pearson's correlation coefficient (r)
PI4KIIIβ/Rab11
1
0.8
0.6
0.4
0.2
0
**
**
Vector
WT-PI4KIIIβ-1
KD-PI4KIIIβ-2

Figure 3.9: Ectopic expression of either WT- or KD-PI4KIIIβ enhances the recruitment of PI4KIIIβ to recycling endosomes.

A. Confocal images of PI4KIIIβ (green) and the recycling endosome marker, transferrin receptor (red), in the vector control, WT- PI4KIIIβ-overexpressing and KD-PI4KIIIβ expressing BT549 cell lines. Scale bar indicates 10 μm. **B.** The Pearson's correlation coefficient (*r*) for PI4KIIIβ and the transferrin receptor (TfR) in the vector control, WT-PI4KIIIβ-overexpressing and KD-PI4KIIIβ expressing BT549 cell lines. Data is presented as the mean +/- S.E.M. for 15 cells imaged from three independent experiments for each cell line. Statistical significance ($p < 0.01$, Student's *t*-test) is indicated by (**).

A

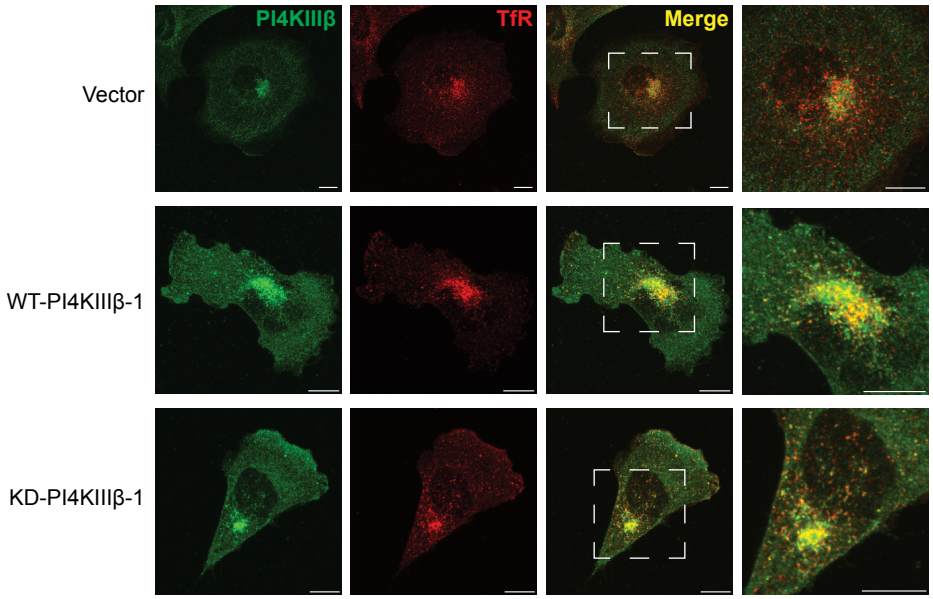
PI4KIIIβ
TfR
Merge
Vector
WT-PI4KIIIβ-1
KD-PI4KIIIβ-1

B

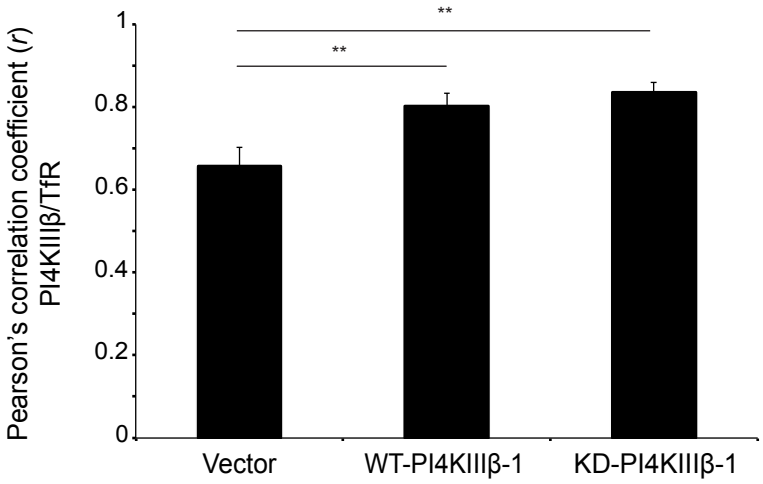
Pearson's correlation coefficient (r)
PI4KIIIβ/TfR
1
0.8
0.6
0.4
0.2
0
**
**
Vector
WT-PI4KIIIβ-1
KD-PI4KIIIβ-1

Figure 3.10: Ectopic expression of either WT- or KD-PI4KIIIβ alters the cellular distribution of Rab11.

A. Confocal images taken during live cell imaging of vector control, WT- PI4KIIIβ-overexpressing and KD-PI4KIIIβ expressing BT549 cells co-transfected with Rab11-GFP and GalT-CFP (trans-Golgi network marker; pseudo-coloured magenta). Scale bars indicate 10 μm. **B.** Quantification of the Golgi and extra-Golgi distribution of GFP-Rab11 in vector control, WT- PI4KIIIβ-overexpressing and KD-PI4KIIIβ-expressing BT549 cells, presented as the mean, ± S.E.M., proportion of total cellular GFP fluorescence in 15 cells from each cell line. Statistical significance ($p < 0.05$, Student's *t*-test) is indicated by (*).

A

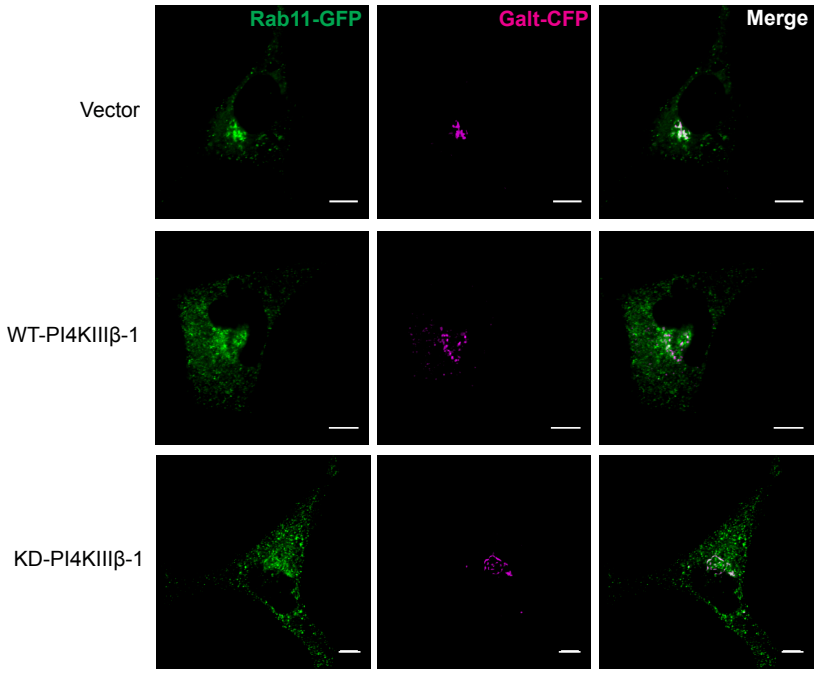
Rab11-GFP
Galt-CFP
Merge
Vector
WT-PI4KIIIβ-1
KD-PI4KIIIβ-1

B

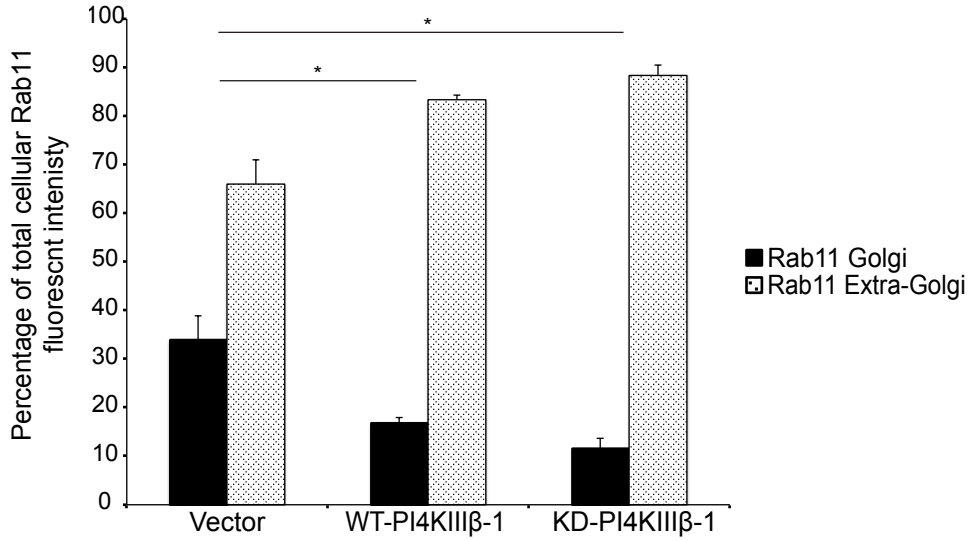
Percentage of total cellular Rab11 fluorescnt intenisty
100
90
80
70
60
50
40
30
20
10
0
*
*
Vector
WT-PI4KIIIβ-1
KD-PI4KIIIβ-1
Rab11 Golgi
Rab11 Extra-Golgi

Golgi. In WT-PI4KIIIβ-overexpressing and KD-PI4KIIIβ-expressing cells, Rab11 shows a broader punctate distribution in addition to Golgi localization. Rab11 Golgi versus extra-Golgi distribution was quantified and showed a significant shift from Golgi to extra-Golgi localization in WT-PI4KIIIβ-overexpressing and KD-PI4KIIIβ-expressing cells, as compared to vector control cells ($p < 0.05$, Student's *t*-test) (Fig. 3.10B). This indicates that enhanced expression of PI4KIIIβ, either WT or a KD mutant, relocalizes Rab11 from the Golgi to a broader punctate cellular distribution. This suggests that enhanced PI4KIIIβ expression shifts Rab11 localization from the Golgi onto endosomes.

To determine if the PI4KIIIβ/Rab11 interaction might be involved in PI4KIIIβ-mediated Akt activation, the vector control, WT- and KD-expressing cell lines were treated with siRNA against Rab11. Depletion of Rab11 protein led to a consistent and significant decrease (~ 50%) in Akt phosphorylation in all cell lines ($p < 0.05$, Student's *t*-test) (Fig. 3.11A-B). Therefore, loss of Rab11 impairs Akt activation in both the control BT549 breast cancer cells and in those with enhanced PI4KIIIβ expression, suggesting that Rab11 plays a role in mediating the activation of PI3K/Akt signalling.

Figure 3.11: siRNA depletion of Rab11 decreases Akt activation in vector control, WT-PI4KIIIβ-overexpressing and KD-PI4KIIIβ-expressing BT549 cells.

A. Western blot analysis showing Akt phosphorylation at Ser473 and Thr308 in vector control, WT-PI4KIIIβ-overexpressing and KD-PI4KIIIβ-expressing BT549 cells treated with siRNA targeted to Rab11 as compared to cells treated with the negative control siRNA. **B.** Quantification of the relative decrease in Akt phosphorylation in cells treated with siRNA targeted to Rab11 as compared to cells treated with negative control siRNA. Data are presented as mean ± S.E.M. of three independent trials and (*) indicates statistical significance ($p < 0.05$, Student's *t*-test).

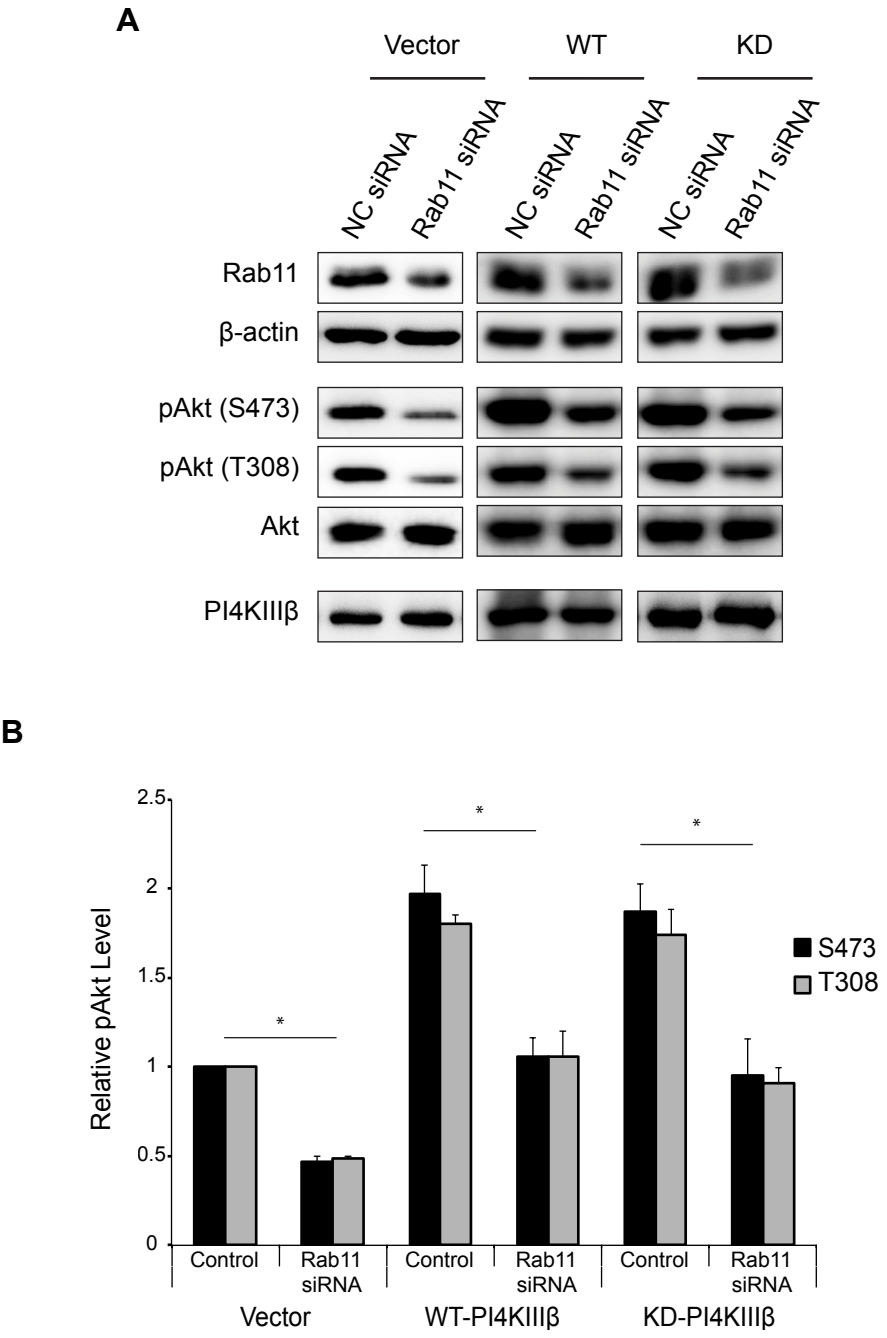
A
Vector
WT
KD
NC siRNA
Rab11 siRNA
NC siRNA
Rab11 siRNA
NC siRNA
Rab11 siRNA
Rab11
β-actin
pAkt (S473)
pAkt (T308)
Akt
PI4KIIIβ
B
Relative pAkt Level
2.5
2
1.5
1
0.5
0
*
*
*
S473
T308
Control
Rab11 siRNA
Control
Rab11 siRNA
Control
Rab11 siRNA
Vector
WT-PI4KIIIβ
KD-PI4KIIIβ

3.4 Discussion

A role for PI4KIIIβ in breast cancer has been recently emerging (146, 162-164, 179). However, the mechanism through which PI4KIIIβ regulates breast oncogenesis has not yet been elucidated. Aberrant expression of the PI4KIIIβ activator and breast oncogene, eEF1A2, activates Akt (157, 163, 164, 168). This suggested that PI4KIIIβ may itself regulate the Akt signalling pathway.

Here we report that enhanced PI4KIIIβ expression increases Akt activation in PTEN-null BT549 cells and the loss of PI4KIIIβ by siRNA silencing decreases Akt activity. This suggests that endogenous PI4KIIIβ is involved in regulating Akt activation in this breast cancer cell line and that enhanced expression of PI4KIIIβ further activates the Akt oncogenic signalling pathway. We also show that this increase in Akt activity is dependent on increased $PI(3,4,5)P_3$ production. Though PI3K-independent modes of Akt activation have been reported (338), our data supports the hypothesis that PI4KIIIβ expression impacts Akt activation upstream of the canonical activation pathway regulated by PI3K.

We also show that Akt phosphorylation levels are returned to control levels in the PI4KIIIβ-overexpressing cells upon expression of PTEN, the phosphatase that antagonises PI3K signalling. This result suggests that PI4KIIIβ expression may have the greatest impact on Akt activation in a PTEN null background. A loss of PTEN expression has been reported in 30-50% of breast cancers, with PTEN loss correlating with lymph node metastasis and disease-related death (339, 340). It is possible that a combination of enhanced PI4KIIIβ expression and PTEN deficiency may help contribute to the aggressive nature of PTEN-null breast tumours.

We found that the enhanced $PI(3,4,5)P_3$ production and Akt activation due to increased PI4KIIIβ expression is unlikely to be driven by changes in abundance or

intracellular localization of PI(4)P and PI(4,5)P_2. No changes in PI(4)P and PI(4,5)P_2 lipid abundance were detected in cells overexpressing PI4KIIIβ, nor were we able to detect substantial changes in cellular lipid distribution using immunofluorescence. It was a surprise to find that enhanced PI4KIIIβ expression did not lead to an overall increase in PI(4)P levels. It is possible that a higher rate of phosphoinositide phosphorylation occurs in cells ectopically expressing PI4KIIIβ but only in a local and transitory manner. Small and/or compartmentalized changes in PI(4)P lipid composition may not have been detectable by HPLC analysis or dramatic enough to be observable by reporter construct imaging or lipid immunostaining. However, the fact that the PI4KIIIβ inhibitor, Pik93, had no effect on PI4KIIIβ-mediated Akt activation and the ability of a catalytically inactive PI4KIIIβ protein to activate Akt rule out a necessary role for PI(4)P in PI4KIIIβ-dependent Akt activation. The work presented here suggests that PI4KIIIβ-mediated Akt activation is not dependent on its catalytic function.

Our data suggests that PI4KIIIβ likely activates Akt in conjunction with Rab11. We demonstrate, that in BT549 cells, Rab11 interacts with PI4KIIIβ in the vector control, WT-PI4KIIIβ-overexpressing and KD-PI4KIIIβ-expressing cell lines, though to a greater extent in the cell lines with enhanced PI4KIIIβ expression. Moreover, down-regulation of Rab11 (using RNAi) inhibits Akt activation. We speculate that PI4KIIIβ activates Akt in concert with Rab11 at the cell's endosomal membranes. Consistent with this idea, PI4KIIIβ was found to co-localize more strongly with the recycling endosomal marker, transferrin receptor, in both the WT- and KD-PI4KIIIβ expressing cell lines. These results suggest that in the overexpressing cell lines, PI4KIIIβ is recruited to recycling endosomes, as they traffic through the TGN. Coupled to the fact that in the WTPI4KIIIβ-overexpressing and KD-PI4KIIIβ-expressing cells the distribution of Rab11 is altered, showing a broader punctate

cellular distribution, this suggests that enhanced expression of PI4KIIIβ leads to greater endosomal recruitment of Rab11 in BT549 cells.

In *Drosophila*, the PI4KIIIβ homologue, four wheel drive (Fwd), has also been previously shown to regulate Rab11 recruitment and trafficking events. More specifically, Fwd is required for Rab11 localization to secretory granules at the midzone of dividing spermatocyte cells, allowing successful completion of cytokinesis (126). Of interest to our study, a non-catalytic role for Fwd in Rab11 regulation was determined as expression of a kinase-dead mutant of Fwd, which also binds to Rab11, partially rescues male *Drosophila* spermatocyte cytokinesis defects in *fwd* null flies.

A role for Rab11 in regulating Akt activation at endosomes has also previously been reported (145). Garcia-Regalado *et al*. showed that the LPA-stimulated interaction between Rab11 and the heteromeric G protein sub-unit Gβγ on intracellular membranes contributes to the recruitment of PI3K and the activation of Akt via phosphorylation on early and recycling endosomes (145). Interestingly, ectopic expression of Rab11a was shown to be sufficient to translocate Gβγ to endocytic structures; with constitutively active Rab11 showing a higher affinity for Gβγ (145). In addition, expression of a dominant-negative Rab11 led to a loss of Gβγ and PI3K recruitment to early and recycling endosomes, suggesting that Rab11 has a critical role in recruiting PI3K to endosomes (145). Therefore, we propose that PI4KIIIβ-dependent recruitment of Rab11 could enhance PI3K and Akt signalling on endosomal vesicles exiting the TGN. Endosomal membranes have been emerging for some time as sites of signal transduction. A number of receptor tyrosine kinases (RTKs) have been demonstrated to signal from endosomes (341). For example, it has been reported that in adipocytes, insulin-stimulated PI3K activation, via phosphorylation of insulin receptor substrate (IRS-1), occurs preferentially in internal membranes rather than at the plasma

membrane (342). Endosome specific signalling of EGFR has also been shown to activate PI3K/Akt signalling (343, 344). In addition, the endosomal proteins adaptor protein, phosphotyrosine interaction, PH domain and leucine zipper containing 1 (Appl1) and EEA1 have been shown to regulate Akt endosome recruitment and activation (345, 346). Furthermore, Sato et al., demonstrated using a targetable probe, that in response to platelet derived growth factor (PDGR), $PI(3,4,5)P_3$, was rapidly produced at the plasma membrane, followed by accumulation in endomembranes of Chinese hamster ovary (CHO) cells (347). They further showed that $PI(3,4,5)P_3$ was produced *in situ* in endomembranes, a process stimulated by receptor tyrosine kinase endocytosis. This previously published work sets a precedence for endosome localized PI3K/Akt activation, with a specific role for Rab11 reported in directing Akt activation on these internal membranes. We believe that the interaction between PI4KIIIβ and Rab11 at the TGN and on endosomal membranes is likely regulating Akt activation on endosomes themselves. We speculate that PI4KIIIβ is co-operating with Rab11 to increase Akt activation through one or more membrane receptors and subcellular PI3K signalling in breast cancer cells. Rab GTPases have been previously linked to breast cancer oncogenesis in their role as central regulators of cell trafficking (140, 348, 349).

It is important to note that Rab11 siRNA depletion leads to a similar decrease in Akt activation in vector control cells as well as in cells ectopically expressing either WT- or KD-PI4KIIIβ. We have shown that endogenous PI4KIIIβ plays a role in Akt activation, as siRNA depletion of PI4KIIIβ in BT549 parental cells impairs Akt activation. Thus, it is anticipated that, similarly, loss of Rab11, as a putative downstream effector of PI4KIIIβ in the regulation of Akt signalling, would impair Akt activation in cells without PI4KIIIβ overexpression. Even in the cell lines with Rab11 expression decreased, Akt phosphorylation in PI4KIIIβ-

overexpressing cells is greater than the levels observed in vector control cells. This could be due to the fact that the Rab11 knockdown is only partial, leaving sufficient Rab11 remaining to interact with the exogenous PI4KIIIβ in the overexpressing cell lines, to together drive increased Akt activation. Further work needs to be done to conclusively say whether Rab11 is acting downstream of PI4KIIIβ in the regulation of Akt activation. An important experiment to perform would be to study what effect ectopic expression of a mutant PI4KIIIβ, deficient in Rab11 binding, has on Akt activation, Another, would be to express a dominant negative Rab11 in the PI4KIIIβ-overexpressing cells to determine if this leads to a loss of PI4KIIIβ-mediated Akt activation. In addition, expression of a constitutively active Rab11 should lead to increased Akt activation, even when PI4KIIIβ expression is knocked down using siRNA, if Rab11 is truly acting downstream of PI4KIIIβ.

In conclusion, we find that enhanced PI4KIIIβ expression in BT549 breast cancer cells activates Akt signalling and that PI4KIIIβ overexpression leads to PI3K/Akt activation independently of its kinase function, and likely via its interaction with the endosomal trafficking protein Rab11.

CHAPTER 4: GENERAL DISCUSSION

4.1 Summary of Thesis

Recent findings have implicated PI4KIIIβ in breast cancer. PI4KIIIβ has been reported genetically amplified in breast tumours (178). Dr. Lee's research group has previously found that PI4KIIIβ is a downstream effector of the breast cancer oncogene, eEF1A2, which is aberrantly expressed in 60% of breast tumours (146, 147, 163, 164). Additionally, our laboratory has also reported that PI4KIIIβ overexpression disrupts breast epithelial cell *in vitro* morphogenesis (179). Furthermore, PI4KIIIβ expression has been reported to inhibit apoptosis in breast cancer cells (180). However, whether PI4KIIIβ protein is upregulated in breast tumours and the specific oncogenic processes regulated by PI4KIIIβ remained to be determined. Thus, the focus of my research has been on investigating the mechanism of oncogenesis of PI4KIIIβ in breast cancer.

As PI4KIIIβ protein expression was found to be increased in ~20% of primary human breast tumours, the first aim of my research was to identify a role for PI4KIIIβ protein expression in breast cancer. Ectopic expression of eEF1A2, a PI4KIIIβ activator, in breast cancer cells leads to enhanced filopodia formation, enhanced cell migration and increased activation of the pro-proliferative kinase Akt (168). Therefore, I wanted to determine whether PI4KIIIβ expression itself could impact filopodia formation, cell migration and proliferation in breast cancer cells. I found that ectopic expression of PI4KIIIβ increases filopodia formation in both human breast cancer and rodent fibroblast cells. Enhanced PI4KIIIβ expression is not sufficient, however, to increase the migration rate of breast cancer cells. PI4KIIIβ overexpression does enhance the *in vitro* proliferative capacity of breast cancer cells. Therefore, enhanced PI4KIIIβ expression is likely implicated in breast tumour progression and impacts both breast cancer cell architecture and proliferation *in vitro*.

The second aim of my thesis examined the role of PI4KIIIβ in Akt activation. I found that PI4KIIIβ expression regulates Akt activation in BT549 invasive human ductal epithelial breast cancer cells. Overexpression of PI4KIIIβ increases Akt activation and, concomitantly, its siRNA depletion decreases Akt activation. PI4KIIIβ likely activates Akt via canonical PI3K signalling, as enhanced PI4KIIIβ expression leads to increased abundance of $PI(3,4,5)P_3/PI(3,4)P_2$ at the plasma membrane. Concordantly, PI4KIIIβ-mediated Akt activation is lost upon reintroduction of functional PTEN, a $PI(3,4,5)P_3/PI(3,4)P_2$ lipid phosphatase, in the PTEN-null BT549 breast cancer cell line. Upstream of $PI(3,4,5)P_3$, PI(4)P and $PI(4,5)P_2$ cellular lipid levels and distribution are not detectably altered by ectopic expression of PI4KIIIβ. In addition, treatment of the BT549 cells with a PI4KIIIβ inhibitor, Pik93, does not affect PI4KIIIβ-mediated Akt activation. Together, this data suggests that ectopic PI4KIIIβ expression activates PI3K and Akt independently from its ability to synthesize PI(4)P lipid in BT549 breast cancer cells. Supporting the hypothesis that PI4KIIIβ is regulating Akt activation independently of its kinase function, ectopic expression of a catalytically inactive PI4KIIIβ mutant protein also leads to increased Akt activation and plasma membrane abundance of $PI(3,4,5)P_3/PI(3,4)P_2$. It appears likely that PI4KIIIβ is mediating Akt activation through an interacting protein, the small GTPase, Rab11. Enhanced expression of PI4KIIIβ leads to increased amount of Rab11 binding to PI4KIIIβ and enhances the co-localization of PI4KIIIβ with a recycling endosome marker. This suggests that enhanced PI4KIIIβ expression is leading to greater localization of PI4KIIIβ and Rab11 to recycling endosomes. Furthermore, siRNA depletion of Rab11 leads to a decrease in Akt activation, suggesting that these two proteins work in concert to activate Akt through a cell trafficking mechanism. Therefore enhanced PI4KIIIβ expression likely plays a role in activating PI3K/Akt signalling in breast tumours. My work reveals a novel

role for PI4KIIIβ in Akt activation, in a manner that appears to be independent of the lipid kinase's catalytic function but is dependent on Rab11.

4.2 A Role for PI4KIIIβ in Filopodia Formation

As described in chapter 2, enhanced expression of PI4KIIIβ induces filopodia formation in both Rat2 rodent fibroblast cells and BT549 breast cancer cells. Phosphoinositides have been shown to play important roles in the regulation of filopodia initiation and growth (200, 222). However, PI4KIIIβ is likely regulating filopodia polymerization through different mechanisms in these two cell types. I hypothesize that PI4KIIIβ contributes to filopodia formation in two ways: one dependent on phosphoinositide generation and the other independent of its kinase activity.

In Rat2 cells, previous work published by our laboratory shows that the PI4KIIIβ activator, eEF1A2, regulates filopodia formation through the small GTPase Cdc42 (147). eEF1A2 expression also leads to enhanced PI(4,5)P_2 cellular abundance and plasma membrane localization (147). Cdc42 and PI(4,5)P_2 have well established roles in regulating actin filament growth through WASP protein activation, which leads to Arp2/3 complex-mediated actin nucleation (210, 222). In addition, PI(4,5)P_2 promotes actin polymerization by regulating the function of a number of actin-binding proteins (200). Using mutant constructs, our laboratory has also previously shown that eEF1A2-mediated filopodia formation is dependent on the protein's interaction with PI4KIIIβ and PI4KIIIβ overexpression is sufficient to lead to an increase in PI(4,5)P_2 plasma membrane accumulation (147). Together, these results suggest that, in Rat2 cells, enhanced activation of PI4KIIIβ by eEF1A2 and enhanced expression of PI4KIIIβ lead to an increase in PI(4,5)P_2 pools at the plasma membrane. This increase in plasma membrane PI(4,5)P_2 could then

increasingly activate N-WASP, in concert with Cdc42, which would drive more Arp2/3 complex actin nucleation and produce longer and more numerous filopodia (45, 210).

It may appear surprising that a Golgi localized enzyme such as PI4KIIIβ could be responsible for the generation of $PI(4,5)P_2$ at the plasma membrane. Balla et al. showed that PI4KIIIα, which localizes to the ER in mammalian cells, is responsible for the generation of plasma membrane pools of PI(4)P and $PI(4,5)P_2$ during PLC activation in agonist stimulated cells, leading to IP_3 and Ca^{2+} signalling (106). In addition, it has been reported that plasma membrane pools of $PI(4,5)P_2$ are independently regulated from plasma membrane pools of PI(4)P (350, 351). In effect, Hammond et al. showed that plasma membrane PI(4)P is not required for the maintenance of plasma membrane $PI(4,5)P_2$ (351). Depletion of plasma membrane PI(4)P, using a targetable Sac phosphatase, very minimally altered levels of plasma membrane $PI(4,5)P_2$ and had no effect on the endocytosis of clathrin, generation of Ca^{2+}-mobilizing IP_3 or in the generation of $PI(3,4,5)P_3$/$PI(3,4)P_2$ (351). The authors postulated that plasma membrane PI(4)P and $PI(4,5)P_2$ may have independent signalling functions. Proteins can be targeted to the plasma membrane through basic clusters that interact with negatively charged phosphoinositide headgroups (8). A steady state plasma membrane pool of PI(4)P may primarily be responsible for this electrostatic interaction targeting proteins to the plasma membrane (351). This raises the possibility that specific signalling pools of plasma membrane $PI(4,5)P_2$ are generated from PI(4)P delivered from internal organelle membranes. I propose that PI4KIIIβ may be trafficking PI(4)P to the plasma membrane in vesicles derived from the TGN for $PI(4,5)P_2$ generation. $PI(4,5)P_2$ may be generated at the plasma membrane or on endosomes themselves by PI(4)P 5-kinases (352). As PI4KIIIβ is not an integral Golgi protein but a soluble protein recruited to the

Golgi by Arf1 (113), it is also possible that eEF1A2 expression or PI4KIIIβ overexpression mislocalize the protein to other cellular membranes, which facilitates the generation of plasma membrane pools of $PI(4,5)P_2$.

PI4KIIIβ-generated PI(4)P at the Golgi and $PI(4,5)P_2$ may also play an indirect role in regulating filopodia production through vesicular trafficking. Enhanced PI4KIIIβ catalytic activity leads to increased transport to the plasma membrane, demonstrating a direct role for PI4KIIIβ derived PI(4)P in vesicular transport (134, 353). PI(4)P has been shown to regulate vesicular trafficking by mediating a number of interactions. PI(4)P recruits clathrin-coated vesicle (CCV)-associated proteins, such as AP-1, GGAs and EpsinR, as well as binding the lipid transfer proteins CERT, FAPP1 and FAPP2 (19, 31, 34, 354). PI(4)P also binds GOLPH3, which connects the Golgi to F-actin, as GOLPH3 binds myosin MYO18A (28). This conveys a tensile force required for efficient vesicle budding (28). $PI(4,5)P_2$ also regulates vesicular trafficking by regulating both endocytosis and exocytosis. $PI(4,5)P_2$ regulates endocytosis as a co-receptor for the endocytic clathrin adaptors AP-2 and epsin and as a regulator of dynamin catalysed membrane fission (18, 56, 57). $PI(4,5)P_2$ regulates exocytosis, by acting on both plasma membrane and vesicle proteins at a pre-fusion stage (50, 51). Enhanced vesicular trafficking, due to more abundant cellular $PI(4,5)P_2$ and PI(4)P, could impact filopodia formation through increased delivery of filopodial components to the leading edge, as the formation of membrane protrusions is supported by vesicle delivery and recycling (355). Most vesicular trafficking is regulated by soluble N-ethylmaleimide-sensitive factor activating protein receptor (SNARE) proteins (356). Inhibition of SNARE-mediated membrane traffic has been shown to lead to a decrease in cell protrusions and migration (356), demonstrating the importance of cell trafficking in the formation of

membrane protrusions. Vesicles directed to nascent filopodia deliver new membrane for extension (357, 358). They also supply membrane protrusions with necessary molecular components. Integrins, cell surface adhesion receptors that bind the ECM, are constantly endocytosed from the retracting end of a motile cell and recycled for exocytosis at the leading edge (359). There is also evidence that the N-WASP/Cdc42 complex, which drives filopodia protrusions, is assembled at the perinuclear recycling compartment (also termed the endocytic recycling compartment (ERC)) in breast cancer cells (360), which suggests a role for the slow recycling pathway in filopodia formation through the regulation of the actin nucleation promoting N-WASP/Cdcd42 complex assembly.

As Rat2 cells ectopically expressing PI4KIIIβ have been shown to have an increase in PI(4,5)P_2 plasma membrane lipid abundance (147), it is likely that this overexpression is driving filopodia formation via PI(4,5)P_2 and possibly via PI(4)P lipid production. A model depicting the possible phosphoinositide-driven mechanisms of PI4KIIIβ-mediated filopodia production in Rat2 cells is depicted in Fig. 4.1A. Enhanced PI(4,5)P_2 abundance at the plasma membrane promotes filopodia production through the WASP/Arp2/3 complex actin nucleating pathway (Fig. 4.1A (i)). Enhanced PI(4,5)P_2 and PI(4)P abundance on Golgi-derived vesicles could also impact filopodia formation by enhancing the trafficking of filopodial components to sites of membrane protrusions (Fig. 4.1A (ii)). It is important to note that though PI(4,5)P_2 levels have been reported elevated in PI4KIIIβ-overexpressing Rat2 cells (147), it remains to be conclusively determined whether this is in fact due to an increase in PI(4)P lipid precursor or whether it may be through an alternative mechanism, such as increased activation of PI(4)P 5-kinases or inhibition of INPP5 phosphatases.

Unlike in Rat2 cells, PI4KIIIβ-mediating filopodia formation is likely not through

Figure 4.1: Models depicting the possible roles of PI4KIIIβ in filopodia formation.

A. Phosphoinositide-dependent mechanisms by which enhanced PI4KIIIβ expression could drive filopodia formation. **(i)** Enhanced PI(4,5)P_2 abundance at the plasma membrane promotes filopodia formation through activation of WASP, in concert with Cdc42, and induction of Arp2/3 actin polymerization. **(ii)** Enhanced PI(4)P and PI(4,5)P_2 abundance on Golgi-derived vesicles could enhance the trafficking of integrins and N-WASP/Cdc42 complex to sites of membrane protrusions. **B.** Non-catalytic roles for PI4KIIIβ in promoting filopodia formation. **(i)** Enhanced PI(3,4,5)P_3 plasma membrane abundance leads to the recruitment of Cdc42 GEFs (Vav/Asef) that activate Cdc42, leading to WASP activation, and Arp2/3 actin polymerization, as well as IRSp53 recruitment and induction of membrane protrusions. **(ii)** Enhanced PI(3,4,5)P_3 plasma membrane abundance also leads to the activation of Myosin X, which promotes filopodial extensions by delivering integrins and ENA/VASP proteins to the tips of filopodia. **(iii)** Enhanced PI4KIIIβ-directed recruitment of Rab11 to recycling endosomes could increase the provision of integrins to sites of membrane protrusions.

A

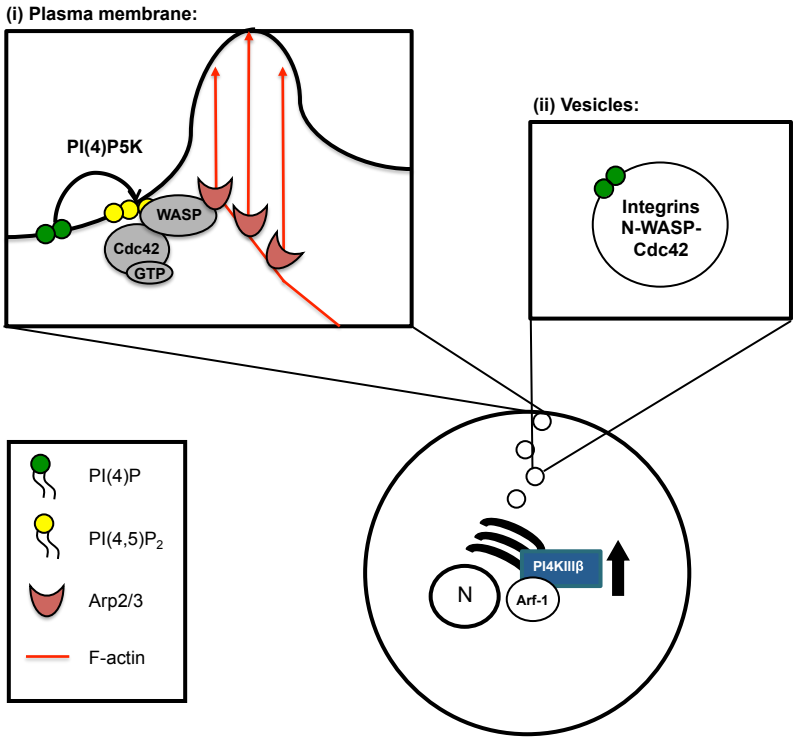
(i) Plasma membrane:
PI(4)P5K
WASP
Cdc42
GTP
(ii) Vesicles:
Integrins
N-WASP-
Cdc42
PI(4)P
PI(4,5)P2
Arp2/3
F-actin
PI4KIIIβ
N
Arf-1

B

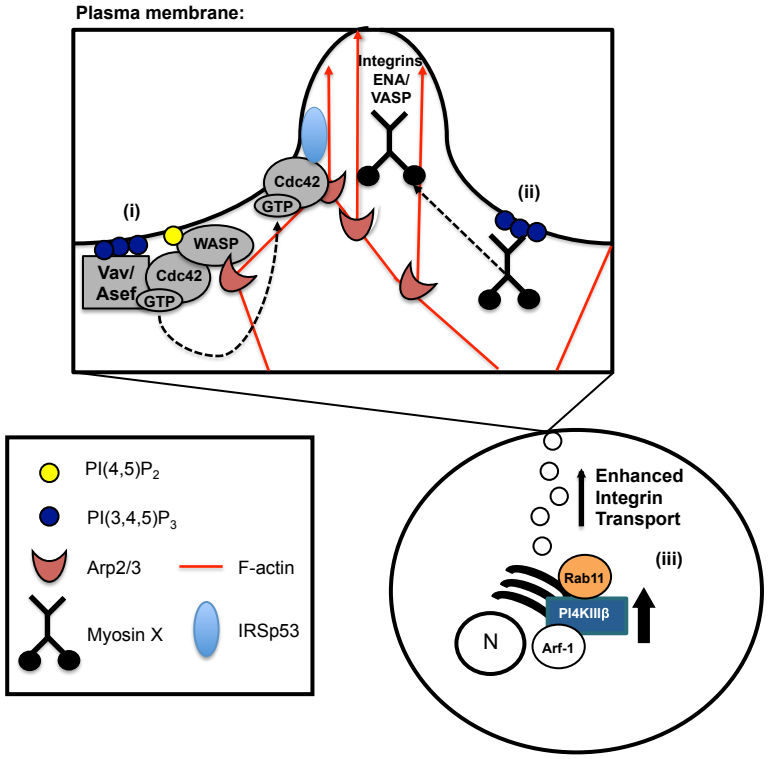
Plasma membrane:
Integrins
ENA/
VASP
Cdc42
GTP
(i)
WASP
Vav/
Asef
Cdc42
GTP
(ii)
PI(4,5)P2
PI(3,4,5)P3
Arp2/3
F-actin
Myosin X
IRSp53
Enhanced
Integrin
Transport
(iii)
Rab11
PI4KIIIβ
N
Arf-1

$PI(4,5)P_2$ production in BT549 breast cancer cells. This hypothesis is based on the oberservation that BT549 cells overexpressing PI4KIIIβ show no change in PI(4)P or $PI(4,5)P_2$ lipid abundance or localization, as was shown in the HPLC analysis, phosphoinositide reporter imaging and immunostaining presented in chapter 2. This suggests that, in these breast cancer cells, enhanced PI4KIIIβ expression is not leading to the generation of more $PI(4,5)P_2$. It remains however to be determined experimentally, whether ectopic expression KD-PI4KIIIβ has any effect on filopodia production. PI4KIIIβ is activated by PKD phosphorylation and by interacting partners such as NCS-1 (115, 117, 134). It is possible that in PI4KIIIβ-overexpressing BT549 cells, ectopic PI4KIIIβ protein may not have access to the factors and interacting partners necessary for activation. It is also possible that excess PI(4)P is being rapidly converted back to PtdIns by Sac1 in BT549 cells. As a consequence, PI4KIIIβ overexpression is likely regulating filopodia formation independently of its lipid kinase activity in BT549 cells. In chapter 3, enhanced PI4KIIIβ expression was shown to generate, in a kinase independent fashion, an increase in plasma membrane $PI(3,4,5)P_3$ abundance, as well as an increase in Rab11 recruitment to recycling endosomes. Both $PI(3,4,5)P_3$ and Rab11 have been shown to impact the processes of actin filament initiation and growth and could mediate PI4KIIIβ-directed filopodia formation independently of the enzyme's kinase activity in BT549 breast cancer cells (Fig. 4.1B).

$PI(3,4,5)P_3$ phospholipids can regulate filopodia formation by two distinct mechanisms, one involving Cdc42 and the other myosin X. First, $PI(3,4,5)P_3$ regulates Cdc42 activation (Fig 4.1B (i)). Cdc42 is active in its GTP bound state and GEFs facilitate the exchange of GDP for GTP (66). The Cdc42 GEFs Vav and Asef are both recruited by $PI(3,4,5)P_3$ via their PH domains (361, 362). Therefore, increased plasma membrane pools of

$PI(3,4,5)P_3$ would lead to enhanced Cdc42 GEF recruitment, increased Cdc42 activation, and along with $PI(4,5)P_2$, induce WASP/Arp2/3-mediated actin nucleation (210). Additionally, active Cdc42 can also direct filopodia formation, through its interaction with IRSp53, which promotes membrane curvature via its I-BAR domain and filopodia protrusions by binding WAVE2 and the ENA/VASP protein MENA (192, 212, 213). Secondly, activation of the myosin X motor protein is mediated by $PI(3,4,5)P_3$ (Fig. 4.1B (ii)). Myosin X binds to $PI(3,4,5)P_3$ via a PH domain in its tail, inducing a change in conformation which activates the cargo transporter function of Myosin X. Myosin X regulates filopodia formation by delivering ENA/VASP proteins and integrins to the tips of filopodia (218, 363, 364).

Rab11 also plays a role in regulating the production of filopodial protrusions (Fig. 4.1B (iii)). Rab11 has been shown to regulate the slow endosomal recycling of key filopodial components from the perinuclear recycling compartment to the plasma membrane (142, 365, 366). Several integrins have been shown to recycle to the plasma membrane via the Rab11-positive perinuclear recycling compartment (366, 367). In addition, the N-WASP/Cdc42 complex has been shown to assemble at the perinuclear recycling compartment and as Rab11 controls recycling at the perinuclear recycling compartment, it likely regulates the delivery of this complex to the plasma membrane as well (360, 368). Furthermore, Rab11-dependent recycling appears to be necessary for the migration of different cell types (349, 366, 369, 370). As membrane protrusions guide directed cell migration, Rab11 likely has a vital role in providing cell protrusion components to the leading edge of a motile cell via the endocytic recycling pathway.

Therefore, PI4KIIIβ likely has the capacity to regulate filopodia production through several different pathways, some of which are dependent on the enzyme's kinase activity and

others can be regulated independently of its kinase activity. It is possible that PI4KIIIβ can regulate filopodia formation in different ways depending on the cell context in which PI4KIIIβ is expressed. How PI4KIIIβ has the capacity to enhance $PI(3,4,5)P_3$ lipid generation and alter Rab11 function independently of its kinase function will be explored in more detail in the following section.

4.3 A Role for PI4KIIIβ in Akt Activation

In chapter 3, enhanced expression of PI4KIIIβ was shown to increase activation of PI3K/Akt signalling in the BT549 breast cancer cell line. The increased activation of this pro-proliferative kinase likely explains why BT549 cells ectopically expressing PI4KIIIβ were found to have increased *in vitro* proliferative capacity in chapter 2. PI4KIIIβ appears to activate PI3K/Akt signalling independently of its lipid kinase activity. Rather, PI4KIIIβ-mediated Akt activation is likely dependent on cell trafficking via Rab11, as enhanced expression of PI4KIIIβ alters the cellular distribution of Rab11 and siRNA depletion of Rab11 impedes Akt activation. Rab11 has previously been shown to regulate PI3Kγ recruitment to recycling endosomes in HEK-293T, human embryonic kidney cells, leading to enhanced Akt activation on endosomal vesicles in an agonist stimulated, GPCR-regulated fashion (145). A model depicting this Rab11-mediated activation of PI3K and Akt can be seen in Fig. 1.7. As shown in chapter 3, PI4KIIIβ overexpression appears to enhance the recycling endosome localization of Rab11. Coupled to the fact that $PI(3,4,5)P_3$ generation and Akt activation have been shown to occur on endomembranes in a number of studies (345-347), it is likely that enhanced PI4KIIIβ expression is directing Rab11-mediated

PI3K/Akt activation on recycling endosomes. A model depicting how enhanced PI4KIIIβ expression activates Akt via Rab11 on recycling endosomes is presented in Fig. 4.2. We hypothesize that enhanced PI4KIIIβ expression leads to the enhanced recruitment of Rab11to endocytic structures trafficking through the TGN (Fig 4.2 (i)). Rab11 then likely recruits an as yet to be identified PI3K, which leads to enhanced $PI(3,4,5)P_3$ generation and Akt activation on endomembranes (Fig. 4.2 (ii)). Vesicles trafficking to the plasma membrane post Rab11-directed PI3K activation would also contain more abundant $PI(3,4,5)P_3$ lipids, which upon fusion with the plasma membrane would create localized sites of $PI(3,4,5)P_3$/$PI(3,4)P_2$ enrichment that could also activate Akt (Fig. 4.2 (iii)). Thus, the plasma membrane increase in $PI(3,4,5)P_3$/$PI(3,4)P_2$ lipids observed in the PI4KIIIβ-overexpressing BT549 cells in chapter 3, could be due to enhanced trafficking of $PI(3,4,5)P_3$ rich vesicles to the plasma membrane. Finally, as reintroduction of a functional PTEN in the PTEN-null BT549 cell line led to a loss of PI4KIIIβ-mediated Akt activation, it is likely that upregulated expression of PI4KIIIβ activates Akt only in the context of PTEN-null cells (Fig. 4.2 (iv)).

Future research is required to assess whether PI3K is in fact increasingly recruited to recycling endosomes by PI4KIIIβ overexpression, via Rab11, as depicted in the presented model. The PI4KIIIβ inhibitor, Pik93, used in chapter 3, also inhibits PI3Kγ in the same micromolar range used to inhibit PI4KIIIβ (336). However, PI4KIIIβ-mediated Akt activation was not inhibited by Pik93 treatment. This suggests, that in the context BT549 breast cancer cells, Rab11 may be interacting with another PI3K isoform that remains to be identified. It is also possible that PI3Kγ is upregulated or its activity is enhanced in BT549 cells, therefore a greater concentration of Pik93 would be required to see an effect on PI4KIIIβ-mediated activation. PI3Kγ (p110γ catalytic subunit) expression has been shown to

Figure 4.2: Model depicting the role of PI4KIIIβ in Akt activation.

(i) Enhanced PI4KIIIβ expression leads to increased recruitment of Rab11 to recycling endosomes cycling through the TGN. **(ii)** Rab11 then directs $PI(3,4,5)P_3$ generation on recycling endosomes, through an as yet to be identified PI3K, leading to Akt activation. **(iii)** Enhanced $PI(3,4,5)P_3$ production on recycling endosomes leads to enhanced plasma membrane pools of $PI(3,4,5)P_3/PI(3,4)P_2$ at sites of vesicular fusion, which would also direct Akt activation at the plasma membrane. **(iv)** PI4KIIIβ-mediated Akt activation is likely dependent on loss of PTEN.

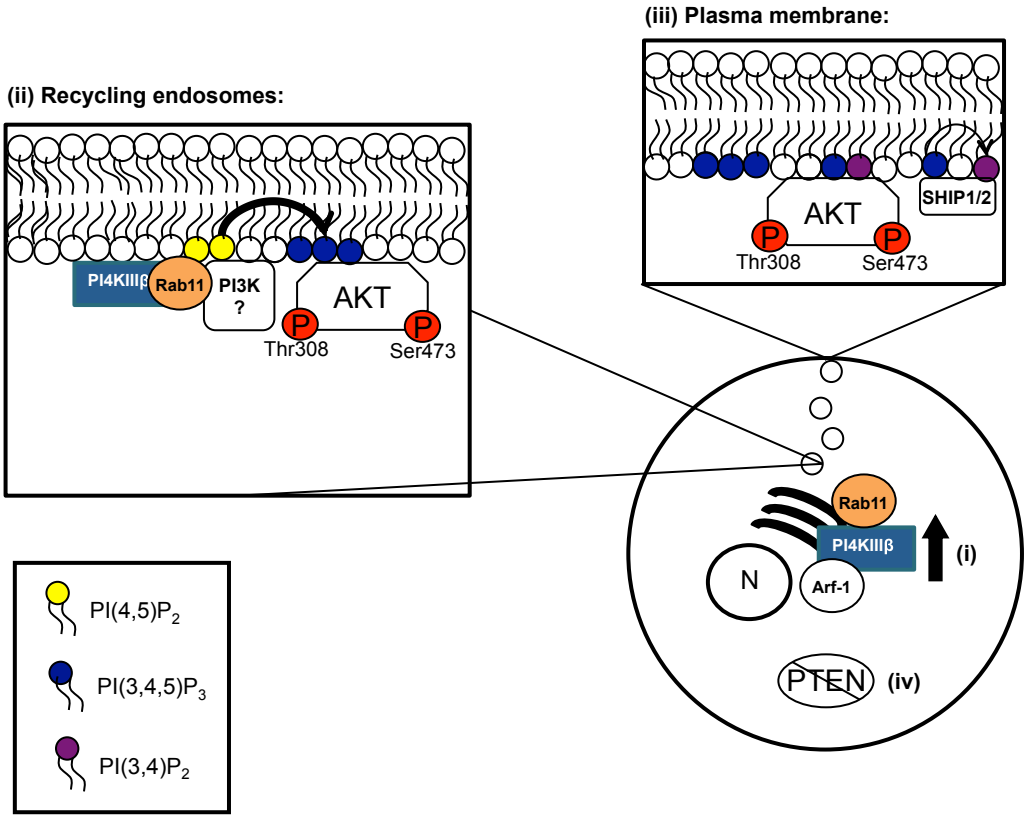
(iii) Plasma membrane:
(ii) Recycling endosomes:
PI4KIIIβ
Rab11
PI3K
?
AKT
P
P
Thr308
Ser473
AKT
P
P
Thr308
Ser473
SHIP1/2
Rab11
PI4KIIIβ
(i)
N
Arf-1
PTEN
(iv)
PI(4,5)P2
PI(3,4,5)P3
PI(3,4)P2

be upregulated in pancreatic and ductal carcinomas (371, 372).

It is also likely that ectopic expression of PI4KIIIβ is impacting intracellular trafficking, as PI4KIIIβ has been implicated in neuroendocrine exocytosis, TGN to plasma membrane protein delivery in polarized MDCK cells, as well as ERK1/2 trafficking through the endocytic recycling compartment (117-119). In addition, Rab11 itself has been shown to regulate EGFR recycling, with Rab11 expression enhancing recycling of this RTK back to the cell surface (373). It is possible that overexpression of PI4KIIIβ is enhancing recycling of RTKs back to the plasma membrane, via Rab11, thus enhancing the activation of PI3K and Akt via growth factor stimulation of RTKs at the cell surface. It remains to be determined experimentally what possible impact PI4KIIIβ overexpression has on trafficking from the TGN to the plasma membrane and endocytic recycling and whether the alteration of these trafficking events plays a role in PI4KIIIβ-mediated Akt activation in BT549 cells. Alternatively, it is possible that PI4KIIIβ driven recruitment of Rab11 to recycling endosomes, in PI4KIIIβ overexpressing breast cancer cells, is enhancing the localized recruitment of PI3K and activation of Akt on endosomes, as modelled in Fig. 4.2, leading to RTK independent Akt activation. The internalizing and recycling of EGFR molecules have been shown to enhance and prolong signalling, as internalized EGFR continues to bind and phosphorylate downstream targets, activating signalling pathways linked to proliferation and survival (343, 374, 375). This could be a way in which breast cancer cell oncogenic signalling becomes growth factor independent and evades drugs that target RTKs.

4.3.1 Enhanced Akt Signalling in Tumour Progression and Therapeutic Implications in Breast Cancer

Mutations in genes found in the PI3K/Akt signalling pathway occur in >70% of breast cancers and mutations and/or amplifications occur in all the major elements of this pathway (376). Amplification, overexpression and/or activating mutations have been reported, in human breast cancers, for RTKs, such as HER2 and the insulin-like growth factor receptor (IRG-1), which activate PI3Ks, for PIKCA, for the Akt-activating kinase PDK1 and for Akt1 and Akt2 (376). The phosphatases responsible for shutting off $PI(3,4,5)P_3$ and $PI(3,4)P_2$ lipid-directed activation of Akt, PTEN and INPP4B, are also frequently lost in breast cancers (376). PI3K/Akt pathway alterations also frequently co-occur in breast cancer, suggesting that they present non-overlapping mechanisms of oncogenicity (293). Increased Akt/PI3K/mTOR activation has been linked to resistance to chemotherapy and radiation treatments (252, 377). Enhanced Akt activation also promotes resistance to other therapeutic agents such as tamoxifen, which antagonises estrogen receptors in luminal breast tumours, and trastuzumab, a monoclonal antibody that interferes with HER2 receptors in $HER2^+$ breast tumours (378). In addition, triple negative breast tumours, which in general lack hormone receptors and HER2 expression, display PI3KCA and PDK1 mutations in approximately a third of tumours, as well as frequent PTEN and INPP4B losses (376). As there is no one therapeutic agent that has been proven effective in treating triple negative tumours and only 20% of this breast tumour subtype respond well to chemotherapy (186), the PI3K/Akt signalling pathway may be a promising target to treat this breast tumour subtype.

Multiple agents targeting the PI3K/Akt pathway are in various stages of development by both commercial and academic researchers (379-381). PI3K/Akt pathway nodes currently

targeted by drugs in clinical development are shown in Fig. 4.3. Coexisting PI3K/Akt pathway mutations likely amplify Akt activation and arise due to the fact that each mutated gene activates non-overlapping pathways that activate Akt or relieve negative feedback on the PI3K/Akt pathway (293). Due to this, the use of combination therapy for PI3K-dependent tumours appears most promising. Combination therapy has the potential to overcome drug resistance and oncogene addiction (293). Breast tumours treated with both HER2 inhibitors or antibodies and mTORC1 inhibitors had a higher response rate than the single agents would have predicted (382, 383). Similar results were seen in clinical trials done using mTORC1 inhibitors in combination with aromatase inhibitors, which block the synthesis of estrogen (384, 385).

The work presented in this thesis shows that PI4KIIIβ has a role in the PI3K/Akt pathway, likely through the regulation of Rab11-direted cell trafficking. Therefore, PI4KIIIβ appears to regulate PI3K/Akt activation through a novel mechanism. PI4KIIIβ may also regulate oncogenesis through other non-overlapping pathways, such as through increased provision of membrane protrusion components to the leading edge, increasing filopodia production as shown in chapter 2. This posits PI4KIIIβ as a possible new drug target in breast cancer, which could prove to be useful in combination therapies used to treat breast tumours. As this work has demonstrated that the catalytic activity of PI4KIIIβ does not appear to be critical for its role in Akt activation in breast cancer cells, kinase inhibitors would not be effective in targeting PI4KIIIβ in breast cast cancer cells, but alternatively PI4KIIIβ could be targeted for degradation siRNA delivered via nanoparticle which are engineered to specifically bind to cancer cells (386).

Figure 4.3: Diagram of PI3K/Akt signalling pathway and the nodes targeted by drugs in clinical development.

Tumour promoters and suppressors are labelled in pink and blue, respectively. Nodes targeted by drugs in clinical development are shown in red. AMPK, AMP-activated protein kinase; GPCR, G-protein-coupled receptor; GSK3, glycogen synthase kinase 3; INPP4B, inositol polyphosphate-4-phosphatase type II; LKB1, liver kinase B1; PDK1, phosphoinositide-dependent kinase 1; PI3K, phosphatidylinositol 3-kinase; PIP1, phosphatidylinositol monophosphate; PIP2, phosphatidylinositol 4,5-bisphosphate; PIP3, phosphatidylinositol 3,4,5-trisphophate; PTEN, phosphatase and tensin homolog; RTK, receptor tyrosine kinase. Adapted from (376).

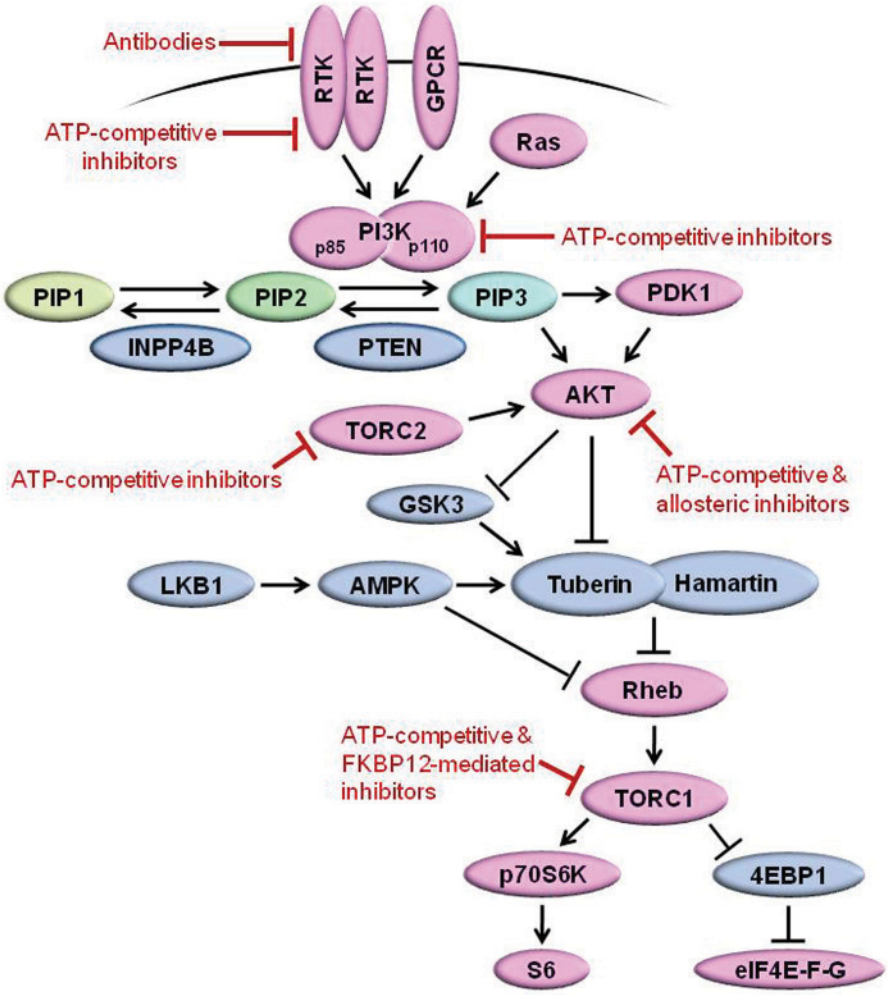
Antibodies
RTK
RTK
GPCR
ATP-competitive inhibitors
Ras
PI3K
p85
p110
ATP-competitive inhibitors
PIP1
PIP2
PIP3
PDK1
INPP4B
PTEN
AKT
TORC2
ATP-competitive inhibitors
ATP-competitive & allosteric inhibitors
GSK3
LKB1
AMPK
Tuberin
Hamartin
Rheb
ATP-competitive & FKBP12-mediated inhibitors
TORC1
p70S6K
4EBP1
S6
eIF4E-F-G

4.4 Future Directions

PI4KIIIβ protein expression was found enhanced in a subset of 169 breast tumours. This results serves as a rationale to assess the expression of PI4KIIIβ in a larger TMA study with breast tumours annotated for molecular sub-type, survial, and tumour aggressiveness, to determine the prognostic significance of enhanced PI4KIIIβ expression in breast cancer. It would be important to know if enhanced expression of PI4KIIIβ correlates with a loss of PTEN or other PI3K/Akt pathway alterations, such as the mutation or amplification of RTKs, Akt or PI3K isoforms in human breast tumours. Furthermore, it remains to be shown whether enhanced PI4KIIIβ expression is an early or late transforming event in human breast tumours. This resolution would shed light on whether enhanced PI4KIIIβ expression is linked to initial transforming events or tumour progression and metastasis. Whether enhanced PI4KIIIβ expression is linked to breast cancer recurrence should also be assessed. These studies on the clinical significance and mode of action of PI4KIIIβ on breast tumour progression would help determine whether PI4KIIIβ could be a possible drug target for breast cancer therapy. Additionally, the results presented in this thesis focus on the role of PI4KIIIβ in breast cancer, however it would be of interest to know whether PI4KIIIβ expression plays a role in any other cancer types.

In chapter 2, enhanced PI4KIIIβ expression is shown to promote greater filopodia production in breast cancer cells. It is possible that PI4KIIIβ expression is impacting filopodia formation via both phosphoinositide dependent and independent pathways and possibly through different mechanisms depending on the cell type. Research remains to be done to uncover the specific mechanisms through which PI4KIIIβ expression is driving filopodia formation in non-transformed and transformed cells. As this increase in filopodia

production did not enhance breast cancer cell migration as assessed by wound closure assay, the role of PI4KIIIβ-mediated filopodia formation also needs to be examined. It may be that increased PI4KIIIβ-mediated filopodia formation is involved in breast cancer cell invasion. It is also possible that enhanced PI4KIIIβ expression must be coupled with the alteration of another actin remodelling pathway to impact cell migration and invasion.

Finally, in chapter 3, PI4KIIIβ overexpression was shown to enhance $PI(3,4,5)P_3$/$PI(3,4)P_2$ generation and Akt activation. This PI4KIIIβ-mediated PI3K/Akt activation appears to be independent of the lipid kinase's enzymatic function and likely dependent on the protein's interaction with Rab11. These results were demonstrated in BT549 cells, immortalized basal-like breast cancer cells, which do not express estrogen and progesterone receptors or HER2 and are PTEN-null (333, 387). These experiments should be replicated in other breast cancer cell lines to assess the impact of PI4KIIIβ overexpression on Akt activation in different molecular contexts and determine if specific cellular alterations are needed in a cancer cell for PI4KIIIβ overexpression to have an impact on Akt activation.

To investigate whether PI4KIIIβ is in fact regulating Akt activation through Rab11, PI4KIIIβ-overexpressing cells should be transfected with a dominant negative Rab11 to see if Akt activation is lost. In addition, Akt activation should be assayed in cells expressing a constitutively active Rab11 and treated with siRNA against PI4KIIIβ. Moreover, breast cancers cells that ectopically express a PI4KIIIβ mutant, which cannot bind to Rab11, should be generated to determine whether PI4KIIIβ binding to Rab11 is required for its activation of Akt. It still remains to be determined if enhanced PI4KIIIβ expression is leading to enhanced PI3K and Akt recruitment to recycling endosomes, as proposed in the model in Fig. 4.2. Cell fractionation of early and recycling endosomes could be done in the vector control and

PI4KIIIβ overexpressing cell lines, as outlined in the work of Garcia-Regalado et al. (145), and then PI3K isoforms as well as pAkt levels probed for in the isolated endocytic fraction, to determine if PI4KIIIβ overexpression drives the enhanced recruitment of PI3K and the activation of Akt directly on endocytic vesicles. I hypothesis that PI4KIIIβ overexpression is leading to the enhanced recruitment of Rab11 to endocytic vesicles, which is then recruiting PI3K and activating Akt. It remains to be determined however, how Rab11 recruits PI3K to endocytic structures. Whether these two proteins interact directly or through intermediates needs to be determined. It has also remains to be demonstrated that PI4KIIIβ itself does not bind Akt, acting as a scaffold protein recruiting it to sites of activation at membrane microdomains within the cell. Work should be undertaken to show whether PI4KIIIβ directly binds Akt.

Lastly, it would be beneficial to know if rates of vesicular transport and endocytic recycling are upregulated in cells overexpressing PI4KIIIβ, as enhanced endocytic trafficking of signalling proteins may be driving both the formation of membrane protrusions and Akt activation. Uncovering the detailed mechanism of action of PI4KIIIβ-mediated PI3K/Akt activation will allow a better understanding of how this novel oncogenic activation pathway can impact PI3K-tumour dependent progression and treatment.

REFERENCES

1. **Carlton JG, Cullen PJ.** 2005. Coincidence detection in phosphoinositide signaling. Trends Cell Biol **15:**540-547.
2. **Di Paolo G, De Camilli P.** 2006. Phosphoinositides in cell regulation and membrane dynamics. Nature **443:**651-657.
3. **Downes CP, Gray A, Lucocq JM.** 2005. Probing phosphoinositide functions in signaling and membrane trafficking. Trends Cell Biol **15:**259-268.
4. **Holub BJ.** 1986. Metabolism and function of myo-inositol and inositol phospholipids. Annu Rev Nutr **6:**563-597.
5. **Nielsen E.** 2008. Investigating lipid signalling: it's all about finding the right PI. Biochem J **413:**e5-6.
6. **Antonsson B.** 1997. Phosphatidylinositol synthase from mammalian tissues. Biochim Biophys Acta **1348:**179-186.
7. **Fruman DA, Meyers RE, Cantley LC.** 1998. Phosphoinositide Kinases. Annual Review of Biochemistry **67:**481-507.
8. **Heo WD, Inoue T, Park WS, Kim ML, Park BO, Wandless TJ, Meyer T.** 2006. PI(3,4,5)P3 and PI(4,5)P2 lipids target proteins with polybasic clusters to the plasma membrane. Science **314:**1458-1461.
9. **Yin HL, Janmey PA.** 2003. Phosphoinositide regulation of the actin cytoskeleton. Annu Rev Physiol **65:**761-789.
10. **Sechi AS, Wehland J.** 2000. The actin cytoskeleton and plasma membrane connection: PtdIns(4,5)P(2) influences cytoskeletal protein activity at the plasma membrane. J Cell Sci **113 Pt 21:**3685-3695.
11. **Lemmon MA.** 2003. Phosphoinositide recognition domains. Traffic **4:**201-213.
12. **Overduin M, Cheever ML, Kutateladze TG.** 2001. Signaling with phosphoinositides: better than binary. Mol Interv **1:**150-159.
13. **Maffucci T, Falasca M.** 2001. Specificity in pleckstrin homology (PH) domain membrane targeting: a role for a phosphoinositide-protein co-operative mechanism. FEBS Lett **506:**173-179.
14. **Lemmon MA, Ferguson KM, O'Brien R, Sigler PB, Schlessinger J.** 1995. Specific and high-affinity binding of inositol phosphates to an isolated pleckstrin homology domain. Proc Natl Acad Sci U S A **92:**10472-10476.
15. **Frech M, Andjelkovic M, Ingley E, Reddy KK, Falck JR, Hemmings BA.** 1997. High affinity binding of inositol phosphates and phosphoinositides to the pleckstrin

homology domain of RAC/protein kinase B and their influence on kinase activity. J Biol Chem **272:**8474-8481.

16. **Kavran JM, Klein DE, Lee A, Falasca M, Isakoff SJ, Skolnik EY, Lemmon MA.** 1998. Specificity and promiscuity in phosphoinositide binding by pleckstrin homology domains. J Biol Chem **273:**30497-30508.

17. **Kutateladze TG.** 2010. Translation of the phosphoinositide code by PI effectors. Nat Chem Biol **6:**507-513.

18. **Gaidarov I, Keen JH.** 1999. Phosphoinositide-AP-2 interactions required for targeting to plasma membrane clathrin-coated pits. J. Cell Biol. **146:**755-764.

19. **Wang YJ, Wang J, Sun HQ, Martinez M, Sun YX, Macia E, Kirchhausen T, Albanesi JP, Roth MG, Yin HL.** 2003. Phosphatidylinositol 4 phosphate regulates targeting of clathrin adaptor AP-1 complexes to the Golgi. Cell **114:**299-310.

20. **Munro S.** 2002. Organelle identity and the targeting of peripheral membrane proteins. Curr Opin Cell Biol **14:**506-514.

21. **Balla T, Varnai P.** 2002. Visualizing Cellular Phosphoinositide Pools with GFP-Fused Protein-Modules. Sci. STKE **2002:**pl3-.

22. **Várnai P, Balla T.** 2006. Live cell imaging of phosphoinositide dynamics with fluorescent protein domains. Biochimica et Biophysica Acta (BBA) - Molecular and Cell Biology of Lipids **1761:**957-967.

23. **Balla T.** 2007. Imaging and manipulating phosphoinositides in living cells. J Physiol **582:**927-937.

24. **Halet G.** 2005. Imaging phosphoinositide dynamics using GFP-tagged protein domains. Biol Cell **97:**501-518.

25. **Hammond GR, Schiavo G, Irvine RF.** 2009. Immunocytochemical techniques reveal multiple, distinct cellular pools of PtdIns4P and PtdIns(4,5)P(2). Biochem J **422:**23-35.

26. **Sasaki T, Takasuga S, Sasaki J, Kofuji S, Eguchi S, Yamazaki M, Suzuki A.** 2009. Mammalian phosphoinositide kinases and phosphatases. Prog Lipid Res **48:**307-343.

27. **Lemmon MA.** 2008. Membrane recognition by phospholipid-binding domains. Nat Rev Mol Cell Biol **9:**99-111.

28. **Dippold HC, Ng MM, Farber-Katz SE, Lee SK, Kerr ML, Peterman MC, Sim R, Wiharto PA, Galbraith KA, Madhavarapu S, Fuchs GJ, Meerloo T, Farquhar MG, Zhou H, Field SJ.** 2009. GOLPH3 bridges phosphatidylinositol-4-phosphate and actomyosin to stretch and shape the Golgi to promote budding. Cell **139:**337-351.

29. **Graham TR, Burd CG.** 2011. Coordination of Golgi functions by phosphatidylinositol 4-kinases. Trends Cell Biol **21:**113-121.

30. **Nakayama K, Wakatsuki S.** 2003. The structure and function of GGAs, the traffic controllers at the TGN sorting crossroads. Cell Struct Funct **28:**431-442.

31. **Wang J, Sun HQ, Macia E, Kirchhausen T, Watson H, Bonifacino JS, Yin HL.** 2007. PI4P promotes the recruitment of the GGA adaptor proteins to the trans-Golgi network and regulates their recognition of the ubiquitin sorting signal. Mol Biol Cell **18:**2646-2655.

32. **Hirst J, Robinson MS.** 1998. Clathrin and adaptors. Biochim Biophys Acta **1404:**173-193.

33. **Levine TP, Munro S.** 2002. Targeting of Golgi-specific pleckstrin homology domains involves both PtdIns 4-kinase-dependent and -independent components. Curr Biol **12:**695-704.

34. **Godi A, Campli AD, Konstantakopoulos A, Tullio GD, Alessi DR, Kular GS, Daniele T, Marra P, Lucocq JM, Matteis MAD.** 2004. FAPPs control Golgi-to-cell-surface membrane traffic by binding to ARF and PtdIns(4)P. Nat Cell Biol **6:**393-404.

35. **Santiago-Tirado FH, Bretscher A.** 2011. Membrane-trafficking sorting hubs: cooperation between PI4P and small GTPases at the trans-Golgi network. Trends Cell Biol **21:**515-525.

36. **Fugmann T, Hausser A, Schoffler P, Schmid S, Pfizenmaier K, Olayioye MA.** 2007. Regulation of secretory transport by protein kinase D-mediated phosphorylation of the ceramide transfer protein. J Cell Biol **178:**15-22.

37. **Banerji S, Ngo M, Lane CF, Robinson CA, Minogue S, Ridgway ND.** 2010. Oxysterol binding protein-dependent activation of sphingomyelin synthesis in the golgi apparatus requires phosphatidylinositol 4-kinase IIalpha. Mol Biol Cell **21:**4141-4150.

38. **Zhu Y, Traub LM, Kornfeld S.** 1998. ADP-ribosylation factor 1 transiently activates high-affinity adaptor protein complex AP-1 binding sites on Golgi membranes. Mol Biol Cell **9:**1323-1337.

39. **Liu Y, Boukhelifa M, Tribble E, Morin-Kensicki E, Uetrecht A, Bear JE, Bankaitis VA.** 2008. The Sac1 phosphoinositide phosphatase regulates Golgi membrane morphology and mitotic spindle organization in mammals. Mol Biol Cell **19:**3080-3096.

40. **Whitters EA, Cleves AE, McGee TP, Skinner HB, Bankaitis VA.** 1993. SAC1p is an integral membrane protein that influences the cellular requirement for phospholipid transfer protein function and inositol in yeast. J Cell Biol **122:**79-94.

41. **Tahirovic S, Schorr M, Mayinger P.** 2005. Regulation of intracellular phosphatidylinositol-4-phosphate by the Sac1 lipid phosphatase. Traffic **6:**116-130.

42. **Szentpetery Z, Varnai P, Balla T.** 2010. Acute manipulation of Golgi phosphoinositides to assess their importance in cellular trafficking and signaling. Proc Natl Acad Sci U S A **107:**8225-8230.

43. **Heath CM, Stahl PD, Barbieri MA.** 2003. Lipid kinases play crucial and multiple roles in membrane trafficking and signaling. Histol Histopathol **18:**989-998.

44. **Rebecchi MJ, Pentyala SN.** 2000. Structure, function, and control of phosphoinositide-specific phospholipase C. Physiol Rev **80:**1291-1335.

45. **Rohatgi R, Ho H-yH, Kirschner MW.** 2000. Mechanism of N-WASP Activation by CDC42 and Phosphatidylinositol 4,5-bisphosphate. J. Cell Biol. **150:**1299-1310.

46. **Di Paolo G, Pellegrini L, Letinic K, Cestra G, Zoncu R, Voronov S, Chang S, Guo J, Wenk MR, De Camilli P.** 2002. Recruitment and regulation of phosphatidylinositol phosphate kinase type 1 gamma by the FERM domain of talin. Nature **420:**85-89.

47. **Fukami K, Furuhashi K, Inagaki M, Endo T, Hatano S, Takenawa T.** 1992. Requirement of phosphatidylinositol 4,5-bisphosphate for alpha-actinin function. Nature **359:**150-152.

48. **Gilmore AP, Burridge K.** 1996. Regulation of vinculin binding to talin and actin by phosphatidyl-inositol-4-5-bisphosphate. Nature **381:**531-535.

49. **Huttelmaier S, Mayboroda O, Harbeck B, Jarchau T, Jockusch BM, Rudiger M.** 1998. The interaction of the cell-contact proteins VASP and vinculin is regulated by phosphatidylinositol-4,5-bisphosphate. Curr Biol **8:**479-488.

50. **Gong LW.** 2005. Phosphatidylinositol phosphate kinase type I [gamma] regulates dynamics of large dense-core vesicle fusion. Proc. Natl Acad. Sci. USA **102:**5204-5209.

51. **Di Paolo G.** 2004. Impaired PtdIns(4,5)P2 synthesis in nerve terminals produces defects in synaptic vesicle trafficking. Nature **431:**415-422.

52. **Eberhard DA, Cooper CL, Low MG, Holz RW.** 1990. Evidence that the inositol phospholipids are necessary for exocytosis. Loss of inositol phospholipids and inhibition of secretion in permeabilized cells caused by a bacterial phospholipase C and removal of ATP. Biochem. J. **268:**15-25.

53. **Hay JC, Martin TF.** 1993. Phosphatidylinositol transfer protein required for ATP-dependent priming of Ca(2+)-activated secretion. Nature **366:**572-575.

54. **Hay JC, Fisette PL, Jenkins GH, Fukami K, Takenawa T, Anderson RA, Martin TF.** 1995. ATP-dependent inositide phosphorylation required for Ca(2+)-activated secretion. Nature **374:**173-177.

55. **Bai J, Tucker WC, Chapman ER.** 2004. PIP2 increases the speed of response of synaptotagmin and steers its membrane-penetration activity toward the plasma membrane. Nature Struct. Mol. Biol. **11:**36-44.

56. **Schmid SL, Frolov VA.** 2011. Dynamin: functional design of a membrane fission catalyst. Annu Rev Cell Dev Biol **27:**79-105.

57. **Jakobsson J, Gad H, Andersson F, Low P, Shupliakov O, Brodin L.** 2008. Role of epsin 1 in synaptic vesicle endocytosis. Proc Natl Acad Sci U S A **105:**6445-6450.

58. **Hilgemann DW, Feng S, Nasuhoglu C.** 2001. The complex and intriguing lives of PIP2 with ion channels and transporters. Sci. STKE **2001:**RE19.

59. **Suh BC, Hille B.** 2005. Regulation of ion channels by phosphatidylinositol 4,5-bisphosphate. Curr Opin Neurobiol **15:**370-378.

60. **Prescott ED, Julius D.** 2003. A modular PIP2 binding site as a determinant of capsaicin receptor sensitivity. Science **300:**1284-1288.

61. **Franke TF, Kaplan DR, Cantley LC, Toker A.** 1997. Direct regulation of the Akt proto-oncogene product by phosphatidylinositol-3,4-bisphosphate. Science **275:**665-668.

62. **Vivanco I, Sawyers CL.** 2002. The phosphatidylinositol 3-Kinase AKT pathway in human cancer. Nat Rev Cancer **2:**489-501.

63. **Xue G, Hemmings BA.** 2013. PKB/Akt-dependent regulation of cell motility. J Natl Cancer Inst **105:**393-404.

64. **Alessi DR, Deak M, Casamayor A, Caudwell FB, Morrice N, Norman DG, Gaffney P, Reese CB, MacDougall CN, Harbison D, Ashworth A, Bownes M.** 1997. 3-Phosphoinositide-dependent protein kinase-1 (PDK1): structural and functional homology with the Drosophila DSTPK61 kinase. Curr Biol **7:**776-789.

65. **Oikawa T.** 2004. PtdIns(3,4,5)P3 binding is necessary for WAVE2-induced formation of lamellipodia. Nature Cell Biol. **6:**420-426.

66. **Schmidt A, Hall A.** 2002. Guanine nucleotide exchange factors for Rho GTPases: turning on the switch. Genes Dev **16:**1587-1609.

67. **Krugmann S, Stephens L, Hawkins PT.** 2006. Purification of ARAP3 and characterization of GAP activities. Methods Enzymol **406:**91-103.

68. **Kimber WA, Deak M, Prescott AR, Alessi DR.** 2003. Interaction of the protein tyrosine phosphatase PTPL1 with the PtdIns(3,4)P2-binding adaptor protein TAPP1. Biochem J **376:**525-535.

69. **Wullschleger S, Wasserman DH, Gray A, Sakamoto K, Alessi DR.** 2011. Role of TAPP1 and TAPP2 adaptor binding to PtdIns(3,4)P2 in regulating insulin sensitivity defined by knock-in analysis. Biochem J **434:**265-274.

70. **Hoepfner S, Severin F, Cabezas A, Habermann B, Runge A, Gillooly D, Stenmark H, Zerial M.** 2005. Modulation of receptor recycling and degradation by the endosomal kinesin KIF16B. Cell **121:**437-450.

71. **Mills IG, Urbe S, Clague MJ.** 2001. Relationships between EEA1 binding partners and their role in endosome fusion. J Cell Sci **114:**1959-1965.

72. **Petiot A, Faure J, Stenmark H, Gruenberg J.** 2003. PI3P signaling regulates receptor sorting but not transport in the endosomal pathway. J Cell Biol **162:**971-979.

73. **Ikonomov OC, Sbrissa D, Shisheva A.** 2001. Mammalian cell morphology and endocytic membrane homeostasis require enzymatically active phosphoinositide 5-kinase PIKfyve. J Biol Chem **276:**26141-26147.

74. **Rutherford AC, Traer C, Wassmer T, Pattni K, Bujny MV, Carlton JG, Stenmark H, Cullen PJ.** 2006. The mammalian phosphatidylinositol 3-phosphate 5-

kinase (PIKfyve) regulates endosome-to-TGN retrograde transport. J Cell Sci **119:**3944-3957.

75. **Cabezas A, Pattni K, Stenmark H.** 2006. Cloning and subcellular localization of a human phosphatidylinositol 3-phosphate 5-kinase, PIKfyve/Fab1. Gene **371:**34-41.

76. **de Lartigue J, Polson H, Feldman M, Shokat K, Tooze SA, Urbe S, Clague MJ.** 2009. PIKfyve regulation of endosome-linked pathways. Traffic **10:**883-893.

77. **Ikonomov OC, Sbrissa D, Mlak K, Kanzaki M, Pessin J, Shisheva A.** 2002. Functional dissection of lipid and protein kinase signals of PIKfyve reveals the role of PtdIns 3,5-P2 production for endomembrane integrity. J Biol Chem **277:**9206-9211.

78. **Zolov SN, Bridges D, Zhang Y, Lee WW, Riehle E, Verma R, Lenk GM, Converso-Baran K, Weide T, Albin RL, Saltiel AR, Meisler MH, Russell MW, Weisman LS.** 2012. In vivo, Pikfyve generates PI(3,5)P2, which serves as both a signaling lipid and the major precursor for PI5P. Proc Natl Acad Sci U S A **109:**17472-17477.

79. **Sbrissa D, Ikonomov OC, Shisheva A.** 1999. PIKfyve, a mammalian ortholog of yeast Fab1p lipid kinase, synthesizes 5-phosphoinositides. Effect of insulin. J Biol Chem **274:**21589-21597.

80. **Ungewickell A.** 2005. The identification and characterization of two phosphatidylinositol-4,5-bisphosphate 4-phosphatases. Proc. Natl Acad. Sci. USA **102:**18854-18859.

81. **Pagliarini DJ, Worby CA, Dixon JE.** 2004. A PTEN-like phosphatase with a novel substrate specificity. J Biol Chem **279:**38590-38596.

82. **Clarke JH, Letcher AJ, D'Santos C S, Halstead JR, Irvine RF, Divecha N.** 2001. Inositol lipids are regulated during cell cycle progression in the nuclei of murine erythroleukaemia cells. Biochem J **357:**905-910.

83. **Sarkes D, Rameh LE.** 2010. A novel HPLC-based approach makes possible the spatial characterization of cellular PtdIns5P and other phosphoinositides. Biochem J **428:**375-384.

84. **Jones DR, Bultsma Y, Keune WJ, Halstead JR, Elouarrat D, Mohammed S, Heck AJ, D'Santos CS, Divecha N.** 2006. Nuclear PtdIns5P as a transducer of stress signaling: an in vivo role for PIP4Kbeta. Mol Cell **23:**685-695.

85. **Bunce MW, Boronenkov IV, Anderson RA.** 2008. Coordinated activation of the nuclear ubiquitin ligase Cul3-SPOP by the generation of phosphatidylinositol 5-phosphate. J Biol Chem **283:**8678-8686.

86. **Carricaburu V, Lamia KA, Lo E, Favereaux L, Payrastre B, Cantley LC, Rameh LE.** 2003. The phosphatidylinositol (PI)-5-phosphate 4-kinase type II enzyme controls insulin signaling by regulating PI-3,4,5-trisphosphate degradation. Proc Natl Acad Sci U S A **100:**9867-9872.

87. **Pendaries C, Tronchere H, Arbibe L, Mounier J, Gozani O, Cantley L, Fry MJ, Gaits-Iacovoni F, Sansonetti PJ, Payrastre B.** 2006. PtdIns5P activates the host

cell PI3-kinase/Akt pathway during Shigella flexneri infection. Embo J **25:**1024-1034.

88. **Ramel D, Lagarrigue F, Dupuis-Coronas S, Chicanne G, Leslie N, Gaits-Iacovoni F, Payrastre B, Tronchere H.** 2009. PtdIns5P protects Akt from dephosphorylation through PP2A inhibition. Biochem Biophys Res Commun **387:**127-131.

89. **Lecompte O, Poch O, Laporte J.** 2008. PtdIns5P regulation through evolution: roles in membrane trafficking? Trends Biochem Sci **33:**453-460.

90. **Balla A, Balla T.** 2006. Phosphatidylinositol 4-kinases: old enzymes with emerging functions. Trends in Cell Biology **16:**351-361.

91. **Balla A, Tuymetova G, Barshishat M, Geiszt M, Balla T.** 2002. Characterization of type II phosphatidylinositol 4-kinase isoforms reveals association of the enzymes with endosomal vesicular compartments. J Biol Chem **277:**20041-20050.

92. **Gehrmann T, Heilmeyer LM, Jr.** 1998. Phosphatidylinositol 4-kinases. Eur J Biochem **253:**357-370.

93. **Barylko B, Gerber SH, Binns DD, Grichine N, Khvotchev M, Sudhof TC, Albanesi JP.** 2001. A novel family of phosphatidylinositol 4-kinases conserved from yeast to humans. J Biol Chem **276:**7705-7708.

94. **Salazar G, Craige B, Wainer BH, Guo J, De Camilli P, Faundez V.** 2005. Phosphatidylinositol-4-kinase type II alpha is a component of adaptor protein-3-derived vesicles. Mol Biol Cell **16:**3692-3704.

95. **Minogue S, Waugh MG, De Matteis MA, Stephens DJ, Berditchevski F, Hsuan JJ.** 2006. Phosphatidylinositol 4-kinase is required for endosomal trafficking and degradation of the EGF receptor. J Cell Sci **119:**571-581.

96. **Simons JP, Al-Shawi R, Minogue S, Waugh MG, Wiedemann C, Evangelou S, Loesch A, Sihra TS, King R, Warner TT, Hsuan JJ.** 2009. Loss of phosphatidylinositol 4-kinase 2alpha activity causes late onset degeneration of spinal cord axons. Proc Natl Acad Sci U S A **106:**11535-11539.

97. **Jung G, Wang J, Wlodarski P, Barylko B, Binns DD, Shu H, Yin HL, Albanesi JP.** 2008. Molecular determinants of activation and membrane targeting of phosphoinositol 4-kinase IIbeta. Biochem J **409:**501-509.

98. **Wei YJ, Sun HQ, Yamamoto M, Wlodarski P, Kunii K, Martinez M, Barylko B, Albanesi JP, Yin HL.** 2002. Type II Phosphatidylinositol 4-Kinase beta Is a Cytosolic and Peripheral Membrane Protein That Is Recruited to the Plasma Membrane and Activated by Rac-GTP. J. Biol. Chem. **277:**46586-46593.

99. **Li J, Barylko B, Johnson J, Mueller JD, Albanesi JP, Chen Y.** 2012. Molecular brightness analysis reveals phosphatidylinositol 4-Kinase IIbeta association with clathrin-coated vesicles in living cells. Biophys J **103:**1657-1665.

100. **Varnai P, Balla T.** 1998. Visualization of Phosphoinositides That Bind Pleckstrin Homology Domains: Calcium- and Agonist-induced Dynamic Changes and

Relationship to Myo-[3H]inositol-labeled Phosphoinositide Pools. J. Cell Biol. **143:**501-510.

101. **Han GS, Audhya A, Markley DJ, Emr SD, Carman GM.** 2002. The Saccharomyces cerevisiae LSB6 gene encodes phosphatidylinositol 4-kinase activity. J Biol Chem **277:**47709-47718.

102. **Shelton SN, Barylko B, Binns DD, Horazdovsky BF, Albanesi JP, Goodman JM.** 2003. Saccharomyces cerevisiae contains a Type II phosphoinositide 4-kinase. Biochem J **371:**533-540.

103. **Chang FS, Han GS, Carman GM, Blumer KJ.** 2005. A WASp-binding type II phosphatidylinositol 4-kinase required for actin polymerization-driven endosome motility. J Cell Biol **171:**133-142.

104. **Burgess J, Del Bel LM, Ma CI, Barylko B, Polevoy G, Rollins J, Albanesi JP, Kramer H, Brill JA.** 2012. Type II phosphatidylinositol 4-kinase regulates trafficking of secretory granule proteins in Drosophila. Development **139:**3040-3050.

105. **Wong K, Cantley LC.** 1997. Subcellular Locations of Phosphatidylinositol 4-Kinase Isoforms. J. Biol. Chem. **272:**13236-13241.

106. **Balla A, Kim YJ, Varnai P, Szentpetery Z, Knight Z, Shokat KM, Balla T.** 2008. Maintenance of Hormone-sensitive Phosphoinositide Pools in the Plasma Membrane Requires Phosphatidylinositol 4-Kinase III{alpha}. Mol. Biol. Cell **19:**711-721.

107. **Nakatsu F, Baskin JM, Chung J, Tanner LB, Shui G, Lee SY, Pirruccello M, Hao M, Ingolia NT, Wenk MR, De Camilli P.** 2012. PtdIns4P synthesis by PI4KIIIalpha at the plasma membrane and its impact on plasma membrane identity. J Cell Biol **199:**1003-1016.

108. **Berger KL, Cooper JD, Heaton NS, Yoon R, Oakland TE, Jordan TX, Mateu G, Grakoui A, Randall G.** 2009. Roles for endocytic trafficking and phosphatidylinositol 4-kinase III alpha in hepatitis C virus replication. Proc Natl Acad Sci U S A **106:**7577-7582.

109. **Ma H, Blake T, Chitnis A, Liu P, Balla T.** 2009. Crucial role of phosphatidylinositol 4-kinase IIIalpha in development of zebrafish pectoral fin is linked to phosphoinositide 3-kinase and FGF signaling. J Cell Sci **122:**4303-4310.

110. **Audhya A, Emr SD.** 2002. Stt4 PI 4-kinase localizes to the plasma membrane and functions in the Pkc1-mediated MAP kinase cascade. Dev Cell **2:**593-605.

111. **Audhya A, Foti M, Emr SD.** 2000. Distinct roles for the yeast phosphatidylinositol 4-kinases, Stt4p and Pik1p, in secretion, cell growth, and organelle membrane dynamics. Mol Biol Cell **11:**2673-2689.

112. **de Graaf P, Klapisz EE, Schulz TK, Cremers AF, Verkleij AJ, van Bergen en Henegouwen PM.** 2002. Nuclear localization of phosphatidylinositol 4-kinase beta. J Cell Sci **115:**1769-1775.

113. **Godi A, Pertile P, Meyers R, Marra P, Di Tullio G, Iurisci C, Luini A, Corda D, De Matteis MA.** 1999. ARF mediates recruitment of PtdIns-4-OH kinase-[bgr] and stimulates synthesis of PtdIns(4,5)P2 on the Golgi complex. Nat Cell Biol **1:**280-287.

114. **O'Callaghan DW, Ivings L, Weiss JL, Ashby MC, Tepikin AV, Burgoyne RD.** 2002. Differential use of myristoyl groups on neuronal calcium sensor proteins as a determinant of spatio-temporal aspects of Ca2+ signal transduction. J Biol Chem **277:**14227-14237.

115. **Haynes LP, Thomas GM, Burgoyne RD.** 2005. Interaction of neuronal calcium sensor-1 and ADP-ribosylation factor 1 allows bidirectional control of phosphatidylinositol 4-kinase beta and trans-Golgi network-plasma membrane traffic. J Biol Chem **280:**6047-6054.

116. **Bourne Y, Dannenberg J, Pollmann V, Marchot P, Pongs O.** 2001. Immunocytochemical localization and crystal structure of human frequenin (neuronal calcium sensor 1). J Biol Chem **276:**11949-11955.

117. **de Barry J, Janoshazi A, Dupont JL, Procksch O, Chasserot-Golaz S, Jeromin A, Vitale N.** 2006. Functional implication of neuronal calcium sensor-1 and phosphoinositol 4-kinase-beta interaction in regulated exocytosis of PC12 cells. J Biol Chem **281:**18098-18111.

118. **Bruns JR, Ellis MA, Jeromin A, Weisz OA.** 2002. Multiple roles for phosphatidylinositol 4-kinase in biosynthetic transport in polarized Madin-Darby canine kidney cells. J Biol Chem **277:**2012-2018.

119. **Kapp-Barnea Y, Ninio-Many L, Hirschberg K, Fukuda M, Jeromin A, Sagi-Eisenberg R.** 2006. Neuronal calcium sensor-1 and phosphatidylinositol 4-kinase beta stimulate extracellular signal-regulated kinase 1/2 signaling by accelerating recycling through the endocytic recycling compartment. Mol Biol Cell **17:**4130-4141.

120. **Kholodenko BN.** 2002. MAP kinase cascade signaling and endocytic trafficking: a marriage of convenience? Trends Cell Biol **12:**173-177.

121. **Miaczynska M, Pelkmans L, Zerial M.** 2004. Not just a sink: endosomes in control of signal transduction. Curr Opin Cell Biol **16:**400-406.

122. **Teis D, Wunderlich W, Huber LA.** 2002. Localization of the MP1-MAPK scaffold complex to endosomes is mediated by p14 and required for signal transduction. Dev Cell **3:**803-814.

123. **Grant BD, Donaldson JG.** 2009. Pathways and mechanisms of endocytic recycling. Nat Rev Mol Cell Biol **10:**597-608.

124. **Sridhar S, Patel B, Aphkhazava D, Macian F, Santambrogio L, Shields D, Cuervo AM.** 2013. The lipid kinase PI4KIIIbeta preserves lysosomal identity. Embo J **32:**324-339.

125. **Toth B, Balla A, Ma H, Knight ZA, Shokat KM, Balla T.** 2006. Phosphatidylinositol 4-Kinase IIIbeta Regulates the Transport of Ceramide between the Endoplasmic Reticulum and Golgi. J. Biol. Chem. **281:**36369-36377.

126. **Polevoy G, Wei HC, Wong R, Szentpetery Z, Kim YJ, Goldbach P, Steinbach SK, Balla T, Brill JA.** 2009. Dual roles for the Drosophila PI 4-kinase four wheel drive in localizing Rab11 during cytokinesis. J Cell Biol **187:**847-858.

127. **Brill JA, Hime GR, Scharer-Schuksz M, Fuller MT.** 2000. A phospholipid kinase regulates actin organization and intercellular bridge formation during germline cytokinesis. Development **127:**3855-3864.

128. **Flanagan CA, Schnieders EA, Emerick AW, Kunisawa R, Admon A, Thorner J.** 1993. Phosphatidylinositol 4-kinase: gene structure and requirement for yeast cell viability. Science **262:**1444-1448.

129. **Walch-Solimena C, Novick P.** 1999. The yeast phosphatidylinositol-4-OH kinase pik1 regulates secretion at the Golgi. Nat Cell Biol **1:**523-525.

130. **Strahl T, Hama H, DeWald DB, Thorner J.** 2005. Yeast phosphatidylinositol 4-kinase, Pik1, has essential roles at the Golgi and in the nucleus. J Cell Biol **171:**967-979.

131. **Huttner IG, Strahl T, Osawa M, King DS, Ames JB, Thorner J.** 2003. Molecular interactions of yeast frequenin (Frq1) with the phosphatidylinositol 4-kinase isoform, Pik1. J Biol Chem **278:**4862-4874.

132. **Gloor Y, Schone M, Habermann B, Ercan E, Beck M, Weselek G, Muller-Reichert T, Walch-Solimena C.** 2010. Interaction between Sec7p and Pik1p: the first clue for the regulation of a coincidence detection signal. Eur J Cell Biol **89:**575-583.

133. **Suer S, Sickmann A, Meyer HE, Herberg FW, Heilmeyer LM, Jr.** 2001. Human phosphatidylinositol 4-kinase isoform PI4K92. Expression of the recombinant enzyme and determination of multiple phosphorylation sites. Eur J Biochem **268:**2099-2106.

134. **Hausser A, Storz P, Martens S, Link G, Toker A, Pfizenmaier K.** 2005. Protein kinase D regulates vesicular transport by phosphorylating and activating phosphatidylinositol-4 kinase IIIbeta at the Golgi complex. Nat Cell Biol **7:**880-886.

135. **Hausser A, Link G, Hoene M, Russo C, Selchow O, Pfizenmaier K.** 2006. Phospho-specific binding of 14-3-3 proteins to phosphatidylinositol 4-kinase III beta protects from dephosphorylation and stabilizes lipid kinase activity. J Cell Sci **119:**3613-3621.

136. **Szivak I, Lamb N, Heilmeyer LM.** 2006. Subcellular localization and structural function of endogenous phosphorylated phosphatidylinositol 4-kinase (PI4K92). J Biol Chem **281:**16740-16749.

137. **de Graaf P, Zwart WT, van Dijken RA, Deneka M, Schulz TK, Geijsen N, Coffer PJ, Gadella BM, Verkleij AJ, van der Sluijs P, van Bergen en Henegouwen PM.** 2004. Phosphatidylinositol 4-kinasebeta is critical for functional association of rab11 with the Golgi complex. Mol Biol Cell **15:**2038-2047.

138. **Wennerberg K, Rossman KL, Der CJ.** 2005. The Ras superfamily at a glance. J Cell Sci **118:**843-846.

139. **Schwartz SL, Cao C, Pylypenko O, Rak A, Wandinger-Ness A.** 2007. Rab GTPases at a glance. J Cell Sci **120:**3905-3910.

140. **Agola J, Jim P, Ward H, Basuray S, Wandinger-Ness A.** 2011. Rab GTPases as regulators of endocytosis, targets of disease and therapeutic opportunities. Clin Genet.

141. **Seachrist JL, Ferguson SS.** 2003. Regulation of G protein-coupled receptor endocytosis and trafficking by Rab GTPases. Life Sci **74:**225-235.

142. **Ullrich O, Reinsch S, Urbe S, Zerial M, Parton RG.** 1996. Rab11 regulates recycling through the pericentriolar recycling endosome. J Cell Biol **135:**913-924.

143. **Chen W, Feng Y, Chen D, Wandinger-Ness A.** 1998. Rab11 is required for trans-golgi network-to-plasma membrane transport and a preferential target for GDP dissociation inhibitor. Mol Biol Cell **9:**3241-3257.

144. **Takahashi S, Kubo K, Waguri S, Yabashi A, Shin HW, Katoh Y, Nakayama K.** 2012. Rab11 regulates exocytosis of recycling vesicles at the plasma membrane. J Cell Sci **125:**4049-4057.

145. **Garcia-Regalado A, Guzman-Hernandez ML, Ramirez-Rangel I, Robles-Molina E, Balla T, Vazquez-Prado J, Reyes-Cruz G.** 2008. G protein-coupled receptor-promoted trafficking of Gbeta1gamma2 leads to AKT activation at endosomes via a mechanism mediated by Gbeta1gamma2-Rab11a interaction. Mol Biol Cell **19:**4188-4200.

146. **Jeganathan S, Lee JM.** 2007. Binding of elongation factor eEF1A2 to phosphatidylinositol 4-kinase beta stimulates lipid kinase activity and phosphatidylinositol 4-phosphate generation. J Biol Chem **282:**372-380.

147. **Jeganathan S, Morrow A, Amiri A, Lee JM.** 2008. Eukaryotic Elongation Factor 1A2 Cooperates with Phosphatidylinositol-4 Kinase III {beta} To Stimulate Production of Filopodia through Increased Phosphatidylinositol-4,5 Bisphosphate Generation. Mol. Cell. Biol. **28:**4549-4561.

148. **Hershey JWB.** 1991. Translational Control in Mammalian Cells. Annual Review of Biochemistry **60:**717-755.

149. **Browne GJ, Proud CG.** 2002. Regulation of peptide-chain elongation in mammalian cells. Eur J Biochem **269:**5360-5368.

150. **Knudsen SM, Frydenberg J, Clark BF, Leffers H.** 1993. Tissue-dependent variation in the expression of elongation factor-1 alpha isoforms: isolation and characterisation of a cDNA encoding a novel variant of human elongation-factor 1 alpha. Eur J Biochem **215:**549-554.

151. **Durso NA, Cyr RJ.** 1994. A calmodulin-sensitive interaction between microtubules and a higher plant homolog of elongation factor-1 alpha. Plant Cell **6:**893-905.

152. **Moore RC, Durso NA, Cyr RJ.** 1998. Elongation factor-1alpha stabilizes microtubules in a calcium/calmodulin-dependent manner. Cell Motil Cytoskeleton **41:**168-180.

153. **Liu G, Tang J, Edmonds BT, Murray J, Levin S, Condeelis J.** 1996. F-actin sequesters elongation factor 1alpha from interaction with aminoacyl-tRNA in a pH-dependent reaction. J Cell Biol **135:**953-963.

154. **Murray JW, Edmonds BT, Liu G, Condeelis J.** 1996. Bundling of actin filaments by elongation factor 1 alpha inhibits polymerization at filament ends. J Cell Biol **135:**1309-1321.

155. **Khacho M, Mekhail K, Pilon-Larose K, Pause A, Cote J, Lee S.** 2008. eEF1A is a novel component of the mammalian nuclear protein export machinery. Mol Biol Cell **19:**5296-5308.

156. **Chang R, Wang E.** 2007. Mouse translation elongation factor eEF1A-2 interacts with Prdx-I to protect cells against apoptotic death induced by oxidative stress. J Cell Biochem **100:**267-278.

157. **Li Z, Qi CF, Shin DM, Zingone A, Newbery HJ, Kovalchuk AL, Abbott CM, Morse HC, 3rd.** 2010. Eef1a2 promotes cell growth, inhibits apoptosis and activates JAK/STAT and AKT signaling in mouse plasmacytomas. PLoS One **5:**e10755.

158. **Li R, Wang H, Bekele BN, Yin Z, Caraway NP, Katz RL, Stass SA, Jiang F.** 2006. Identification of putative oncogenes in lung adenocarcinoma by a comprehensive functional genomic approach. Oncogene **25:**2628-2635.

159. **Iwabuchi H, Sakamoto M, Sakunaga H, Ma YY, Carcangiu ML, Pinkel D, Yang-Feng TL, Gray JW.** 1995. Genetic analysis of benign, low-grade, and high-grade ovarian tumors. Cancer Res **55:**6172-6180.

160. **Kallioniemi A, Kallioniemi OP, Piper J, Tanner M, Stokke T, Chen L, Smith HS, Pinkel D, Gray JW, Waldman FM.** 1994. Detection and mapping of amplified DNA sequences in breast cancer by comparative genomic hybridization. Proc Natl Acad Sci U S A **91:**2156-2160.

161. **Pinke DE, Kalloger SE, Francetic T, Huntsman DG, Lee JM.** 2008. The prognostic significance of elongation factor eEF1A2 in ovarian cancer. Gynecol Oncol **108:**561-568.

162. **Anand N, Murthy S, Amann G, Wernick M, Porter LA, Cukier IH, Collins C, Gray JW, Diebold J, Demetrick DJ, Lee JM.** 2002. Protein elongation factor EEF1A2 is a putative oncogene in ovarian cancer. Nat Genet **31:**301-305.

163. **Kulkarni G, Turbin DA, Amiri A, Jeganathan S, Andrade-Navarro MA, Wu TD, Huntsman DG, Lee JM.** 2007. Expression of protein elongation factor eEF1A2 predicts favorable outcome in breast cancer. Breast Cancer Res Treat **102:**31-41.

164. **Tomlinson VA, Newbery HJ, Wray NR, Jackson J, Larionov A, Miller WR, Dixon JM, Abbott CM.** 2005. Translation elongation factor eEF1A2 is a potential oncoprotein that is overexpressed in two-thirds of breast tumours. BMC Cancer **5:**113.

165. **Cao H, Zhu Q, Huang J, Li B, Zhang S, Yao W, Zhang Y.** 2009. Regulation and functional role of eEF1A2 in pancreatic carcinoma. Biochem Biophys Res Commun **380:**11-16.

166. **Joseph P, O'Kernick CM, Othumpangat S, Lei YX, Yuan BZ, Ong TM.** 2004. Expression profile of eukaryotic translation factors in human cancer tissues and cell lines. Mol Carcinog **40:**171-179.

167. **Grassi G, Scaggiante B, Farra R, Dapas B, Agostini F, Baiz D, Rosso N, Tiribelli C.** 2007. The expression levels of the translational factors eEF1A 1/2 correlate with cell growth but not apoptosis in hepatocellular carcinoma cell lines with different differentiation grade. Biochimie **89:**1544-1552.

168. **Amiri A, Noei F, Jeganathan S, Kulkarni G, Pinke DE, Lee JM.** 2006. eEF1A2 activates Akt and stimulates Akt-dependent actin remodeling, invasion and migration. Oncogene **26:**3027-3040.

169. **Li J, Lu Y, Zhang J, Kang H, Qin Z, Chen C.** 2010. PI4KIIalpha is a novel regulator of tumor growth by its action on angiogenesis and HIF-1alpha regulation. Oncogene **29:**2550-2559.

170. **Mazzocca A, Liotta F, Carloni V.** 2008. Tetraspanin CD81-regulated cell motility plays a critical role in intrahepatic metastasis of hepatocellular carcinoma. Gastroenterology **135:**244-256 e241.

171. **Sjoblom B, Salmazo A, Djinovic-Carugo K.** 2008. Alpha-actinin structure and regulation. Cell Mol Life Sci **65:**2688-2701.

172. **Ishikawa S, Egami H, Kurizaki T, Akagi J, Tamori Y, Yoshida N, Tan X, Hayashi N, Ogawa M.** 2003. Identification of genes related to invasion and metastasis in pancreatic cancer by cDNA representational difference analysis. J Exp Clin Cancer Res **22:**299-306.

173. **Giroux V, Iovanna J, Dagorn JC.** 2006. Probing the human kinome for kinases involved in pancreatic cancer cell survival and gemcitabine resistance. FASEB J **20:**1982-1991.

174. **Guerreiro AS, Fattet S, Kulesza DW, Atamer A, Elsing AN, Shalaby T, Jackson SP, Schoenwaelder SM, Grotzer MA, Delattre O, Arcaro A.** 2011. A sensitized RNA interference screen identifies a novel role for the PI3K p110gamma isoform in medulloblastoma cell proliferation and chemoresistance. Mol Cancer Res **9:**925-935.

175. **Tirkkonen M, Tanner M, Karhu R, Kallioniemi A, Isola J, Kallioniemi OP.** 1998. Molecular cytogenetics of primary breast cancer by CGH. Genes Chromosomes Cancer **21:**177-184.

176. **Mesquita B, Lopes P, Rodrigues A, Pereira D, Afonso M, Leal C, Henrique R, Lind GE, Jeronimo C, Lothe RA, Teixeira MR.** 2013. Frequent copy number gains at 1q21 and 1q32 are associated with overexpression of the ETS transcription factors ETV3 and ELF3 in breast cancer irrespective of molecular subtypes. Breast Cancer Res Treat.

177. **Larramendy ML, Lushnikova T, Bjorkqvist AM, Wistuba, II, Virmani AK, Shivapurkar N, Gazdar AF, Knuutila S.** 2000. Comparative genomic hybridization reveals complex genetic changes in primary breast cancer tumors and their cell lines. Cancer Genet Cytogenet **119:**132 - 138.

178. **Curtis C, Shah SP, Chin SF, Turashvili G, Rueda OM, Dunning MJ, Speed D, Lynch AG, Samarajiwa S, Yuan Y, Graf S, Ha G, Haffari G, Bashashati A, Russell R, McKinney S, Langerod A, Green A, Provenzano E, Wishart G, Pinder S, Watson P, Markowetz F, Murphy L, Ellis I, Purushotham A,**

Borresen-Dale AL, Brenton JD, Tavare S, Caldas C, Aparicio S. 2012. The genomic and transcriptomic architecture of 2,000 breast tumours reveals novel subgroups. Nature **486:**346-352.

179. **Pinke DE, Lee JM.** 2011. The lipid kinase PI4KIIIbeta and the eEF1A2 oncogene co-operate to disrupt three-dimensional in vitro acinar morphogenesis. Exp Cell Res **317:**2503-2511.

180. **Chu KM, Minogue S, Hsuan JJ, Waugh MG.** 2010. Differential effects of the phosphatidylinositol 4-kinases, PI4KIIalpha and PI4KIIIbeta, on Akt activation and apoptosis. Cell Death Dis **1:**e106.

181. **Chappell H, De P, Dryer D, Ellison L, Logan H, MacIntyre M.** 2011. Canadian cancer statistics 2011. Toronto: Canadian Cancer Society **4**.

182. **Sharma GN, Dave R, Sanadya J, Sharma P, Sharma KK.** 2010. Various types and management of breast cancer: an overview. J Adv Pharm Technol Res **1:**109-126.

183. **Maxmen A.** 2012. The hard facts. Nature **485:**S50-51.

184. Rosen PP (2009) *Rosen's breast pathology* (Lippincott Williams & Wilkins).

185. **Redig AJ, McAllister SS.** 2013. Breast cancer as a systemic disease: a view of metastasis. J Intern Med **274:**113-126.

186. **Polyak K.** 2011. Heterogeneity in breast cancer. J Clin Invest **121:**3786-3788.

187. **Tinoco G, Warsch S, Gluck S, Avancha K, Montero AJ.** 2013. Treating breast cancer in the 21st century: emerging biological therapies. J Cancer **4:**117-132.

188. **Allinen M, Beroukhim R, Cai L, Brennan C, Lahti-Domenici J, Huang H, Porter D, Hu M, Chin L, Richardson A, Schnitt S, Sellers WR, Polyak K.** 2004. Molecular characterization of the tumor microenvironment in breast cancer. Cancer Cell **6:**17-32.

189. **Cho SH, Jeon J, Kim SI.** 2012. Personalized medicine in breast cancer: a systematic review. J Breast Cancer **15:**265-272.

190. **Friedl P, Wolf K.** 2003. Tumour-cell invasion and migration: diversity and escape mechanisms. Nat Rev Cancer **3:**362-374.

191. **Jiang P, Enomoto A, Takahashi M.** 2009. Cell biology of the movement of breast cancer cells: intracellular signalling and the actin cytoskeleton. Cancer Lett **284:**122-130.

192. **Mattila PK, Lappalainen P.** 2008. Filopodia: molecular architecture and cellular functions. Nat Rev Mol Cell Biol **9:**446-454.

193. **Yamaguchi H, Condeelis J.** 2007. Regulation of the actin cytoskeleton in cancer cell migration and invasion. Biochim Biophys Acta **1773:**642-652.

194. **Yang C, Svitkina T.** 2011. Visualizing branched actin filaments in lamellipodia by electron tomography. Nat Cell Biol **13:**1012-1013; author reply 1013-1014.

195. **Gupton SL, Gertler FB.** 2007. Filopodia: the fingers that do the walking. Sci STKE **2007:**re5.

196. **Bowden ET, Onikoyi E, Slack R, Myoui A, Yoneda T, Yamada KM, Mueller SC.** 2006. Co-localization of cortactin and phosphotyrosine identifies active invadopodia in human breast cancer cells. Exp Cell Res **312:**1240-1253.

197. **Dominguez R, Holmes KC.** 2011. Actin structure and function. Annu Rev Biophys **40:**169-186.

198. **Pollard TD, Blanchoin L, Mullins RD.** 2001. Actin dynamics. J Cell Sci **114:**3-4.

199. **Shi W, Inamdar MV, Sastry AM, Lastoskie CM.** 2007. Divalent Cation Adsorption on the Actin Monomer. The Journal of Physical Chemistry C **111:**15642-15652.

200. **Saarikangas J, Zhao H, Lappalainen P.** 2010. Regulation of the actin cytoskeleton-plasma membrane interplay by phosphoinositides. Physiol Rev **90:**259-289.

201. **Bugyi B, Carlier MF.** 2010. Control of actin filament treadmilling in cell motility. Annu Rev Biophys **39:**449-470.

202. **Carlsson L, Nystrom LE, Sundkvist I, Markey F, Lindberg U.** 1977. Actin polymerizability is influenced by profilin, a low molecular weight protein in non-muscle cells. J Mol Biol **115:**465-483.

203. **Goldschmidt-Clermont PJ, Furman MI, Wachsstock D, Safer D, Nachmias VT, Pollard TD.** 1992. The control of actin nucleotide exchange by thymosin beta 4 and profilin. A potential regulatory mechanism for actin polymerization in cells. Mol Biol Cell **3:**1015-1024.

204. **Pantaloni D, Carlier MF.** 1993. How profilin promotes actin filament assembly in the presence of thymosin beta 4. Cell **75:**1007-1014.

205. **Kwiatkowski DJ.** 1999. Functions of gelsolin: motility, signaling, apoptosis, cancer. Curr Opin Cell Biol **11:**103-108.

206. **Silacci P, Mazzolai L, Gauci C, Stergiopulos N, Yin HL, Hayoz D.** 2004. Gelsolin superfamily proteins: key regulators of cellular functions. Cell Mol Life Sci **61:**2614-2623.

207. **Carlier MF, Laurent V, Santolini J, Melki R, Didry D, Xia GX, Hong Y, Chua NH, Pantaloni D.** 1997. Actin depolymerizing factor (ADF/cofilin) enhances the rate of filament turnover: implication in actin-based motility. J Cell Biol **136:**1307-1322.

208. **Pavlov D, Muhlrad A, Cooper J, Wear M, Reisler E.** 2007. Actin filament severing by cofilin. J Mol Biol **365:**1350-1358.

209. **Pollard TD.** 1990. Actin. Curr Opin Cell Biol **2:**33-40.

210. **Higgs HN, Pollard TD.** 2000. Activation by Cdc42 and PIP2 of Wiskott-Aldrich Syndrome protein (WASp) Stimulates Actin Nucleation by Arp2/3 Complex. J. Cell Biol. **150:**1311-1320.

211. **Schirenbeck A, Bretschneider T, Arasada R, Schleicher M, Faix J.** 2005. The Diaphanous-related formin dDia2 is required for the formation and maintenance of filopodia. Nat Cell Biol **7:**619-625.

212. **Scita G, Confalonieri S, Lappalainen P, Suetsugu S.** 2008. IRSp53: crossing the road of membrane and actin dynamics in the formation of membrane protrusions. Trends Cell Biol **18:**52-60.

213. **Krugmann S, Jordens I, Gevaert K, Driessens M, Vandekerckhove J, Hall A.** 2001. Cdc42 induces filopodia by promoting the formation of an IRSp53:Mena complex. Curr Biol **11:**1645-1655.

214. **Miki H, Takenawa T.** 2002. WAVE2 serves a functional partner of IRSp53 by regulating its interaction with Rac. Biochem Biophys Res Commun **293:**93-99.

215. **Nakagawa H, Miki H, Nozumi M, Takenawa T, Miyamoto S, Wehland J, Small JV.** 2003. IRSp53 is colocalised with WAVE2 at the tips of protruding lamellipodia and filopodia independently of Mena. J Cell Sci **116:**2577-2583.

216. **Barzik M, Kotova TI, Higgs HN, Hazelwood L, Hanein D, Gertler FB, Schafer DA.** 2005. Ena/VASP proteins enhance actin polymerization in the presence of barbed end capping proteins. J Biol Chem **280:**28653-28662.

217. **Pasic L, Kotova T, Schafer DA.** 2008. Ena/VASP proteins capture actin filament barbed ends. J Biol Chem **283:**9814-9819.

218. **Tokuo H, Ikebe M.** 2004. Myosin X transports Mena/VASP to the tip of filopodia. Biochem Biophys Res Commun **319:**214-220.

219. **Tokuo H, Mabuchi K, Ikebe M.** 2007. The motor activity of myosin-X promotes actin fiber convergence at the cell periphery to initiate filopodia formation. J Cell Biol **179:**229-238.

220. **DeRosier DJ, Edds KT.** 1980. Evidence for fascin cross-links between the actin filaments in coelomocyte filopodia. Exp Cell Res **126:**490-494.

221. **Kureishy N, Sapountzi V, Prag S, Anilkumar N, Adams JC.** 2002. Fascins, and their roles in cell structure and function. Bioessays **24:**350-361.

222. **Arjonen A, Kaukonen R, Ivaska J.** 2011. Filopodia and adhesion in cancer cell motility. Cell Adh Migr **5:**421-430.

223. **Lee K, Gallop JL, Rambani K, Kirschner MW.** 2010. Self-assembly of filopodia-like structures on supported lipid bilayers. Science **329:**1341-1345.

224. **Mattila PK, Pykalainen A, Saarikangas J, Paavilainen VO, Vihinen H, Jokitalo E, Lappalainen P.** 2007. Missing-in-metastasis and IRSp53 deform PI(4,5)P2-rich membranes by an inverse BAR domain-like mechanism. J Cell Biol **176:**953-964.

225. **Kobayashi K, Kuroda S, Fukata M, Nakamura T, Nagase T, Nomura N, Matsuura Y, Yoshida-Kubomura N, Iwamatsu A, Kaibuchi K.** 1998. p140Sra-1 (specifically Rac1-associated protein) is a novel specific target for Rac1 small GTPase. J Biol Chem **273:**291-295.

226. **Lebensohn AM, Kirschner MW.** 2009. Activation of the WAVE complex by coincident signals controls actin assembly. Mol Cell **36:**512-524.

227. **Pollard TD.** 2007. Regulation of actin filament assembly by Arp2/3 complex and formins. Annu Rev Biophys Biomol Struct **36:**451-477.

228. **Oikawa T, Yamaguchi H, Itoh T, Kato M, Ijuin T, Yamazaki D, Suetsugu S, Takenawa T.** 2004. PtdIns(3,4,5)P3 binding is necessary for WAVE2-induced formation of lamellipodia. Nat Cell Biol **6:**420-426.

229. **Das B, Shu X, Day GJ, Han J, Krishna UM, Falck JR, Broek D.** 2000. Control of intramolecular interactions between the pleckstrin homology and Dbl homology domains of Vav and Sos1 regulates Rac binding. J Biol Chem **275:**15074-15081.

230. **Plantard L, Arjonen A, Lock JG, Nurani G, Ivaska J, Stromblad S.** 2010. PtdIns(3,4,5)P(3) is a regulator of myosin-X localization and filopodia formation. J Cell Sci **123:**3525-3534.

231. **Oikawa T, Takenawa T.** 2009. PtdIns(3,4)P2 instigates focal adhesions to generate podosomes. Cell Adh Migr **3:**195-197.

232. **Kolsch V, Charest PG, Firtel RA.** 2008. The regulation of cell motility and chemotaxis by phospholipid signaling. J Cell Sci **121:**551-559.

233. **Lacalle RA, Peregil RM, Albar JP, Merino E, Martinez AC, Merida I, Manes S.** 2007. Type I phosphatidylinositol 4-phosphate 5-kinase controls neutrophil polarity and directional movement. J Cell Biol **179:**1539-1553.

234. **Nishio M, Watanabe K, Sasaki J, Taya C, Takasuga S, Iizuka R, Balla T, Yamazaki M, Watanabe H, Itoh R, Kuroda S, Horie Y, Forster I, Mak TW, Yonekawa H, Penninger JM, Kanaho Y, Suzuki A, Sasaki T.** 2007. Control of cell polarity and motility by the PtdIns(3,4,5)P3 phosphatase SHIP1. Nat Cell Biol **9:**36-44.

235. **Vignjevic D, Schoumacher M, Gavert N, Janssen KP, Jih G, Lae M, Louvard D, Ben-Ze'ev A, Robine S.** 2007. Fascin, a novel target of beta-catenin-TCF signaling, is expressed at the invasive front of human colon cancer. Cancer Res **67:**6844-6853.

236. **Yang LY, Tao YM, Ou DP, Wang W, Chang ZG, Wu F.** 2006. Increased expression of Wiskott-Aldrich syndrome protein family verprolin-homologous protein 2 correlated with poor prognosis of hepatocellular carcinoma. Clin Cancer Res **12:**5673-5679.

237. **Wang WS, Zhong HJ, Xiao DW, Huang X, Liao LD, Xie ZF, Xu XE, Shen ZY, Xu LY, Li EM.** 2010. The expression of CFL1 and N-WASP in esophageal squamous cell carcinoma and its correlation with clinicopathological features. Dis Esophagus **23:**512-521.

238. **Semba S, Iwaya K, Matsubayashi J, Serizawa H, Kataba H, Hirano T, Kato H, Matsuoka T, Mukai K.** 2006. Coexpression of actin-related protein 2 and Wiskott-Aldrich syndrome family verproline-homologous protein 2 in adenocarcinoma of the lung. Clin Cancer Res **12:**2449-2454.

239. **Iwaya K, Oikawa K, Semba S, Tsuchiya B, Mukai Y, Otsubo T, Nagao T, Izumi M, Kuroda M, Domoto H, Mukai K.** 2007. Correlation between liver metastasis of the colocalization of actin-related protein 2 and 3 complex and WAVE2 in colorectal carcinoma. Cancer Sci **98:**992-999.

240. **Fernando HS, Davies SR, Chhabra A, Watkins G, Douglas-Jones A, Kynaston H, Mansel RE, Jiang WG.** 2007. Expression of the WASP verprolin-homologues (WAVE members) in human breast cancer. Oncology **73:**376-383.

241. **Iwaya K, Norio K, Mukai K.** 2007. Coexpression of Arp2 and WAVE2 predicts poor outcome in invasive breast carcinoma. Mod Pathol **20:**339-343.

242. **Nurnberg A, Kitzing T, Grosse R.** 2011. Nucleating actin for invasion. Nat Rev Cancer **11:**177-187.

243. **Machesky LM, Li A.** 2010. Fascin: Invasive filopodia promoting metastasis. Commun Integr Biol **3:**263-270.

244. **Yoder BJ, Tso E, Skacel M, Pettay J, Tarr S, Budd T, Tubbs RR, Adams JC, Hicks DG.** 2005. The expression of fascin, an actin-bundling motility protein, correlates with hormone receptor-negative breast cancer and a more aggressive clinical course. Clin Cancer Res **11:**186-192.

245. **Takikita M, Hu N, Shou JZ, Giffen C, Wang QH, Wang C, Hewitt SM, Taylor PR.** 2011. Fascin and CK4 as biomarkers for esophageal squamous cell carcinoma. Anticancer Res **31:**945-952.

246. **Pelosi G, Pastorino U, Pasini F, Maissoneuve P, Fraggetta F, Iannucci A, Sonzogni A, De Manzoni G, Terzi A, Durante E, Bresaola E, Pezzella F, Viale G.** 2003. Independent prognostic value of fascin immunoreactivity in stage I nonsmall cell lung cancer. Br J Cancer **88:**537-547.

247. **Hashimoto Y, Skacel M, Lavery IC, Mukherjee AL, Casey G, Adams JC.** 2006. Prognostic significance of fascin expression in advanced colorectal cancer: an immunohistochemical study of colorectal adenomas and adenocarcinomas. BMC Cancer **6:**241.

248. **Yamashiro S, Yamakita Y, Ono S, Matsumura F.** 1998. Fascin, an actin-bundling protein, induces membrane protrusions and increases cell motility of epithelial cells. Mol Biol Cell **9:**993-1006.

249. **Lizarraga F, Poincloux R, Romao M, Montagnac G, Le Dez G, Bonne I, Rigaill G, Raposo G, Chavrier P.** 2009. Diaphanous-related formins are required for invadopodia formation and invasion of breast tumor cells. Cancer Res **69:**2792-2800.

250. **Qian Y, Corum L, Meng Q, Blenis J, Zheng JZ, Shi X, Flynn DC, Jiang B-H.** 2004. PI3K induced actin filament remodeling through Akt and p70S6K1: implication of essential role in cell migration. Am J Physiol Cell Physiol **286:**C153-163.

251. **Vivanco I, Sawyers CL.** 2002. The phosphatidylinositol 3-kinase AKT pathway in human cancer. Nat Rev Cancer **2:**489 - 501.

252. **LoPiccolo J, Blumenthal GM, Bernstein WB, Dennis PA.** 2008. Targeting the PI3K/Akt/mTOR pathway: effective combinations and clinical considerations. Drug Resist Updat **11:**32-50.

253. **Datta SR, Dudek H, Tao X, Masters S, Fu H, Gotoh Y, Greenberg ME.** 1997. Akt Phosphorylation of BAD Couples Survival Signals to the Cell-Intrinsic Death Machinery. Cell **91:**231-241.

254. **Diehl JA, Cheng M, Roussel MF, Sherr CJ.** 1998. Glycogen synthase kinase-3Î² regulates cyclin D1 proteolysis and subcellular localization. Genes & Development **12:**3499-3511.

255. **Laplante M, Sabatini DM.** 2009. mTOR signaling at a glance. J Cell Sci **122:**3589-3594.

256. **Inoki K, Li Y, Zhu T, Wu J, Guan KL.** 2002. TSC2 is phosphorylated and inhibited by Akt and suppresses mTOR signalling. Nat Cell Biol **4:**648-657.

257. **Richter JD, Sonenberg N.** 2005. Regulation of cap-dependent translation by eIF4E inhibitory proteins. Nature **433:**477-480.

258. **Ma XM, Blenis J.** 2009. Molecular mechanisms of mTOR-mediated translational control. Nat Rev Mol Cell Biol **10:**307-318.

259. **Thiery JP, Acloque H, Huang RY, Nieto MA.** 2009. Epithelial-mesenchymal transitions in development and disease. Cell **139:**871-890.

260. **Julien S, Puig I, Caretti E, Bonaventure J, Nelles L, van Roy F, Dargemont C, de Herreros AG, Bellacosa A, Larue L.** 2007. Activation of NF-kappaB by Akt upregulates Snail expression and induces epithelium mesenchyme transition. Oncogene **26:**7445-7456.

261. **Brock C, Schaefer M, Reusch HP, Czupalla C, Michalke M, Spicher K, Schultz G, Nurnberg B.** 2003. Roles of G beta gamma in membrane recruitment and activation of p110 gamma/p101 phosphoinositide 3-kinase gamma. J Cell Biol **160:**89-99.

262. **Sarbassov DD, Guertin DA, Ali SM, Sabatini DM.** 2005. Phosphorylation and Regulation of Akt/PKB by the Rictor-mTOR Complex. Science **307:**1098-1101.

263. **Andjelkovic M, Alessi DR, Meier R, Fernandez A, Lamb NJC, Frech M, Cron P, Cohen P, Lucocq JM, Hemmings BA.** 1997. Role of Translocation in the Activation and Function of Protein Kinase B. J. Biol. Chem. **272:**31515-31524.

264. **Riaz A, Zeller KS, Johansson S.** 2012. Receptor-specific mechanisms regulate phosphorylation of AKT at Ser473: role of RICTOR in beta1 integrin-mediated cell survival. PLoS One **7:**e32081.

265. **Kumar CC, Madison V.** 2005. AKT crystal structure and AKT-specific inhibitors. Oncogene **24:**7493-7501.

266. **Huang BX, Kim H-Y.** 2006. Interdomain Conformational Changes in Akt Activation Revealed by Chemical Cross-linking and Tandem Mass Spectrometry. Mol Cell Proteomics **5:**1045-1053.

267. **Kirkegaard T, Witton CJ, Edwards J, Nielsen KV, Jensen LB, Campbell FM, Cooke TG, Bartlett JM.** 2010. Molecular alterations in AKT1, AKT2 and AKT3 detected in breast and prostatic cancer by FISH. Histopathology **56:**203-211.

268. **Dillon RL, Marcotte R, Hennessy BT, Woodgett JR, Mills GB, Muller WJ.** 2009. Akt1 and akt2 play distinct roles in the initiation and metastatic phases of mammary tumor progression. Cancer Res **69:**5057-5064.

269. **Chen WS, Xu PZ, Gottlob K, Chen ML, Sokol K, Shiyanova T, Roninson I, Weng W, Suzuki R, Tobe K, Kadowaki T, Hay N.** 2001. Growth retardation and increased apoptosis in mice with homozygous disruption of the Akt1 gene. Genes Dev **15:**2203-2208.

270. **Garofalo RS, Orena SJ, Rafidi K, Torchia AJ, Stock JL, Hildebrandt AL, Coskran T, Black SC, Brees DJ, Wicks JR, McNeish JD, Coleman KG.** 2003. Severe diabetes, age-dependent loss of adipose tissue, and mild growth deficiency in mice lacking Akt2/PKB beta. J Clin Invest **112:**197-208.

271. **Tschopp O, Yang ZZ, Brodbeck D, Dummler BA, Hemmings-Mieszczak M, Watanabe T, Michaelis T, Frahm J, Hemmings BA.** 2005. Essential role of protein kinase B gamma (PKB gamma/Akt3) in postnatal brain development but not in glucose homeostasis. Development **132:**2943-2954.

272. **Peng XD, Xu PZ, Chen ML, Hahn-Windgassen A, Skeen J, Jacobs J, Sundararajan D, Chen WS, Crawford SE, Coleman KG, Hay N.** 2003. Dwarfism, impaired skin development, skeletal muscle atrophy, delayed bone development, and impeded adipogenesis in mice lacking Akt1 and Akt2. Genes Dev **17:**1352-1365.

273. **Gonzalez E, McGraw TE.** 2009. The Akt kinases: isoform specificity in metabolism and cancer. Cell Cycle **8:**2502-2508.

274. **Zinda MJ, Johnson MA, Paul JD, Horn C, Konicek BW, Lu ZH, Sandusky G, Thomas JE, Neubauer BL, Lai MT, Graff JR.** 2001. AKT-1, -2, and -3 are expressed in both normal and tumor tissues of the lung, breast, prostate, and colon. Clin Cancer Res **7:**2475-2479.

275. **Bellacosa A, de Feo D, Godwin AK, Bell DW, Cheng JQ, Altomare DA, Wan M, Dubeau L, Scambia G, Masciullo V, Ferrandina G, Benedetti Panici P, Mancuso S, Neri G, Testa JR.** 1995. Molecular alterations of the AKT2 oncogene in ovarian and breast carcinomas. Int J Cancer **64:**280-285.

276. **Stal O, Perez-Tenorio G, Akerberg L, Olsson B, Nordenskjold B, Skoog L, Rutqvist LE.** 2003. Akt kinases in breast cancer and the results of adjuvant therapy. Breast Cancer Res **5:**R37-44.

277. **Carpten JD, Faber AL, Horn C, Donoho GP, Briggs SL, Robbins CM, Hostetter G, Boguslawski S, Moses TY, Savage S, Uhlik M, Lin A, Du J, Qian YW, Zeckner DJ, Tucker-Kellogg G, Touchman J, Patel K, Mousses S, Bittner M, Schevitz R, Lai MH, Blanchard KL, Thomas JE.** 2007. A transforming mutation in the pleckstrin homology domain of AKT1 in cancer. Nature **448:**439-444.

278. **Sun M, Wang G, Paciga JE, Feldman RI, Yuan ZQ, Ma XL, Shelley SA, Jove R, Tsichlis PN, Nicosia SV, Cheng JQ.** 2001. AKT1/PKBalpha kinase is frequently elevated in human cancers and its constitutive activation is required for oncogenic transformation in NIH3T3 cells. Am J Pathol **159:**431-437.

279. **Amundadottir LT, Leder P.** 1998. Signal transduction pathways activated and required for mammary carcinogenesis in response to specific oncogenes. Oncogene **16:**737-746.

280. **Shayesteh L, Lu Y, Kuo WL, Baldocchi R, Godfrey T, Collins C, Pinkel D, Powell B, Mills GB, Gray JW.** 1999. PIK3CA is implicated as an oncogene in ovarian cancer. Nat Genet **21:**99-102.

281. **Philp AJ, Campbell IG, Leet C, Vincan E, Rockman SP, Whitehead RH, Thomas RJ, Phillips WA.** 2001. The phosphatidylinositol 3'-kinase p85alpha gene is an oncogene in human ovarian and colon tumors. Cancer Res **61:**7426-7429.

282. **Gershtein ES, Shatskaya VA, Ermilova VD, Kushlinsky NE, Krasil'nikov MA.** 1999. Phospatidylinositol 3-kinase expression in human breast cancer. Clinica chimica acta **287:**59-67.

283. **Sun M, Paciga JE, Feldman RI, Yuan Z, Coppola D, Lu YY, Shelley SA, Nicosia SV, Cheng JQ.** 2001. Phosphatidylinositol-3-OH Kinase (PI3K)/AKT2, activated in breast cancer, regulates and is induced by estrogen receptor alpha (ERalpha) via interaction between ERalpha and PI3K. Cancer Res **61:**5985-5991.

284. **Wu X, Senechal K, Neshat MS, Whang YE, Sawyers CL.** 1998. The PTEN/MMAC1 tumor suppressor phosphatase functions as a negative regulator of the phosphoinositide 3-kinase/Akt pathway. Proc Natl Acad Sci U S A **95:**15587-15591.

285. **Whang YE, Wu X, Suzuki H, Reiter RE, Tran C, Vessella RL, Said JW, Isaacs WB, Sawyers CL.** 1998. Inactivation of the tumor suppressor PTEN/MMAC1 in advanced human prostate cancer through loss of expression. Proc Natl Acad Sci U S A **95:**5246-5250.

286. **Li J, Yen C, Liaw D, Podsypanina K, Bose S, Wang SI, Puc J, Miliaresis C, Rodgers L, McCombie R, Bigner SH, Giovanella BC, Ittmann M, Tycko B, Hibshoosh H, Wigler MH, Parsons R.** 1997. PTEN, a putative protein tyrosine phosphatase gene mutated in human brain, breast, and prostate cancer. Science **275:**1943-1947.

287. **Georgescu MM, Kirsch KH, Akagi T, Shishido T, Hanafusa H.** 1999. The tumor-suppressor activity of PTEN is regulated by its carboxyl-terminal region. Proc Natl Acad Sci U S A **96:**10182-10187.

288. **Ali IU, Schriml LM, Dean M.** 1999. Mutational spectra of PTEN/MMAC1 gene: a tumor suppressor with lipid phosphatase activity. J Natl Cancer Inst **91:**1922-1932.

289. **Lu Y, Lin YZ, LaPushin R, Cuevas B, Fang X, Yu SX, Davies MA, Khan H, Furui T, Mao M, Zinner R, Hung MC, Steck P, Siminovitch K, Mills GB.** 1999. The PTEN/MMAC1/TEP tumor suppressor gene decreases cell growth and induces apoptosis and anoikis in breast cancer cells. Oncogene **18:**7034-7045.

290. **Gewinner C, Wang ZC, Richardson A, Teruya-Feldstein J, Etemadmoghadam D, Bowtell D, Barretina J, Lin WM, Rameh L, Salmena L, Pandolfi PP, Cantley LC.** 2009. Evidence that inositol polyphosphate 4-phosphatase type II is a tumor suppressor that inhibits PI3K signaling. Cancer Cell **16:**115-125.

291. **Ling K, Schill NJ, Wagoner MP, Sun Y, Anderson RA.** 2006. Movin' on up: the role of PtdIns(4,5)P(2) in cell migration. Trends Cell Biol **16:**276-284.

292. **Funamoto S, Meili R, Lee S, Parry L, Firtel RA.** 2002. Spatial and temporal regulation of 3-phosphoinositides by PI 3-kinase and PTEN mediates chemotaxis. Cell **109:**611-623.

293. **Yuan TL, Cantley LC.** 2008. PI3K pathway alterations in cancer: variations on a theme. Oncogene **27:**5497-5510.

294. **Bunney TD, Katan M.** 2010. Phosphoinositide signalling in cancer: beyond PI3K and PTEN. Nat Rev Cancer **10:**342-352.

295. **Waugh MG.** 2012. Phosphatidylinositol 4-kinases, phosphatidylinositol 4-phosphate and cancer. Cancer Lett **325:**125-131.

296. **Hanahan D, Weinberg RA.** 2000. The hallmarks of cancer. Cell **100:**57-70.

297. **Kopnin BP.** 2000. Targets of oncogenes and tumor suppressors: key for understanding basic mechanisms of carcinogenesis. Biochemistry (Mosc) **65:**2-27.

298. **Sporn MB.** 1996. The war on cancer. Lancet **347:**1377-1381.

299. **Edmonds BT, Wyckoff J, Yeung YG, Wang Y, Stanley ER, Jones J, Segall J, Condeelis J.** 1996. Elongation factor-1 alpha is an overexpressed actin binding protein in metastatic rat mammary adenocarcinoma. J Cell Sci **109 (Pt 11):**2705-2714.

300. **Chen L, Yang S, Jakoncic J, Zhang JJ, Huang XY.** 2010. Migrastatin analogues target fascin to block tumour metastasis. Nature **464:**1062-1066.

301. **Debnath J, Muthuswamy SK, Brugge JS.** 2003. Morphogenesis and oncogenesis of MCF-10A mammary epithelial acini grown in three-dimensional basement membrane cultures. Methods **30:**256-268.

302. **Nilufar S, Morrow AA, Lee JM, Perkins TJ.** 2013. FiloDetect: automatic detection of filopodia from fluorescence microscopy images. BMC Syst Biol **7:**66.

303. **Jones LJ, Gray M, Yue ST, Haugland RP, Singer VL.** 2001. Sensitive determination of cell number using the CyQUANT cell proliferation assay. J Immunol Methods **254:**85-98.

304. **Husainy AN, Morrow AA, Perkins TJ, Lee JM.** 2010. Robust patterns in the stochastic organization of filopodia. BMC Cell Biol **11:**86.

305. **Kahns S, Lund A, Kristensen P, Knudsen CR, Clark BF, Cavallius J, Merrick WC.** 1998. The elongation factor 1 A-2 isoform from rabbit: cloning of the cDNA and characterization of the protein. Nucleic Acids Res **26:**1884-1890.

306. **Lee S, Wolfraim LA, Wang E.** 1993. Differential expression of S1 and elongation factor-1 alpha during rat development. J Biol Chem **268:**24453-24459.

307. **Thornton S, Anand N, Purcell D, Lee J.** 2003. Not just for housekeeping: protein initiation and elongation factors in cell growth and tumorigenesis. J Mol Med **81:**536-548.

308. **Hershey JW.** 1991. Translational control in mammalian cells. Annu Rev Biochem **60:**717-755.

309. **Bernaciak TM, Zareno J, Parsons JT, Silva CM.** 2009. A novel role for signal transducer and activator of transcription 5b (STAT5b) in beta1-integrin-mediated human breast cancer cell migration. Breast Cancer Res **11:**R52.

310. **Yoon CH, Kim MJ, Lee H, Kim RK, Lim EJ, Yoo KC, Lee GH, Cui YH, Oh YS, Gye MC, Lee YY, Park IC, An S, Hwang SG, Park MJ, Suh Y, Lee SJ.** 2012. PTTG1 oncogene promotes tumor malignancy via epithelial to mesenchymal transition and expansion of cancer stem cell population. J Biol Chem **287:**19516-19527.

311. **Garcia-Marcos M, Kietrsunthorn PS, Pavlova Y, Adia MA, Ghosh P, Farquhar MG.** 2012. Functional characterization of the guanine nucleotide exchange factor (GEF) motif of GIV protein reveals a threshold effect in signaling. Proc Natl Acad Sci U S A **109:**1961-1966.

312. **Goldbeter A, Koshland DE, Jr.** 1981. An amplified sensitivity arising from covalent modification in biological systems. Proc Natl Acad Sci U S A **78:**6840-6844.

313. **Huang CY, Ferrell JE, Jr.** 1996. Ultrasensitivity in the mitogen-activated protein kinase cascade. Proc Natl Acad Sci U S A **93:**10078-10083.

314. **Ridley AJ, Schwartz MA, Burridge K, Firtel RA, Ginsberg MH, Borisy G, Parsons JT, Horwitz AR.** 2003. Cell migration: integrating signals from front to back. Science **302:**1704-1709.

315. **Edmonds BT, Murray J, Condeelis J.** 1995. pH regulation of the F-actin binding properties of Dictyostelium elongation factor 1 alpha. J Biol Chem **270:**15222-15230.

316. **Lopez-Valenzuela JA, Gibbon BC, Hughes PA, Dreher TW, Larkins BA.** 2003. eEF1A isoforms change in abundance and actin-binding activity during maize endosperm development. Plant Physiol **133:**1285-1295.

317. **Yang W, Burkhart W, Cavallius J, Merrick WC, Boss WF.** 1993. Purification and characterization of a phosphatidylinositol 4-kinase activator in carrot cells. J Biol Chem **268:**392-398.

318. **Munshi R, Kandl KA, Carr-Schmid A, Whitacre JL, Adams AE, Kinzy TG.** 2001. Overexpression of translation elongation factor 1A affects the organization and function of the actin cytoskeleton in yeast. Genetics **157:**1425-1436.

319. **Baker BM, Chen CS.** 2012. Deconstructing the third dimension: how 3D culture microenvironments alter cellular cues. J Cell Sci **125:**3015-3024.

320. **Meyer AS, Hughes-Alford SK, Kay JE, Castillo A, Wells A, Gertler FB, Lauffenburger DA.** 2012. 2D protrusion but not motility predicts growth factor-induced cancer cell migration in 3D collagen. J Cell Biol **197:**721-729.

321. **Chen HC.** 2005. Boyden chamber assay. Methods Mol Biol **294:**15-22.

322. **Qian Y, Corum L, Meng Q, Blenis J, Zheng JZ, Shi X, Flynn DC, Jiang BH.** 2004. PI3K induced actin filament remodeling through Akt and p70S6K1:

implication of essential role in cell migration. Am J Physiol Cell Physiol **286:**C153-163.

323. **Cheng JQ, Ruggeri B, Klein WM, Sonoda G, Altomare DA, Watson DK, Testa JR.** 1996. Amplification of AKT2 in human pancreatic cells and inhibition of AKT2 expression and tumorigenicity by antisense RNA. Proceedings of the National Academy of Sciences of the United States of America **93:**3636-3641.

324. **Cheng JQ, Godwin AK, Bellacosa A, Taguchi T, Franke TF, Hamilton TC, Tsichlis PN, Testa JR.** 1992. AKT2, a putative oncogene encoding a member of a subfamily of protein-serine/threonine kinases, is amplified in human ovarian carcinomas. Proceedings of the National Academy of Sciences of the United States of America **89:**9267-9271.

325. **Bachman KE, Argani P, Samuels Y, Silliman N, Ptak J, Szabo S, Konishi H, Karakas B, Blair BG, Lin C.** 2004. The PIK3CA gene is mutated with high frequency in human breast cancers. Cancer Biol Ther **3:**772 - 775.

326. **Yamamoto H, Shigematsu H, Nomura M, Lockwood WW, Sato M, Okumura N, Soh J, Suzuki M, Wistuba II, Fong KM, Lee H, Toyooka S, Date H, Lam WL, Minna JD, Gazdar AF.** 2008. PIK3CA Mutations and Copy Number Gains in Human Lung Cancers. Cancer Res **68:**6913-6921.

327. **Lopez-Knowles E, O'Toole SA, McNeil CM, Millar EK, Qiu MR, Crea P, Daly RJ, Musgrove EA, Sutherland RL.** 2010. PI3K pathway activation in breast cancer is associated with the basal-like phenotype and cancer-specific mortality. Int J Cancer **126:**1121-1131.

328. **Chalhoub N, Baker SJ.** 2009. PTEN and the PI3-kinase pathway in cancer. Annu Rev Pathol **4:**127-150.

329. **Song MS, Salmena L, Pandolfi PP.** 2012. The functions and regulation of the PTEN tumour suppressor. Nat Rev Mol Cell Biol **13:**283-296.

330. **Ivetac I, Gurung R, Hakim S, Horan KA, Sheffield DA, Binge LC, Majerus PW, Tiganis T, Mitchell CA.** 2009. Regulation of PI(3)K/Akt signalling and cellular transformation by inositol polyphosphate 4-phosphatase-1. EMBO Rep **10:**487-493.

331. **Bridges D, Ma JT, Park S, Inoki K, Weisman LS, Saltiel AR.** 2012. Phosphatidylinositol 3,5-bisphosphate plays a role in the activation and subcellular localization of mechanistic target of rapamycin 1. Mol Biol Cell **23:**2955-2962.

332. **Zimmermann S, Moelling K.** 1999. Phosphorylation and regulation of Raf by Akt (protein kinase B). Science **286:**1741-1744.

333. **Li J.** 1997. PTEN, a putative protein tyrosine phosphatase gene mutated in human brain, breast, and prostate cancer. Science **275:**1943-1947.

334. **He X, Saji M, Radhakrishnan D, Romigh T, Ngeow J, Yu Q, Wang Y, Ringel MD, Eng C.** 2012. PTEN lipid phosphatase activity and proper subcellular localization are necessary and sufficient for down-regulating AKT phosphorylation in the nucleus in Cowden syndrome. J Clin Endocrinol Metab **97:**E2179-2187.

335. **Toth B, Balla A, Ma H, Knight ZA, Shokat KM, Balla T.** 2006. Phosphatidylinositol 4-kinase IIIbeta regulates the transport of ceramide between the endoplasmic reticulum and Golgi. J Biol Chem **281:**36369-36377.

336. **Knight ZA, Gonzalez B, Feldman ME, Zunder ER, Goldenberg DD, Williams O, Loewith R, Stokoe D, Balla A, Toth B, Balla T, Weiss WA, Williams RL, Shokat KM.** 2006. A pharmacological map of the PI3-K family defines a role for p110alpha in insulin signaling. Cell **125:**733-747.

337. **Hsu NY, Ilnytska O, Belov G, Santiana M, Chen YH, Takvorian PM, Pau C, van der Schaar H, Kaushik-Basu N, Balla T, Cameron CE, Ehrenfeld E, van Kuppeveld FJ, Altan-Bonnet N.** 2010. Viral reorganization of the secretory pathway generates distinct organelles for RNA replication. Cell **141:**799-811.

338. **Mahajan K, Mahajan NP.** 2012. PI3K-independent AKT activation in cancers: a treasure trove for novel therapeutics. J Cell Physiol **227:**3178-3184.

339. **Depowski PL, Rosenthal SI, Ross JS.** 2001. Loss of expression of the PTEN gene protein product is associated with poor outcome in breast cancer. Mod Pathol **14:**672-676.

340. **Perren A, Weng LP, Boag AH, Ziebold U, Thakore K, Dahia PL, Komminoth P, Lees JA, Mulligan LM, Mutter GL, Eng C.** 1999. Immunohistochemical evidence of loss of PTEN expression in primary ductal adenocarcinomas of the breast. Am J Pathol **155:**1253-1260.

341. **Murphy JE, Padilla BE, Hasdemir B, Cottrell GS, Bunnett NW.** 2009. Endosomes: a legitimate platform for the signaling train. Proc Natl Acad Sci U S A **106:**17615-17622.

342. **Kelly KL, Ruderman NB.** 1993. Insulin-stimulated phosphatidylinositol 3-kinase. Association with a 185-kDa tyrosine-phosphorylated protein (IRS-1) and localization in a low density membrane vesicle. J Biol Chem **268:**4391-4398.

343. **Wang Y, Pennock S, Chen X, Wang Z.** 2002. Endosomal signaling of epidermal growth factor receptor stimulates signal transduction pathways leading to cell survival. Mol Cell Biol **22:**7279-7290.

344. **Vieira AV, Lamaze C, Schmid SL.** 1996. Control of EGF receptor signaling by clathrin-mediated endocytosis. Science **274:**2086-2089.

345. **Nazarewicz RR, Salazar G, Patrushev N, San Martin A, Hilenski L, Xiong S, Alexander RW.** 2011. Early endosomal antigen 1 (EEA1) is an obligate scaffold for angiotensin II-induced, PKC-alpha-dependent Akt activation in endosomes. J Biol Chem **286:**2886-2895.

346. **Schenck A, Goto-Silva L, Collinet C, Rhinn M, Giner A, Habermann B, Brand M, Zerial M.** 2008. The endosomal protein Appl1 mediates Akt substrate specificity and cell survival in vertebrate development. Cell **133:**486-497.

347. **Sato M, Ueda Y, Takagi T, Umezawa Y.** 2003. Production of PtdInsP3 at endomembranes is triggered by receptor endocytosis. Nat Cell Biol **5:**1016-1022.

348. **Cheng KW, Lahad JP, Gray JW, Mills GB.** 2005. Emerging role of RAB GTPases in cancer and human disease. Cancer Res **65:**2516-2519.

349. **Yoon SO, Shin S, Mercurio AM.** 2005. Hypoxia stimulates carcinoma invasion by stabilizing microtubules and promoting the Rab11 trafficking of the alpha6beta4 integrin. Cancer Res **65:**2761-2769.

350. **Wuttke A, Sagetorp J, Tengholm A.** 2010. Distinct plasma-membrane PtdIns(4)P and PtdIns(4,5)P2 dynamics in secretagogue-stimulated beta-cells. J Cell Sci **123:**1492-1502.

351. **Hammond GR, Fischer MJ, Anderson KE, Holdich J, Koteci A, Balla T, Irvine RF.** 2012. PI4P and PI(4,5)P2 are essential but independent lipid determinants of membrane identity. Science **337:**727-730.

352. **Brown FD, Rozelle AL, Yin HL, Balla T, Donaldson JG.** 2001. Phosphatidylinositol 4,5-bisphosphate and Arf6-regulated membrane traffic. J Cell Biol **154:**1007-1017.

353. **Rajebhosale M, Greenwood S, Vidugiriene J, Jeromin A, Hilfiker S.** 2003. Phosphatidylinositol 4-OH kinase is a downstream target of neuronal calcium sensor-1 in enhancing exocytosis in neuroendocrine cells. J Biol Chem **278:**6075-6084.

354. **Hirst J, Motley A, Harasaki K, Peak Chew SY, Robinson MS.** 2003. EpsinR: an ENTH domain-containing protein that interacts with AP-1. Mol Biol Cell **14:**625-641.

355. **Lanzetti L.** 2007. Actin in membrane trafficking. Curr Opin Cell Biol **19:**453-458.

356. **Tayeb MA, Skalski M, Cha MC, Kean MJ, Scaife M, Coppolino MG.** 2005. Inhibition of SNARE-mediated membrane traffic impairs cell migration. Exp Cell Res **305:**63-73.

357. **Sesaki H, Ogihara S.** 1997. Protrusion of cell surface coupled with single exocytotic events of secretion of the slime in Physarum plasmodia. J Cell Sci **110 (Pt 7):**809-818.

358. **Tsaneva-Atanasova K, Burgo A, Galli T, Holcman D.** 2009. Quantifying neurite growth mediated by interactions among secretory vesicles, microtubules, and actin networks. Biophys J **96:**840-857.

359. **Pellinen T, Ivaska J.** 2006. Integrin traffic. J Cell Sci **119:**3723-3731.

360. **Parsons M, Monypenny J, Ameer-Beg SM, Millard TH, Machesky LM, Peter M, Keppler MD, Schiavo G, Watson R, Chernoff J, Zicha D, Vojnovic B, Ng T.** 2005. Spatially distinct binding of Cdc42 to PAK1 and N-WASP in breast carcinoma cells. Mol Cell Biol **25:**1680-1695.

361. **Abe K, Rossman KL, Liu B, Ritola KD, Chiang D, Campbell SL, Burridge K, Der CJ.** 2000. Vav2 is an activator of Cdc42, Rac1, and RhoA. J Biol Chem **275:**10141-10149.

362. **Gotthardt K, Ahmadian MR.** 2007. Asef is a Cdc42-specific guanine nucleotide exchange factor. Biol Chem **388:**67-71.

363. **Bohil AB, Robertson BW, Cheney RE.** 2006. Myosin-X is a molecular motor that functions in filopodia formation. Proc Natl Acad Sci U S A **103:**12411-12416.

364. **Zhang H, Berg JS, Li Z, Wang Y, Lang P, Sousa AD, Bhaskar A, Cheney RE, Stromblad S.** 2004. Myosin-X provides a motor-based link between integrins and the cytoskeleton. Nat Cell Biol **6:**523-531.

365. **Jones MC, Caswell PT, Norman JC.** 2006. Endocytic recycling pathways: emerging regulators of cell migration. Curr Opin Cell Biol **18:**549-557.

366. **Powelka AM, Sun J, Li J, Gao M, Shaw LM, Sonnenberg A, Hsu VW.** 2004. Stimulation-dependent recycling of integrin beta1 regulated by ARF6 and Rab11. Traffic **5:**20-36.

367. **Caswell PT, Norman JC.** 2006. Integrin trafficking and the control of cell migration. Traffic **7:**14-21.

368. **Innamorati G, Le Gouill C, Balamotis M, Birnbaumer M.** 2001. The long and the short cycle. Alternative intracellular routes for trafficking of G-protein-coupled receptors. J Biol Chem **276:**13096-13103.

369. **Fan GH, Lapierre LA, Goldenring JR, Sai J, Richmond A.** 2004. Rab11-family interacting protein 2 and myosin Vb are required for CXCR2 recycling and receptor-mediated chemotaxis. Mol Biol Cell **15:**2456-2469.

370. **Prigozhina NL, Waterman-Storer CM.** 2006. Decreased polarity and increased random motility in PtK1 epithelial cells correlate with inhibition of endosomal recycling. J Cell Sci **119:**3571-3582.

371. **Edling CE, Selvaggi F, Buus R, Maffucci T, Di Sebastiano P, Friess H, Innocenti P, Kocher HM, Falasca M.** 2010. Key role of phosphoinositide 3-kinase class IB in pancreatic cancer. Clin Cancer Res **16:**4928-4937.

372. **El Haibi CP, Sharma PK, Singh R, Johnson PR, Suttles J, Singh S, Lillard JW, Jr.** 2010. PI3Kp110-, Src-, FAK-dependent and DOCK2-independent migration and invasion of CXCL13-stimulated prostate cancer cells. Mol Cancer **9:**85.

373. **Palmieri D, Bouadis A, Ronchetti R, Merino MJ, Steeg PS.** 2006. Rab11a differentially modulates epidermal growth factor-induced proliferation and motility in immortal breast cells. Breast Cancer Res Treat **100:**127-137.

374. **Babst M, Odorizzi G, Estepa EJ, Emr SD.** 2000. Mammalian tumor susceptibility gene 101 (TSG101) and the yeast homologue, Vps23p, both function in late endosomal trafficking. Traffic **1:**248-258.

375. **Wiley HS.** 2003. Trafficking of the ErbB receptors and its influence on signaling. Exp Cell Res **284:**78-88.

376. **Miller TW, Rexer BN, Garrett JT, Arteaga CL.** 2011. Mutations in the phosphatidylinositol 3-kinase pathway: role in tumor progression and therapeutic implications in breast cancer. Breast Cancer Res **13:**224.

377. **Montemurro F, Di Cosimo S, Arpino G.** 2013. Human epidermal growth factor receptor 2 (HER2)-positive and hormone receptor-positive breast cancer: new insights into molecular interactions and clinical implications. Ann Oncol.

378. **Clark AS, West K, Streicher S, Dennis PA.** 2002. Constitutive and inducible Akt activity promotes resistance to chemotherapy, trastuzumab, or tamoxifen in breast cancer cells. Mol Cancer Ther **1:**707-717.

379. **Nahta R, O'Regan RM.** 2010. Evolving strategies for overcoming resistance to HER2-directed therapy: targeting the PI3K/Akt/mTOR pathway. Clin Breast Cancer **10 Suppl 3:**S72-78.

380. **Sheri A, Martin LA, Johnston S.** 2010. Targeting endocrine resistance: is there a role for mTOR inhibition? Clin Breast Cancer **10 Suppl 3:**S79-85.

381. **Hennessy BT, Smith DL, Ram PT, Lu Y, Mills GB.** 2005. Exploiting the PI3K/AKT pathway for cancer drug discovery. Nat Rev Drug Discov **4:**988-1004.

382. **Morrow PK, Wulf GM, Ensor J, Booser DJ, Moore JA, Flores PR, Xiong Y, Zhang S, Krop IE, Winer EP, Kindelberger DW, Coviello J, Sahin AA, Nunez R, Hortobagyi GN, Yu D, Esteva FJ.** 2011. Phase I/II study of trastuzumab in combination with everolimus (RAD001) in patients with HER2-overexpressing metastatic breast cancer who progressed on trastuzumab-based therapy. J Clin Oncol **29:**3126-3132.

383. **Gandhi L, Bahleda R, Tolaney SM, Kwak EL, Cleary JM, Pandya SS, Hollebecque A, Abbas R, Ananthakrishnan R, Berkenblit A, Krygowski M, Liang Y, Turnbull KW, Shapiro GI, Soria JC.** 2013. Phase I Study of Neratinib in Combination With Temsirolimus in Patients With Human Epidermal Growth Factor Receptor 2-Dependent and Other Solid Tumors. J Clin Oncol Dec 9 [Epub ahead of print].

384. **Baselga J, Campone M, Piccart M, Burris HA, 3rd, Rugo HS, Sahmoud T, Noguchi S, Gnant M, Pritchard KI, Lebrun F, Beck JT, Ito Y, Yardley D, Deleu I, Perez A, Bachelot T, Vittori L, Xu Z, Mukhopadhyay P, Lebwohl D, Hortobagyi GN.** 2012. Everolimus in postmenopausal hormone-receptor-positive advanced breast cancer. N Engl J Med **366:**520-529.

385. **Baselga J, Semiglazov V, van Dam P, Manikhas A, Bellet M, Mayordomo J, Campone M, Kubista E, Greil R, Bianchi G, Steinseifer J, Molloy B, Tokaji E, Gardner H, Phillips P, Stumm M, Lane HA, Dixon JM, Jonat W, Rugo HS.** 2009. Phase II randomized study of neoadjuvant everolimus plus letrozole compared with placebo plus letrozole in patients with estrogen receptor-positive breast cancer. J Clin Oncol **27:**2630-2637.

386. **Gao W, Xiao Z, Radovic-Moreno A, Shi J, Langer R, Farokhzad OC.** 2010. Progress in siRNA delivery using multifunctional nanoparticles. Methods Mol Biol **629:**53-67.

387. **Davison Z, de Blacquiere GE, Westley BR, May FE.** 2011. Insulin-like growth factor-dependent proliferation and survival of triple-negative breast cancer cells: implications for therapy. Neoplasia **13:**504-515.

CONTRIBUTIONS OF COLLABORATORS

This thesis was written by me, Anne Morrow, with editing done by Dr. Jonathan Lee, Dr. Dixie Pinke, Sandy Szeto and Elena Young. The work presented in Chapter 2 was done by myself, with the exception of the tissue microarray analysis which was performed by Dr. Jonathan Lee and the quantification of BT549 filopodia, using FiloDetect, which was performed by Dr. Sharmin Nilufar in Dr. Theodore Perkins laboratory at the University of Ottawa. In addition, Lisa Montgomery assisted in performing the scratch wound and cell proliferation assays presented. The work presented in Chapter 3 was done by myself, with the exception of the HPLC phosphoinositide analysis which was performed by Dr. Dave Bridges, while in Dr. Alain Saltiel's laboratory at the University of Michigan, the live cell microscopy imaging of FAPP1-GFP-PH transfected BT549 cells, which was done by Dr. Jonathan Lee and the live cell microscopy imaging of GFP-Rab11 and CFP-Galt transfected vector control and PI4KIIIβ-expressing BT549 cells, which was performed by Dr. Mohsen Amir Alipour, while in Dr. Zemin Yao's laboratory at the University of Ottawa. I would like to thank Dr. Heidi McBride for the use of her confocal microscope. I would also like to thank Dr. Tamas Balla and Dr. Angelika Hausser for providing various plasmids and Dr. Menq-jer Lee for providing the PTEN adenoviral particles. I am thankful to Dr. Dixie Pinke, Dr. Ilona Skerjanc, Dr. Dave Bridges and Dr. Zemin Yao for helpful discussions and critical reviews of the work presented here.

APPENDIX A: PUBLISHED PAPERS

BMC Systems Biology

SOFTWARE Open Access

FiloDetect: automatic detection of filopodia from fluorescence microscopy images

Sharmin Nilufar[1*], Anne A Morrow[2], Jonathan M Lee[2] and Theodore J Perkins[1,2,3*]

Abstract

Background: Filopodia are small cellular projections that help cells to move through and sense their environment. Filopodia play crucial roles in processes such as development and wound-healing. Also, increases in filopodia number or size are characteristic of many invasive cancers and are correlated with increased rates of metastasis in mouse experiments. Thus, one possible route to developing anti-metastatic therapies is to target factors that influence the filopodia system. Filopodia can be detected by eye using confocal fluorescence microscopy, and they can be manually annotated in images to quantify filopodia parameters. Although this approach is accurate, it is slow, tedious and not entirely objective. Manual detection is a significant barrier to the discovery and quantification of new factors that influence the filopodia system.

Results: Here, we present FiloDetect, an automated tool for detecting, counting and measuring the length of filopodia in fluorescence microscopy images. The method first segments the cell from the background, using a modified triangle threshold method, and then extracts the filopodia using a series of morphological operations. We verified the accuracy of FiloDetect on Rat2 and B16F1 cell images from three different labs, showing that per-cell filopodia counts and length estimates are highly correlated with the manual annotations. We then used FiloDetect to assess the role of a lipid kinase on filopodia production in breast cancer cells. Experimental results show that PI4KIIIβ expression leads to an increase in filopodia number and length, suggesting that PI4KIIIβ is involved in driving filopodia production.

Conclusion: FiloDetect provides accurate and objective quantification of filopodia in microscopy images, and will enable large scale comparative studies to assess the effects of different genetic and chemical perturbations on filopodia production in different cell types, including cancer cell lines.

Keywords: Filopodia, Morphology, FiloDetect, Microscopy image

Background

Filopodia are thin, finger-like protrusions comprised of tight parallel bundles of filamentous actin (Figure 1(a) and (b)). These protrusions are found at the leading edge of motile cells and are used to sense the cell's microenvironment [1,2]. Filopodia have been shown to regulate cancer cell motility *in vitro*, and metastasis *in vivo* in mouse experiments [3,4]. As enhanced filopodia production is a characteristic of many invasive cancers, understanding the genetic and chemical factors that regulate filopodia is an important problem. There are presently no algorithms that automatically detect and accurately quantify filopodia in the range of sizes and numbers that are relevant to cancer cell motility. Instead, filopodia are detected by eye, and length or other spatial information are extracted by manually tracing filopodia using image manipulation software. Figure 1(c) shows the manually labeled filopodia. This approach is tedious and slow, limiting the potential size of studies and their statistical power. Our previous work shows that there is high variability in filopodia characteristics, even among genetically identical cells in identical culture conditions [5]. Thus to study filopodia under several different conditions can require tens, if not hundreds,

*Correspondence: snilufar@gmail.com; tperkins@ohri.ca
[1]Ottawa Hospital Research Institute, 501 Smyth Road, Ottawa, Ontario, K1Y 4E9, Canada
[2]Department of Biochemistry, Microbiology and Immunology, University of Ottawa, 451 Smyth Road, Ottawa, Ontario, K1H 8M5, Canada
[3]School of Electrical Engineering and Computer Science, University of Ottawa, Ottawa, Ontario, K1N 6N5, Canada

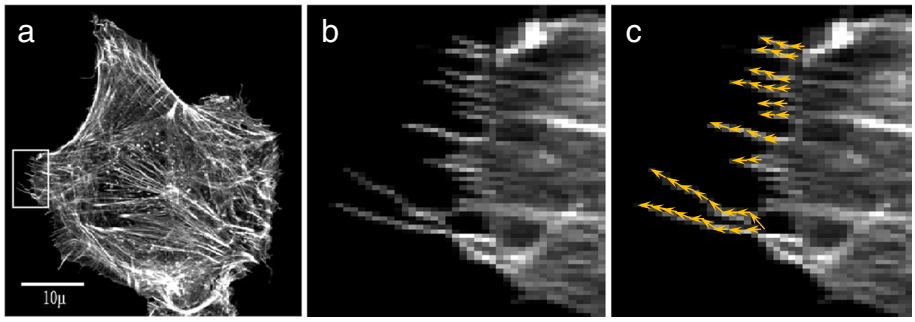

Figure 1 Images of cells displaying filopodia. (a) Fluorescence confocal microscopy image of a Rat2 fibroblast cell. **(b)** Close up of the region of subfigure **(a)** shown by the red rectangle. **(c)** Manual labelling of the filopodia are shown by yellow arrows.

of manually annotated images. High-throughput image-based screens, which may generate thousands or even millions of images, are simply infeasible.

Although there are no automated tools for filopodia detection on cancer cell images, there is considerable work on the closely related problem of tracing neurites in images of neurons. Neurites are any cellular extension of a neuron. Usually, the term refers to axons and dendrites, though it is sometimes used with filopodia. There are sophisticated algorithms for tracing neurites in images, and good public software packages are available [6-12]. The general neurite tracing problem differs in some details from the filopodia detection problem we study. Neurites can have complex branching structures, and it is commonly required to trace them in congested images with multiple cells and many visually crossing neurites. We focus on single-cell images. In these images, filopdia do not branch or cross so extensively as some neurites—although it is not unusual for longer filopodia to cross over other ones, and detection of these filopodia is challenging. Neurites such as axons and dendrites are significantly larger than filopodia, especially in comparison with the cell body. The filopodia we wish to detect can be little more than a pixel wide. Moreover, unless global context is taken into account, other cytoskeletal features within the cell can be confused with filopodia, and the bases of the filopodia, where they enter the cell body, have a considerably heterogeneous appearance.

The neurite tracing literature includes methods to detect and quantify filopodia on the growth cones of axons during development. However, most of these algorithms are only semi-automated, requiring user interaction to set algorithm parameters for each image or movie. For example [10] target only the larger, and thus easier to detect, filopodia. In a pilot study, we applied three popular software tools, namely fTacker [10], NeuriteQuant [13] and WIS-NeuroMath [11], on our non-neural cell. fTracker, which was originally designed to quantify filopodial dynamics from cultured neurons imaged by time-lapse fluorescence microscopy, works by binarizing the cell image, simplifying the boundary with morphological operators, and skeletonizing. Two types of binarization are used in fTracker: intensity based and edge based. NeuriteQuant is a freely available open-source tool which enables automated morphological analysis of large-scale image data from neuronal cultures or brain sections. Recently proposed software WIS-NeuroMath is based on efficient multiscale detection of edges and fibers in two-dimensional images allowing direct and accurate detection of neurites in various conditions. Figure 2 shows the results of these three existing tools on a sample image. From this figure we can see the existing neurite detection method failed to detect filopodia accurately in non-neural cell. fTracker correctly identifies some filopodia tips, but it traces them back far into the cell, and it misses many other tips. NeuriteQuant and WIS-NeuroMath detect many internal cellular structures, confusing them with cellular protrusions.

Our recent work suggests that filopodia sizes in non-neural cells are lognormally distributed [5]. The few, longest filopodia are not representative of the majority of the filopodia distribution, and thus we must detect all or nearly all filopodia to accurately assess the length distribution. Thus, new algorithms that can accurately detect and quantify filopodia in non-neural cells are greatly needed, as this will allow more rigorous and thorough study of the relationships between filopodia characteristics and the factors that control them.

In this paper, we propose FiloDetect, a fully automated method to detect filopodia from the cell body and measure filopodia length. The approach is inspired by neurite detection methods, including NeuriteQuant and fTracker, but designed in such a way as to avoid the problems they have with our kind of images. We employ intensity-based thresholding and a combination of morphological operations to detect the filopodia. The algorithm is implemented in Matlab and is publicly available at http://www.perkinslab.ca/Software.html. We validated FiloDetect on

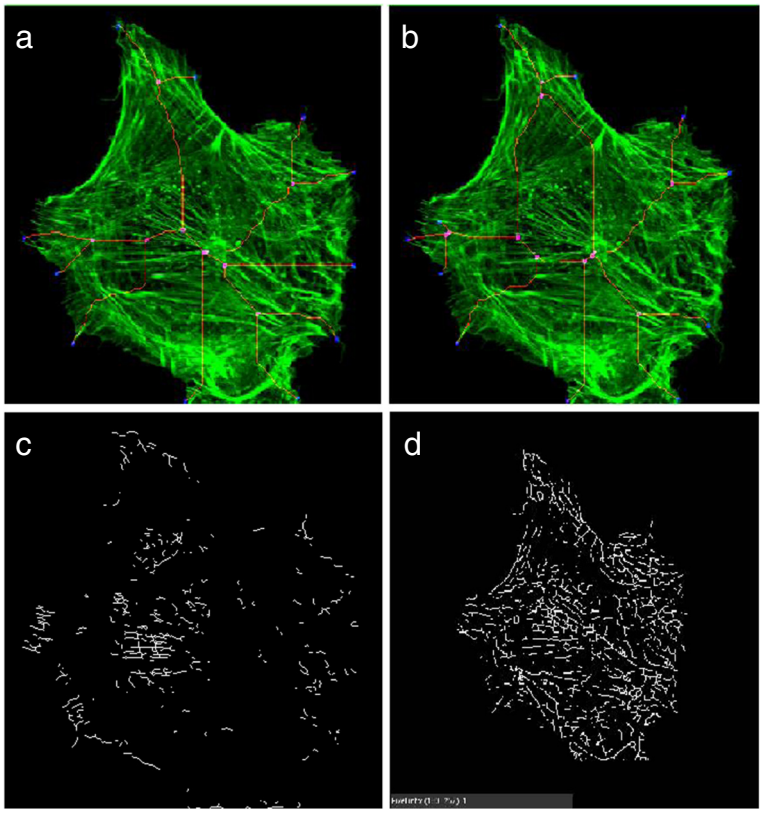

Figure 2 Filopodia detection in non neural cell of Figure 1. (a) result of edge based fTracker (where filopodia tips are represented by blue color and base by pink color) and **(b)** result of intensity based fTracker (where filopodia tips are represented by blue color and base by pink color), **(c)** result of NeuriteQuant (where the white lines represent filopodia) and **(d)** result of WIS-NeuroMath (where the black lines represent filopodia).

the non-transformed rodent cell line Rat2 and mouse melanoma cell line B16F1. The Rat2 images used to test the algorithm have been previously manually annotated for filopodia length and number [5], allowing us to assess the accuracy. The B16F1 images were annotated newly for this study.

We then used FiloDetect on a novel dataset, to determine whether expression of the lipid kinase, PI4KIIIβ, impacts filopodia production in breast cancer cells. We were interested in this question because of several lines of evidence implicating a role for PI4KIIIβ in breast cancer and filopodia production: it is activated by eEF1A2 (eukaryotic elongation factor 1 alpha 2) [14], which is amplified in approximately two-thirds of breast tumours [15,16]; it was recently identified as a putative breast cancer driver gene, in a large-scale copy number and gene expression analysis of 2000 breast tumours [17]; and ectopic expression of PI4KIIIβ in fibroblast cells increases filopodia number and length [5,14]. Thus, we hypothesized that PI4KIIIβ may drive filopodia formation in breast cancer cells, potentially enhancing their invasivenes. Our analysis shows this is indeed the case, with PI4KIIIβ involved in both increasing the filopodia length and number in the breast cancer cells.

Implementation

Dataset

Experiments were carried out on three datasets from three different cell lines. Rat2 rodent fibroblasts, B16F1 mouse melanoma cells, and BT549 human breast ductal carcinoma cells.

Rat2 dataset

This dataset consists of a subset of 38 single Rat2, rodent fibroblast, cell images taken from [5]. The details of fixation and imaging of these cells can be found in that publication. In this work, all filopodia at least 0.4 microns long were manually annotated, yielding the total number of filopodia on each cell, as well as the lengths and positions of those filopodia (Figure 1(c)). The subset of Rat2 cells studied in this paper were not genetically altered or chemically stimulated. Out of these 38 cells, 12 images were used in the training phase for the development of the

automatic detection method and the remaining 26 images were used to test the method.

B16F1 dataset

This dataset consists of images of B16F1 mouse melanoma cells, and was used for additional validation of FiloDetect, without any further tuning of parameters. We used five images provided by Dr. J. Schober [18] and seven images provided by Dr. T. Svitkina [19,20]. We call these two groups of images the Schober and Svitkina datasets respectively. We manually annotated these images for filopodia, as described previously [5].

BT549 dataset

This data set consists of images of BT549, human breast cancer cells, that have been manipulated to express the protein phosphatidylinositol 4-kinase III beta (PI4KIIIβ). The BT549 cells ectopically expressing PI4KIIIβ were generated using the pLXSN retroviral system as described by [21]. Human PI4KIIIβ cDNA was cloned into the pLXSN retroviral expression vector (Clontech). Polyclonal pools of BT549 cells stably expressing PI4KIIIβ were selected with 0.4 mg/ml G418. Cells selected to contain the empty pLXSN vector (EV) were also isolated and used as a control. For filopodia imaging, the cells were seeded onto coverslips in 6-well plates (1×10^5 cells/well), and allowed to adhere for 24hrs. Cells were then fixed in 3.7% paraformaldehyde, permeabilized with 0.1% Triton X-100, blocked with 1% BSA and stained with Phalloidin-546 (Invitrogen). Following staining, cells were mounted on slides using fluorescence mounting media (Dako). All images were acquired with a 100X NA 1.4 oil immersion objective (Olympus) at 1 airy U on a laser-scanning confocal microscope (IX80, Olympus) with Olympus Fluoview FV1000 software. From each group, empty vector control (EV) and PI4KIIIβ expressing (PI4Kβ), 5 images were used in the training phase to fine-tune parameters and 30 images were used in the testing phase.

Approach

As shown in Figure 3, the FiloDetect approach is divided into three basic steps: 1) Intensity thresholding is used to segment the cell body. 2) A series of morphological methods is applied to detect the filopodia. 3) The lengths of the detected filopodia are calculated by thinning them to one pixel wide and counting the pixels that remain. We expand on this outline below.

Step 1: Cell segmentation

Intensity thresholding Intensity thresholding is used to segment an image by setting all pixels whose intensity values are above a threshold to a foreground value and all the remaining pixels to a background value. In broad brush-strokes, it is easy to separate the cell from the background. However, fluorescence confocal microscopy images are usually noisy, and some parts of the cell body typically have low intensity that is very close to the background intensity. Moreover, because we are dealing with fine structures at the periphery of the cell, which may not have high intensity, high precision segmentation is important. Some of our images are background-subtracted and

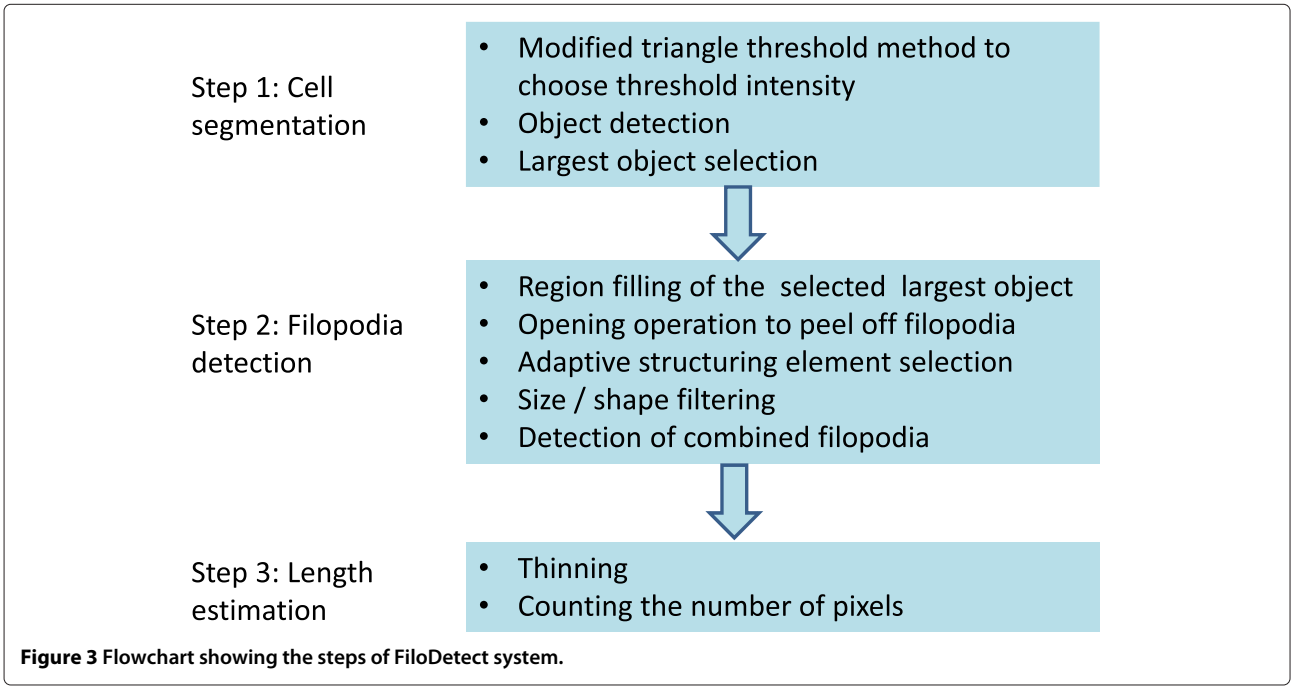

Figure 3 Flowchart showing the steps of FiloDetect system.

intensity-enhanced for better visibility and some are raw images. As a result, we need an automatic method that can apply for all of these different kinds of images. The popular Otsu's thresholding method [22,23] which chooses the threshold to minimize the intra-class variance of the black and white pixels, was initially applied by [10] to segment fluorescence microscopy images. However this thresholding technique failed to properly segment the cell body from the background in our images. Here we propose a modified triangle threshold method to segment the cell body from the background. The triangle thresholding method was originally proposed by [24] to segment sister chromatids from microscopy images. In triangle thresholding, a line is constructed between the peak of the histogram b to the last non-zero value a on the longer tail of the histogram (Figure 4).

The level where the normal distance between the histogram and the line is maximal is the threshold value (level). However in our case, we searched for local minima at the right side of the threshold value (within 10 neighbouring gray level values). This technique allows us to eliminate some of the background pixels that are detected as foreground pixels in traingle threshold method due to their close intensity level to the foreground pixels. Figure 4 shows the gray level values used in various different popular thresholding methods namely Otsu [22], IsoData [25], mean [26], maximum entropy [27], triangle [24] and the proposed modified triangle methods. The intensity histogram of Figure 4 is generated using the image of Figure 5(a). Figure 5(b) shows an enlargement of part of that image where filopodia can be observed. Figure 5(c–h) show the results of different thresholding methods.

Cell body selection There can be substantial noise in images and debris in culture due to cell culturing, fixing and/or imaging conditions. Collectively, these factors result in a variety of objects of different sizes appearing in the thresholded image. Therefore we must select the primary cell from the image. To do this, we use an eight-connected neighborhood to define individual objects. This assigns all ON or white pixels touching vertically, horizontally or diagonally to the same object. The areas of all of the objects present in the image are calculated, and the object with largest area is preserved and considered as the main cell body. All other pixels are set to OFF or zero.

Step 2: Filopodia detection

After obtaining an initial segmented image, a series of morphological operations is applied to detect the filopodia. Morphology, originally defined as operations on sets, is applied to process images based on shapes [28].

Region filling After intensity thresholding, usually some parts of the cell body that have very low image intensity are set to background pixels, as shown is Figure 6(b). The foreground regions can simply be filled by applying a morphological hole filling operation on the thresholded image. A hole is a set of background pixels that cannot be

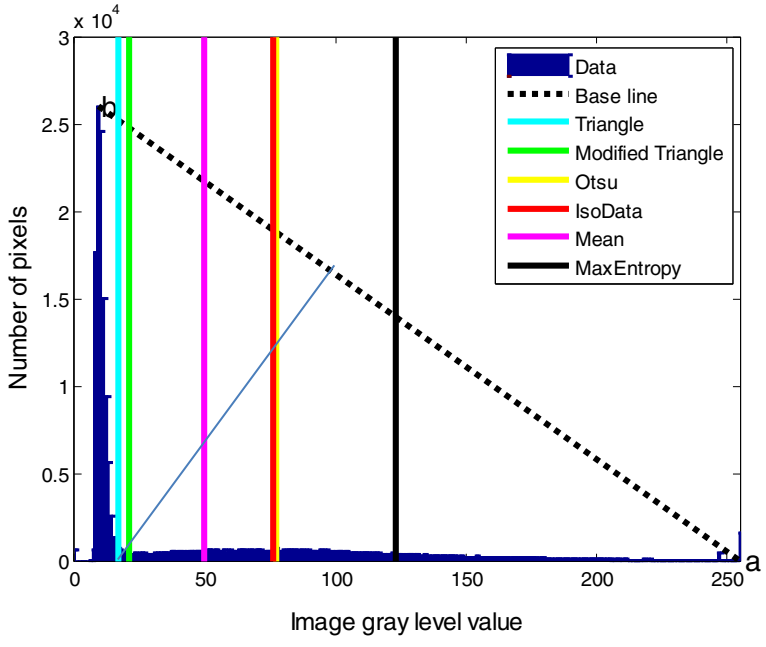

Figure 4 Image pixel intensity histogram with selected threshold values generated by different thresholding methods.

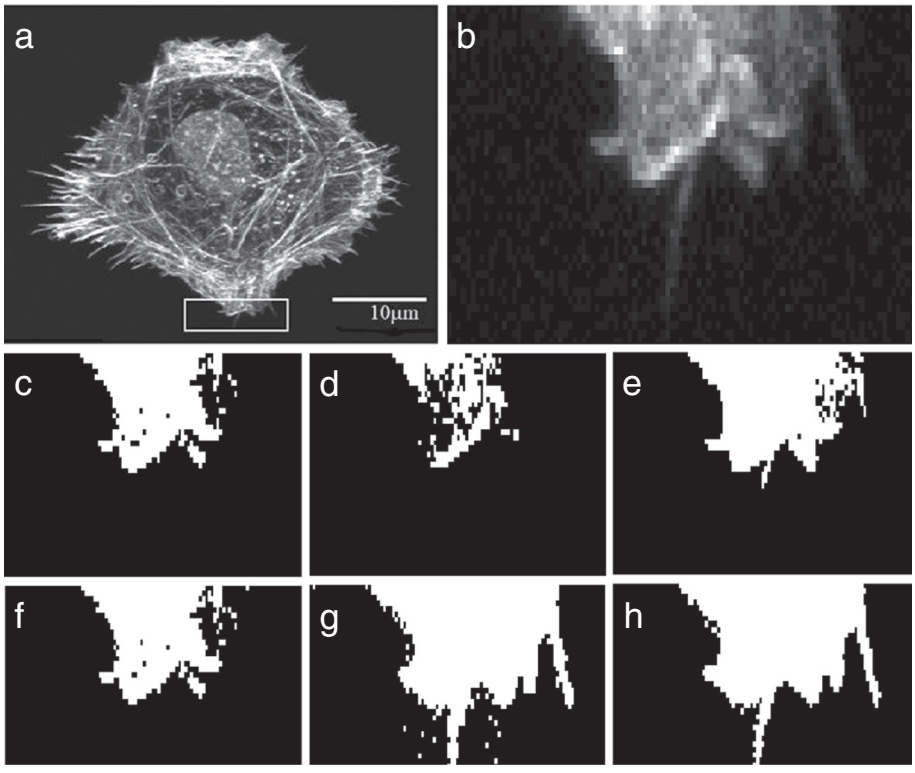

Figure 5 Results with different thresholding methods. (a) Original image. **(b)** Magnified part of original image. Thresholded images by: **(c)** Otsu, **(d)** MaxEntropy, **(e)** mean, **(f)** IsoData, **(g)** triangle and **(h)** modified triangle method.

reached by filling in the background from the edge of the image. Figure 6(c) shows the result after the region filling operation.

Splitting the filopodia from the cell body To split the filopodia from the main cell body, we begin by applying the morphological opening operation. Opening consists of an erosion step (in which a pixel remains ON only if all pixels in its neighborhood are ON), followed by a dilation step (in which a pixel is turned ON if any pixel in its neighborhood is ON). The opening operation tends to remove small protrusions from the periphery of a larger object. In this case, the fragments removed from the cell body are considered candidate filopodia. However, it is unclear what size of neighborhood is ideal for detecting filopodia. To address this problem, we initially take the neighborhood of a pixel P to be all those pixels whose centers are ≤ 0.5 microns from the center of pixel P. We chose this threshold because the filopodia in our images generally had a width of ≤ 0.4 microns, and thus are eliminated by the opening operation. We further filter objects that are not sufficiently filament-like, by fitting an ellipse to the pixels in the object and discarding objects whose major axis in less than 1.5 times as long as the minor axis. This removes cellular protrusions too thick to be considered single filopodia. We use the remaining objects to get a more precise, cell-specific estimate of filopodia width, by calculating their average minor axis length L. We then apply the opening operation again to the original image using a structuring element of radius L, generating a revised set of candidate filopodia. Finally, we filter this set to remove objects less than 0.4 microns long. The same criterion was used in the [5] study, on the grounds that human annotators could not always agree on whether such small objects represented filopodia or not.

Detection of combined filopodia Combined filopodia represent filopodia that are either fused at the base or that cross over along the length of the filopodia. We call these filopodia "combined" filopodia based on their appearance in the image. They may or may not actually touch in the cell (Figure 7). Detection of these combined filopodia needs additional processing on the split filopodia. The bounding box around each detected filopodium is first obtained. The morphological thinning operation is applied on that bounding box image and the number of endpoints and branch points of the thinned filopodia are calculated. If the number of branch points is greater than 1 and endpoints are greater than or equal to 4, the detected filopodium is considered to be combined.

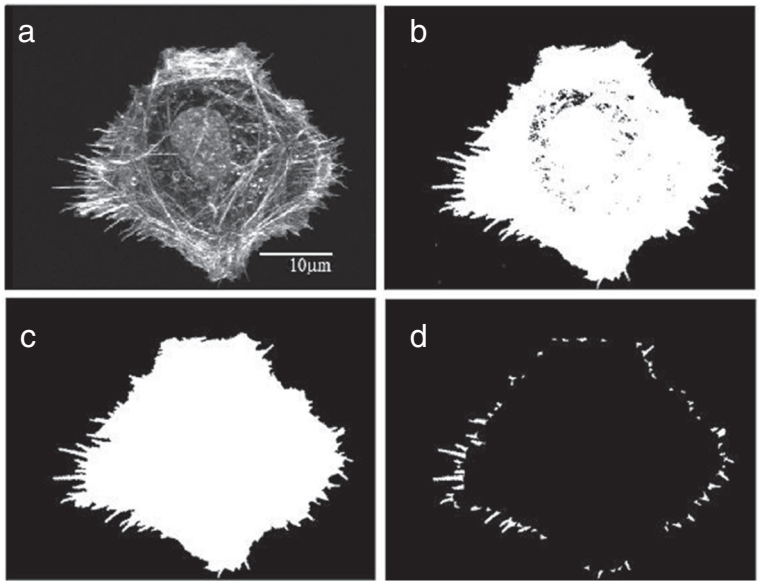

Figure 6 Step-by-step results for the filopodia detection system. (a) input image, **(b)** thresholded image, **(c)** image after hole filling and **(d)** final set of split filopodia.

Step 3: Length estimation of the filopodia

The split filopodia are morphologically thinned into one pixel connected lines and the lengths of the filopodia are calculated by the area of each thinned filopodium. In this way, combined filopodia are length equivalent to the total length of all filopodia in the combined group. In the Rat2 cells images, the majority of the combined filopodia represent fused or bifurcating filopodia, which share a common base, and are not due to crossing over events. We have considered these fused filopodia as one object and have calculated the length of the fused filopodia using the method detailed above. In the manual count, combined filopodia were also considered as a single object, as they share the same base [5].

Results and discussion

Filopodia size and number can vary greatly across individual cells. To gauge the ability of the proposed detection system to effectively identify filopodia and substitute for a human expert, we compared the manual count and length measurements of filopodia to the proposed detection method in 26 Rat2 cell images. The density of filopodia of this test set varies from 10 filopodia per cell to 64 filopodia per cell. Also the images are captured in different resolutions. The scatter diagram of Figure 8 shows the automatic and manual filopodia counts on our 26 Rat2 test images. The mean absolute error of FiloDetect counts is 15.69%.[1] We next compared the manual and FiloDetect-computed lengths of Rat2 filopodia. For

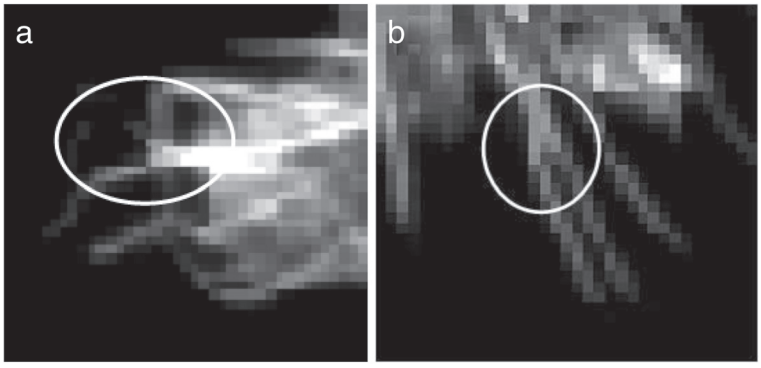

Figure 7 Two examples of combined filopodia. (a) cross over along length and **(b)** fused at base.

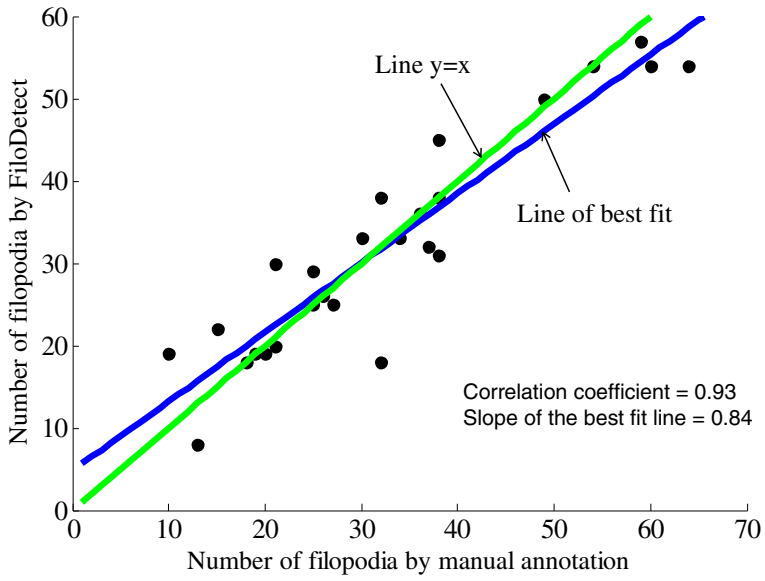

Figure 8 Scatter plot showing the correlation between manual and automatic count in Rat2 dataset (correlation coefficient = 0.93 and slope of the best fit line = 0.84). Each point represents one of 26 test images.

the majority of cases, the automatic length measurement generated a slightly lower value than the manual calculation (Figure 9; this plot excludes one cell image which contained very long filopodia, a point agreed upon by both manual annotation and FiloDetect.) This systematic difference in assessed filopodia lengths is due to the fact that there is a certain ambiguity in defining where the base of a filopodium begins on the cell body. The manual annotations appear to consistently begin counting the filopodia pixels further down in the cell body. However, using FiloDetect, the filopodia base points, determined by the size of the structuring element, is the point where the filopodia touches the border of the cell body. Even with this difference between the manual and automatic lengths, the mean lengths obtained across all 26 Rat2 cell test images by automatic versus

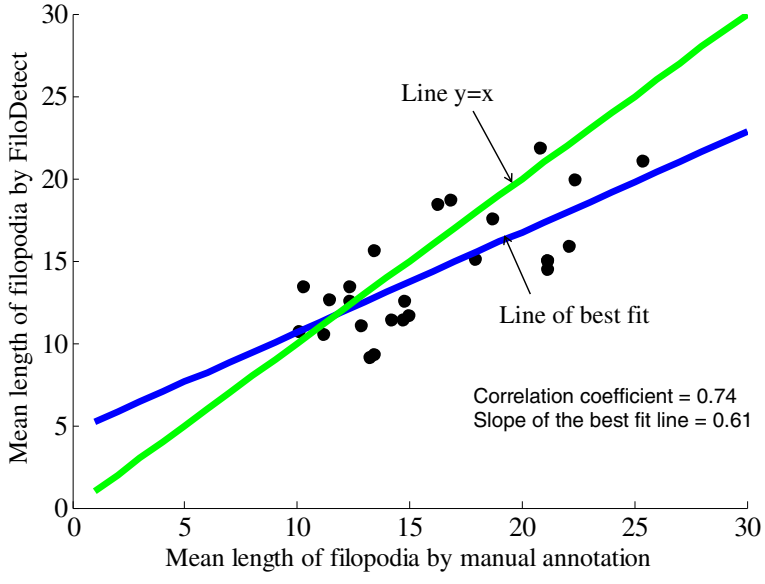

Figure 9 Scatter plot showing the correlation between manual and automatic length calculation in Rat2 dataset (correlation coefficient = 0.74 and slope of the best fit line = 0.61). Each point represents one of 25 test images.

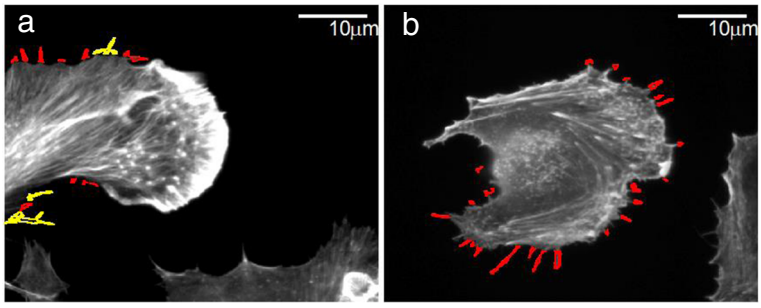

Figure 10 Example results on images of B16F1 mouse melanoma cells. (a) detected filopodia of a sample cell of Schober dataset and **(b)** detected filopodia of a sample cell of Svitkina dataset, where single filopodia are shown in red and combined filopodia are shown in yellow.

manual detection, 15.89μm and 19.27μm with standard errors 3.26 and 6.23 respectively, are not statistically different. To further validate the performance of FiloDetect, we applied it to images of B16F1 mouse melanoma cells used in [18] and [19,20]. For the Schober dataset, the *MAE* of the automated count to the manual count is 6.8%, and the mean length obtained by automatic versus manual detection is 13.64μm and 13.89μm with standard errors 2.37 and 2.27 respectively. For the Svitkina dataset, the *MAE* of the automated count to the manual count is 19.96% and the mean length obtained by automatic versus manual detection is 15.95μm and 18.18μm with standard error 1.21 and 2.78 respectively. Figure 10 shows a sample image from each of these datasets and corresponding detected filopodia with FiloDetect. Thus, we can conclude that the automated algorithm designed effectively identifies and measures filopodia length in a manner that replicates results obtained by manual count.

To detect the robustness of the proposed method we applied FiloDetect on noisy images. We added artificial poisson and salt & pepper noise to our test set. Poisson noise, a common type of noise for confocal microscopy images, is multiplicative noise described by a Poisson distribution, [29,30]. The MAE of FiloDetect count for this noisy test set is 20.23%. To see the performance of FiloDetect system for different signal to noise ratio, we have recorded the MAE on test set with varying degrees of salt and pepper noise. Figure 11 shows the plot of MAE on test set for different percentages of salt and pepper noise.

Next we applied FiloDetect to assess whether increased PI4KIIIβ expression leads to enhanced filopodia number

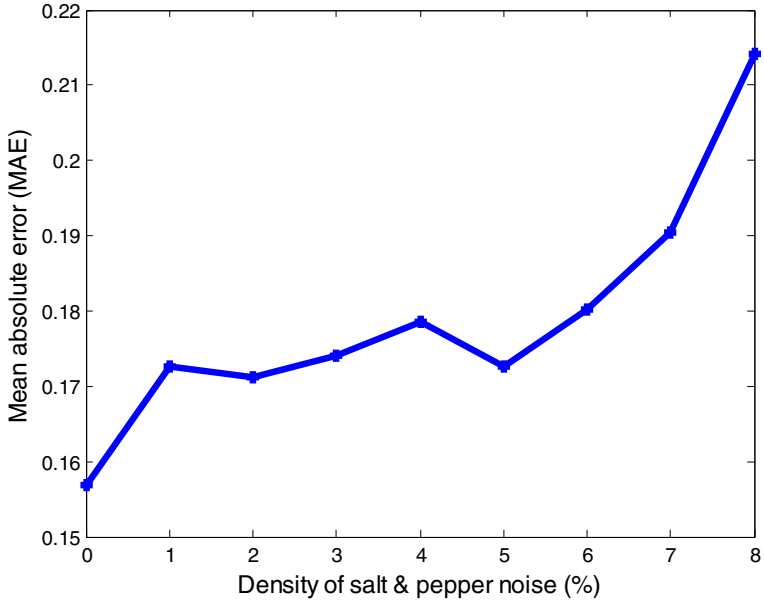

Figure 11 Mean absolute error for different signal to noise ratio.

or length in BT549 breast cancer cells. Here we calculated the length and number of single and combined filopodia separately in response to the fact that filopodia are relatively long in BT549 cells, with many filopodia crossing events.

The box plots in Figure 12(a), (b) and (c) show that the mean number of single, combined and total filopodia per cell are greater in the PI4KIIIβ expressing BT549 cells as compared to the empty vector control cells. From these plots we can see for all cases these results were statistically significant. Using a two-tailed unpaired t-test, the difference in the total number of filopodia per cell in EV and PI4KIIIβ is statistically significant with p-value=0.00001. Filopodia length was measured for each group of cells, PI4KIIIβ versus EV, for the single and combined filopodia separately (Figure 12(d) and (e)) and then for all filopodia (Figure 12(f)). The average filpodium length, for all filopodia, was determined to be 4.45 μm for the empty vector controls and 7.10 μm for the PI4KIIIβ expressing cells. When treated separately, the single and crossing filopodia both showed a greater average length in the PI4KIIIβ expressing cells versus the empty vector controls. In all cases these results were statistically significant. By t-test, the difference of average length of filopodia per cell in EV and PI4KIIIβ is statistically significant with p-value=0.00001. Therefore, we can conclude from these results that PI4KIIIβ expression leads to a greater number of filopodia, and filopodia that are longer on average, in BT549 breast cancer cells.

Conclusion

In this paper, we proposed FiloDetect to automate the quantification of filopodia, making more reliable and reproducible the task of quantifying filopodia from static microscopy images. The proposed FiloDetect system was evaluated on Rat2 fibroblast and B16F1 mouse melanoma cell images, manually annotated for filopodia number and length. A comparative analysis of the results shows the good performance of FiloDetect, in both number and length determination. This method was then applied to measure the effect of PI4KIIIβ's expression on filopodia production in BT549 breast cancer cells. We found that PI4KIIIβ expression leads to an increase in filopodia number and length, suggesting that PI4KIIIβ is involved in driving filopodia production in the cell. When overexpressed, PI4KIIIβ may promote cancer cell metastasis, as filopodia are a characteristic of invasive cells.

Although FiloDetect compared favorably to manual annotations and was accurate enough to carry out the PI4KIIIβ analysis, further improvements may be possible. In Costantino's work on detecting filopodia on

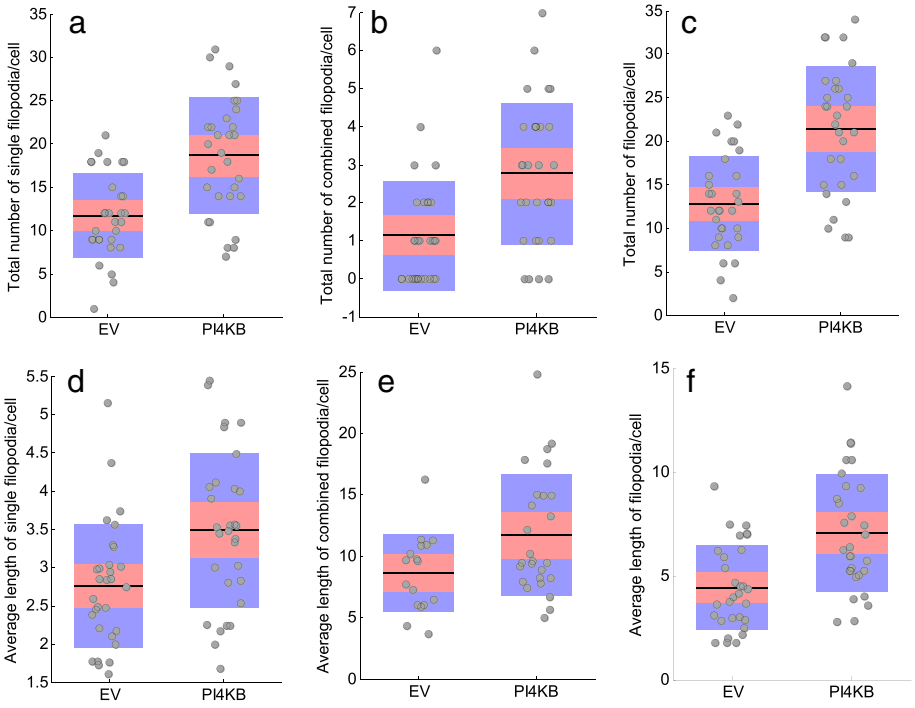

Figure 12 Boxplots showing different conditions. (a) total number of single filopodia, **(b)** total number of combined filopodia, **(c)** total number of filopodia, **(d)** average length (in μm) of single filopodia, **(e)** average length (in μm) of combined filopodia and **(f)** average length (in μm) of filopodia between EV and PI4KIIIβ. Points are layed over a 1.96 standard error of mean (95% confidence interval) in pink and a 1 standard deviation in blue.

neural growth cones [10] they found that segmentation based on edge detection was superior to intensity based thresholding–although both are options in their software. In pilot studies, we did not find an advantage to edge detection. However this might be true for other image sets. Adaptive intensity thresholding methods, where the threshold varies for different parts of the image, or methods that combine intensity and edge information might also yield improvements. Because the filopodia are comparatively small objects in typical images, and because it can be difficult for morphological analysis to correct for errors in segmentation, high quality segmentation is key to our approach. A completely different approach would be to forego segmentation and use a tracing-based approach to delineate filopodia. In the neurite detection literature, tracing-based approaches are generally considered to be the most accurate, although their computational burden is higher than that of morphology-based approaches.

Another area for possible improvement is in the untangling of combined filopodia. Following the policy of our previous manual annotations, we have not attempted untangling. However, some combined filopodia are truly physically joined, whereas others are really separate but overlap visually. By analyzing joined structure in more detail, it may be possible to discriminate between these cases. We have conducted preliminary analysis of 3D image stacks, to see if they might be informative in this regard. However, segmenting the cell is much more difficult in this case, because each layer of the stack contains differing and only partial information on where the cell boundaries are.

Filopodia are just one of many cytoskeletal features that are biologically relevant and that we might want to quantify automatically from images. For instance, it would be of interest in the study of cytoskeleton remodelling to be able to automatically define and measure the relative size/cellular proportion of a cell's lamellipodium, which defines the flat and broad cellular protrusion containing a meshwork of branched F-actin found at the leading edge [2]. In addition, it would be useful to develop an algorithm that is able to quantify the number/proportion of stress fibers, contractile acto-myosin structures, which span the length of a cell, and are involved in adhesion and motility [31]. Robust and automated quantification of the size of the lamellipodium and the number of stress fibers in a cell under genetic and chemical perturbations, along with the measure of filopodial protrusions would allow a broader study of events of cytoskeletal rearrangement. Also, it would be interesting to see if our algorithm to measure filopodia number and length could be applied in a live cell imaging context, allowing real-time actin dynamic remodelling events to be studied quantitatively.

Availability and requirements

Algorithms were implemented in Matlab2009. The FiloDetect system and some sample cell images are available at http://www.perkinslab.ca/Software.html. There is no restrictions on non-commercial use of this software.

Endnote

[1]Here we define, $\mathrm{MAE} = \sum_{i=1}^{N} |M_i - F_i|/NM_i$ where $M_i = M_1, M_2, \cdots M_N$ are the manual counts and $F_i = F_1, F_2, \cdots F_N$ are the FiloDetect counts for N different cells.

Competing interests

The authors declare that they have no competing interests.

Authors' contributions

SN and TJP proposed and designed the filoDetect method and drafted the manuscript. AM generated and imaged the Rat2 and BT549 cell lines used in this study and helped to draft the manuscript and to generate manual annotation. JML helped to generate manual annotation and to draft the manuscript. All authors read and approved the final manuscript.

Acknowledgements

We thank Dr. J. Schober and Dr. T. Svitkina for the B16F1 cell images we used to validate our system. This work was supported in part by a Government of Ontario Ministry of Economic Development and Innovation (MEDI) grant to TJP, an NSERC Discovery grant to TJP, a MITACS Elevate fellowship to SN, a CIHR Doctoral Research Award to AAM and an NSERC Discovery grant to JML.

Received: 30 December 2012 Accepted: 11 July 2013
Published: 23 July 2013

References

1. Gupton SL, Gertler FB: **Filopodia: the fingers that do the walking.** *Sci STKE* 2007, **2007**(400):re5.
2. Mattila PK, Lappalainen P: **Filopodia: molecular architecture and cellular functions.** *Nat Rev Mol Cell Biol* 2008, **9**(6):446–454.
3. Arjonen A, Kaukonen R, Ivaska J: **Filopodia and adhesion in cancer cell motility.** *Cell Adh Migration* 2011, **5**(5):421–430.
4. Chen L, Yang S, Jakoncic J, Zhang JJ, Huang XY: **Migrastatin analogues target fascin to block tumour metastasis.** *Nature* 2010, **464**(7291):1062–1066.
5. Husainy A, Morrow A, Perkins T, Lee J: **Robust patterns in the stochastic organization of filopodia.** *BMC Cell Biol* 2010, **11:**86+.
6. Al-kofahi KA, Lasek S, Szarowski DH, Pace CJ, Nagy G, Member S, Turner JN, Roysam B: **Rapid automated three-dimensional tracing of neurons from confocal image stacks.** *IEEE Trans Inf Technol Biomed* 2002, **6:**171–187.
7. Meijering E: **Neuron tracing in perspective.** *Cytom Part A* 2010, **77**(7):693–704.
8. He W, Hamilton TA, Cohen AR, Holmes TJ, Pace C, Szarowski DH, Turner JN, Roysam B: **Automated three-dimensional tracing of neurons in confocal and brightfield images.** *Microsc Microanal* 2003, **9:**296–310.
9. Meijering E, Jacob M, Sarria JC, Steiner P, Hirling H, Unser M: **Design and validation of a tool for neurite tracing and analysis in fluorescence microscopy images.** *Cytom Part A* 2004, **58A**(2):167–176.
10. Costantino S, Kent CB, Godin AG, Kennedy TE, Wiseman PW, Fournier AE: **Semi-automated quantification of filopodial dynamics.** *J Neurosci Methods* 2008, **171:**165–173.
11. Rishal I, Golani O, Rajman M, Costa B, Ben-Yaakov K, Schoenmann Z, Yaron A, Basri R, Fainzilber M, Galun M: **WIS-Neuromath enables versatile high throughput analyses of neuronal processes.** *Dev Neurobiol* 2013, **73**(3):247–56.
12. Fanti Z, Martinez-Perez M, De-Miguel F: **NeuronGrowth, a software for automatic quantification of neurite and filopodial dynamics from time-lapse sequences of digital images.** *Dev Neurobiol* 2011, **71**(10):870–81.

13. Dehmelt L, Poplawski G, Hwang E, Halpain S: **NeuriteQuant: an open source toolkit for high content screens of neuronal morphogenesis.** *BMC Neurosci* 2011, **1:**1–13.
14. Jeganathan S, Morrow A, Amiri A, Lee JM: **Eukaryotic elongation factor 1A2 cooperates with phosphatidylinositol-4 kinase III beta to stimulate production of filopodia through increased phosphatidylinositol-4,5 bisphosphate generation.** *Mol Cell Biol* 2008, **28**(14):4549–1561.
15. Kulkarni G, Turbin D, Amiri A, Jeganathan S, Andrade-Navarro M, Wu T, Huntsman D, Lee J: **Expression of protein elongation factor eEF1A2 predicts favorable outcome in breast cancer.** *Breast Cancer Res Treat* 2007, **102:**31–41.
16. Tomlinson VAL, Newbery HJ, Wray NR, Jackson J, Larionov A, Miller WR, Dixon JM, Abbott CM: **Translation elongation factor eEF1A2 is a potential oncoprotein that is overexpressed in two-thirds of breast tumours.** *BMC Cancer* 2005, **5**(113):1471–2407.
17. Curtis C, Shah SP, Chin SF, Turashvili G, Rueda OM, Dunning MJ, Speed D, Lynch AG, Samarajiwa S, Yuan Y, et al: **The genomic and transcriptomic architecture of 2,000 breast tumours reveals novel subgroups.** *Nature* 2012, **486**(7403):346–352.
18. Schober JM, Komarova YA, Chaga OY, Akhmanova A, Borisy GG: **Microtubule-targeting-dependent reorganization of filopodia.** *J Cell Sci* 2007, **120:**1235–1244.
19. Yang C, Czech L, Gerboth S, Kojima Si, Scita G, Svitkina T: **Novel roles of Formin mDia2 in Lamellipodia and filopodia formation in motile cells.** *PLoS Biol* 2007, **5**(11):e317+.
20. Svitkina TM, Bulanova EA, Chaga OY, Vignjevic DM, Kojima Si, Vasiliev JM, Borisy GG: **Mechanism of filopodia initiation by reorganization of a dendritic network.** *J Cell Biol* 2003, **160**(3):409–421.
21. Debnath J, Muthuswamy SK, Brugge JS: **Morphogenesis and oncogenesis of MCF-10A mammary epithelial acini grown in three-dimensional basement membrane cultures.** *Methods (San Diego, Calif)* 2003, **30**(3):256–268.
22. Otsu N: **A threshold selection method from gray-level histograms.** *Ieee Trans Syst Man Cybern* 1979, **9:**62–66.
23. Sezgin M, Sankur B: **Survey over image thresholding techniques and quantitative performance evaluation.** *J Electron Imaging* 2004, **13:**146–168.
24. Zack GW, Rogers WE, Latt SA: **Automatic measurement of sister chromatid exchange frequency.** *J Histochem Cytochem* 1977, **25**(7):741–753.
25. Flavio: **Thresholding using the ISODATA clustering algorithm.** *IEEE Trans Syst Man Cybernet* 1980, **10**(11):771–774.
26. Glasbey C: **An analysis of histogram-based thresholding algorithms.** *CVGIP: Graphical Models Image Process* 1993, **55**(6):532–537. http://www.sciencedirect.com/science/article/pii/S1049965283710400
27. Kapur J, Sahoo P, Wong A: **A new method for gray-level picture thresholding using the entropy of the histogram.** *Comput Vis, Graphics, Image Process* 1985, **29**(3):273–285.
28. Haralick RM, Sternberg SR, Zhuang X: **Image analysis using mathematical morphology.** *IEEE Trans Pattern Anal Mach Intell* 1987, **9**(4):532–550.
29. Rodrigues I, Xavier J, Sanches J: **Fluorescence confocal microscopy imaging denoising with photobleaching.** In *IEEE Engineering in Medicine and Biology Society*. Vancouver, BC, Canada: IEEE; 2008:2205–2208.
30. Srivastava R, Gupta J, Parthasarathy H: **Enhancement and restoration of microscopic images corrupted with poisson's noise using a nonlinear partial differential equation-based filter.** *Defence Sci J* 2011, **61**(5):437–442.
31. Naumanen P, Lappalainen P, Hotulainen P: **Mechanisms of actin stress fibre assembly.** *J Microsc* 2008, **231**(3):446–454.

doi:10.1186/1752-0509-7-66
Cite this article as: Nilufar *et al.*: FiloDetect: automatic detection of filopodia from fluorescence microscopy images. *BMC Systems Biology* 2013 **7**:66.

BMC Cell Biology

RESEARCH ARTICLE Open Access

Robust patterns in the stochastic organization of filopodia

Asma N Husainy[1], Anne A Morrow[1], Theodore J Perkins[1,2], Jonathan M Lee[1*]

Abstract

Background: Filopodia are actin-based cellular projections that have a critical role in initiating and sustaining directional migration in vertebrate cells. Filopodia are highly dynamic structures that show a rich diversity in appearance and behavior. While there are several mathematical models of filopodia initiation and growth, testing the capacity of these theoretical models in predicting empirical behavior has been hampered by a surprising shortage of quantitative data related to filopodia. Neither is it clear how quantitatively robust the cellular filopodial network is and how perturbations alter it.

Results: We have measured the length and interfilopodial separation distances of several thousand filopodia in the rodent cell line Rat2 and measured these parameters in response to genetic, chemical and physical perturbation. Our work shows that length and separation distance have a lognormal pattern distribution over their entire detection range (0.4 μm to 50 μm).

Conclusions: We find that the lognormal distribution of length and separation is robust and highly resistant to perturbation. We also find that length and separation are independent variables. Most importantly, our empirical data is not entirely in agreement with predictions made based on existing theoretical models and that filopodial size and separation are an order of magnitude larger than what existing models suggest.

Background

When mammalian cells migrate, they do so by generating protrusive actin structures in the form of advancing lammellipodia or filopodia [1,2]. The lamellipodium is a broad cellular extension composed of a mesh-like network of crosslinked actin fibers. Filopodia, on the other hand, are finger-like cellular projections composed of a core of actin filaments bundled in a parallel array [3,4]. Filopodia are the first cellular structures to reach new space during cell migration and their growth factor receptors guide movement towards chemoattractants [5]. Filopodial adhesion molecules also provide traction [6]. During migration, filopodia are often overtaken by advancing lamellipodia and filopodial actin bundles contribute to the formation of contractile structures within the cell body [7]. Filopodia have an important role in controlling cell migration *in vivo* and are essential for neurogenesis in mice and for cell-cell adhesion during Drosophila embryogenesis [3,4]. Filopodia are also involved in cancer progression, as many filopodial proteins are known to regulate tumor invasion and metastatic development [8,9].

The simple composition of filopodia belies the complex biochemical events that shape their initiation and growth. The pathways controlling the assembly of mature filopodia are controversial, and two different models, convergent elongation and *de novo* nucleation, compete for general acceptance [3,4,10]. During convergent elongation, linear actin bundles in the lamellipod, termed microspikes, fuse into a lambda-shaped structure that becomes a filopodium as is grows outward from the plasma membrane [10,11]. In *de novo* nucleation, filopodia are created by actin nucleating proteins at or near the plasma membrane and are independent of lamellar actin [4,10,12]. Experimental evidence supports both models and it therefore seems likely that there are multiple mechanisms of filopodia initiation.

In mammalian cells, filopodia have a strikingly varied appearance and behavior. Their lengths span greater than two orders of magnitude and they can grow to

* Correspondence: jlee@uottawa.ca
[1]Department of Biochemistry, Microbiology & Immunology, University of Ottawa, 451 Smyth Road, Ottawa, Ontario, K1H 8M5, Canada
Full list of author information is available at the end of the article

50 μm or more in size [3,4]. Filopodial behavior is also highly variable, and filopodia in the same cell are observed undergoing phases of growth, retraction or stasis. The velocity of growth and retraction is variable, and filopodia can have velocities ranging from 0.25-1 μm/minute [13]. Several theoretical models have been used to describe filopodia formation and growth [14-20]. Parameters that have been incorporated into these models include the number of actin filaments in a filopodium, plasma membrane elasticity, G-actin concentration, actin retrograde flow, actin depolymerization and the mechanical strength of the actin polymers [14-20]. These studies make predictions as to the length distribution of filopodia and interfilopodial separation distances. However, there is a surprising paucity of quantitative data related to these parameters. In addition, it is unclear how perturbation quantitatively affects the filopodial system. In this report, we have measured the length and distance separation of several thousand filopodia in the non-transformed rodent cell line Rat2. Analysis of this data indicates that filopodia length and interfilopodial distance are distributed lognormally and this distribution is highly robust and resistant to perturbation.

Methods

Cell lines and treatments

Rat2 fibroblasts were purchased from American Type Culture Collection (Manassa, VA) and cultured in Dubecco's Modified Eagle Medium High Glucose 1X from Gibco, Invitrogen (Grand Island, NY) containing 10% Fetal Bovine Serum (FBS) (Gibco) and 1% antibiotic/antimycotic (Gibco). The cultured cells were incubated in 10 cm plates at 37°C in 5% $CO\rightarrow_2$. Cells were treated with bradykinin at 100 ng/ml for 30 minutes using DMSO as a vehicle. For poly-D-lysine experiments, cover slips were coated with 50 μg/ml poly-D-lysine for 2 hours prior to cell plating. Rat2 fibroblast cells ectopically expressing PI4KIIIβ and empty vector controls have been previously described [21,22].

Immunofluorescence

Rat2 cells were grown to 70-80% confluency, trypsinized with 0.05% 1X Trypsin-EDTA (Gibco), diluted 1:100 and plated in 6 well plates containing glass coverslips (Fisher; Pittsburg, PA). 24 hrs later, cells were fixed in 3.7% paraformaldehyde for 20 minutes, permeabilized with 0.5% Triton-X for 15 minutes and left overnight in IF Buffer (130 mM NaCl, 7 mM $Na\rightarrow_2HPO_4$, 3.5 mM NaH_sPO_4, 7 mM NaN_3, 0.2% Triton X-100, 0.1% BSA, 0.05% Tween-20, ph 7.4). The following day, cells were stained for 1 hr with Phalloidin-488 (Invitrogen) diluted 1:200 in 1X PBS (pH7.4) and subsequently stained with Hoescht-405 (Invitrogen) diluted 1:40 in 1X PBS. Coverslips were mounted on glass microscope slides (Fisher) with Fluorescent Mounting Medium (Dako; Carpinteria, CA). Images of single Rat2 cells were obtained from an Olympus Fluoview FV1000 laser scanning confocal microscope. Openlab Software (Improvision, MA) was used to measure filopodia lengths and separation.

Data Analysis

For each length or distance data set, histograms were plotted on a logarithmic axis, with bins of equal width in log-space. For both visualization and statistical fitting purposes, as described below, the empirical cumulative distribution function, F(x), is defined as the fraction of the data having a value strictly less than x. The empirical probability density function, which was used only for visualization purposes, was taken to be the Parzen windows estimator with a radius parameter of h = 0.25 applied in the log-transformed space. That is, if x_1 ... x_n are the original data and y_1 ... y_n are the transformed data ($y_i = \log_{10} x_i$) then the probability density function is f(y) = c(y)/n, where c(y) is the number of points y_1 ... y_n for which the absolute difference to point y is less than or equal to h.

We fit different distributions to the data by comparison of idealized and empirical cumulative distribution functions. Let G(x, θ) denote the cumulative distribution function of a statistical distribution with parameter or parameters θ. We judged that filopodia lengths or interfilopodial distances less than 0.4 μm could not be reliably quantified from the images. So, no such measurements were included in our data set. To fit θ based on the data we first defined the "cut-off cumulative distribution function" as $G_C(x, \theta) = 0$ if $x \le 0.4$ and $G_C(x, \theta) = (G(x, \theta)-G(0.4, \theta))/(1-G(0.4, \theta))$ if $x > 0.4$. The cut-off function recognizes that our data collection procedure does not record any values smaller than 0.4 μm; in essence, any part of the statistical distribution falling below that threshold is zeroed out and the remainder of the distribution is rescaled so that it integrates to one. We define the error of parameters θ as the sum of squared residuals: $E(\theta) = \Sigma_X(F(x)- G_C(x, \theta))$, where the sum is over $x = 10^{-0.40}, 10^{-0.39}, 10^{-0.38}, ..., 10^{1.60}$ for length data and $x = 10^{-0.40}, 10^{-0.39}, 10^{-0.38}, ..., 10^{2.30}$ for distance data. Parameters θ are fit by minimizing the error E(θ). We fit four different families of distributions in this way: the exponential, which has probability density function $g(x, \lambda) = \lambda \exp(-\lambda x)$ and cumulative distribution function $G(x, \lambda) = 1- \exp(-\lambda x)$; the powerlaw, which has probability density function $g(x, x_{min}, \alpha) = ((\alpha-1)/x_{min})(x/x_{min})^{-\alpha}$ and cumulative distribution function $G(x, x_{min}, \alpha) = 1 - (x/x_{min})^{1-\alpha}$ for $x \ge x_{min}$; the Gaussian, which has probability density function $g(x, \mu, \sigma) = (2\pi\sigma^2)^{-1/2} \exp(-(x-\mu)^2/2\sigma^2)$; and the lognormal,

which has probability density function $g(x, \mu, \sigma) = (2\pi\sigma^2x^2)^{-1/2} \exp(-(\ln(x)-\mu)^2/2\sigma^2)$ for $x > 0$.

Results

Quantitation of Filopodia

Filopodia span a wide range of observable lengths and individual cells show high variability in the size and number of filopodia they possess. To understand filopodia in their cellular context, we observed filopodia production in rodent fibroblast Rat2 cells. We chose this cell line because it is non-cancerous and individual cells have filopodia that span nearly two orders of magnitude in length. The appearance of the actin cytoskeleton in typical Rat2 cells is shown in Figure 1. In interphase, two types of linear actin polymers are commonly seen, stress fibers (S) and filopodia (F). Stress fibers traverse the cell in a lengthwise manner. Filopodia, on the other hand, are visible as linear projections from the cell body that emanate from multiple places and proceed in multiple directions. Filopodia are distinguishable from the less frequently observed and visibly similar retraction fibers. Retraction fibers are seen primarily in mitotic cells but also appear in cells in interpahse, at the trailing edge during migration. Based on our previously published work with living Rat2 cells [23], filopodia can be visually distinguished from retraction fibers (R) based on their relative thickness and extended presence behind the plasma membrane. We have purposely excluded mitotic cells from our analysis to avoid potential confusion between filopodia and retraction fibers. Moreover, Rat2 cells are relatively non-migratory so they have very few retraction fibers relative to filopodia in non-mitotic cells.

To quantitate filopodial properties in Rat2 cells, we used image analysis software to manually trace the lengths of individual filopodia in fixed Rat2 cells. The length of a filopodium was extrapolated from the pixel length of the trace line. Based on the resolution of our fluorescence microscopy system, we estimate that we can accurately determine the length of filopodia > 0.4 μm in length. Filopodia shorter than this cannot accurately be distinguished from lamellar actin structures and therefore were not counted. We also measured the distance that separates a given filopodium from its nearest neighbor. Cells visualized were non-mitotic and not visibly attached to other cells but were otherwise randomly chosen. The cell population as a whole was in a logarithmic phase of growth and no attempt was made to synchronize filopodia growth cycles. As such, the filopodia that we measure represent structures in undetermined phases of growth, shrinkage and stasis. We collected this data for all filopodia in the individual cells that we imaged. Thus, each filopodium is defined by a length (L_x) and a separation distance (D_x) measurement.

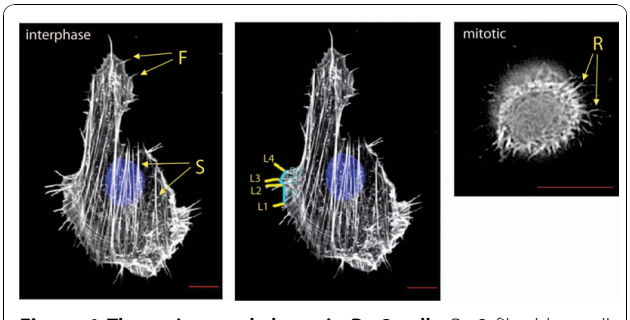

Figure 1 The actin cytoskeleton in Rat2 cells. Rat2 fibroblast cell stained for actin (white) and DNA (blue). The leftmost panel shows transverse actin stress fibers (S) and filopodia (F) as hair-like projections from the cell perimeter. The central panel shows counting of individual filopodia lengths (L1, L2, L3, L4) and distance separation (D1, D2, D3). The right panel shows a mitotic cell with retraction fibers (R) indicated. The red scale bar is 10 μm.

Filopodia lengths are distributed lognormally

We compiled filopodia length measurements from three independent experiments. We counted filopodia from a total of 52 Rat2 cells (experiment 1 = 25; experiment 2 = 18; experiment 3 = 10). The total number of filopodia was 1,682 (experiment 1 = 745; experiment 2 = 573; experiment 3 = 364). As shown in Figure 2A, filopodia distribution in the total data set is unimodal with a mean of 2.70 μm. The length distribution of the individual experiments was also unimodal with a respective mean of 2.79 μm, 2.49 μm, and 2.84 μm for Experiments 1, 2 and 3. Approximately 82% of the filopodia fall within the range of 1 μm to 10 μm in length.

We next determined the statistical model that would best fit the empirical cumulative probability distribution (CDF) of filopodia lengths and distances. We found that the length distribution of the collective dataset was best modeled as a lognormal distribution ($p(x)= (2\pi\sigma^2x^2)^{-1/2} \exp(-(\ln(x)-\mu)^2/2\sigma^2)$) (Figure 2B). That is, the logarithm of the length is approximately normally distributed. The dataset is poorly modeled as an exponential ($p(x) = \lambda \exp(-\lambda x)$), Gaussian ($p(x) = (2\pi\sigma^2)^{-1/2}\exp(-(x-\mu)^2/2\sigma^2)$) or power law ($p(x) = ((\alpha-1)/x_{min})(x/x_{min})^{-\alpha}$) distribution (Figure 2B). The power law and exponential distributions fit least well, as they are incapable of capturing the unimodality of the observed data. The exponential, however does provide a reasonable fit for the distribution of filopodia larger than ~1.5 μm. The Gaussian is the next most accurate, capturing the unimodal data, but it overestimates the left tail while underestimating the right tail. The lognormal captures both unimodality and the heavy right tail. The datasets of individual experiments are also fit well by lognormal distributions (Figure 2A, B), as are the length distributions from each individual cell (Figure 2C). The similarity in CDF distribution

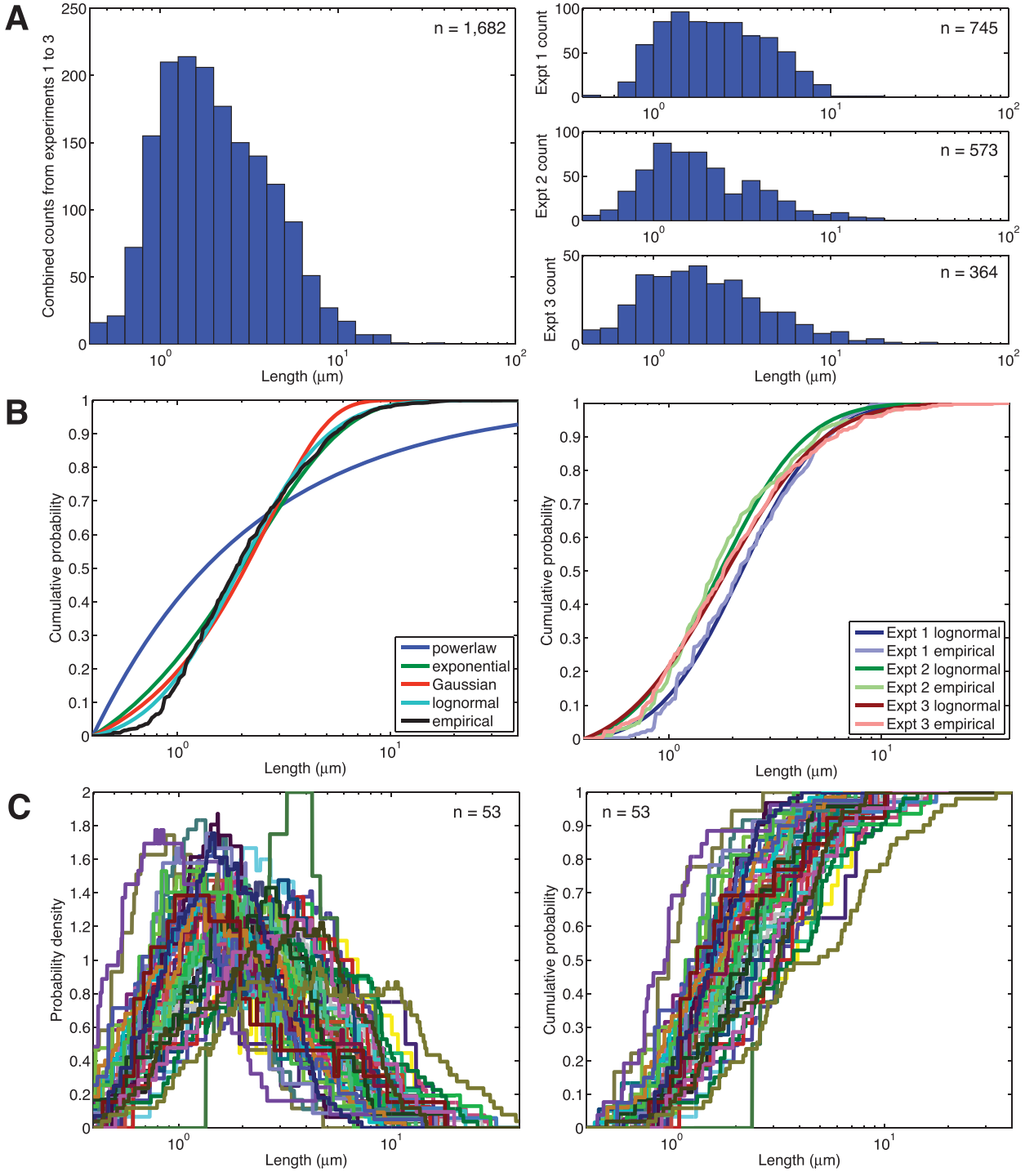

Figure 2 Filopodia length distribution is unimodal and best fits a lognormal model. **(A)** Histogram of all the filopodia lengths (n = 1,682), and independent experiments 1, 2 and 3 with n = 745, n = 573 and n = 364 respectively. **(B)** Empirical cumulative distribution functions (CDFs) of lengths with the lognormal and other statistical models for all the experiments combined and each independent experiment 1, 2 and 3. **(C)** Empirical PDFs and CDFs of filopodia lengths for 53 cells.

between individual cells in a population indicates that the system regulating filopodia length shows robust behavior in the Rat2 population.

Filopodia distance separations are distributed lognormally

As we did for filopodia lengths, we compiled the data for the separation distances between adjacent filopodia. As with filopodia length, the separation distance is unimodal in both the total data set and in the three separate experiments (Figure 3A). The mean distance for the collective dataset was 6.18 μm and experiments 1, 2 and 3 had respective means of 5.52 μm, 5.11 μm, and 9.23 μm. When we calculated the CDF for the distance distribution, lognormal was the best fit of the distribution data (Figure 3B). As is the case of filopodial length, the separation dataset is poorly modeled as an exponential, Gaussian, or power law distribution (Figure 3B). The power law distribution is the poorest fit, while an exponential distribution may fit the distribution of filopodia that are separated by 10 μm or more. Nearly all of the cells in a Rat2 population show a good lognormal fit of separation distance data. The similarity in CDF distribution between individual cells in a population indicates that the system regulating filopodia distance separation shows robust behavior between cells. 74% of the interfilopodial distance separation falls within the range of 1 μm to 10 μm.

Length and separation distance are independent variables

The polymerization of actin polymers within a filopodium depends on an intracellular pool of G-actin. It is possible that as an individual filopodium grows, it might locally deplete the G-actin pool around it and thereby interfere with *de novo* filopodia creation or actin polymerization in pre-existing filopodia. If this were the case, then there may be some empirical relationship between filopodia length and separation. To test this idea, we determined whether or not the length of an individual filopodium is detectably correlated with separation distance between its neighbours (Figure 4A). The figure shows the length of individual filopodia versus the average separation distance between its two nearest filopodia plotted on a log-log scale. On the whole, however, there is no substantial correlation between filopodial length and interfilopodial separation distance ($r \sim 0.02$). On a per cell basis, there are some cells that show a weak negative correlation between length and separation ($r \sim -0.6$) and some with a weak positive correlation ($r \sim 0.25$). We next determined whether or not there was any substantial correlation between the distance separating adjacent filopodia and whether there might be correlation between the lengths of filopodial neighbours. Such a correlation would be predicted should the concentration of a G-actin pool be a limiting factor in either the initiation of an individual filopodium or in its total length. Figure 4B shows that there is a mild correlation between the separation distance of adjacent filopodia. A similar weak correlation exists between the length of filopodial neighbours (Figure 4C). This suggests that any spatial constraints linking filopodia length and separation are likely to be quite small and, together with Figure 4A, suggests that filopodial length and separation distance are likely to be independent variables.

Perturbation Analysis of Filopodia

We next wanted to investigate how the filopodia system quantitatively responds to perturbation. There are many agents that have been described to be inducers of filopodia formation, but high-quality empirical measurement of what these agents do to filopodia are not common. Since we have been able to mathematically describe the filopodia system with some degree of confidence, we are now able to define how known filopodial perturbations affect the system as a whole. We chose to alter filopodia production in three distinct manners: genetically, chemically and physically. For the genetic perturbation, we engineered Rat2 cells to ectopically express the lipid kinase PI4KIIIβ, which we have reported stimulates filopodia production [22]. To chemically induce filopodia, we used the peptide hormone bradykinin, which induces filopodia through activation of G-protein coupled receptors [24]. To physically induce filopodia, we coated the growth substrate with poly-D-lysine, which could increase filopodia size by increasing the positive charge of the substrate and enhancing adhesion.

As shown in Figure 5A, expression of PI4KIIIβ causes a large increase in the length of filopodia. The mean length in PI4KIIIβ-expressing cells was 5.13 μm, significantly longer than the 2.03 μm mean length in the vector-only controls (t-test, $p < 0.0001$). The length distribution remains unimodal, and an increase in the number of long filopodia (10 μm - 100 μm) is visible. The longest filopodium in PI4KIIIβ expressing cells was 65.71 μm. Interestingly, the separation distance between the filopodia also increases following PI4KIIIβ expression and the mean separation in PI4KIIIβ-expressing cells was 12.00 μm, significantly higher than the 4.16 μm distance in vector-only controls (t-test, $p < 0.00005$). Importantly, even though the length and separation of filopodia have increased substantially, the distribution of both parameters remains lognormal. This indicates that the lognormal distribution is a robust aspect of filopodia length and separation distance control.

Bradykinin treatment causes an increase in filopodia length, albeit to a much lesser extent than PI4KIIIβ

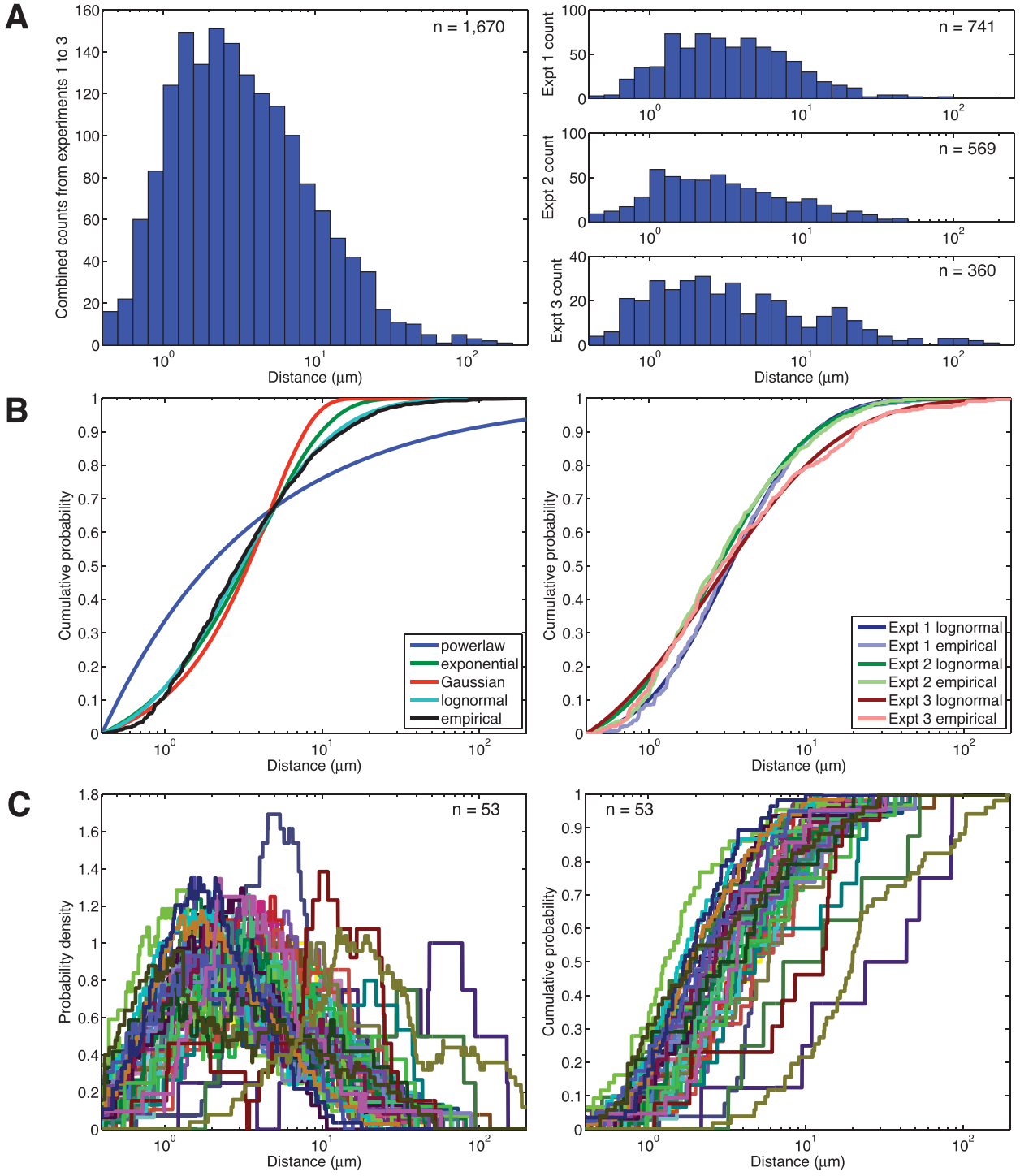

Figure 3 Filopodia distance separation distribution is unimodal and best fits a lognormal model. **(A)** Histogram of all the filopodia distances (n = 1,670), and independent experiments 1, 2 and 3 with n = 741, n = 569 and n = 360 respectively. **(B)** Empirical cumulative distribution functions (CDFs) of distances with the lognormal and other statistical models for all the experiments combined and each independent experiment 1, 2 and 3. **(C)** Empirical PDFs and CDFs of filopodia distances for 53 cells.

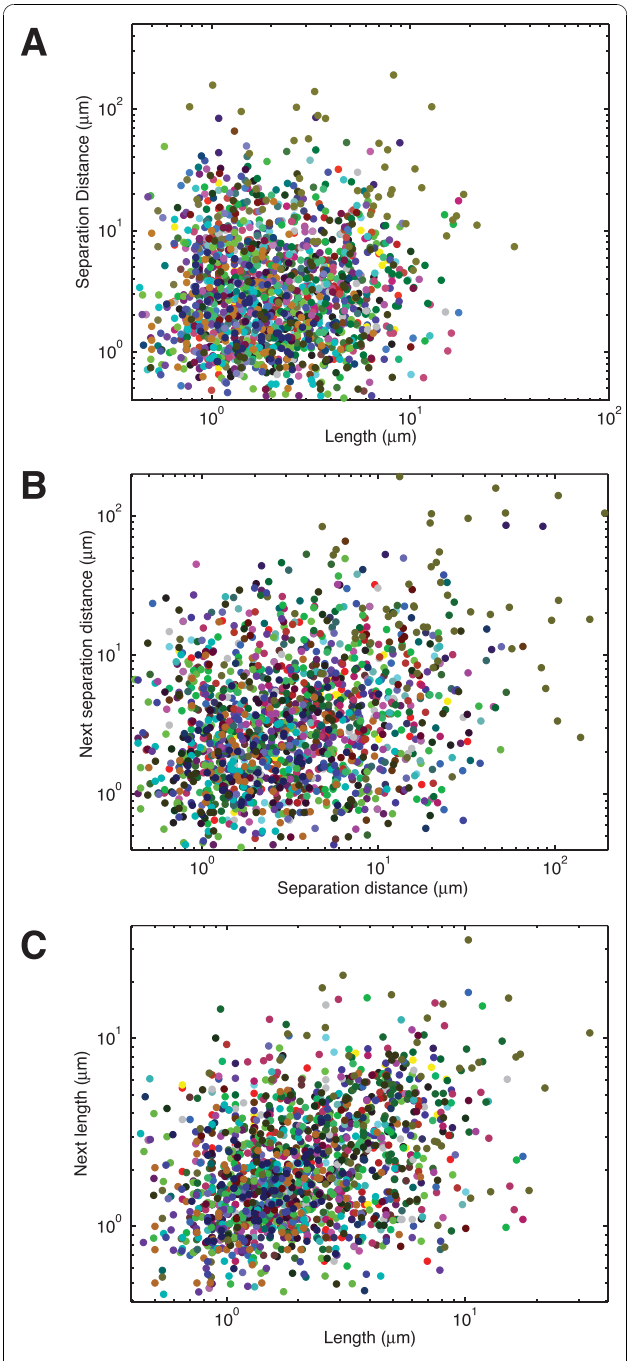

Figure 4 Filopodia length and distance separation are independent. **(A)** Scatter plot of filopodia lengths against the neighboring distances shows no correlation. Identically coloured data points represent measurements from the same cell. **(B)** Scatter plot of the distances between filopodia versus the distances between the next filopodia in a clockwise direction around the edge of the cell. **(C)** Scatter plot of the lengths of filopodia versus the lengths of the next filopodia in a clockwise direction around the edge of the cell.

expression. The mean length of bradykinin treated filopodia was 5.19 μm, significantly longer than the 3.95 μm mean length in DMSO treated controls (t-test, $p < 0.04773$). The change that bradykinin makes to filopodia length distribution is primarily in the longer filopodia as 27% of filopodia in bradykinin treated cells were > 6 μm in length, compared to only 17% (48/282) of filopodia in the DMSO controls. The mean separation did not change appreciably, with a mean distance of 4.97 μm in the bradykinin-treated cells compared to 5.16 μm in the DMSO-treated cells. The lack of significant change in distance separation (t-test, $p < 0.4386$) further strengthens our assertion that filopodia length and distance separation are independent variables. As in the case with PI4KIIIβ expression, the distributions of length and separation following bradykinin remain unimodal and are best fit by lognormal distributions.

The effects of poly-D-lysine on filopodia were very modest (Figure 5C). The mean length of filopodia in cells grown on poly-D-lysine was 3.13 μm which is not much longer than the 2.82 μm mean filopodia length of Rat2 cells grown on plain glass slides. This difference is statistically significant (t-test, $p < 0.02968$) due to the large number of samples, but it is not readily apparent in the PDF and CDF distribution. Like bradykinin, no change in filopodia separation distances is apparent (5.90 μm compared to 5.49 μm). The distribution of filopodia is unimodal and fits a lognormal distribution. Collectively, the effects of genetic, chemical and physical filopodia inducers show that increases in filopodia length do not apparently alter the lognormal distribution pattern of filopodia length nor the lognormal distribution of the distances that separate them.

Lastly, we chose to analyze the relationship between length and separation distance in the perturbed cells. Figure 6 shows this relationship, plotted on a log-log scale, for all three perturbations. In the case of bradykinin and poly-D lysine, there was no obvious relationship between length and separation. In this respect, these two perturbations do not cause changes from the wild-type situation. In the case of PI4KIIIβ expression, there is a weak, albeit statistically significant, positive correlation ($r \sim 0.39$). This appears to result from two individual cells (coloured black and purple) with very long and highly separated filopodia. Filopodia length and separation are not highly correlated in these two cells, but the magnitude of the length and separation measurements leads to an apparent correlation in the overall population. As such, we conclude that length and filopodial separation remain independent variables even following perturbation.

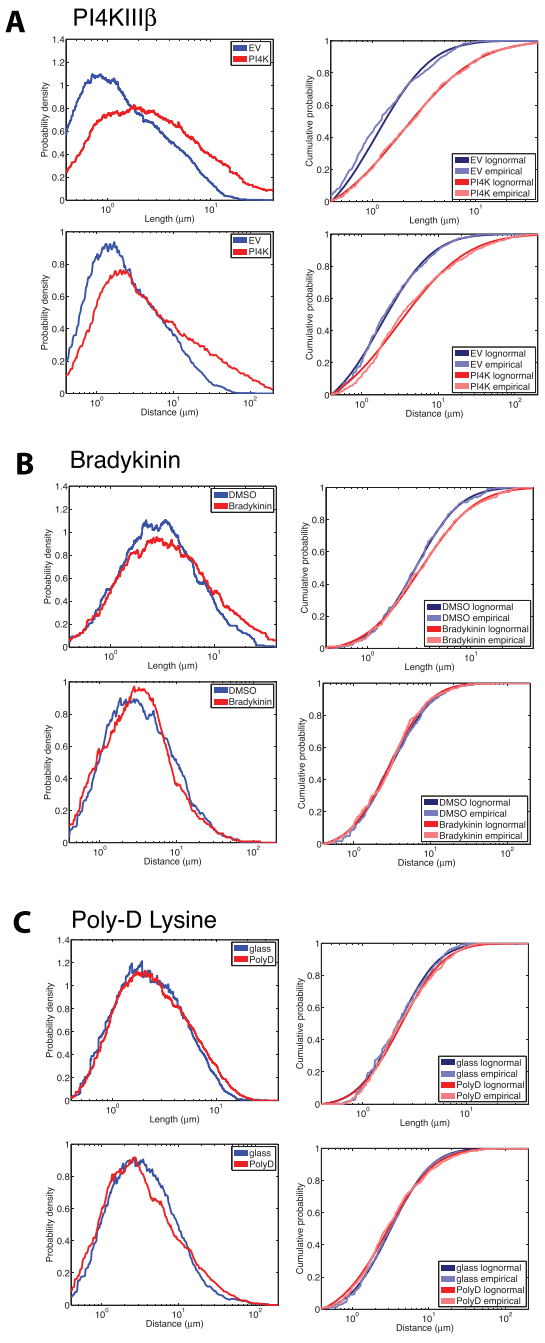

Figure 5 Robust nature of the filopodial length and distance separation lognormal distribution. Perturbation analysis of Rat2 cells after genetic, chemical and physical induction of filopodia. **(A)** PΠI4KIIIβ expression induces filopodia and increases both length and separation distance relative to the empty vector control. Rat2 cells stably expressing PI4KIIIβ and controls have been previously described [22]. **(B)** Bradykinin, a chemical inducer of filopodia, increased the length but had no effect on the interfilopodial distances compared to the DMSO control. Rat2 cells were treated with 100 ng/mL bradykinin. **(C)** Poly-D-lysine, a physical inducer of filopodia, increased the length of filopodia modestly but had no effect on distances.

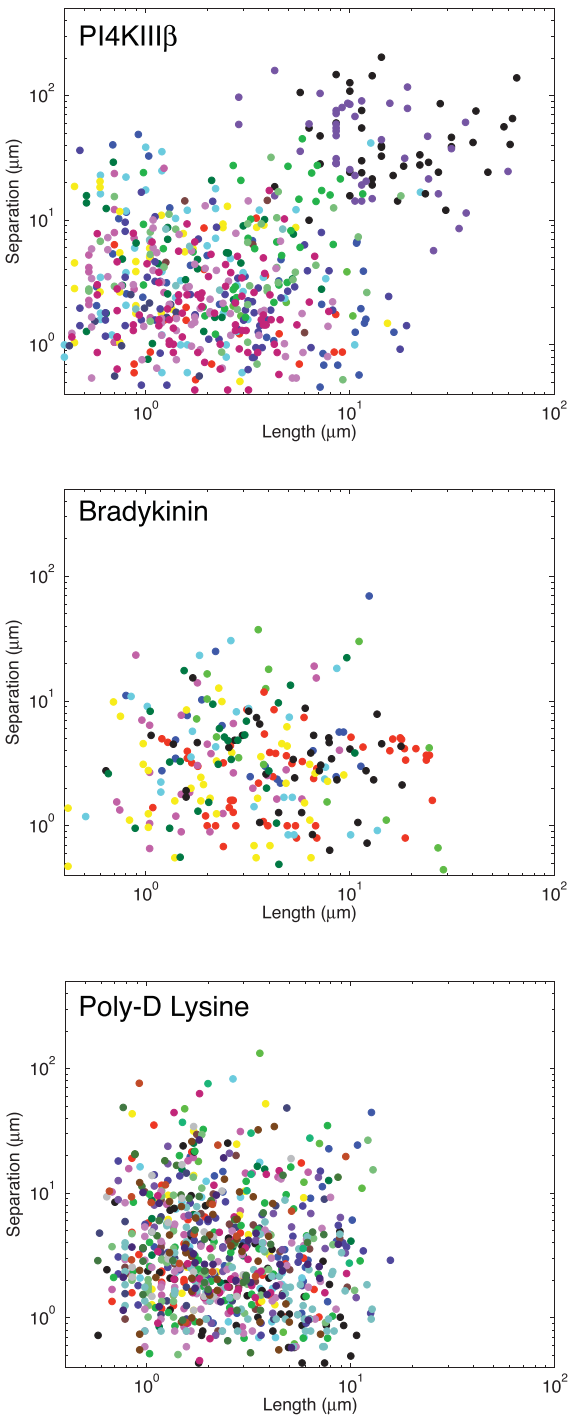

Figure 6 Filopodia length and distance separation are independent after perturbation. Graph of filopodial length and separation distance for PI4KIIIβ, Bradykinin and Poly-D-lysine perturbations. Identically coloured data points represent measurements from the same cell.

Discussion and Conclusions

Among the goals for this study was to identify a method to quantitatively describe the filopodial system in a given cell population. Our interest in this idea first arose when we began to quantitate the effect that PI4KIIIβ expression had on filopodia in the mammalian breast cancer cell line BT549 [22]. PI4KIIIβ is one of four mammalian kinases, PI4KIIα, PI4KIIβ, PI4KIIIα and PI4KIIIβ, which generate PI4P (Phosphatidylinositol 4-phosphate) from PI (phosphatidylinositol) [25,26]. Our work with this kinase and an oncogenic protein that activates it, eEF1A2, suggested that eEF1A2 and PI4KIIIβ stimulated filopodia production by activating the production of $PI(4,5)P_2$ [21-23]. $PI(4,5)P_2$ abundance regulates filopodia by recruiting actin-remodeling proteins to the migratory leading edge [27]. While the effect that PI4KIIIβ expression had on filopodia was visually striking and qualitatively apparent, quantitative description proved difficult because of the highly variable appearance of filopodia in a given cell population. Filopodia numbers vary per cell; their lengths in a single cell frequently span more than an order of magnitude and very long filopodia sometimes appear even in unstimulated cells. In the end, we adopted a system that approximated our qualitative visual evaluation [22]. We scored cells that had 10 or more filopodia > 3 μm in length as positive and the remainder as negative [22]. Based on this criterion, PI4KIIIβ expression has a demonstrable and significant numerical effect on filopodia production [22]. However, this descriptive system was unsatisfying because there is nothing intrinsically unique about filopodia longer than 3 μm nor is having 10 or more long filopodia of obvious biologic importance. In this study, we hoped to identify objective and quantitative parameters of the filopodial system to determine whether or not any given stimulus was altering filopodia production. Based on our current analysis, we propose that μ the peak of the density of the lognormal distribution represents a useful quantitation parameter of the filopodial network. The robust nature of the lognormal distribution (Figure 2) among independent replicates of the same cell population indicates that it appears to be a tightly regulated feature of the cell type. Moreover, individual cells of the same population have a similar CDF distribution (Figure 2C). Based on our analysis of the bradykinin, poly-D-lysine perturbation, and PI4KIIIβ expression, we believe that counting ~300 filopodia in a population will allow quantitative determination of the effect that a given stimulus has on filopodial appearance based on alterations in μ.

The extensive filopodia length data that we have collected provide an empirical base on which to test existing theoretical models of filopodia growth [14-16]. Our empirical data does not closely match many existing theoretical models. For example, Lan and Papoian predict that the frequency distribution of filopodia lengths will be tight and will peak at ~0.6 μm [16] while our empirical peak is ~3 μm. Moreover, we frequently observe filopodia >5 μm in length, which is not readily accounted for in their work. The presence of these long filopodia is also not in agreement with Atligan et al., who propose that mechanical buckling forces provide strong limits on filopodia growth beyond a length of 1.7 μm [14]. It is possible that adhesion between filopodia and the growth substrate may reduce the effect that buckling forces have in retarding filopodial growth, but this remains to be empirically tested. While Mogilner & Rubinstein predict that most of the filopodia will be of 2 μm in length [15], in closer agreement with our studies, their modeling does not account for the lognormal distribution of the filopodial nor the large numbers of long filopodia that we observe. Mogilner & Rubinstein postulate that three different parameters limit filopodia growth dependent on filopodial length [15]. According to their model, membrane resistance limits filopodia below 0.4 μm in length, between 0.4-1.5 μm filopodia length is limited by buckling, while longer filopodia growth is limited by the diffusion of G-actin. More recent modeling has suggested that the generation of long filopodia (~4-6 μm length) may be the result of active G-actin transport within filopodia or the loss of capping protein function [17,18]. However, we consistently observe filopodia in the > 6 μm range, therefore we hypothesize that additional factors must be at work.

It is worth mentioning that existing models of filopodia formation are based on the assumption that the actin filaments within an individual filopodium are as long as the filopodium itself [14-16]. Because of the directionality of the filopodial actin fibers, filopodial growth directly reflects actin polymerization at the tips. Many studies support this model [4,10,12], but a recent cryo-electron tomographic analysis of filopodia in *Dictyostelium* suggests otherwise [28]. This ultrastructural analysis indicates that filopodia are composed of discontinuous actin filament bundles ~100 nm in length. The discontinuous nature of the actin filaments within these filopodia could therefore allow for longer filopodia because the buckling forces that affect individual filaments would be predicted to be smaller. However, the commonality of this structure in filopdia in other cell types remains to be determined.

It is important to note some limitations in our current study. Firstly, we have relied exclusively on the Rat2 cell line and other cells may behave differently. The B16 melanoma line is commonly used to study filopodia and these cells show much smaller filopodia and more

uniform length distribution relative to Rat2 [13]. The cell-type specificity of filopodial quantitative parameters indicates that differing biochemical pathways are at play in individual cell lines. Another limitation of our study is that we have not measured filopodia in living cells. Individual filopodia undergo phases of growth, stasis and retraction during their lifespan [13]. Our use of fixed (non-living) cells, treats filopodia as stationary objects and, in a sense, ignores their dynamism. To help circumvent this issue, we have collected data from a large population of cells. Because we have made no attempt to synchronize or otherwise manipulate the filopodial growth cycle, our collective dataset represents filopodia in all their dynamic phases. Large-scale analysis of filopodia in living cells will be necessary to betterunderstand and measure filopodial dynamics.

The inter-filopodial distance separation data that we collected also allow sus to test the predictions made by Mogilner et al. [15]. Mogilner based their model on previous work by Svitkina et al. [11], which provided evidence that filopodia are initiated from the fusion of cytosolic actin fibers. These lamellar actin fibers fuse into a λ-shaped precursor and subsequent actin polymerization creates a filopodium. Based on the distribution of λ-precursors and their lateral motion, Mogilner modeled interfilopodial spacing to a range of 1-3 μm, with a tight distribution. Another theoretical study, based on the idea that membrane protein adhesion complexes regulate the initiation of protrusive structures, also suggests that filopodia will have separation distances in this range [29]. However, we observe that filopodia are often widely spaced, frequently having separation distances of 10 μm or more. It should be noted that lambda precursors are not the only proposed pathway of filopodia initiation, and filopodia may also form from *de novo* nucleation by Formin proteins independent of lamellar actin strands [4,10,12]. Moreover, filopodial fusion, an event predicted [14,20] but not yet reported may also function to increase inter-filopodial distances. These may account for our large filopodial spacing.

We were initially surprised to find that PI4KIIIβ expression not only increases filopodial length, but also increases their separation (Figure 5). Since no biochemical regulators of interfilopodial separation have been identified to date, it is not immediately apparent how PI4KIIIβ increases this parameter. However, it is possible that concomitant with an increase in filopodial length, PI4KIIIβ may be depleting a pool of G-actin or actin polymerizing factors that control filopodial initiation. On the other hand, our work indicates that filopodia length and separation are independent variables (Figure 4), suggesting they are regulated by different mechanisms. This is also further buttressed by our observation that PI4KIIIβ affects both length and separation, while bradykinin and poly-D-lysine only affect filopodial length.

We find that both filopodial length and separation distance have a lognormal distribution. Earlier biophysical modeling of filopodia-like structures in lymphocytes shorter than 1.1 μm has suggested the restraining force of the membrane might account for a heavy right-tailed length distribution [20]. In this work, a Gaussian distribution accounts for filopodia up to ~0.3 μm in length and then an exponential distribution of longer filopodia generates a heavy right tail. Qualitatively, this is consistent with our data. The presence of some experimental skew even in our log-transformed length dataset indicates that the lognormal does not wholly account for the data. Indeed, fitting a distribution of the type described by Gov [27] results in a tighter fit to the data (results not shown). However, it is not clear that the biophysical model studied by Gov has relevance to our data, as the lengths that we observe are an order of magnitude larger than the ones modeled by Gov. Moreover, we found that much of the skew in the log-transformed data is due to cell-to-cell variation. Some individual cells showed positive skew, but others showed negative skew. As such, we did not feel there was sufficient support to adopt the four-parameter Gov model [27] or even a three-parameter skew-lognormal model for filopodial length distribution.

The lognormal distribution is not uncommon in biology. For example, species abundance distributions and long-term survival in breast cancer are lognormal functions [30,31]. Fruit and flower sizes also show lognormal distributions [32]. With respect to filopodia, the cellular significance of lognormal length and separation distance distributions is unclear. However, this distribution is highly robust and resistant to perturbation. PI4KIIIβ expression and bradykinin treatment affect filopodia length but do not change the lognormal distribution. This suggests that the lognormal distribution is robust and likely reflects strong biophysical constraints on the pathways controlling filopodial dynamics. Filopodia length distribution is lognormal from the smallest length that we confidently detect (0.4 μm) up to almost 100 μm. Generally speaking, a lognormal distribution can arise as the product of a number of random variables. There are dozens, perhaps hundreds of proteins that affect actin polymerization and higher-ordered polymer assembly [1,2]. The biochemical mechanism(s) through which their combinatorial action creates a lognormal distributed function is unclear to us. Nevertheless, fluctuations in the concentrations of these proteins may be among the factors influencing filopodia length and separation. Membrane forces are also likely to be important [19,20]. Further theoretical modeling of the actin

cytoskeleton is likely to be necessary to resolve this issue.

Authors' contributions

ANH carried out the cell biology studies, performed the microscopy and measurements, participated in the data analysis and drafted the manuscript; AAM generated cell lines, assisted in the cell biology, participated in the microscopy and measurements and assisted in manuscript revision; TJP participated in the design of the study, performed the mathematical analysis of the data, participated in manuscript writing and revision and generated the figures; JML conceived of the study, participated in its design and coordination, participated in the data analysis and participated in manuscript writing and figure generation. All authors read and approved the final manuscript.

Acknowledgements

Supported by grants from the Natural Sciences and Engineering Research Council of Canada (JML, TJP). AAM is supported by a fellowship from the Canadian Institute of Health Research. We thank D. Bickel, J. Copeland, H. McBride, S. Michnick, D. Pinke, and S. Shaikh for helpful discussion and reading of this manuscript. We also thank H. McBride for help with and use of the confocal microscope.

Author details

[1]Department of Biochemistry, Microbiology & Immunology, University of Ottawa, 451 Smyth Road, Ottawa, Ontario, K1H 8M5, Canada. [2]Ottawa Hospital Research Institute, 501 Smyth Road, Ottawa, Ontario, K1H 8L6, Canada.

Received: 13 July 2010 Accepted: 17 November 2010
Published: 17 November 2010

References

1. Pollard TD, Borisy GG: **Cellular motility driven by assembly and disassembly of actin filaments.** *Cell* 2003, **112(4)**:453-465.
2. Borisy GG, Svitkina TM: **Actin machinery: pushing the envelope.** *Curr Opin Cell Biol* 2000, **12(1)**:104-112.
3. Gupton SL, Gertler FB: **Filopodia: the fingers that do the walking.** *Sci STKE* 2007, **2007(400)**:re5.
4. Faix J, Rottner K: **The making of filopodia.** *Curr Opin Cell Biol* 2006, **18(1)**:18-25.
5. Lidke DS, Lidke KA, Rieger B, Jovin TM, Arndt-Jovin DJ: **Reaching out for signals: filopodia sense EGF and respond by directed retrograde transport of activated receptors.** *J Cell Biol* 2005, **170(4)**:619-626.
6. Steketee MB, Tosney KW: **Three functionally distinct adhesions in filopodia: shaft adhesions control lamellar extension.** *J Neurosci* 2002, **22(18)**:8071-8083.
7. Nemethova M, Auinger S, Small JV: **Building the actin cytoskeleton: filopodia contribute to the construction of contractile bundles in the lamella.** *J Cell Biol* 2008, **180(6)**:1233-1244.
8. Condeelis J, Singer RH, Segall JE: **The great escape: when cancer cells hijack the genes for chemotaxis and motility.** *Annu Rev Cell Dev Biol* 2005, **21**:695-718.
9. Yamaguchi H, Wyckoff J, Condeelis J: **Cell migration in tumors.** *Curr Opin Cell Biol* 2005, **17(5)**:559-564.
10. Faix J, Breitsprecher D, Stradal TE, Rottner K: **Filopodia: Complex models for simple rods.** *Int J Biochem Cell Biol* 2009, **41(8-9)**:1656-1664.
11. Svitkina TM, Bulanova EA, Chaga OY, Vignjevic DM, Kojima S, Vasiliev JM, Borisy GG: **Mechanism of filopodia initiation by reorganization of a dendritic network.** *J Cell Biol* 2003, **160(3)**:409-421.
12. Faix J, Grosse R: **Staying in shape with formins.** *Dev Cell* 2006, **10(6)**:693-706.
13. Mallavarapu A, Mitchison T: **Regulated actin cytoskeleton assembly at filopodium tips controls their extension and retraction.** *J Cell Biol* 1999, **146(5)**:1097-1106.
14. Atilgan E, Wirtz D, Sun SX: **Mechanics and dynamics of actin-driven thin membrane protrusions.** *Biophys J* 2006, **90(1)**:65-76.
15. Mogilner A, Rubinstein B: **The physics of filopodial protrusion.** *Biophys J* 2005, **89(2)**:782-795.
16. Lan Y, Papoian GA: **The stochastic dynamics of filopodial growth.** *Biophys J* 2008, **94(10)**:3839-3852.
17. Zhuravlev PI, Papoian GA: **Molecular noise of capping protein binding induces macroscopic instability in filopodial dynamics.** *Proc Natl Acad Sci USA* 2009, **106(28)**:11570-11575.
18. Zhuravlev PI, Der BS, Papoian GA: **Design of active transport must be highly intricate: a possible role of myosin and Ena/VASP for G-actin transport in filopodia.** *Biophys J* **98(8)**:1439-1448.
19. Gov NS, Gopinathan A: **Dynamics of membranes driven by actin polymerization.** *Biophys J* 2006, **90(2)**:454-469.
20. Gov NS: **Dynamics and morphology of microvilli driven by actin polymerization.** *Phys Rev Lett* 2006, **97(1)**:018101.
21. Jeganathan S, Lee JM: **Binding of elongation factor eEF1A2 to phosphatidylinositol 4-kinase beta stimulates lipid kinase activity and phosphatidylinositol 4-phosphate generation.** *J Biol Chem* 2007, **282(1)**:372-380.
22. Jeganathan S, Morrow A, Amiri A, Lee JM: **Eukaryotic elongation factor 1A2 cooperates with phosphatidylinositol-4 kinase III beta to stimulate production of filopodia through increased phosphatidylinositol-4,5 bisphosphate generation.** *Mol Cell Biol* 2008, **28(14)**:4549-4561.
23. Amiri A, Noei F, Jeganathan S, Kulkarni G, Pinke DE, Lee JM: **eEF1A2 activates Akt and stimulates Akt-dependent actin remodeling, invasion and migration.** *Oncogene* 2007, **26(21)**:3027-3040.
24. Kozma R, Ahmed S, Best A, Lim L: **The Ras-related protein Cdc42Hs and bradykinin promote formation of peripheral actin microspikes and filopodia in Swiss 3T3 fibroblasts.** *Mol Cell Biol* 1995, **15(4)**:1942-1952.
25. Balla T: **Phosphatidylinositol 4-kinases.** *Biochim Biophys Acta* 1998, **1436(1-2)**:69-85.
26. Balla A, Balla T: **Phosphatidylinositol 4-kinases: old enzymes with emerging functions.** *Trends Cell Biol* 2006, **16(7)**:351-361.
27. Ling K, Schill NJ, Wagoner MP, Sun Y, Anderson RA: **Movin' on up: the role of PtdIns(4,5)P(2) in cell migration.** *Trends Cell Biol* 2006, **16(6)**:276-284.
28. Medalia O, Beck M, Ecke M, Weber I, Neujahr R, Baumeister W, Gerisch G: **Organization of actin networks in intact filopodia.** *Curr Biol* 2007, **17(1)**:79-84.
29. Veksler A, Gov NS: **Phase transitions of the coupled membrane-cytoskeleton modify cellular shape.** *Biophys J* 2007, **93(11)**:3798-3810.
30. Tai P, Yu E, Shiels R, Pacella J, Jones K, Sadikov E, Mahmood S: **Short- and long-term cause-specific survival of patients with inflammatory breast cancer.** *BMC Cancer* 2005, **5**:137.
31. de Aguiar MA, Baranger M, Baptestini EM, Kaufman L, Bar-Yam Y: **Global patterns of speciation and diversity.** *Nature* 2009, **460(7253)**:384-387.
32. Limpert A, Stahel WA, Abbt M: **Log-normal Distributions across the Sciences: Keys and Clues.** *BioScience* 2001, **51(5)**:341-352.

doi:10.1186/1471-2121-11-86
Cite this article as: Husainy *et al.*: Robust patterns in the stochastic organization of filopodia. *BMC Cell Biology* 2010 **11**:86.

MOLECULAR AND CELLULAR BIOLOGY, July 2008, p. 4549–4561 Vol. 28, No. 14
0270-7306/08/$08.00+0 doi:10.1128/MCB.00150-08

Eukaryotic Elongation Factor 1A2 Cooperates with Phosphatidylinositol-4 Kinase III β To Stimulate Production of Filopodia through Increased Phosphatidylinositol-4,5 Bisphosphate Generation▽

Sujeeve Jeganathan, Anne Morrow, Anahita Amiri, and Jonathan M. Lee*

Department of Biochemistry, Microbiology, and Immunology, University of Ottawa, 451 Smyth Road, Ottawa, Ontario, Canada K1H 8M5

Received 21 January 2008/Returned for modification 4 March 2008/Accepted 5 May 2008

Eukaryotic elongation factor 1 alpha 2 (eEF1A2) is a transforming gene product that is highly expressed in human tumors of the ovary, lung, and breast. eEF1A2 also stimulates actin remodeling, and the expression of this factor is sufficient to induce the formation of filopodia, long cellular processes composed of bundles of parallel actin filaments. Here, we find that eEF1A2 stimulates formation of filopodia by increasing the cellular abundance of cytosolic and plasma membrane-bound phosphatidylinositol-4,5 bisphosphate [$PI(4,5)P_2$]. We have previously reported that the eEF1A2 protein binds and activates phosphatidylinositol-4 kinase III beta (PI4KIIIβ), and we find that production of eEF1A2-dependent $PI(4,5)P_2$ and generation of filopodia require PI4KIIIβ. Furthermore, PI4KIIIβ is itself capable of activating both the production of $PI(4,5)P_2$ and the creation of filopodia. We propose a model for extrusion of filopodia in which eEF1A2 activates PI4KIIIβ, and activated PI4KIIIβ stimulates production of $PI(4,5)P_2$ and filopodia by increasing PI4P abundance. Our work suggests an important role for both eEF1A2 and PI4KIIIβ in the control of $PI(4,5)P_2$ signaling and actin remodeling.

Filopodia are fingerlike projections from the plasma membrane that are the first cellular structures to reach new spaces during cell migration. Filopodia are composed of bundled actin filaments and actin-associated proteins (9, 13). Transmembrane receptors within filopodia respond to extracellular cues and guide directional movement toward chemoattractants (26). In addition, filopodia contain abundant adhesion molecules that regulate cellular attachment to growth substrates and cell-cell interactions (37). As such, filopodia regulate several key physiological processes, including cell migration, wound healing, and development. For example, filopodia are essential for neurogenesis in mice and for cell-cell adhesion during *Drosophila melanogaster* embryogenesis (9, 13).

We have previously described a role for eukaryotic elongation factor 1 alpha 2 (eEF1A2) in the initiation and maintenance of filopodia (1). In several types of mammalian cells, eEF1A2 expression is sufficient to stimulate formation of filopodia (1). eEF1A2 is one of two members of the eEF1A family of proteins, eEF1A1 and eEF1A2. During the elongation phase of protein synthesis, GTP-bound eEF1A proteins interact with amino-acylated tRNA and recruit them to the ribosome (18). While eEF1A1 and eEF1A2 are believed to have equivalent roles in protein translation, their tissue-specific expression patterns are each markedly different. eEF1A1 is expressed ubiquitously, whereas eEF1A2 is detectably expressed only in normal tissues of mammalian heart, brain, and skeletal muscle (24a, 24b, 28). Homozygous deletion of eEF1A2 occurs in the wasted mouse (7). These mice develop normally but suffer from neuromuscular abnormalities and immunodeficiency and die at approximately 1 month of age (35, 36). Importantly, eEF1A2 is likely to be a human oncogene, it is highly expressed, and its gene is amplified in 30 to 60% of human tumors of the breast, ovary, and lung (2, 24, 24a, 25, 40). eEF1A2 is transforming, and its expression in mammalian cells increases the cells' in vitro growth rate, allows cells to grow in soft agar, and enhances cells' tumorigenicity in xenograft models (2).

The mechanism by which eEF1A2 stimulates production of filopodia is currently unclear. The production of filopodia is regulated in major part by the plasma membrane abundance of phosphatidylinositol-4,5 bisphosphate [$PI(4,5)P_2$] (9). $PI(4,5)P_2$ cooperates with the WASP family of proteins and the Cdc42 GTPase to stimulate the ability of the Arp2-Arp3 complex to assemble actin (9). As such, proteins that control $PI(4,5)P_2$ abundance are likely to have critical roles in controlling initiation of filopodia. Consistent with a role for eEF1A2 in phospholipid signaling, we have previously reported that eEF1A2 binds to the lipid kinase phosphatidylinositol-4 kinase III beta (PI4KIIIβ) and increases its kinase activity (21). PI4KIIIβ is a member of the PI4K family of lipid kinases that phosphorylates the D4 carbon of the inositol ring in phosphatidylinositol to yield phosphatidylinositol-4 phosphate (PI4P) (5, 17). PI4Ks are emerging as important mediators of cell physiology because PI4P is itself a regulatory phospholipid and additionally an obligate precursor for $PI(4,5)P_2$ and $PI(3,4,5)P_3$ (4, 29).

Here, we investigated whether eEF1A2 might activate production of filopodia through PI4KIIIβ. We find that eEF1A2 expression is sufficient to increase the cytoplasmic and plasma membrane abundance of $PI(4,5)P_2$. This increase in plasma membrane $PI(4,5)P_2$ is necessary for eEF1A2-induced filopo-

* Corresponding author. Mailing address: Department of Biochemistry, Microbiology, and Immunology, University of Ottawa, 451 Smyth Road, Ottawa, Ontario, Canada K1H 8M5. Phone: (613) 562-5800, ext. 8640. Fax: (613) 562-5452. E-mail: jlee@uottawa.ca.

▽ Published ahead of print on 12 May 2008.

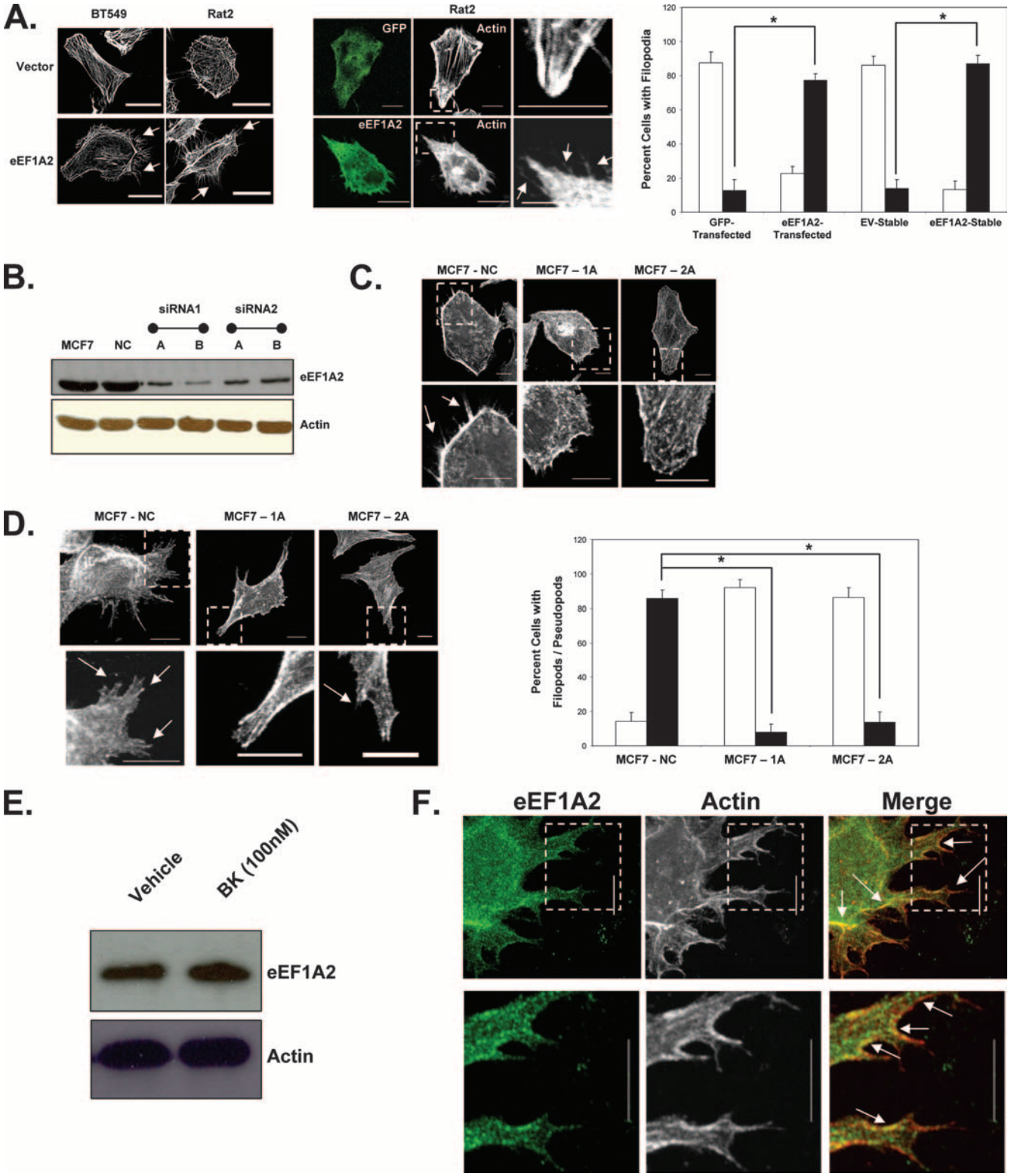

FIG. 1. eEF1A2 regulates formation of filopodia. (A) Left panel, BT549 and Rat2 cells stably expressing eEF1A2 have more filopodia (arrows) than do the empty vector control cells. Middle panel, transient transfection of eEF1A2 in Rat2 cells increases the number of filopodia (arrows) relative to those of GFP-transfected controls. Right panel, quantification of the number of cells with filopodia (n = 138, 152, 131 and 157, for GFP-transfected, eEF1A2-transfected, stable-EV, and stable-eEF1A2 cells, respectively). Filled columns indicate cells with at least 10 filopodia greater than or equal to 3 μm in length. Open columns indicate cells with any number of filopodia less than 3 μm in length. Significance ($P < 0.05$, Student's t test) is indicated by an asterisk. (B) Expression of eEF1A2 protein in MCF7 variants with stable downregulation of eEF1A2 by RNAi. NC, negative control. (C) MCF7 stable cell lines with control RNAi (NC) cells show abundant filopodia (arrows), while those showing constitutive eEF1A2 downregulation (1A and 2A) show little or none. (D) Left panel, MCF7 cells grown in the presence of 100 nM

dium formation. eEF1A2-mediated formation of filopodia and $PI(4,5)P_2$ accumulation are both dependent on PI4KIIIβ. Cdc42 activation is also required for eEF1A2-induced formation of filopodia, and eEF1A2 expression is sufficient to activate Cdc42. Furthermore, we find that PI4KIIIβ expression is sufficient to induce formation of filopodia and localization of plasma membrane $PI(4,5)P_2$. Our work is consistent with a model for filopodium production in which eEF1A2 stimulates production of filopodia through Cdc42 activation and a PI4KIIIβ-mediated increase in $PI(4,5)P_2$ abundance. Our work also suggests an important regulatory role for PI4KIIIβ in controlling actin remodeling.

MATERIALS AND METHODS

Cell lines and vectors. Rat2, BT549, and MCF7 cells were obtained from the American Type Culture Collection (Manassas, VA) and grown according to their instructions. MCF7 cell lines with stable eEF1A2 ablation were generated using a pSilencer Neo short interfering RNA (siRNA) expression vector (Ambion) with eEF1A2-directed siRNA, using sequences previously described (21). Bradykinin was purchased from Calbiochem (San Diego, CA). Generation of the eEF1A2 plasmid (eEF1A2-pcDNA3.1) is described in the report by Anand et al. (2). Generation of the adenoviral vectors (Ad-eEF1A2 and Ad-GFP) was described previously (1, 24). The PI4KIIIβ-expressing stable cell lines and the vector controls were generated using the pLXSN retroviral system described by Grignani et al. (12). PI4K111B, PM-FRB-CFP, mRFP-FKBP-5-ptase, and PLCδ-PH-GFP plasmids were a generous gift of T. Balla (41, 42).

Antibodies. Generation of the rabbit polyclonal eEF1A2 antibody and its validation by Western blotting and immunohistochemistry were described previously (24). eEF1A2 expression was also detected using a V5-horseradish peroxidase (HRP) antibody (Invitrogen or Sigma). The PI4KIIIβ and goat anti-mouse, HRP-conjugated immunoglobulin G (IgG) antibodies were from Upstate Cell Signaling Solutions (Charlottesville, VA). Actin antibody was from Sigma (Oakville, Ontario), and HRP-conjugated anti-rabbit IgG was from Cell Signaling Technology (Danvers, MA). $PI(4,5)P_2$ was visualized by using an anti-$PI(4,5)P_2$ IgM antibody (Echelon Biosciences Inc., Salt Lake City, UT) and a goat anti-mouse IgM, (*R*)-phycoerythrin secondary antibody (Caltag Laboratories, Carlsbad, CA).

siRNA and transfections. The sequence of the PI4KIIIβ siRNA is 5′-GGAG GUGUUGGA-GAAAGUCtt-3′. This siRNA and the negative control siRNA (catalog no. 4611) were purchased from Ambion (Austin, TX). siRNA transfections were performed using siPORT Lipid (Ambion) according to the manufacturer's instructions.

During the immunofluorescence experiments, parental Rat2 cells were triply transfected with the PLCδ-PH-GFP plasmid, with eEF1A2-pcDNA3.1, and either the negative control siRNA or the PI4KIIIβ siRNA. The eEF1A2 or vector plasmid was always at a 10-fold molar excess over that of the PLCδ-PH-GFP plasmid. When the Rat2 cells stably expressing eEF1A2 were used, the transfections were done using only the PLCδ-PH-GFP plasmid and the siRNA. For transfections, the total plasmid amount was 4 μg. When the stable cell lines were used for the siRNA experiments, cells were transfected with 3.7 μg of the PLCδ-PH-GFP plasmid and 20 nM of either the negative control siRNA or the PI4KIIIβ siRNA. To study the $PI(4,5)P_2$ levels induced upon transient eEF1A2 or empty vector expression, Rat2 cells were transfected with the PLCδ-PH-GFP plasmid and either an eEF1A2-pcDNA3.1 or a pcDNA3.1 plasmid. For all transient eEF1A2 transfections, the eEF1A2 or vector plasmid was at a 10-fold molar excess over that of the other plasmids. All transfections were performed using Lipofectamine 2000 reagent (Invitrogen) according to the manufacturer's protocol.

Immunofluorescence. Cells were plated in six-well plates containing coverslips. The next day, cells were fixed in 3.7% paraformaldehyde (15 min), permeabilized with 0.1% Triton-X (20 min), and blocked with 5% fetal bovine serum/phosphate-buffered saline (1 h; 37°C). Following staining, cells were mounted on slides, using fluorescence mounting medium (Dako Cytomation, Golstrup, Denmark). Actin was stained with either Alexa Fluor phalloidin 546 or Alexa Fluor 594 (Invitrogen). In experiments where eEF1A2 was analyzed, eEF1A2 was stained by using one of two methods. For the first method, we used an eEF1A2-specific rabbit polyclonal antibody (MCF7 cells, 1:100, overnight), followed by Alexa Fluor 488 goat anti-rabbit IgG secondary antibody (1:300, 2 h, room temperature). In the second method, we used a monoclonal anti-V5 antibody (Rat2 cells, 1:1000, 1 h, room temperature), followed by Alexa Fluor 680 goat anti-mouse IgG secondary antibody (1:300, 1 h, room temperature). The $PI(4,5)P_2$-specific antibody was used at 1:100 (overnight), followed by the goat anti-mouse IgM, (R)-phycoerythrin secondary antibody (1:500, 1 h, room temperature). All images were acquired using an Olympus FluoView FV1000 laser scanning confocal microscope. $PI(4,5)P_2$ fluorescence was quantified with Olympus software (FV1000, version 01.04a; Center Valley, PA) and analyzed using GraphPad Prism version 4 software (San Diego, CA).

Phosphoinositide labeling. The medium of near-confluent Rat2 cell cultures was removed and replaced with phosphate-free Dulbecco's modified Eagle's medium (Invitrogen) and labeled inorganic phosphate (40 μCi/ml; GE Healthcare, Piscataway, NJ) for 4 h. Following the incubation, cells were pelleted, and phospholipids were extracted with 40 μl of 1:1 methanol-water, 10 μl of salt-saturated NaCl, 2 μl of glacial acetic acid, and 40 μl of chloroform. The sample was vortexed vigorously and frozen at −20°C. Samples were thawed at room temperature, 40-μl aliquots of the organic phase were spotted onto precoated thin-layer chromatography (TLC) plates, and the plates were placed in the appropriate solvent system. The precoating protocol and details of the solvent system were described previously (21). The phosphatidylinositol-stained cells were visualized with storage phosphor screens (GE Healthcare), which were placed on top of the plates for a 24-h period. For the adenoviral experiments, Rat2 cells were incubated with the Ad-eEF1A2 or Ad-GFP virus (multiplicity of infection of 500) when they were 50 to 60% confluent for an overnight period. The next day, medium was replaced with phosphate-free medium, and the above-described procedure was followed.

In vitro PI4KIIIβ lipid kinase assay. Total cellular protein (20 μl) from PI4KIIIβ or vector stable cells was added to 35 μl of kinase buffer (1 mM EDTA, 30 mM HEPES [pH 7.4], 100 mM NaCl, 2 mM $MgCl_2$, and 0.2% Triton X-100) and 5 μl of 10 mM ATP containing 10 μCi of [^{32}P]ATP. Following a 20-min incubation, the reactions were stopped by the addition of 60 μl of 1 N HCl. Phospholipids were then extracted by adding 160 μl of chloroform-methanol (1:2 [vol/vol]). After samples were vortexed briefly, they were centrifuged for 10 min at 10,000 × *g*. Aliquots of the organic phase were spotted onto precoated TLC plates, and the plates were placed in the same solvent system as that mentioned previously. Once complete, the plates were placed in a cassette and covered with a phosphor screen (GE Healthcare) for a 24-h period. The screen was then analyzed with a Storm 860 phosphorimager unit (GE Healthcare).

Generation of eEF1A2 mutants. eEF1A2 mutant proteins were generated by using a PCR-mediated deletion protocol (14). Briefly, we used the eEF1A2pLXSN retroviral plasmid (1) as the template (50 ng) and *Pfu* Turbo DNA polymerase (Stratagene) with the appropriate primers (0.2 μM each), 1× *Pfu* buffer, and 0.2 mM of each deoxynucleoside triphosphate. The 5′-phosphorylated primers used were as follows: 5′-TCGGTGAAGGACATCGGTAAGCCTATCCCTAACCCTCTC-3′ (Δ321 to 464, forward); 5′-AGGGATAGGCTTACCGATGTCCTTCACCGACA CGTTCTT-3′ (Δ321 to 464, reverse); 5′-ACAGAGCCGGCCTACGGTAAGCCT ATCCCTAACCCTCTC-3′ (Δ163 to 464, forward); 5′-AGGGATAGGCTTACCG TAGGCCGGCTCTGTGGAGTCCAT-3′ (Δ163 to 464, reverse); 5′-GCGCCGG AATTCATGCGGCGGGGCAACGTGTGTGGGGAC-3′ (Δ1 to 320, forward); and 5′-CACGTTGCCCCGCCGCATGAATTCCGGCGCCTAGAGAAG-3′ (Δ1 to 320, reverse). The PCR was carried out as follows: denaturation at 95°C for 45 s,

bradykinin. eEF1A2-deficient 1A and 2A cells show fewer filopodia and pseudopodia (arrows) than control cells. Right panel, quantification of filopodia/pseudopodia (n = 148, 165, and 154 for MCF7-NC, MCF7-1A and MCF7-2A cells, respectively). Filled columns indicate cells with at least 10 pseudopodia/filopodia greater than or equal to 5 μm in length. Open columns indicate cells with any number of filopodia/pseudopodia less than 5 μm in length. (E) eEF1A2 protein levels in MCF7 cells are not detectably altered upon bradykinin treatment. (F) MCF7 cells grown in the presence of bradykinin were stained for eEF1A2 and actin. eEF1A2 is found in filopodia and pseudopodia, as well as along their bases (arrows). Scale bars represent 10 μm.

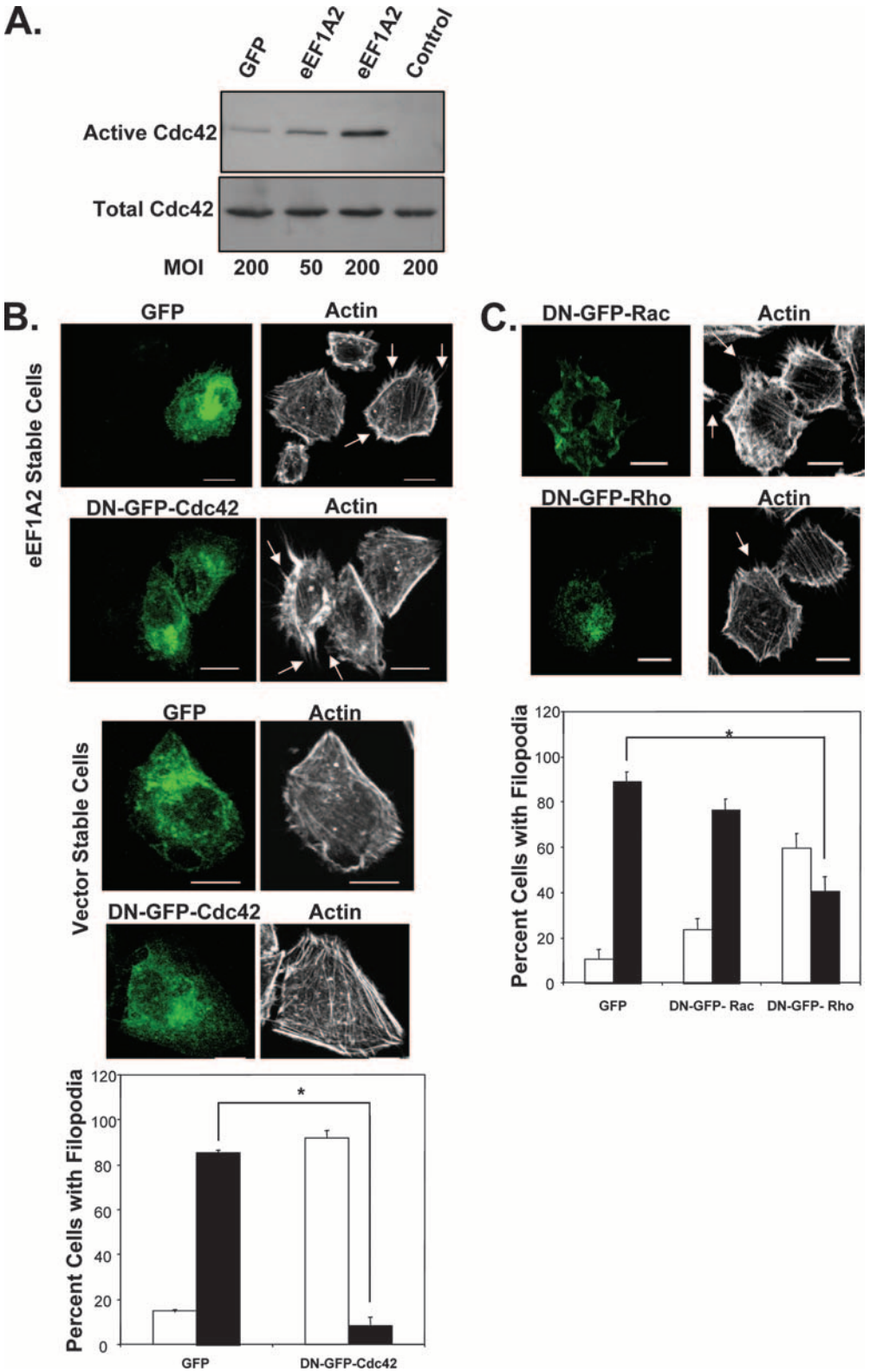

FIG. 2. eEF1A2 regulates development of filopodia through Cdc42. (A) Cdc42 activation in cells transduced with a GFP adenovirus or an eEF1A2 adenovirus. Multiplicity of infection (MOI) is as indicated. Cdc42 activity, as measured by glutathione *S*-transferase (GST)-Pak1 precipitation, is increased in cells transduced with the eEF1A2 adenovirus in a dose-dependent manner. Total Cdc42 protein is derived from a whole-cell lysate of infected cells. The control is GST-rhotekin precipitation. (B) Expression of a dominant-negative GFP-Cdc42 (DN-GFP-Cdc42) in eEF1A2-expressing cells inhibits development of filopodia (arrows). Expression of DN-GFP-Cdc42 has no noticeable effect on the overall shape or actin architecture in vector control cells. Scale bars represent 10 μm. Bottom panel, quantification of filopodia after Cdc42 inhibition ($n = 137$ and 144 for GFP and DN-GFP-Cdc42 cells, respectively). Filled columns indicate cells with at least 10 filopodia greater than or equal to 3 μm in

annealing at 43°C (Δ163 to 464 and Δ321 to 464) or 55°C (Δ1 to 320) for 45 s, and elongation at 72°C for 14 min (2 min/kb). Following the PCR, the 50-μl reaction product was DpnI digested for 1 to 2 h at 37°C and heat inactivated for 20 min at 80°C. One to two microliters of the treated reaction mixture were then transformed into competent cells. Rat2 cells stably expressing the mutants were generated as described previously (1).

Coimmunoprecipitation. For coimmunoprecipitation, cells were grown to 80 to 95% confluence in 100-mm cell culture plates. Cells were lysed by sonication on ice in detergent-free buffer (137 mM NaCl, 8 mM KH_2PO_4 [pH 7.5], 2.7 mM KCl, 2.5 mM EDTA, 1% aprotinin, 1 mg/ml leupeptin, 50 mM NaF, 1 mM Na_3VO_4, 10 μg/ml pepstatin, 1 mM phenylmethylsulfonyl fluoride) and centrifuged at 10,000 × *g* for 20 min to remove membranes. Supernatants were collected, and protein levels were quantified by using a Bradford assay (Bio-Rad) according to the manufacturer's instructions. Total protein (250 μg) was precleared with protein A-agarose (Amersham Biosciences) for 1 h at 4°C. Following this, 2 to 4 μg of PI4KIIIβ antibody (rabbit polyclonal; Upstate Cell Signaling Solutions), anti-V5 agarose affinity gel (Sigma) or anti-FLAG affinity gel (Sigma) was added and incubated overnight at 4°C. Beads were washed three times in phosphate-buffered saline, centrifuged, and boiled for 5 min in sample buffer, and the supernatant was subjected to sodium dodecyl sulfate-polyacrylamide gel electrophoresis. The antibodies used to detect the proteins were mouse anti-PI4KIIIβ antibody (BD Biosciences), anti-V5-HRP (Invitrogen), and anti-FLAG-HRP (Sigma).

RESULTS

eEF1A2 regulates formation of filopodia. We have previously reported that eEF1A2 expression induces formation of filopodia in rodent and mammalian cell lines (1). For example, stable expression of eEF1A2 in the Rat2 fibroblast line and the BT549 breast carcinoma cell line visibly increases the number and size of filopodia (Fig. 1A). This also occurs in Rat2 cells transiently transfected with eEF1A2 (Fig. 1A). In general, eEF1A2 expression causes a significant, eight- to ninefold, increase in the number of cells with filopodia greater than 3 μm in length relative to that of empty vector controls ($P < 0.05$, Student's *t* test). To further investigate a role for eEF1A2 in production of filopodia, we studied the MCF7 human breast cancer cell line. These cells express abundant eEF1A2 message and protein (24). We generated MCF7 variants, in which endogenous eEF1A2 expression had been stably reduced by using RNA interference (Fig. 1B). While abundant filopodia are observed for control cells, their size and number are visibly reduced upon eEF1A2 ablation (Fig. 1C). To quantify the reduction in filopodia, the eEF1A2-deficient cells and control cell lines were incubated with bradykinin, a soluble stimulator of filopodium formation (23). After cells were incubated with 100 nM bradykinin, there was a significant, ninefold, decrease in the number of eEF1A2-ablated MCF7 cells with filopodia and pseudopodia relative to those of control MCF7 cells (Fig. 1D). Bradykinin has no effect on eEF1A2 protein levels (Fig. 1E). Thus, eEF1A2 likely has a physiological role in formation of filopodia. For the most part, the eEF1A2 protein is diffusely cytoplasmic but can be found within filopodia and also in the bases and edges of pseudopods, colocalizing there with actin (Fig. 1F).

eEF1A2 regulates development of filopodia through Cdc42 activation. One of the key proteins that regulates formation of filopodia is the Rho family GTPase Cdc42 (9). Bradykinin, for example, stimulates filopodia through Cdc42 activation (23). eEF1A2 expression is sufficient to increase Cdc42 activity (Fig. 2A). In four separate experiments, eEF1A2 expression increased Cdc42 activity two- to eightfold relative to that of green fluorescent protein (GFP) controls. To investigate whether Cdc42 played a role in eEF1A2-dependent filopodium production, we inhibited Cdc42 activity in eEF1A2-expressing Rat2 cells by using dominant-negative GFP-tagged Cdc42 (DN-GFP-Cdc42) (39). Untransfected eEF1A2-expressing cells or those transfected with a GFP control plasmid showed many filopodia, but those expressing DN-GFP-Cdc42 showed a visibly reduced number of filopodia (Fig. 2B). Moreover, the filopodia that remained were reduced in length relative to those of controls. Overall, there was a significant, eightfold, decrease ($P < 0.05$, Student's *t* test) in the number of eEF1A2/DN-GFP-Cdc42-expressing cells with filopodia greater than 3 μm in length relative to those of eEF1A2/GFP-expressing control cells (Fig. 2B). DN-GFP-Cdc42 expression had no visible effect on the overall shape or cytoplasmic actin architecture in the vector control cell lines. To confirm the specificity of these effects for dominant-negative Cdc42, we repeated the experiments using dominant-negative Rac (DN-GFP-Rac) or a dominant-negative Rho (DN-GFP-Rho). Cells expressing DN-GFP-Rac showed no significant decrease in the size or length of filopodia relative to those of the GFP-expressing controls (Fig. 2C). However, there was a nearly twofold increase in the number of DN-GFP-Rho-expressing cells with filopodia greater than 3 μm in length compared to those of GFP controls (Fig. 2C). This is still fourfold more filopodia than in cells expressing DN-GFP-Cdc42 (Fig. 2B), suggesting that either eEF1A2 may regulate development of filopodia through a mechanism that is partially Rho dependent or that DN-Rho is interfering with Cdc42 function. Taken together, however, our findings indicate that eEF1A2 regulates filopodia primarily through Cdc42.

eEF1A2 stimulates PI(4,5)P_2 accumulation and membrane localization. A major pathway for the production of filopodia is controlled through Cdc42 and the abundance of PI(4,5)P_2 (9). Active Cdc42 and PI(4,5)P_2 cooperate to activate actin nucleation by the Arp2/3 complex (19). We have previously found that eEF1A2 can activate PI4KIIIβ, leading to an increase in the intracellular abundance of PI4P (21), a precursor for PI(4,5)P_2. We reasoned that eEF1A2 might be inducing filopodia through an increase in cellular PI(4,5)P_2 abundance. To test this idea, we first used TLC to measure total PI(4,5)P_2 levels in Rat2 cells transduced with an eEF1A2 adenovirus and in Rat2 cells stably expressing eEF1A2. We observed an increase in PI(4,5)P_2 levels upon eEF1A2 expression relative to that of controls (2.1-fold ± 0.4-fold in adenovirally transduced

length. Open columns indicate cells with any number of filopodia less than 3 μm in length. Significance ($P < 0.05$, Student's *t* test) is indicated by an asterisk. (C) eEF1A2-expressing Rat2 cells transfected with a dominant-negative Rho (DN-GFP-Rho) or Rac (DN-GFP-Rac) and stained for actin. DN-GFP-Rac-expressing cells show filopodia similar to those of untransfected cells, but those expressing DN-GFP-Rho show a decrease. Bottom panel, quantification of filopodia after Rac or Rho inhibition ($n = 125$, 166, and 176 for GFP, DN-GFP-Rac, and DN-GFP-Rho cells, respectively). Filled columns indicate cells with at least 10 filopodia greater than or equal to 3 μm in length. Open columns indicate cells with any number of filopodia less than 3 μm in length. Significance ($P < 0.05$, Student's *t* test) is indicated by an asterisk. Scale bars represent 10 μm.

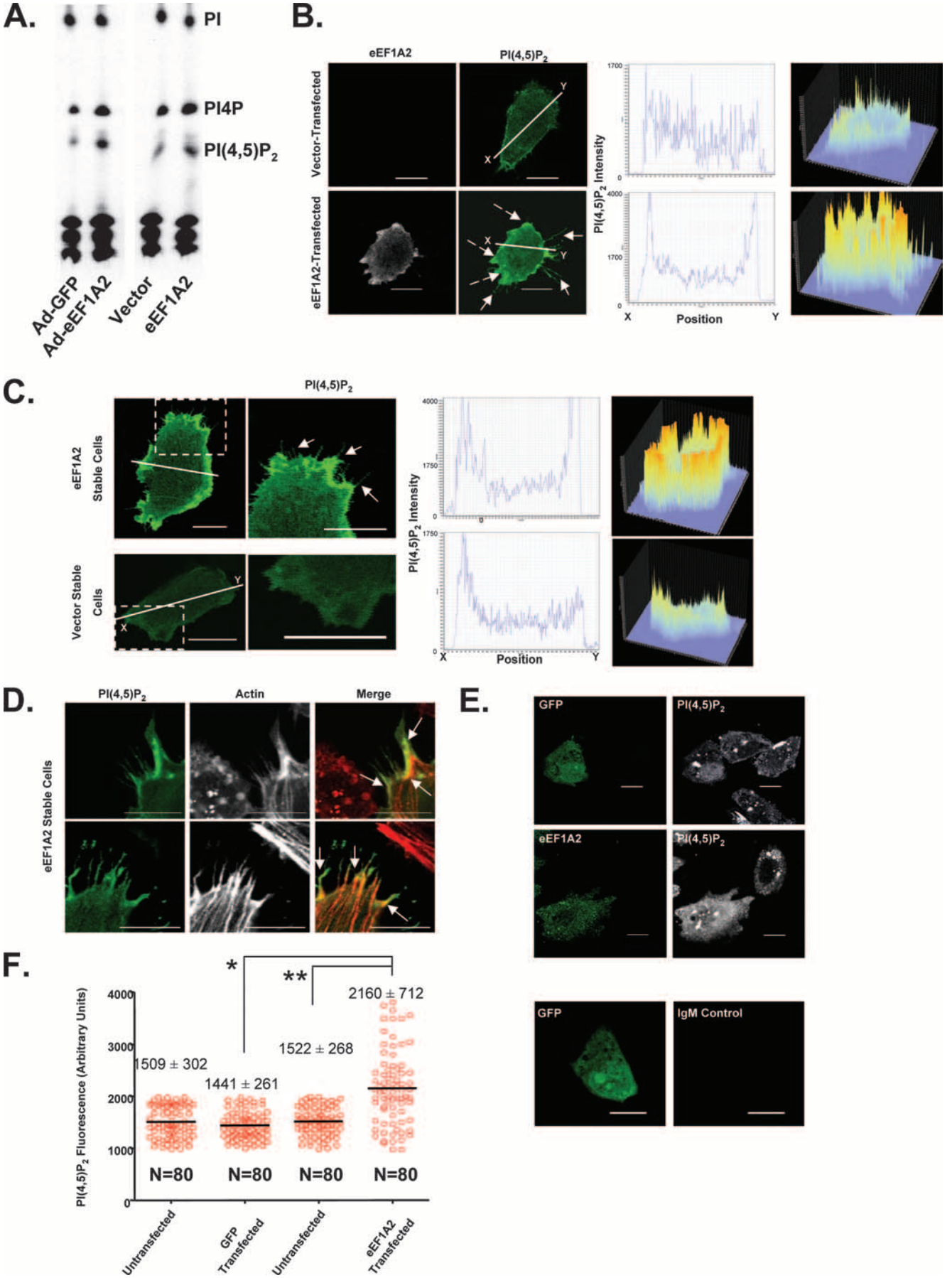
A.
PI
PI4P
PI(4,5)P2
Ad-GFP
Ad-eEF1A2
Vector
eEF1A2
B.
eEF1A2
PI(4,5)P2
Vector-Transfected
eEF1A2-Transfected
PI(4,5)P2 Intensity
Position
C.
PI(4,5)P2
eEF1A2 Stable Cells
Vector Stable Cells
PI(4,5)P2 Intensity
Position
D.
PI(4,5)P2
Actin
Merge
eEF1A2 Stable Cells
E.
GFP
PI(4,5)P2
eEF1A2
PI(4,5)P2
GFP
IgM Control
F.
PI(4,5)P2 Fluorescence (Arbitrary Units)
1509 ± 302
1441 ± 261
1522 ± 268
2160 ± 712
N=80
N=80
N=80
N=80
Untransfected
GFP Transfected
Untransfected
eEF1A2 Transfected

cells and 1.5-fold ± 0.2-fold in the eEF1A2 stable cell line) (Fig. 3A). Because Cdc42 cooperates with membrane-bound $PI(4,5)P_2$ during filopodium generation, we next investigated $PI(4,5)P_2$ localization in eEF1A2-expressing cells. To this end, cells were transfected with a fluorescent $PI(4,5)P_2$ reporter constructed from the fusion of the $PI(4,5)P_2$-binding pleckstrin homology (PH) domain of phospholipase C delta (PLCδ) and GFP as described previously (41). PLCδ-PH-GFP binds to membrane-bound $PI(4,5)P_2$. When Rat2 cells were cotransfected with eEF1A2 and PLCδ-PH-GFP, $PI(4,5)P_2$ was observed to be prominent at the cell membrane (Fig. 3B). The staining in eEF1A2-expressing cells was visibly thicker and more intense than that found in control cells transfected with an empty vector and the reporter. Furthermore, the ratio of the $PI(4,5)P_2$ staining in the membrane relative to that in the cytosol was greater in eEF1A2-expressing cells than in vector controls. A similar increase in membrane $PI(4,5)P_2$ staining was observed for cell lines stably expressing eEF1A2 (Fig. 3C). $PI(4,5)P_2$ can also be visualized within filopodium-like structures and at their bases (Fig. 3D). To further extend these studies, we used a $PI(4,5)P_2$ antibody to quantify cytosolic $PI(4,5)P_2$. This antibody does not detect $PI(4,5)P_2$ at the cell membrane. We transiently transfected Rat2 cells with either GFP or eEF1A2 and then stained fixed cells with this antibody (Fig. 3E). Cells transfected with eEF1A2 showed visibly more $PI(4,5)P_2$ staining than untransfected cells or those transfected with GFP. We quantified $PI(4,5)P_2$ fluorescence intensity in individual eEF1A2-transfected and -untransfected cells, as well as in GFP-transfected and -untransfected cells (Fig. 3F). $PI(4,5)P_2$ fluorescence intensity is significantly higher ($P < 0.0001$, Mann-Whitney U test) in eEF1A2-expressing cells (2,160 ± 712 fluorescence units) than in either untransfected (1,522 ± 268 fluorescence units) or GFP-transfected cells (1,441 ± 261 fluorescence units). Thus, eEF1A2 expression increases the abundance of both plasma membrane-bound and cytoplasmic $PI(4,5)P_2$.

eEF1A2-mediated formation of filopodia is dependent on $PI(4,5)P_2$. To determine whether the eEF1A2-mediated increase in $PI(4,5)P_2$ levels was necessary for production of filopodia, we used a rapamycin-inducible system to decrease membrane-bound $PI(4,5)P_2$. This system uses two plasmids, PM-FRB-CFP and mRFP-FKBP-5-ptase (42). The mRFP-FKBP-5-ptase contains the phosphoinositide-5 phosphatase domain of the inositol polyphosphate 5-phosphatase enzyme fused to the rapamycin-binding FKBP12 protein and the red fluorescent protein (mRFP). The PM-FRB-CFP is a fusion of the plasma membrane-bound FRB domain of mTOR (containing the palmitoylation sequence of the human GAP43 protein) and cyan fluorescent protein (CFP). Upon addition of rapamycin, mRFP-FKBP-5-ptase translocates to the membrane, where it heterodimerizes with the PM-FRB-CFP protein via the FRB domain. Once it is localized to the plasma membrane, the phosphatase in mRFP-FKBP-5-ptase depletes plasma membrane $PI(4,5)P_2$ by converting it to PI4P. We transfected Rat2 cells stably expressing eEF1A2 with these plasmids (Fig. 4A). In the presence of rapamycin, the eEF1A2-expressing cells transfected with PM-FRB-CFP and mRFP-FKBP-5-ptase show visibly decreased plasma membrane-bound $PI(4,5)P_2$ and a concomitant reduction in the number and length of filopodia relative to those of cells without rapamycin. Rapamycin treatment of eEF1A2-expressing cells without PM-FRB-CFP and mRFP-FKBP-5-ptase was unable to elicit changes in the appearance of filopodia or $PI(4,5)P_2$ membrane localization in eEF1A2-expressing cells (Fig. 4B). Therefore, the induction of filopodia by eEF1A2 is dependent on plasma membrane $PI(4,5)P_2$.

eEF1A2-mediated formation of filopodia is dependent on eEF1A2 interaction with PI4KIIIβ. Thus far, we have determined that eEF1A2 can increase $PI(4,5)P_2$ production and that membrane $PI(4,5)P_2$ is required for eEF1A2-mediated formation of filopodia. Because we have previously shown that eEF1A2 can increase the cellular pool of PI4P by binding to and activating PI4KIIIβ (21), we next investigated the role of PI4KIIIβ in eEF1A2-dependent $PI(4,5)P_2$ generation and production of filopodia. We first designed eEF1A2 variants that did not interact with PI4KIIIβ. Based on its homology with yeast and *Dictyostelium* eEF1A, the eEF1A2 protein contains domains for GTP binding, GTP hydrolysis, tRNA binding, and two putative actin binding domains (Fig. 5A). We generated mutants lacking amino acids 163 to 464, 321 to 464, and 1 to 320 (Δ163 to 464, Δ321 to 464, and Δ1 to 320) and tagged them with a C-terminal V5 epitope. We generated polyclonal cell lines expressing each of these proteins (protein expression levels in the polyclonal cell lines are shown in Fig. 5B). To determine which of these mutants interact with PI4KIIIβ, we performed coimmunoprecipitation assays with each of these cell lines. As shown in Fig. 5B, both the full-length eEF1A2

FIG. 3. eEF1A2 stimulates overall accumulation and membrane localization of $PI(4,5)P_2$. (A) TLC of labeled phosphatidylinositol from Rat2 cells transduced with either a GFP-adenovirus (Ad-GFP) or an eEF1A2-adenovirus (Ad-eEF1A2) or from vector only or eEF1A2-expressing stable cells. The TLC shown is a representative sample of three independent experiments. (B) Rat2 cells, transiently transfected with eEF1A2, show greater membrane-localized $PI(4,5)P_2$ fluorescence (dashed arrows) than vector-transfected cells. The first and second columns (at left) show eEF1A2 and $PI(4,5)P_2$ staining, respectively. The third column (middle) shows a cross-section of $PI(4,5)P_2$ fluorescence intensity along the white line indicated in the second column. The fourth column (at right) shows a three-dimensional (3D) representation of $PI(4,5)P_2$ staining in the entire cell. (C) eEF1A2-expressing Rat2 stable cells show greater membrane-bound $PI(4,5)P_2$ than vector stable cells. First and second columns (at left) show $PI(4,5)P_2$ staining. The third column (middle) shows a cross-section of $PI(4,5)P_2$ fluorescence intensity along the line indicated in the first column. The fourth column (at right) shows a 3D representation of the $PI(4,5)P_2$ staining pattern of cells seen in the first column. Filopodium-like structures are visible (solid arrows). (D) Colocalization of $PI(4,5)P_2$ and actin in eEF1A2-expressing Rat2 cells. Some colocalization is observed along the bases of the filopodia, as well as along the filopodia (arrows). (E) Rat2 cells transfected with either eEF1A2 or GFP, stained for eEF1A2 (green) or GFP (green) and for $PI(4,5)P_2$ (white). eEF1A2-transfected cells show more intense $PI(4,5)P_2$ staining than either GFP-transfected cells or untransfected control cells. The bottom two panels show a GFP-transfected cell stained with the IgM secondary antibody alone. (F) Quantification of the $PI(4,5)P_2$ fluorescence in the GFP control-transfected cells or the eEF1A2-transfected cells. Red circles represent fluorescence intensity in individual cells, with the means and standard deviations for each transfection condition indicated. eEF1A2-transfected cells have significantly more $PI(4,5)P_2$ fluorescence than controls (* and **, $P < 0.0001$, Mann-Whitney test). Scale bars represent 10 μm.

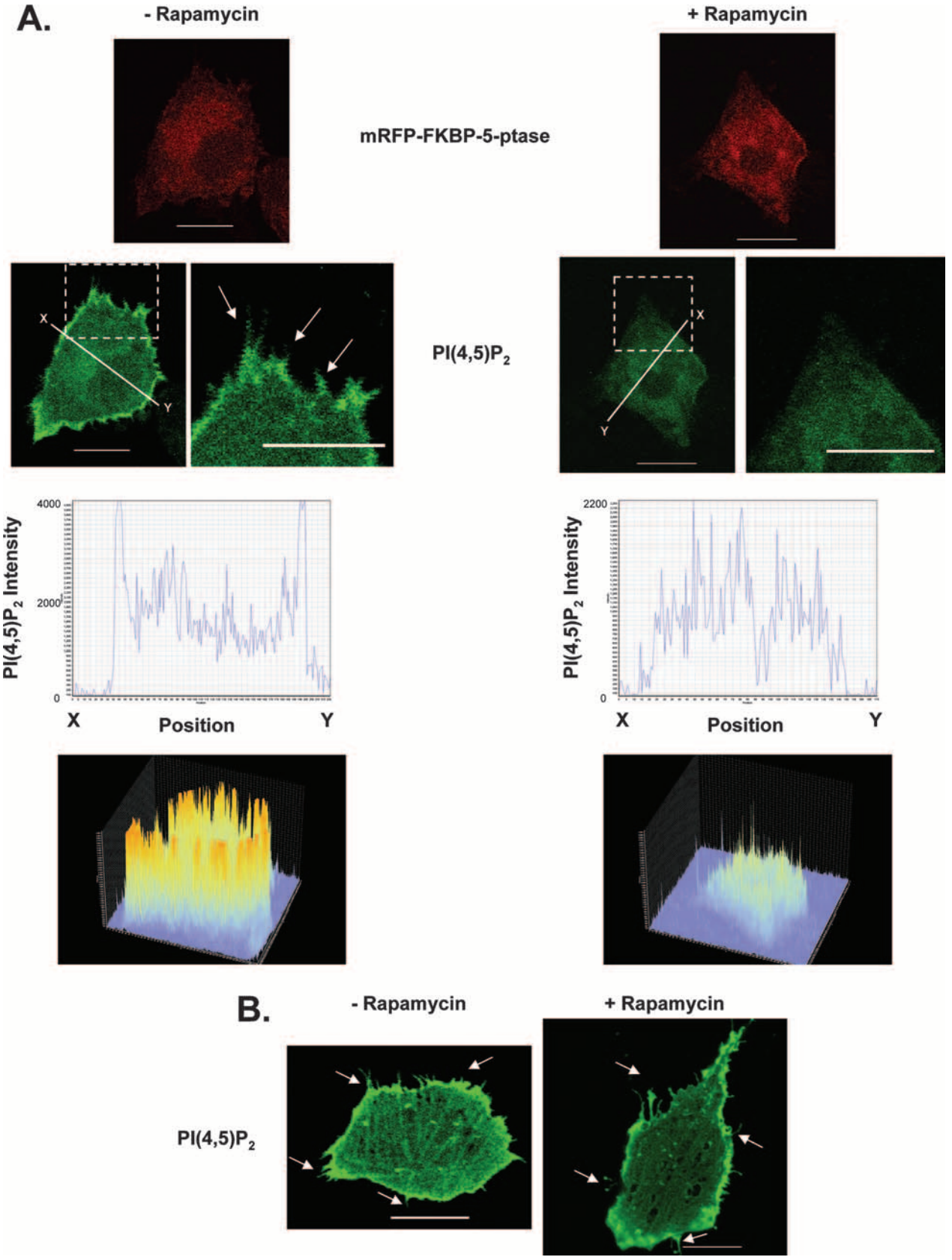

FIG. 4. eEF1A2-mediated formation of filopodia is dependent on $PI(4,5)P_2$. Rat2 cells stably expressing eEF1A2 were transfected with mRFP-FKBP-5-ptase, PM-FRB-CFP, and PLCδ-PH-GFP. (A) Addition of rapamycin (+Rapamycin) depletes the levels of membrane-bound $PI(4,5)P_2$ and reduces production of filopodia (arrows). (B) Addition of rapamycin, without mRFP-FKBP-5-ptase and PM-FRB-CFP, has no effect on eEF1A2-dependent $PI(4,5)P_2$ accumulation on the plasma membrane or on development of filopodia (arrows). Scale bars represent 10 μm.

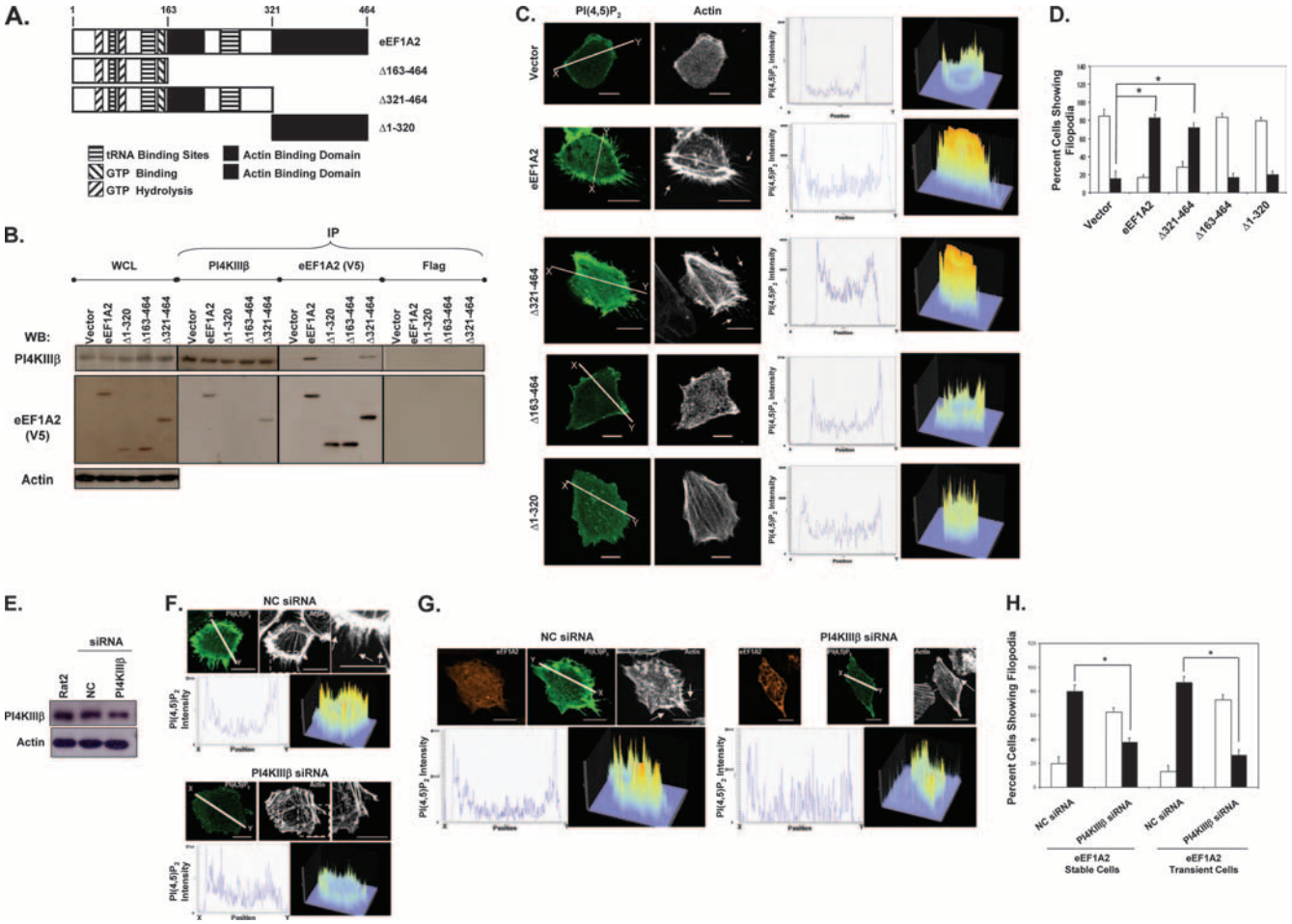

FIG. 5. eEF1A2-PI4KIIIβ interaction is necessary for eEF1A2-mediated development of filopodia. (A) Schematic domain map of eEF1A2 and the generated mutants. (B) Polyclonal cell lines expressing eEF1A2 or mutants were used for coprecipitation analysis with PI4KIIIβ. Whole-cell lysate (WCL) lanes indicate expression of PI4KIIIβ and eEF1A2 in the cell lines used. eEF1A2 is V5 tagged, and actin is used as a loading control. Reciprocal PI4KIIIβ and eEF1A2 coimmunoprecipitation proteins were detected by immunoprecipitation (IP) with the indicated antibody, followed by the indicated Western blotting antibody. No precipitation of either protein was detected using the Flag antibody control. The WCL lane contains 40 μg of total cellular protein, and each IP was performed using 250 μg of protein lysate. (C) eEF1A2 mutants that cannot bind PI4KIIIβ do not show increased membrane-bound PI(4,5)P_2 staining or any formation of filopodia. The first and second columns (at left) show PI(4,5)P_2 and actin staining, respectively. The third column (middle) shows a cross-section of PI(4,5)P_2 fluorescence intensity along the white line indicated in the first column. The fourth column (at right) shows a three-dimensional representation of PI(4,5)P_2 staining in the entire cell. (D) Quantification of filopodia (n = 142, 158, 132, 133, and 135 for vector, eEF1A2, Δ163-to-464, Δ1-to-320, and Δ321-to-464 stable cells, respectively). Filled columns indicate cells with at least 10 filopodia greater than or equal to 3 μm in length. Open columns indicate cells with any number of filopodia less than 3 μm in length. Significance ($P < 0.05$, Student's t test) is indicated by an asterisk. (E) Western blots showing downregulation of PI4KIIIβ in Rat2 cells using siRNA. (F) Downregulation of PI4KIIIβ in eEF1A2-expressing Rat2 stable cells leads to a decrease in membrane-bound PI(4,5)P_2 and a decrease in the number and length of filopodia. (G) Data shown are the same as in panel F, except Rat2 cells are transiently expressing eEF1A2. (H) Quantification of filopodia (n = 141, 157, 122, and 127 for negative control [NC; stable], PI4KIIIβ [stable], NC [transient], and PI4KIIIβ [transient], respectively). Filled columns indicate cells with at least 10 filopodia greater than or equal to 3 μm in length. Open columns indicate cells with any number of filopodia less than 3 μm in length. Significance ($P <$ 0.05, Student's t test) is indicated by an asterisk. Scale bars represent 10 μm.

and the Δ321-to-464 mutant bind to PI4KIIIβ, but the Δ163-to-464 and Δ1-to-320 mutants do not. Thus, a putative PI4KIIIβ interaction domain is likely contained within eEF1A2 residues 163 to 320.

We next investigated whether these eEF1A2 mutants were competent for increasing PI(4,5)P_2 or producing filopodia. As shown in Fig. 5C, both the full-length eEF1A2 and the Δ321-to-464 mutant activate production of filopodia and membrane PI(4,5)P2 accumulation, but the Δ163-to-464 and Δ1-to-320 mutants do not. Overall, the wild-type eEF1A2-expressing cells and the Δ321-to-464 mutant-expressing cells had a significant, ca. fourfold, increase ($P < 0.05$, Student's t test) in the number of cells showing filopodia greater than 3 μm in length (Fig. 5D). The Δ163-to-464 and Δ1-to-320 mutant-expressing cells were no different from vector controls with respect to filopodium appearance (Fig. 5D). Thus, eEF1A2 proteins that do not interact with PI4KIIIβ do not activate PI(4,5)P_2 production or generate filopodia.

To further study the requirement for PI4KIIIβ interaction in eEF1A2-medated formation of filopodia, we used siRNA to decrease PI4KIIIβ protein levels in Rat2 cells (Fig. 5E). The siRNA decreased PI4KIIIβ protein levels by ~60%. We transfected the

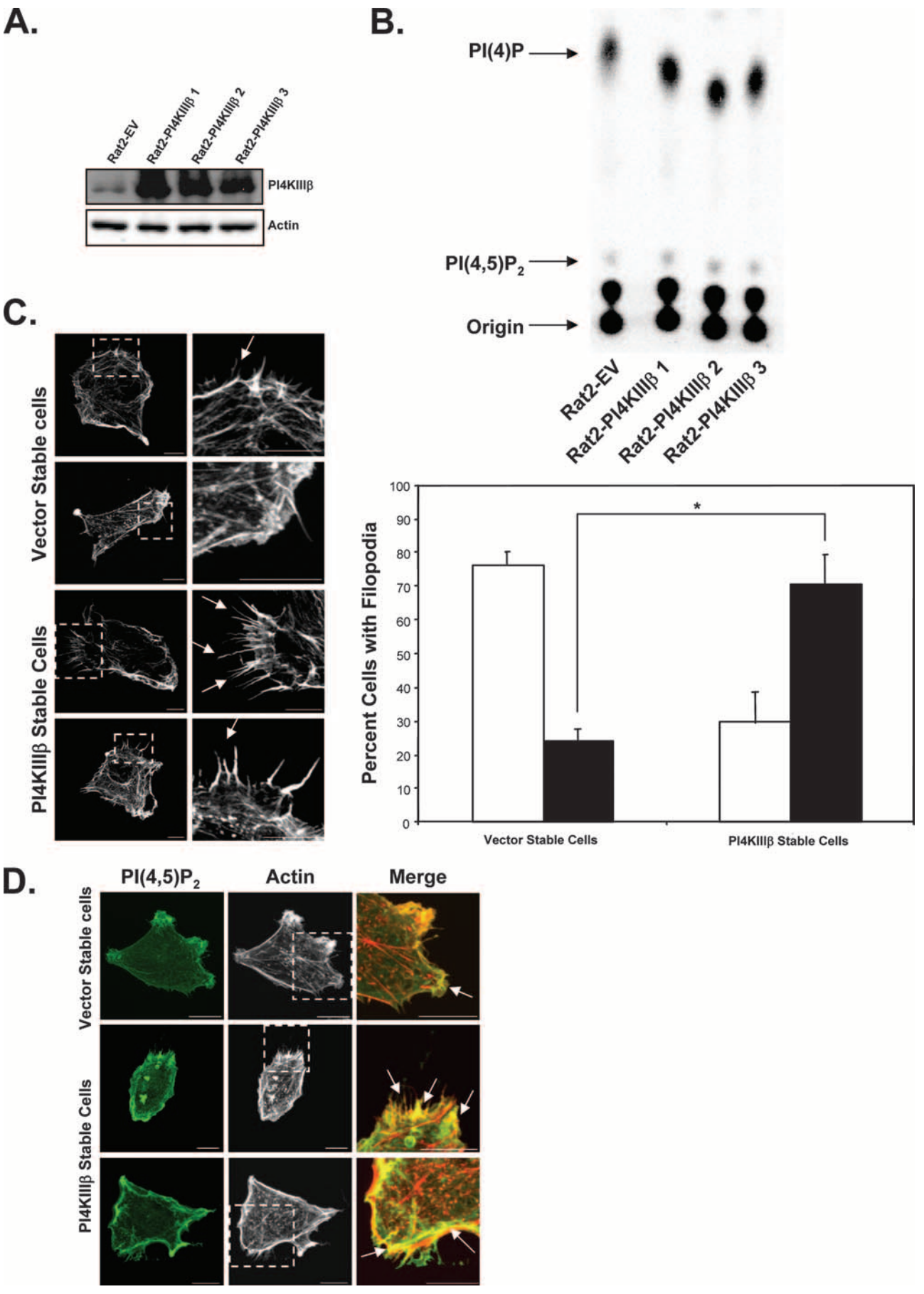
A.
Rat2-EV
Rat2-PI4KIIIβ 1
Rat2-PI4KIIIβ 2
Rat2-PI4KIIIβ 3
PI4KIIIβ
Actin
B.
PI(4)P
PI(4,5)P2
Origin
Rat2-EV
Rat2-PI4KIIIβ 1
Rat2-PI4KIIIβ 2
Rat2-PI4KIIIβ 3
C.
Vector Stable cells
PI4KIIIβ Stable Cells
Percent Cells with Filopodia
100
90
80
70
60
50
40
30
20
10
0
*
Vector Stable Cells
PI4KIIIβ Stable Cells
D.
PI(4,5)P2
Actin
Merge
Vector Stable cells
PI4KIIIβ Stable Cells

eEF1A2-expressing Rat2 stable cell lines with PLCδ-PH-GFP to visualize $PI(4,5)P_2$ production and either PI4KIIIβ or negative control siRNA (Fig. 5F). Cells with the PI4KIIIβ siRNA show a marked decrease in the intensity of $PI(4,5)P_2$ fluorescence relative to that of the control siRNA-treated cells. Importantly, the number of cells with filopodia was similarly decreased. This attenuation was not absolute, however, likely because some PI4KIIIβ was still present in the cells. To confirm these results, we repeated this experiment with Rat2 cells cotransfected with the wild-type eEF1A2 and the siRNAs (Fig. 5G). As with the eEF1A2 stable cell lines, eEF1A2-expressing cells transfected with PLCδ-PH-GFP and the PI4KIIIβ siRNA had decreased filopodia compared to those with the control siRNA. In general, eEF1A2-expressing cells with ablated PI4KIIIβ protein levels had a significant, two- to threefold, decrease ($P < 0.05$, Student's t test) in the number of cells with filopodia greater than 3 μm in length (Fig. 5H).

PI4KIIIβ is sufficient for the formation of filopodia. The data thus far suggest that PI4KIIIβ is necessary for eEF1A2-induced development of filopodia. We thus decided to determine whether PI4KIIIβ alone was sufficient to activate both the generation of $PI(4,5)P_2$ and the production of filopodia. We generated Rat2 cell lines that stably overexpressed PI4KIIIβ (Fig. 6A). These cells have an ~1.5-fold increase in PI4KIIIβ lipid kinase activity (Fig. 6B). Like eEF1A2-expressing cells, there is a significant, ca. fourfold, increase ($P < 0.05$, Student's t test) in the number of PI4KIIIβ-expressing cells with filopodia greater than 3 μm in length (Fig. 6C), as well as an increase in membrane-bound $PI(4,5)P_2$ staining compared to that of vector controls (Fig. 6D). The $PI(4,5)P_2$ also shows some degree of colocalization with the actin in the filopodia (Fig. 6D). PI4KIIIβ has previously been reported to be enriched in the trans-Golgi apparatus network and to have roles in vesicular trafficking (16, 30, 44). However, we have observed no visible changes in Golgi apparatus appearance in cells ectopically expressing eEF1A2 or PI4KIIIβ (not shown). Taken together, these results indicate that PI4KIIIβ is sufficient to increase $PI(4,5)P_2$ levels and activate the development of filopodia.

DISCUSSION

eEF1A2 is a transforming gene, highly expressed in ~50% of breast, ovarian, and lung tumors (2, 24, 24a, 25, 40). eEF1A2 expression also stimulates actin remodeling and cell invasion and migration (1). Here, we propose a pathway of actin remodeling in which eEF1A2 stimulates the extrusion of filopodia through PI4KIIIβ and PI4KIIIβ-mediated accumulation of $PI(4,5)P_2$. This leads to filopodium creation through a Cdc42-dependent pathway. We also identify a region within the eEF1A2 protein that is necessary for its interaction with PI4KIIIβ.

We have previously found that eEF1A2 increases cellular PI4P abundance in a PI4KIIIβ-dependent manner (21). Here we report that eEF1A2 expression increases $PI(4,5)P_2$ abundance as well. eEF1A2 mutants that are unable to interact with PI4KIIIβ activate neither the generation of $PI(4,5)P_2$ nor the production of filopodia. Furthermore, PI4KIIIβ RNA interference (RNAi) ablation attenuates the eEF1A2-mediated increase in $PI(4,5)P_2$ abundance, and PI4KIIIβ expression is sufficient to increase $PI(4,5)P_2$ levels at both the cytosol and the cell membrane. The simplest interpretation of these findings is that the increased $PI(4,5)P_2$ abundance upon eEF1A2 expression is a direct consequence of the larger PI4P precursor pool created by PI4KIIIβ activation. The K_m of mammalian PI4P5 kinases, the enzymes responsible for converting PI4P to $PI(4,5)P_2$, are in the 10 to 45 μM range (20). Thus, an increase in PI4P concentration will stimulate $PI(4,5)P_2$ accumulation wherever PI4P concentrations are in the magnitude of 10 μM or less. In eukaryotic cells, phosphatidylinositol concentrations range from 0.5 to 2.5 μmol/g (31), with an overall concentration of ~10 to 500 pM in cells with a volume range of 500 to 3,000 μm^3 (10). PI4P comprises ~10 to 20% of total phosphatidylinositol, suggesting that the overall cellular PI4P abundance is in the 1 to 100 pM range. However, plasma membrane concentrations of PI4P may be much higher. Stephens et al., for example, estimated that PI4P concentrations in the inner plasma membranes of unstimulated neutrophils approach 3 mM (38). Here, we find that eEF1A2 expression doubles both the total cellular PI4P and the $PI(4,5)P_2$ abundance in cells. Furthermore, increased levels of $PI(4,5)P_2$ are distributed along the plasma membrane, as well as in the cytoplasm. In vitro, purified eEF1A2 doubles the V_{max} of recombinant PI4KIIIβ (21). Thus, PI4P concentration is likely to be limiting in the generation of $PI(4,5)P_2$ in our cell lines. Broadly consistent with this idea, previous reports have suggested the existence of an intracellular pool of $PI(4,5)P_2$ in mammalian cells that was under the control of a wortmannin-sensitive PI4 kinase (32), later identified as PI4KIIIβ (6).

The mechanism of PI4KIIIβ activation by eEF1A2 is unknown. Because purified eEF1A2 increases the lipid kinase activity of PI4KIIIβ in vitro, it is likely that eEF1A2 induces a conformational change in PI4KIIIβ that increases its activity. The small GTPase Ras activates PI3K via a change in conformation, so this method of activation is not unprecedented (33). We have mapped the residues necessary for eEF1A2-PI4KIIIβ interaction to amino acid residues 163 to 320. It is likely that amino acid residues therein are likely to directly bind PI4KIIIβ

FIG. 6. PI4KIIIβ is sufficient to induce production of filopodia. (A) Western blots showing PI4KIIIβ overexpression in Rat2 stable cell lines. (B) Rat2 cells stably overexpressing PI4KIIIβ have greater PI4KIIIβ lipid kinase activity, as seen by an increase in the PI4P product. The TLC is a representative sample of three independent in vitro kinase assays. (C) Left panels, PI4KIIIβ-overexpressing Rat2 stable cells show more and longer filopodia than vector controls. Right panels, quantification of filopodia ($n = 134$ and 118 for vector stable cells and PI4KIIIβ stable cells, respectively). Filled columns indicate cells with at least 10 filopodia greater than or equal to 3 μm in length. Open columns indicate cells with any number of filopodia less than 3 μm in length. Significance ($P < 0.05$, Student's t test) is indicated by an asterisk. (D) PI4KIIIβ-overexpressing Rat2 stable cells show more membrane-bound $PI(4,5)P_2$ than control cells. The $PI(4,5)P_2$ localizes to the plasma membrane as well as to parts of filopodia. Scale bars represent 10 μm.

and induce an as-yet-uncharacterized structural change in the protein that stimulates kinase activity.

The eEF1A2 protein is diffusely cytoplasmic (21, 24), whereas PI4KIIIβ is localized largely in the Golgi apparatus (3, 16, 44, 45). Thus, it was somewhat of a surprise to us that PI4KIIIβ can stimulate plasma membrane $PI(4,5)P_2$ accumulation and activate the generation of filopodia there. Inactivation of PI4KIIIβ in both yeast and mammalian cells impairs Golgi structure and function (11, 16, 43). However we have not observed gross Golgi apparatus abnormalities in eEF1A2- or PI4KIIIβ-overexpressing cells (not shown). Furthermore, the increased cytosolic $PI(4,5)P_2$ accumulation we observed with the $PI(4,5)P_2$ antibody did not appear to be like the distribution observed for the Golgi apparatus. Since eEF1A2 or PI4KIIIβ expression stimulates production of filopodia, we favor the idea that the $PI(4,5)P_2$ generated upon eEF1A2 or PI4KIIIβ expression has primary importance at the cell membrane. eEF1A2-PI4KIIIβ interaction, mediated through amino acid residues 163 to 320 in eEF1A2, and activation could occur on organelle membranes in the cytosol. The resulting PI4P would then be shuttled rapidly to the plasma membrane to generate filopodia. It may even be possible that the PI4P is converted to $PI(4,5)P_2$, coincident with its transport to the plasma membrane. This scenario may explain why we observed a general increase in overall membrane-bound $PI(4,5)P_2$ levels and not distinct pools of the lipid on the membrane. PI4KIIIβ's ability to affect the plasma membrane may not require substantial localization of the protein there. For example, PI4KIIIα is localized primarily to the endoplasmic reticulum in mammalian cells (8, 45), but it controls plasma membrane PI4P levels (5) and is part of the P2X7 ion channel (22). Thus, the interaction between eEF1A2 and PI4KIIIβ could occur away from the plasma membrane, even though the $PI(4,5)P_2$ generated would be functional there. Alternatively, while eEF1A2 and PI4KIIIβ proteins are found in the cytoplasm, the interaction and activation of the kinase may occur transiently, near the plasma membrane.

While we propose that eEF1A2-mediated activation of PI4KIIIβ leads to $PI(4,5)P_2$ accumulation due to a larger PI4P substrate pool, other possibilities do exist. For example, PI4P could also be activating PTEN, the 5′-phosphatase responsible for converting $PI(3,4,5)P_3$ to $PI(4,5)P_2$, thereby increasing $PI(4,5)P_2$ abundance. Alternatively, PI4P could be directly activating a PI4P5K. Monophosphoinositide can influence the activity of other proteins involved in bi-PI and tri-PI generation. For example, Pendaries et al. have recently reported that an increase in cellular PI5P levels upon *Shigella flexneri* infection leads to the activation of a class 1A PI3-kinase, resulting in an increased level of active Akt, a downstream target of PI3-kinase (34a). Thus, it is possible that the generated pool of PI4P could be indirectly regulating $PI(4,5)P_2$ levels.

We have previously reported that eEF1A2 expression can cause activation of the Akt serine threonine kinase (1). The Akt/PKB is a regulator of cell proliferation, insulin responsiveness, and apoptosis (27, 34). Akt activation is dependent, in major part, on plasma membrane levels of $PI(3,4,5)P_3$. The mechanism by which eEF1A2 activates Akt is currently unknown, but we speculate that eEF1A2 activates Akt indirectly, since we have been unable to coimmunoprecipitate or colocalize eEF1A2 with Akt (not shown). We hypothesize that eEF1A2 can increase membrane abundance of $PI(3,4,5)P_3$ in the same manner that it does with $PI(4,5)P_2$.

The ability of PI4KIIIβ to increase production of filopodia also suggests that transcriptional or posttranscriptional control of PI4KIIIβ abundance could be an important facet of both actin remodeling and PI signaling control. To the best of our knowledge, however, no extracellular stimulus is known to increase the abundance of PI4KIIIβ message or protein. It is also unclear whether the ability of eEF1A2 to activate PI4KIIIβ and PI signaling contributes to its ability to transform cells in vitro or to enhance their tumorigenicity. Moreover, eEF1A2 might have effects on other aspects of cell physiology that depend on $PI(4,5)P_2$. For example, hydrolysis of $PI(4,5)P_2$ by phospholipase C yields diacylglycerol and inositol trisphosphate (IP_3). IP_3 is known to release calcium from its storage pools in the endoplasmic reticulum (15). Similarly, $PI(4,5)P_2$ is known to mediate endocytosis/exocytosis and vesicular transport (42). Thus, eEF1A2 could have multiple effects on plasma membrane physiology.

There may be other pathways of eEF1A2-dependent actin remodeling; for example, purified eEF1A proteins bundle actin in vitro, and in *Dictyostelium* sp. they become localized in filopodia extended in response to cyclic AMP stimulation (7a, 7b). This suggests that direct actin bundling by eEF1A2 could also contribute to filopodium production. The localization of eEF1A2 to filopodium bases and within filopodia suggests that both actin bundling and phospholipid regulation may contribute to actin remodeling.

In summary, we have shown that eEF1A2 regulates the formation of filopodia through the binding and activation of PI4KIIIβ. This activation is required to generate a pool of cytosolic and membrane-bound $PI(4,5)P_2$. The membrane $PI(4,5)P_2$ then induces formation of filopodia through a Cdc42-dependent mechanism(s). Moreover, we also show that PI4KIIIβ itself can regulate formation of filopodia, a novel function for this enzyme. This work provides additional evidence for the link between protein translation, phosphatidylinositol signaling, actin remodeling, and oncogenesis.

ACKNOWLEDGMENTS

We thank Heidi McBride, Dixie Pinke, Sanaa Noubir, and Zemin Yao for helpful discussions and critical review of the manuscript. We thank Heidi McBride and Astrid Schauss for use of and assistance with confocal microscopy. We thank T. Balla for the generous gift of many plasmids.

S.J. is supported by a studentship from the CIHR Institute of Gender and Health and the Ontario Women's Health Council. This work was supported by grants from the National Cancer Institute of Canada and by funds from the Canadian Cancer Society and the Canadian Institutes of Health Research.

REFERENCES

1. **Amiri, A., F. Noei, S. Jeganathan, G. Kulkarni, D. E. Pinke, and J. M. Lee.** 2007. eEF1A2 activates Akt and stimulates Akt-dependent actin remodeling, invasion and migration. Oncogene **26:**3027–3040.
2. **Anand, N., S. Murthy, G. Amann, M. Wernick, L. A. Porter, I. H. Cukier, C. Collins, J. W. Gray, J. Diebold, D. J. Demetrick, and J. M. Lee.** 2002. Protein elongation factor EEF1A2 is a putative oncogene in ovarian cancer. Nat. Genet. **31:**301–305.
3. **Balla, A., G. Vereb, H. Gulkan, T. Gehrmann, P. Gergely, L. M. Heilmeyer, Jr., and M. Antal.** 2000. Immunohistochemical localisation of two phosphatidylinositol 4-kinase isoforms, PI4K230 and PI4K92, in the central nervous system of rats. Exp. Brain Res. **134:**279–288.
4. **Balla, T.** 2005. Inositol-lipid binding motifs: signal integrators through protein-lipid and protein-protein interactions. J. Cell Sci. **118:**2093–2104.

5. **Balla, T.** 1998. Phosphatidylinositol 4-kinases. Biochim. Biophys. Acta **1436:** 69–85.
6. **Balla, T., G. J. Downing, H. Jaffe, S. Kim, A. Zolyomi, and K. J. Catt.** 1997. Isolation and molecular cloning of wortmannin-sensitive bovine type III phosphatidylinositol 4-kinases. J. Biol. Chem. **272:**18358–18366.
7. **Chambers, D. M., J. Peters, and C. M. Abbott.** 1998. The lethal mutation of the mouse wasted (wst) is a deletion that abolishes expression of a tissue-specific isoform of translation elongation factor 1alpha, encoded by the Eef1a2 gene. Proc. Natl. Acad. Sci. USA **95:**4463–4468.

7a. **Condeelis, J.** 1995. Elongation factor 1 alpha, translation and the cytoskeleton. Trends Biochem. Sci. **20:**169–170.

7b. **Dharmawardhane, S., M. Demma, F. Yang, and J. Condeelis.** 1991. Compartmentalization and actin binding properties of ABP-50: the elongation factor-1 alpha of Dictyostelium. Cell Motil. Cytoskeleton **20:**279–288.

8. **Ekblad, L., and B. Jergil.** 2001. Localization of phosphatidylinositol 4-kinase isoenzymes in rat liver plasma membrane domains. Biochim. Biophys. Acta **1531:**209–221.
9. **Faix, J., and K. Rottner.** 2006. The making of filopodia. Curr. Opin. Cell Biol. **18:**18–25.
10. **Frame, K. K., and W.-S. Hu.** 1990. Cell volume measurement as an estimation of mammalian cell biomass. Biotechnol. Bioeng. **36:**191–197.
11. **Godi, A., A. Di Campli, A. Konstantakopoulos, G. Di Tullio, D. R. Alessi, G. S. Kular, T. Daniele, P. Marra, J. M. Lucocq, and M. A. De Matteis.** 2004. FAPPs control Golgi-to-cell-surface membrane traffic by binding to ARF and PtdIns(4)P. Nat. Cell Biol. **6:**393–404.
12. **Grignani, F., T. Kinsella, A. Mencarelli, M. Valtieri, D. Riganelli, F. Grignani, L. Lanfrancone, C. Peschle, G. P. Nolan, and P. G. Pelicci.** 1998. High-efficiency gene transfer and selection of human hematopoietic progenitor cells with a hybrid EBV/retroviral vector expressing the green fluorescence protein. Cancer Res. **58:**14–19.
13. **Gupton, S. L., and F. B. Gertler.** 2007. Filopodia: the fingers that do the walking. Sci. STKE **2007:**re5.
14. **Hansson, M. D., K. Rzeznicka, M. Rosenback, M. Hansson, and N. Sirijovski.** 2008. PCR-mediated deletion of plasmid DNA. Anal. Biochem. **375:**373–375.
15. **Haucke, V.** 2005. Phosphoinositide regulation of clathrin-mediated endocytosis. Biochem. Soc. Trans. **33:**1285–1289.
16. **Hausser, A., P. Storz, S. Martens, G. Link, A. Toker, and K. Pfizenmaier.** 2005. Protein kinase D regulates vesicular transport by phosphorylating and activating phosphatidylinositol-4 kinase IIIbeta at the Golgi complex. Nat. Cell Biol. **7:**880–886.
17. **Heilmeyer, L. M., Jr., G. Vereb, Jr., G. Vereb, A. Kakuk, and I. Szivak.** 2003. Mammalian phosphatidylinositol 4-kinases. IUBMB Life **55:**59–65.
18. **Hershey, J. W.** 1991. Translational control in mammalian cells. Annu. Rev. Biochem. **60:**717–755.
19. **Higgs, H. N., and T. D. Pollard.** 2001. Regulation of actin filament network formation through ARP2/3 complex: activation by a diverse array of proteins. Annu. Rev. Biochem. **70:**649–676.
20. **Ishihara, H., Y. Shibasaki, N. Kizuki, T. Wada, Y. Yazaki, T. Asano, and Y. Oka.** 1998. Type I phosphatidylinositol-4-phosphate 5-kinases. Cloning of the third isoform and deletion/substitution analysis of members of this novel lipid kinase family. J. Biol. Chem. **273:**8741–8748.
21. **Jeganathan, S., and J. M. Lee.** 2007. Binding of elongation factor eEF1A2 to phosphatidylinositol 4-kinase beta stimulates lipid kinase activity and phosphatidylinositol 4-phosphate generation. J. Biol. Chem. **282:**372–380.
22. **Kim, M., L. H. Jiang, H. L. Wilson, R. A. North, and A. Surprenant.** 2001. Proteomic and functional evidence for a P2X7 receptor signalling complex. EMBO J. **20:**6347–6358.
23. **Kozma, R., S. Ahmed, A. Best, and L. Lim.** 1995. The Ras-related protein Cdc42Hs and bradykinin promote formation of peripheral actin microspikes and filopodia in Swiss 3T3 fibroblasts. Mol. Cell. Biol. **15:**1942–1952.
24. **Kulkarni, G., D. A. Turbin, A. Amiri, S. Jeganathan, M. A. Andrade-Navarro, T. D. Wu, D. G. Huntsman, and J. M. Lee.** 2007. Expression of protein elongation factor eEF1A2 predicts favorable outcome in breast cancer. Breast Cancer Res. Treat. **102:**31–41.

24a. **Lee, J. M.** 2003. The role of protein elongation factor eEF1A2 in ovarian cancer. Reprod. Biol. Endocrinol. **1:**69.

24b. **Lee, S., L. A. Wolfraim, and E. Wang.** 1993. Differential expression of S1 and elongation factor-1 alpha during rat development. J. Biol. Chem. **268:**24453–24459.

25. **Li, R., H. Wang, B. N. Bekele, Z. Yin, N. P. Caraway, R. L. Katz, S. A. Stass, and F. Jiang.** 2006. Identification of putative oncogenes in lung adenocarcinoma by a comprehensive functional genomic approach. Oncogene **25:** 2628–2635.
26. **Lidke, D. S., K. A. Lidke, B. Rieger, T. M. Jovin, and D. J. Arndt-Jovin.** 2005. Reaching out for signals: filopodia sense EGF and respond by directed retrograde transport of activated receptors. J. Cell Biol. **170:**619–626.
27. **LoPiccolo, J., C. A. Granville, J. J. Gills, and P. A. Dennis.** 2007. Targeting Akt in cancer therapy. Anticancer Drugs **18:**861–874.
28. **Lund, A., S. M. Knudsen, H. Vissing, B. Clark, and N. Tommerup.** 1996. Assignment of human elongation factor 1alpha genes: EEF1A maps to chromosome 6q14 and EEF1A2 to 20q13.3. Genomics **36:**359–361.
29. **McLaughlin, S., and D. Murray.** 2005. Plasma membrane phosphoinositide organization by protein electrostatics. Nature **438:**605–611.
30. **Meyers, R., and L. C. Cantley.** 1997. Cloning and characterization of a wortmannin-sensitive human phosphatidylinositol 4-kinase. J. Biol. Chem. **272:**4384–4390.
31. **Michell, R. H.** 1975. Inositol phospholipids and cell surface receptor function. Biochim. Biophys. Acta **415:**81–147.
32. **Nakanishi, S., K. J. Catt, and T. Balla.** 1995. A wortmannin-sensitive phosphatidylinositol 4-kinase that regulates hormone-sensitive pools of inositolphospholipids. Proc. Natl. Acad. Sci. USA **92:**5317–5321.
33. **Pacold, M. E., S. Suire, O. Perisic, S. Lara-Gonzalez, C. T. Davis, E. H. Walker, P. T. Hawkins, L. Stephens, J. F. Eccleston, and R. L. Williams.** 2000. Crystal structure and functional analysis of Ras binding to its effector phosphoinositide 3-kinase gamma. Cell **103:**931–943.
34. **Parcellier, A., L. A. Tintignac, E. Zhuravleva, and B. A. Hemmings.** 2007. PKB and the mitochondria: AKTing on apoptosis. Cell Signal. **20:**21–30.

34a. **Pendaries, C., H. Tronchere, L. Arbibe, J. Mounier, O. Gozani, L. Cantley, M. J. Fry, F. Gaits-Iacovoni, P. J. Sansonetti, and B. Payrastre.** 2006. PtdIns(5)P activates the host cell PI3-kinase/Akt pathway during Shigella flexneri infection. Embo J. **25:**1024–1034.

35. **Potter, M., A. Bernstein, and J. M. Lee.** 1998. The wst gene regulates multiple forms of thymocyte apoptosis. Cell Immunol. **188:**111–117.
36. **Shultz, L. D., H. O. Sweet, M. T. Davisson, and D. R. Coman.** 1982. "Wasted", a new mutant of the mouse with abnormalities characteristic to ataxia telangiectasia. Nature **297:**402–404.
37. **Steketee, M. B., and K. W. Tosney.** 2002. Three functionally distinct adhesions in filopodia: shaft adhesions control lamellar extension. J. Neurosci. **22:**8071–8083.
38. **Stephens, L. R., T. R. Jackson, and P. T. Hawkins.** 1993. Agonist-stimulated synthesis of phosphatidylinositol(3,4,5)-trisphosphate: a new intracellular signalling system? Biochim. Biophys. Acta **1179:**27–75.
39. **Subauste, M. C., M. Von Herrath, V. Benard, C. E. Chamberlain, T. H. Chuang, K. Chu, G. M. Bokoch, and K. M. Hahn.** 2000. Rho family proteins modulate rapid apoptosis induced by cytotoxic T lymphocytes and Fas. J. Biol. Chem. **275:**9725–9733.
40. **Tomlinson, V. A., H. J. Newbery, N. R. Wray, J. Jackson, A. Larionov, W. R. Miller, J. M. Dixon, and C. M. Abbott.** 2005. Translation elongation factor eEF1A2 is a potential oncoprotein that is overexpressed in two-thirds of breast tumours. BMC Cancer **5:**113.
41. **Varnai, P., X. Lin, S. B. Lee, G. Tuymetova, T. Bondeva, A. Spat, S. G. Rhee, G. Hajnoczky, and T. Balla.** 2002. Inositol lipid binding and membrane localization of isolated pleckstrin homology (PH) domains. Studies on the PH domains of phospholipase C delta 1 and p130. J. Biol. Chem. **277:**27412–27422.
42. **Varnai, P., B. Thyagarajan, T. Rohacs, and T. Balla.** 2006. Rapidly inducible changes in phosphatidylinositol 4,5-bisphosphate levels influence multiple regulatory functions of the lipid in intact living cells. J. Cell Biol. **175:**377–382.
43. **Walch-Solimena, C., and P. Novick.** 1999. The yeast phosphatidylinositol-4-OH kinase pik1 regulates secretion at the Golgi. Nat. Cell Biol. **1:**523–525.
44. **Weixel, K. M., A. Blumental-Perry, S. C. Watkins, M. Aridor, and O. A. Weisz.** 2005. Distinct Golgi populations of phosphatidylinositol 4-phosphate regulated by phosphatidylinositol 4-kinases. J. Biol. Chem. **280:**10501–10508.
45. **Wong, K., R. Meyers dd, and L. C. Cantley.** 1997. Subcellular locations of phosphatidylinositol 4-kinase isoforms. J. Biol. Chem. **272:**13236–13241.

APPENDIX B: CURRICULUM VITAE

Anne A. Morrow

SUMMARY OF QUALIFICATIONS

- Currently completing a Ph.D. in Biochemistry at the University of Ottawa in cancer research
- Experience in project management, including: establishing goals, priorities, deadlines and managing towards expected outcomes
- Experience collecting, analyzing and reporting on quantitative and qualitative data
- Experience in database creation and statistical analysis
- Experience writing reports and research articles
- Experience in science youth outreach
- Experience teaching scientific concepts and laboratory techniques to students at the university, high school and elementary school level
- Strong organizational, time management and multitasking skills
- Ability to work under pressure of deadlines and changing priorities with little or no supervision
- Advanced knowledge of Microsoft Word, Excel, PowerPoint, Outlook and Adobe Creative Suites Software
- Ability to communicate effectively orally and in writing in both English and French

EDUCATION

Ph.D. candidate - Department of Biochemistry **2008-2013**
University of Ottawa, ON
Supervisor: Dr. Jonathan Lee

M.Sc. candidate - Department of Biochemistry **2006-2008**
University of Ottawa, ON
Supervisor: Dr. Jonathan Lee
*Transferred directly into the PhD program

B.Sc. (Honours) - Department of Biochemistry **2002-2006**
University of Ottawa, ON; Graduated Magna Cum Laude

AWARDS, DISTINCTIONS AND SCHOLARSHIPS

Tuition Fee Scholarship **2012-2013**
University of Ottawa

Canada Graduate Scholarships Doctoral Award **2009-2012**
Canadian Institutes of Health Research (CIHR)

Excellence Scholarship **2008-2012**
University of Ottawa

1st Place - Graduate Student Symposium **2010**
Department of Biochemistry, University of Ottawa

Awarded Teaching Assistant of the Year **2009**
University of Ottawa

Ontario Graduate Scholarship (OGS) **2008-2009**
Goverment of Ontario

1st Place - Graduate Student Poster Day **2007**
Department of Biochemistry, University of Ottawa

Admission Scholarship **2006-2008**
University of Ottawa

Dean's Honour List Merit Scholarship **2004-2005**
University of Ottawa

RESEARCH AND WORK EXPERIENCE

Graduate Researcher **2006-Present**
Department of Biochemistry, University of Ottawa, ON

- Managed research goals, planning of research methodology, collection and analysis of data
- Experience in data entry, database creation and statistical analysis
- Responsible for writing manuscripts/reports and presenting research topics
- Assisted in the project planning and supervision of trainees' research projects
- Sought out and maintained collaborations with other science researchers
- Applied to and won two graduate research funding awards
- Technical research experience:
  Nucleic acid and protein extraction and analysis • Western blot • Immunocytochemistry • ELISA • Mammalian cell culture • Cell transformation, transfection and infection • PCR and cloning procedures • Gene and protein engineering • Fluorometric assays • Kinase assays

Teaching Assistant **2006-2013**
Faculty of Science, University of Ottawa, ON

- Trained university students in laboratory techniques and report writing
- Lectured on class material
- Communicated feedback on student's progress (evaluated reports and exams)
- Adapted to different learning styles
- Motivated students with a professional and dynamic attitude

Enrichment Mini-Course Teacher **2013**
Faculty of Science, University of Ottawa, ON

- Taught middle school and high school students
- Lectured on scientific concepts and trained students in laboratory techniques
- Mentored students interested in pursuing a science education
- Used vocabulary appropriate to the audience

Synapse Educator/Facilitator **2011**
Canadian Institutes of Health Research (CIHR), Ottawa, ON

- Worked as a member of CIHR's health research outreach program aimed at high school students
- Operated CIHR's youth outreach booth at regional high school science fairs
- Presented CIHR's mandate to visitors and promoted CIHR-funded science research
- Ecouraged youth interest in science research

Let's Talk Science (Volunteer) - Mentor **2006-2008/2011-2012**
Ottawa, ON

- Participated as a mentor in this science outreach program
- Prepared activities/presentations to spark elementary and high school students interest in science
- Judged high school science fairs

Assistant Coordinator of the Study Group Program **2005-2006**
Student Academic Success Services, University of Ottawa, ON

- Assisted in overseeing the running of the Residence Study Group Program aimed at helping first year university students academically
- Led study groups in chemistry and calculus: helping explain key course concepts and teach study skills
- Assisted in the hiring and training of new study group leaders
- Assisted in running weekly team leader meetings

Federal Election Employee **2004**
Elections Canada - St.Paul's riding, Toronto, ON

- Receptionist at central office: telephone/front desk reception; filing/database and records management
- Central Poll Supervisor on election day: oversaw the running of seven polling stations

PUBLICATIONS

1. **Morrow, A.A.**, Alipour, M.A., Bridges, D., Yao, Z. Saltiel, A. and J.M. Lee. 2013. Elevated expression of PI4KIIIβ in breast cancer leads to Akt activation. *In preparation for submission.*
2. Nilufar, S., **Morrow, A.A.**, Jonathan, J.M. and Perkins, T.J. 2013. FiloDetect: Automatic detection of filopodia from fluorescence microscopy images. *BMC Syst Biol*. 7:66
3. Husainy, A.N., **Morrow, A.A.**, Perkins, T.J. and J. M. Lee. 2010. Robust patterns in the stochastic organization of filopodia. *BMC Cell Biology*. 11:86
4. Jeganathan, S., **Morrow, A,** Amiri, A. and J.M. Lee. 2008. Elongation factor eEF1A2 cooperates with phosphatidylinositol-4 kinase IIIβ to stimulate PI(4,5)P_2 generation and filopodia production. *Mol. Cell. Biol.* 28:4549-61

CONFERENCES ATTENDED

Keystone Symposium on Inositide Signaling in Pharmacology and Disease **2011**
Denver, CO, USA

- Research poster presented: PI4KIIIβ regulates Akt activation

Gordon Conference on the Molecular and Cellular Biology of Lipids **2009**
Waterford Valley, MA, USA

- Research poster presented: PI4KIII beta regulates AKT activation by regulating the generation of a plasma membrane pool of PtdIns(3,4,5)P_3

SKILLS AND ABILITIES

- Strong analytical and problem solving skills
- Ability to convey scientific concepts to various audiences, tailoring language to suit
- Strong organizational and time management skills, both long and short term
- Ability to plan/coordinate multiple projects and duties
- Ability to manage a group/team
- Able to work in a team environment as well as independently
- Ability to synthesize information from a variety of sources
- Ability to conduct source literature/material searches relevant to specific projects
- Advanced knowledge of Microsoft Word, Excel, PowerPoint, Outlook and Adobe Creative Suites Software

LANGUAGES

- Fluent in English and French